Molecular Approaches to Axonal Regeneration

A thesis submitted to the University of London for the degree of Doctor of Philosophy

by

David Hunt

Department of Immunology and Molecular Pathology
Windeyer Institute of Medical Sciences
University College London
46 Cleveland Street
London W1T 4JF
United Kingdom

September, 2004

ProQuest LLC
789 East Eisenhower Parkway
P.O. Box 1346
Ann Arbor, MI 48106-1346

ABSTRACT

The presence of inhibitory molecules is believed to contribute to the failure of axonal regeneration in the adult mammalian CNS. This thesis is focussed on the role of the Nogo-66 receptor (NgR), and its ligands, in preventing axonal regeneration, and the use of genetically modified herpes simplex virus type-1 (HSV-1) for the disruption of these interactions.

The expression of *ngr*, *nogo-66* (i.e. *pan-nogo*), *nogo-a* and *omgp* mRNA in the intact and injured adult rodent nervous system has been examined by *in situ* hybridisation. Nogo-A expression was investigated by immunohistochemistry. The most significant findings were that, although cerebral cortical neurons strongly express *ngr*, many other neurons do not express *ngr* mRNA; indeed, *ngr* transcripts were absent from the corpus striatum and weakly expressed, if at all, by most spinal cord neurons and most primary sensory neurons. In contrast, *nogo* isoforms were expressed by many types of neuron in the CNS and PNS. Nogo-A protein was found to be prominently expressed in growing and regenerating axons. It is therefore unlikely that NgR/Nogo interactions can explain the general failure of axonal regeneration in the CNS.

Several genetically modified HSV-1 vectors were constructed for the disruption of the NgR-ligand interactions. The first of these was constructed for the expression of a tagged-secreted form of the NgR antagonist peptide (NEP1-40); but, this was found to express poorly both *in vitro* and *in vivo*. Additionally, a system for the expression of functional shRNA from HSV-1 is reported. As a proof of principle, eGFP expression was successfully targeted in a cell line *in vitro*. Similarly, NgR was also targeted in primary cultures of cerebellar granule cells *in vitro*, but with less effect.

ACKNOWLEDGEMENTS

I am most grateful to my primary supervisor, Dr. Rob Coffin, for accepting me into his lab and for granting me considerable freedom in determining the course of my research. Also, I owe the utmost thanks to my second supervisor, Professor Patrick Anderson, who has inspired me to take a genuine interest in neuroscience.

I thank those who selected me for a place on the MBPhD programme, as well as University College London and The Royal Free School of Medicine for providing me with funding. I also thank my primary supervisor, Rob, for funding an additional year of my research.

Both the labs in which I have been privileged to work have been full with helpful students and post-docs, unfortunately too numerous to list here. To all of those people, past and present, I express my gratitude since it is they who have issued me with most of my protocols, as well as sensible advice for overcoming any technical difficulties. Several people deserving of specific mention are: Julia Winterbottom, our technician, who has often made time to assist me when there were too few hours in the day; Drs. Greg Campbell and Matt Mason for their willingness to lend their expertise in animal surgery; and Jenny Mills, whom I supervised during her MSc and whose cheerful personality and dedication to our work made her a pleasure to work with. I am also thankful to Professor Bob Lieberman for his ongoing constructive criticism of my work

In addition, I should like to thank Dr. Rabinder Prinjha, of GSK plc., for the provision of the anti-Nogo-A mouse monoclonal antibody; and Sam Wilson, from the Department of Immunology and Molecular Pathology, UCL, for making available his shRNA-expressing lentivirus.

I am greatly indebted to my friends Bobby, Sarita and baby Raya Patel, Tony Greenstein and Richard Eldridge who between them have helped me to maintain some semblance of a social life over the past few years. Likewise, I must sincerely thank my good friends

and fellow research students Emmanuela Costigliola and Sonja Rakic, who not only understand how demoralising lab work can sometimes be, but who also know that laughter is the best antidote.

Finally, I owe my parents, Linda and John, the greatest thanks of all. They alone have taught me to appreciate the value of education, and have provided endless encouragement in all of my endeavours, academic or otherwise. Without their support, it is difficult to believe that I would have come this far. In fact, this thesis is as much the product of their efforts, as it is mine.

PUBLICATIONS

Hunt, D, Hossain-Ibrahim, K, Mason, MR, Coffin, RS, Lieberman, AR, Winterbottom, J, and Anderson, PN (2004) ATF3 upregulation in glia during Wallerian degeneration: differential expression in peripheral nerves and CNS white matter. BMC.Neurosci. 5: 9

Mingorance, A, Fontana, X, Sole, M, Burgaya, F, Urena, JM, Teng, FY, Tang, BL, **Hunt, D**, Anderson, PN, Bethea, JR, Schwab, ME, Soriano, E, and Del Rio, JA (2004) Regulation of Nogo and Nogo receptor during the development of the entorhino-hippocampal pathway and after adult hippocampal lesions. Mol.Cell Neurosci. 26: 34-49.

Hunt, D, Coffin, RS, Prinjha, RK, Campbell, G, and Anderson, PN (2003) Nogo-A expression in the intact and injured nervous system. Mol.Cell Neurosci. 24: 1083-1102.

Hunt, D, Coffin, RS, and Anderson, PN (2002) The Nogo receptor, its ligands and axonal regeneration in the spinal cord; a review. J.Neurocytol. 31: 93-120.

Hunt, D, Mason, MR, Campbell, G, Coffin, R, and Anderson, PN (2002) Nogo receptor mRNA expression in intact and regenerating CNS neurons. Mol.Cell Neurosci. 20: 537-552.

TABLE OF CONTENTS

INDEX OF FIGURES

INDEX OF TABLES

GLOSSARY

AAV	adeno-associated virus
ATF3	activating transcription factor 3
BDNF	brain-derived neurotrophic factor
BSA	bovine serum albumin
CAM	cell adhesion molecule
CDS	coding sequence
CGRP	calcitonin gene related peptide
CMV	cytomegalovirus
CSPG	chondroitin sulphate proteoglycan
CST	corticospinal tract
CNS	central nervous system
CNTF	ciliary neurotrophic factor
DCN	deep cerebellar nuclei
DEPC	diethyl-pyrocarbonate
DIG	digoxigenin
DIV	days *in vitro*
DNA	deoxyribonucleic acid
dpo	days post operation
DREZ	dorsal root entry zone
DRG	dorsal root ganglia
E	embryonic day
ECM	extracellular matrix
EDTA	ethylenediaminetetra acetic acid
eGFP	enhanced green fluorescent protein
FGF	fibroblast growth factor
FGM	full growth media
GAP	growth associated protein
GDNF	glial-derived neurotrophic factor
GFAP	glial fibrillary acidic protein
HCl	hydrochloric acid
HBSS	Hank's buffered saline solution
HIV-1	human immunodeficiency virus type 1
HRP	horse radish peroxidase
HSV-1	herpes simplex virus type 1
Ig	immunoglobulin
IRES	internal ribosomal entry site
JNK	Jun N-terminal kinase
lhRNA	long-hairpin RNA
LRR	leucine rich repeat
LV	lentivirus
MAG	myelin associated glycoprotein
MOI	multiplicity of infection
NaCl	sodium chloride
NaOH	sodium hydroxide
N-CAM	neural cell adhesion molecule
NEP1-40	Nogo extracellular peptide 1-40
NGF	nerve growth factor
NgR	Nogo-66 receptor
NT-3	neurotrophin 3
NT-4/5	neurotrophin 4/5
NT-6	neurotrophin 6
OMgp	oligodendrocyte myelin glycoprotein
P	postnatal day
PBS	phosphate buffered saline
pfu	plaque forming units
PNS	peripheral nervous system
RGC	retinal ganglion cell
RNA	ribonucleic acid
RNAi	RNA interference
SCG	superior cervical ganglion
shRNA	short-hairpin RNA
siRNA	short interfering RNA
SNpc	substantia nigra pars compacta
SSC	standard saline citrate
TRN	thalamic reticular nucleus

CHAPTER 1

Introduction

Injured central nervous system (CNS) neurons of some lower vertebrates exhibit a strong propensity for regeneration (reviewed by Ferretti et al., 2003), often giving rise to target reinnervation and clear functional recovery. In contrast, within the mammalian nervous system, only neurons of the peripheral nervous system (PNS) display a clinically useful capacity for regeneration and functional restitution. That injured adult mammalian CNS neurons demonstrate, at best, an abortive regenerative response is suggestive of an evolutionary loss of the capability to recover function after CNS injuries.

There are several hypotheses which currently seek to explain the abortive regenerative response that occurs following injury to the mammalian CNS: the intrinsic regenerative ability of mature CNS neurons may not be sufficiently strong to allow prolonged axonal regeneration (Richardson and Verge, 1986; Chong et al., 1996; Anderson and Lieberman, 1999); the injured CNS may be deficient in a number of important neurotrophic molecules (Berry et al., 1996; Zhang et al., 1998; Bradbury et al., 1999); or, molecules inhibitory to axonal regeneration may be present after injury to the CNS (Pasterkamp et al., 1999; reviewed by Fawcett and Asher, 1999), or in the intact CNS, especially in myelin (reviewed by Schwab, 1996).

AXONAL REGENERATION

PNS Axonal Regeneration

Neurons which extend axons peripherally have long been known to launch a sustained regenerative response to injury. Clinically, this often results in some degree of functional recovery, dependent on the severity and nature of the lesion. Nonetheless, this innate regenerative process is not entirely without complications, since regenerating axons can

make pathfinding errors resulting in the incorrect innervation of targets which may, for example, manifest in clinical symptoms such as neuropathic pain.

The sequence of events that occurs after axotomy of the peripheral processes of dorsal root ganglia (DRG) neurons, or the axons of extrinsic CNS neurons (e.g. ventral spinal motor neurons), is well documented. Immediately after axotomy, Wallerian degeneration commences (Waller, 1850); this entails the degeneration of the severed distal axons and their myelin sheaths, which are phagocytosed by both Schwann cells and macrophages. As the axonal and myelin debris is eliminated by this process, the Schwann cells begin to proliferate and extend processes longitudinally through the channels formed by columns of Schwann cells, known as the bands of Büngner. All axonal regeneration within the distal segment of injured nerves occurs through these columns. Schwann cells aid the process of axonal regeneration through the synthesis of trophic molecules and membrane-bound cell adhesion molecules, such as N-CAM, L1 and CHL1 (Nieke and Schachner, 1985; Tacke and Martini, 1990). Other molecules that have been implicated in the process of peripheral axonal regeneration as permissive or stimulatory molecular cues include laminin and tenascin-C, both of which are synthesized by Schwann cells and are embedded in the basal lamina as extracellular matrix molecules (Salonen et al., 1987; Martini et al., 1990). At lesion sites in peripheral nerves Schwann cells act to heal the wound, migrating from both proximal and distal stumps to bridge any deficit (Ramon Y Cajal, 1928). This is in marked contrast to the behaviour of CNS glia at injury sites which are characterized by the loss of astrocytes and oligodendrocytes (Berry et al., 1999).

CNS Axonal Regeneration

In contrast to the robust axonal regenerative response of axotomized PNS neurons, there is at best an abortive regenerative response to mechanical injury by intrinsic CNS neurons. The most effective regenerative response by axons in CNS tissue is found in the optic nerve and optic tract where a few axons can regenerate a few millimetres beyond injury sites (Harvey and Tan, 1992; Campbell et al., 1999), although they never regenerate back to their targets in the brain.

Autologous Nerve Grafts for the Enhancement of CNS Axonal Regeneration

Although almost all intrinsic CNS neurons fail to regenerate after axotomy when left untreated, many subclasses exhibit the ability to extend axons if provided with a suitably permissive environment. This was first observed by Ramon Y Cajal, and his student Tello, following the implantation of a segment of peripheral nerve to the cerebrum. They found that axons were often present in the grafted nerve, but were unable to prove to the satisfaction of critics that these were derived from CNS neurons. The suspicion that CNS axons could regenerate was finally confirmed in a landmark series of experiments (Richardson et al., 1980; Benfey and Aguayo, 1982). Using novel retrograde labelling techniques to trace the source of axons that had regenerated into peripheral nerve grafts, they were able to show definitively that many classes of intrinsic neuron were able to grow their axons through the permissive environment provided by the peripheral nerve. However, since they had implanted the segments of peripheral nerve in brain or spinal cord, there was some suggestion that the CNS axons invading the grafts may not have been regenerating axons *per se*, but collateral sprouts from intact CNS axons. The latter was disproved when Berry and colleagues reported that retinal ganglion cells (RGCs) were able to regenerate their axons from severed optic nerve into a contiguous peripheral nerve graft (Berry et al., 1986). However, the grafting of a segment of peripheral nerve, depleted of viable cells by repeated freeze-thaw cycles, to transected optic nerve was found to elicit no axonal ingrowth from injured retinal ganglion cells (Berry et al., 1988). Presumably, Schwann cells in the Bands of Büngner of peripheral nerve, with which in-growing axons closely associate (Hall and Berry, 1989), provide an essential stimulus for regeneration. However, this alone does not explain why some classes of CNS neuron are unable to regenerate axons, even in apparently permissive environments. Purkinje cells and corticospinal neurons are just two examples of types of neuron that have consistently been found to be refractory to regeneration into environments containing Schwann cells (Richardson et al., 1982; Chaisuksunt et al., 2003).

Since peripheral nerves are also composed of other cells - including fibroblasts, macrophages and endothelial cells - that might have been contributing to the effect of peripheral nerve grafts on the regeneration of CNS axons, some groups examined the

effects of transplanting purified Schwann cells to the injured CNS (Kromer and Cornbrooks, 1985; Paino and Bunge, 1991; Montero-Menei et al., 1992; Martin et al., 1996). For the most part, these have shown that suspensions of purified Schwann cells administered to the vicinity of axotomized CNS neurons do promote some degree of axonal regeneration.

The Enhancement of CNS Axonal Regeneration by Other Types of Cell

Olfactory Ensheathing Glial Cells (OEGCs)

In addition to the Schwann cell, another class of cell that has received much attention in recent years for its apparent ability to stimulate axonal regeneration of CNS neurons is the olfactory ensheathing glial cell (OEGC). This class of cell is responsible for ensheathing the axons of olfactory receptor neurons, which are generated throughout life and possess an unusual ability to both grow and regenerate their axons into the CNS environment of the olfactory bulb and form functional synapses.

$p75^{NTR}$ immunoaffinity-purified cultures of OEGCs were first transplanted to the injured nervous system by Ramon-Cueto and Nieto-Sampedro (1994), who implanted them into the dorsal horn of the spinal cord at the level of a dorsal rhizotomy. They reported that DRG axons, as detected by DiI labelling and calcitonin gene-related peptide (CGRP) immunoreactivity, regenerated through laminae 1-5 of the ipsilateral dorsal horn. A series of experiments followed, in which different groups attempted to harness these cells for the repair of spinal cord and brain injuries. However, whilst some impressive claims have been made (reviewed by Raisman, 2001), other groups have failed to demonstrate extensive axonal regeneration into, or within, the CNS after grafting of olfactory ensheathing glial cells (Gomez et al., 2003; Riddell et al., 2004). The consensus finding is that these cells seem to be, at best, of moderate value in promoting axonal regeneration from the corticospinal tracts and are less effective in other systems, although they do have a clear, though limited effect on optic nerve regeneration (Li et al., 2003). In the spinal cord, at least one group has found Schwann cells to be more effective in eliciting regeneration of injured tracts (Takami et al., 2002), although there is some evidence that

OEGCs may be able to stimulate functional recovery by other means (Ramer et al., 2004).

The Cell Body Response of Injured PNS and CNS Neurons

Over the past two decades, it has become clear that the expression of certain proteins is important for a sustained axonal regenerative response by neurons. The genes encoding these proteins have become known as regeneration/growth associated genes and include *c-jun*, *atf3*, and *gap-43* which are discussed later. There are many other regeneration associated genes and intrinsic determinants of axonal regeneration which are not addressed here (for review see Caroni, (1997), and for an example of the complexity of the response as revealed by microarray analysis see Costigan et al., (2002).

Most of the neuronal perikarya which are induced to regenerate axons into peripheral nerve grafts in the CNS are found close to the tip of the graft (Richardson et al., 1980). This illustrates an interesting phenomenon – that axons are better able to regenerate after proximal injury than a distal injury, although the likelihood of cell death also increases with a proximal axotomy. The distance between cell body and point of axotomy is inversely correlated with the induction of expression of regeneration associated genes in some classes of neuron. This was first observed in a model of optic nerve transection, in which the GAP-43 was only found to be expressed in the retinal ganglion cell layer if the lesion was within 3mm of the eye (Doster et al., 1991). Similarly, it has been found that regeneration associated genes are strongly upregulated by rubrospinal neurons following cervical, but not thoracic, lesions of the rubrospinal tract (Fernandes et al., 1999). The notion that the neuronal cell body response to axotomy should vary according to the proximity of the axonal lesion to the cell body is somewhat unexpected. However, it may be the result of the cumulative input of inhibitory cues from the CNS environment along the proximal stump (Zagrebelsky et al., 1998). An alternative argument is that the neurons may be maintained in an inert state by the presence of intact collaterals, which are more likely to be preserved by a distal axotomy.

Evaluation of the expression profiles of different subclasses of CNS neurons following peripheral nerve graft revealed that those neurons that are unable to regenerate their axons, such as Purkinje cells, do not initiate the same robust cell body response to injury as those CNS neurons that are able to extend their axons into grafted peripheral nerve (Anderson et al., 1998). This is a crucial discovery since it implies that there exists a variable degree of inherent neuronal potential for regeneration after injury.

Regeneration Associated Gene Expression in Neurons

For successful axonal regeneration to occur, injured neurons must survive the initial insult in sufficient numbers, sprout neurites and subsequently extend axons over long distances towards their original target. The expression of the regeneration associated genes by axotomized neurons, particularly those with proximal injuries, has been reported to be detrimental to cell survival. Overexpression of GAP-43 by motor neurons enhances their chances of undergoing cell death in response to peripheral nerve injury (Harding et al., 1999). Similarly, c-Jun has been implicated in apoptotic neuronal cell death (Ham et al., 1995). Those neurons that appear to be inherently incapable of regeneration, e.g. Purkinje cells and corticospinal neurons, and do not upregulate regeneration associated genes appear to be resistant (although not immune) to cell death after axotomy. In contrast, those subtypes of neuron which appear to be programmed to launch a regenerative response after injury, e.g. retinal ganglion cells, exhibit a high rate of apoptotic cell death (Villegas-Perez et al., 1993; Berkelaar et al., 1994; Garcia-Valenzuela et al., 1994).

c-Jun

C-Jun is a transcription factor that is expressed by many different cell-types, and can dimerise either with itself to form homodimers or with other proteins such as JunB, JunD, c-Fos or CREB/ATF family members, amongst others, to form heterodimers. Any of these dimers constitute an AP-1 transcription factor complex which recognizes the consensus sequence TGACTCA (Lee et al., 1987). The c-Jun N-terminal kinase (JNK), a member of the MAP kinase superfamily, regulates the activity of c-Jun through the phosphorylation of two serine residues within the amino terminal of the protein. In the

nervous system, c-Jun has been implicated in the cellular response to axotomy, as well as the processes of axonal regeneration and apoptosis.

C-Jun is widely expressed throughout the brain during early embryonic development, and its expression has been reported to decrease with cellular maturation and differentiation. In the adult, basal levels of c-Jun expression persist in many classes of neuron throughout the CNS and PNS including spinal motor neurons, neurons of autonomic ganglia and DRG neurons (Herdegen et al., 1991; Herdegen et al., 1995; de Leon et al., 1995).

Upregulation of c-Jun expression is readily detected in motor and sensory neurons, after peripheral nerve injury (Jenkins and Hunt, 1991), and persists until target-tissue reinnervation occurs. This is accompanied by increased JNK activity, which results in the phosphorylation and activation of c-Jun (Kenney and Kocsis, 1998). Interestingly, Schwann cells in the denervated distal stump also upregulate c-Jun; this is thought to occur as a consequence of the loss of axonal contact, since the onset of c-Jun expression coincides with the commencement of Wallerian degeneration. In addition, expression has been reported to subside with the invasion of regenerating axons (Shy et al., 1996; Soares et al., 2001). There has been some suggestion that transforming growth factor beta (TGFβ) may induce phosphorylation of c-Jun in Schwann cells leading to the initiation of apoptotic pathways, after nerve injury (Parkinson et al., 2001).

A null mutation of the *c-jun* gene locus results in an embryonic lethal phenotype in homozygous transgenic mice, with most embryos dying at E12.5. Despite the -/- transgenic embryos being grossly anatomically and histologically normal, primary cultures of -/- transgenic fibroblasts were found to proliferate considerably more slowly than those of wildtype embryos and, furthermore, were found to be less responsive to the effects of mitogens (Johnson et al., 1993); together, these findings implicate c-Jun in both cell survival and mitogen response pathways. That these knockout animals should die *in utero* has proved a hindrance for regeneration studies; however, Raivich et al. (2004) have developed a conditional *c-jun* null mutant, in which it has been demonstrated that peripheral nerve regeneration is impaired. The level of GAP-43 upregulation in

peripherally axotomized neurons in these transgenic mice was also revealed to be considerably lower than in wild-type mice.

In general terms, the upregulation of c-Jun by axotomized intrinsic CNS neurons correlates well with their capacity for regeneration of axons into segments of peripheral nerve grafted to brain. For example, neurons of the thalamic reticular nucleus and the deep cerebellar nuclei which successfully extend axons into peripheral nerve grafts, are known to up-regulate c-Jun for prolonged periods (Vaudano et al., 1998; Chaisuksunt et al., 2000a). Classes of neuron which fail to regenerate axons into the graft exhibit only brief expression of c-Jun. The only neurons which prove to be an exception to this trend are those of the substantia nigra pars compacta which, despite successfully regenerating axons into nerve grafts to striatum, show only modest signs of c-Jun expression (Chaisuksunt et al., 2003). In summary, although many intrinsic CNS neurons that regenerate their axons into peripheral nerve grafts show a prolonged upregulation of c-Jun, there are some successfully regenerating intrinsic neurons that do not, and some non-regenerating cells that transiently upregulate c-Jun after injury.

Activated Transcription Factor 3 (ATF3)

ATF3 belongs to the ATF/CREB family of basic-region leucine zipper (bZip)-containing transcription factors and can either homodimerise to form complexes that bind ATF/CRE consensus TGACGTCA DNA sequence to suppress transcription, or can form heterodimers with other members of the ATF/CREB family to form complexes that stimulate transcription (reviewed by Hai et al., (1999); Hai and Hartman, (2001)). It has been reported that ATF3 can heterodimerise with c-Jun to form a transcription factor complex capable of binding the AP-1 consensus sequence (Hai and Curran, 1991), which is perhaps not surprising given the homology of their consensus DNA binding sites. The upregulation of ATF3 by primary sensory neurons and spinal motor neurons after peripheral nerve axotomy is more widespread than that of c-Jun, and correlates even better with retrograde labelling than does c-Jun. Tsujino et al. (2000) have suggested that ATF3 should be regarded as a neuron-specific marker of injury in the nervous system.

This, however, is in disagreement with more recent findings (see Chapter 5; Hunt et al., 2004).

Both c-Jun and ATF3 have been found to be upregulated by all classes of axotomized peripheral neurons in which they have been studied. Among intrinsic CNS neurons, there are variable patterns of ATF3 expression following axotomy; in general, CNS neurons that can successfully regenerate their axons into peripheral nerve grafts, upregulate ATF3. As with other regeneration associated genes, ATF3 expression by neurons is critically dependent on the site of axotomy. For example, corticospinal neurons upregulate ATF3 and c-Jun after intracortical axotomy, but not after axotomy within the spinal cord (Mason et al., 2003; Chaisuksunt et al., 2003). The downstream targets of ATF3 are for the most part yet to be identified.

Growth-Associated Protein 43 (GAP-43)

Although the neuronal expression of GAP-43 in response to axotomy and the capacity to regenerate axons in a permissive environment are not perfectly correlated, no neurons have been found to regenerate their axons *in vivo* without expressing GAP-43. That some neurons should upregulate GAP-43 and yet fail to regenerate their axons in a permissive environment is probably an indication of an intrinsic deficiency of other regeneration associated molecules. Currently, it is the best molecular marker of regenerating axons.

GAP-43 is a 43KDa growth associated protein that has been identified as being important in both neurite outgrowth (Skene and Willard, 1981) and synaptic plasticity (Routtenberg and Lovinger, 1985). It is a membrane- and cytoskeleton-associated molecule that localizes to the growth cone during neurite outgrowth, and is thought to participate in signal transduction, initiated by axon guidance molecules, which culminate in cytoskeletal rearrangements. It is strongly expressed by neurons during development and regeneration, and diminishes upon target (re-)innervation (reviewed by Benowitz and Routtenberg, 1997). However, it is also detected in presynaptic nerve terminals and remains present at low levels throughout adulthood in some classes of neuron that are

particularly plastic, implying that it is perhaps multifunctional. Interestingly, the *gap-43* promoter sequence contains an AP-1 binding site (Weber and Skene, 1998), suggesting that the high-level of *gap-43* mRNA detected in many injured neurons may be the result of c-Jun transcription factor binding activity, perhaps in conjunction with ATF3.

A number of *in vitro* studies of GAP-43 function have been reported, most of which support the notion that the molecule is important for neurite outgrowth. Targeting the protein, Shea et al. (1991) incubated a neuroblastoma cell line with anti-GAP-43 antibodies, and observed a significant reduction in neurite formation. The PC12 cell line, derived from rat phaeochromocytoma, which upregulates GAP-43 in response to NGF and subsequently differentiates and extends axons (Karns et al., 1987; Federoff et al., 1988), has been used as a model by several groups for assessing the role of GAP-43 in neurite elongation. Using antisense oligonucleotides to *gap-43* mRNA, Jap Tjoen et al. (1992) found neurite outgrowth to be impaired, which was in keeping with an earlier study in which GAP-43 overexpression in PC12 cells was found to result in greater neurite extension (Yankner et al., 1990). However, others have reported that a mutant PC12 cell line, deficient in GAP-43, was still able to extend neurites in response to NGF and have proposed that its role is not in the initial process of sprouting but the function of growth cones and the presynaptic terminal (Baetge and Hammang, 1991). In contrast, Aigner and Caroni (1993, 1995), who also used antisense oligonucleotides, observed fewer neurites sprouting from primary cultures of chick DRG neurons, and reported that the few attendant neurites bore smaller growth cones were more susceptible to retraction when presented with inhibitory central nervous system myelin-derived liposomes.

Two strains of *gap-43* null mutant mice have been generated (Strittmatter et al., 1995; Zhu and Julien, 1999), both of which exhibit similar and significant aberrations in axonal pathfinding within the visual system. In the first strain, it was found that only a few axons traversed the optic chiasm, and that these had done so randomly. In the second strain, axons failed to form synaptic contacts in the lateral geniculate nuclei. Also, in this strain, the anterior and hippocampal commissures, as well as the corpus callosum were reported absent (Shen et al., 2002). There have been no reports of regeneration

experiments undertaken on either of these *gap-43* null mutant mice, presumably because they die within a few weeks of birth. Nonetheless, what these models have revealed is that GAP-43 alone is not critical for axonal outgrowth from all classes of neuron but that it is also likely to be involved in axon guidance/growth cone motility.

Although, there have been no reports of the state of regeneration in *gap-43* knockout animals, Caroni and colleagues developed a GAP-43 dominant negative and subsequently generated a transgenic animal in which this mutant protein was overexpressed within the nervous system (Laux et al., 2000). The rate of regeneration of axotomized peripheral nerves was found to be impaired, although complete regeneration and re-innervation of target tissues was observed. Conversely, overexpression of GAP-43 in the nervous system, results in spontaneous sprouting of neurites at the neuromuscular junction, as well as significantly more sprouting of neurites and terminal arborisation following axotomy (Aigner et al., 1995).

In wild-type animals, *in vivo* experiments have revealed a clear correlation between upregulation and the duration of GAP-43 expression and the capacity to regenerate axons into peripheral nerve grafts in the brain (Vaudano et al., 1995). Those neurons which had successfully regenerated axons into the graft – primarily residing in the thalamic reticular nucleus - exhibited prolonged expression of *gap-43*, compared to those that had failed to regenerate. Similarly, neurons of the deep cerebellar nuclei which also successfully regenerated axons into grafts to cerebellum showed prolonged expression of *gap-43* in contrast to those that did not. Purkinje cells, which have never been shown to regenerate their axons into nerve grafts, do not even transiently upregulate *gap-43* transcript expression (Anderson et al., 1998)). However, overexpression of GAP-43 in transgenic mice is not sufficient to turn non-regenerating neurons into cells which can regenerate axons into peripheral nerve grafts (Buffo et al., 1997; Mason et al., 2000).

Scar and Cavity Formation in the Injured Mammalian CNS

Traumatic CNS lesions result in scarring, which is often accompanied by cavity or cyst formation, at the site of injury. These readily discernible physical features were long ago

recognized as potential physical barriers to axonal regeneration. Subsequent histological studies of the scar revealed that one of the defining characteristics of CNS injury sites is the presence around the lesion site of hypertrophic glial-fibrillary acidic protein (GFAP) immunopositive astrocytes, termed reactive astrocytes (Berry et al., 1996; Zhang et al., 1997).

Astrocytes

The primary function of reactive astrocytes appears to be in the sealing of the wound through their formation of an encapsulating glia limitans (reviewed by Reier and Houle, 1988). At first, it was thought that the mature scar in which astrocytic processes are tightly interwoven was, in itself, a physical deterrent to regenerating axons. However, it was noted that frog RGC axons were able to penetrate dense astrocytic scars, indicating that the failure of mammalian neurons to do so was probably the result of differences in the molecular phenotype of their astrocytes (Reier et al., 1983). Much research has since been undertaken to establish if and how reactive astrocytes may participate in preventing regeneration.

One of the best models for the study of reactive astrocytes involved dorsal root injury (rhizotomy), in which the regenerating central axons of primary sensory neurons can be studied as they reach the Dorsal Root Entry Zone (DREZ). The particular value of this model lies in its elucidation of the role of reactive astrocytes, in the absence of invading meningeal cells, in limiting the extension of otherwise regeneration-competent neurons (Carlstedt, 1988). Astrocytes reside throughout the entire CNS, becoming more numerous and hypertrophic in response to injury or Wallerian degeneration to give rise to glial scar tissue. After dorsal root rhizotomy, the astrocytes of the DREZ of the spinal cord hypertrophy and – although their cell bodies remain in the DREZ – extend astrocytic processes up to 700μm into the basal lamina tubes of the connecting dorsal roots (Zhang et al., 2001). Upon contact with astrocytic processes, most regenerating sensory axons in the dorsal roots either (i) stop regenerating and form end-bulbs (Carlstedt, 1985; Liuzzi and Lasek, 1987), or (ii) are deflected and extended back along the dorsal root towards their somata (Zhang et al., 2001). A small population of sensory axons usually manage to

avoid inhibitory influences and regenerate back into the cord, often along blood vessels (Chong et al., 1999). Liuzzi and Lasek suggested that reactive astrocytes express molecules serving as 'stop signals' for regenerating axons (Liuzzi and Lasek, 1987). However, it should be borne in mind that (i) ultrastructurally similar nerve profiles are seen in the dorsal roots in contact with Schwann cells (Chong et al., 1999), and (ii) these putative molecular cues are not insurmountable and can be overcome by intraspinal injection of adeno-associated virus (AAV) expressing NT-3 or NGF to the dorsal horn (Zhang et al., 1998; Romero et al., 2001), or even by intrathecal infusion of neurotrophins (Ramer et al., 2000).

Further evidence for the significance of the glial scar comes from Davies et al. who reported that GFP-expressing adult mouse DRG neurons, atraumatically transplanted to the dorsal columns of the adult rodent spinal cord, were capable of extending axons over long distances within the spinal dorsal columns that were undergoing Wallerian degeneration. The rate of regeneration was recorded at 2mm per day, comparable with regenerating peripheral nerves, but the axons were found to be arrested on contact with the scar tissue (Davies et al., 1997; Davies et al., 1999). However, this does not preclude the involvement of other factors such as myelin-associated inhibitory molecules, which may be partly responsible for this observation, as will be discussed later.

One of the most successful and reproducible ways of impeding glial scar formation in the injured spinal cord *in vivo*, has been achieved through the use of low dose X-irradiation (Kalderon and Fuks, 1996; Ridet et al., 2000; Zeman et al., 2001). There is some disagreement over the dose and the time post-injury at which this is most effective with one group claiming that, under the wrong conditions (5-20Gy), the treatment group scores were worse than untreated controls in motor performance tasks. On balance, although this procedure does not completely eliminate reactive astrocytes from the injured spinal cord, it does facilitate axonal regeneration and results in moderate improvements in behavioural scoring tasks. Remarkably, it has also been reported that a single high-dose of radiation (40Gy) applied to neonatal rodents has such a profound

effect that organotypic sections of the spinal cord taken from the animals when they have reached adulthood are capable of supporting neurite outgrowth (Wilson et al., 2000).

It is difficult to model the glial scar using living astrocytes *in vitro*. Nonetheless, it is generally agreed that cultured immature astrocytes are permissive for neurite outgrowth from RGC or neocortical neurons *in vitro*, and mature astrocytes are not (McCaffery et al., 1984; Baehr and Bunge, 1990; Le Roux and Reh, 1995). Using a novel culture system, Fawcett et al. (1989) measured the capacity of various ages and subtypes of neurons to extend axons through a three-dimensional matrix of purified astrocytes. They reported that, although embryonic DRG neurons and retinal ganglion cells were able to extend axons through these three-dimensional cultures of astrocytes, adult RGCs and postnatal DRG neurons were not able to do so. In contrast, two-dimensional monolayers of astrocytes were found to be permissive for neurite outgrowth from all ages of RGC and DRG neurons. This is not consistent with the explanation that the molecular phenotype of adult astrocytes is inhibitory to axonal growth. Rather, it would appear that the three dimensional meshwork of astrocytes in a glial scar either forms an effective physical boundary to neurite outgrowth or has a different molecular phenotype from a monolayer of astrocytes. This is supported by the *in vitro* work of Fok-Saeng et al. (1995) who examined different astrocytic cell lines, which exhibit varying degrees of inhibition of neurite outgrowth, for correlations with expression of putative inhibitory chondroitin sulphate proteoglycans (CSPGs); they found no correlation with any given molecule, but did report that the most inhibitory astrocytic cell lines were those which secreted the most extracellular matrix (ECM). Interestingly, however, it has since been shown that the astrocyte cell line, Neu7, which is particularly inhibitory to neurite outgrowth *in vitro*, expresses considerably more NG2 (a cell membrane-associated chondroitin sulphate proteoglycan), versican and CS-56 antigen than less inhibitory astrocyte cell lines (Fidler et al., 1999). Subsequently, a careful series of experiments suggested that NG2 was responsible for the axon-inhibitory nature of the Neu7 cell line. To date, NG2 has not been shown to be widely expressed by mature astrocytes *in vivo*, even after CNS injury; although, oligodendrocyte precursor cells have been found to

express large amounts of NG2 in both the intact and injured CNS (Chen et al., 2002; but see also Greenwood and Butt, 2003).

In vitro, it has been shown that cytokines can be used to modulate the ability of cultured mature astrocytes to support neurite outgrowth. For example, basic fibroblast growth factor (bFGF) together with interleukin-1 can be used to induce a permissive response, whilst interferon gamma and TGFβ induce a non-permissive response (Fok-Seang et al., 1998). This is an important observation, since many cytokines are released following CNS injury which would be expected to influence the nature of the effect that astrocytes have on sprouting axons *in vivo*.

Meningeal Cells

The inhibitory nature of the scars in damaged CNS tissue cannot be attributed wholly to reactive astrocytes. Over the past few years, meningeal cells have received more attention since it has become apparent that they secrete large amounts of keratan sulphate proteoglycans (Hirsch and Bahr, 1999) as well as collagen IV into the lesion site (Rutka et al., 1986; Sievers et al., 1994). They are also important sources of semaphorin expression (Pasterkamp et al., 2001; De Winter et al., 2002). Their importance may have been long overlooked (reviewed by Morgenstern et al., 2002), as co-cultures of astrocytes and meningeal cells have revealed that RGC axons grew almost exclusively over astrocytes, either growing around or terminating upon contact with meningeal cells (Hirsch and Bahr, 1999).

Extracellular Matrix

The dense collagenous extracellular matrix, a major constituent of the scar tissue, and the surrounding basal lamina are also important aspects of the glial scar that together may comprise a potentially formidable physical barrier to regenerating axons. Recently, attempts to reduce collagen IV deposition through the local administration of the iron-chelating agent 2-2' bipyridine have been shown to augment axonal regeneration into the scar in a fimbra-fornix injury model (Stichel et al., 1999), but not in that of the injured corticospinal tract (Weidner et al., 1999). This is not surprising in the light of a

subsequent study that has revealed that 2-2' bipyridine alone is ineffective at reducing scar tissue formation in the spinal cord due to the presence of relatively large numbers of infiltrating meningeal cells, which are a major source of collagen IV (Hermanns et al., 2001).

Scar-Derived Inhibitory Molecules

Scar tissue is the source of a number of putative inhibitory molecules such as proteoglycans, tenascins and semaphorins (Meiners et al., 1995; Pasterkamp et al., 1999; Niclou et al., 2003). These families of potentially inhibitory molecules have been implicated in axon guidance in the developing nervous system (McAdams and McLoon, 1995; Pearlman and Sheppard, 1996; Powell et al., 1997; Powell and Geller, 1999; Joester and Faissner, 2001). The proteoglycans consist of chondroitin sulphate proteoglycans (CSPG), keratan sulphate proteoglycans (KSPG), heparan sulphate proteoglycans (HSPG) and dermatan sulphate proteoglycans (DSPG) (reviewed by Margolis and Margolis, 1994). The proteoglycans are composed of a core protein, linked to glycosaminoglycan (GAG) side-chains. Some of the molecules are predominantly expressed at the cell-surface, such as CSPGs, whilst others are secreted as extracellular matrix molecules, such as KSPGs. Some of these molecules, e.g. CSPGs, are expressed by GFAP-immunopositive reactive astrocytes and meningeal cells (McKeon et al., 1991). DSPG has been reported to support neuron survival *in vitro* (Kappler et al., 1997). In contrast, CSPG and KSPG, whose expression pattern correlates well with glial scar formation after CNS injury (Snow et al., 1990; Krautstrunk et al., 2002), have been described as non-permissive, if not inhibitory, to neurite outgrowth *in vitro* (Rudge and Silver, 1990; Snow et al., 1990; Snow et al., 1991). HSPG has been shown to potentiate the interaction of Slit2 with Robo1, which repels migrating neurons and growing axons during development (Hu, 2001); it is strongly expressed by leptomeningeal cells (David, 1988).

Enzymatic cleavage of the GAG sidechains of CSPG or KSPG has been reported to render the core proteins permissive for axon growth (Snow et al., 1990; Fidler et al., 1999). Using organotypic slice cultures of injured and intact adult rat spinal cord as a

substrate, Zuo et al. (1998b) reported that treatment with Chondroitinase ABC permitted enhanced neurite outgrowth of cultured embryonic chick DRG neurons. Administration of Chondroitinase ABC can promote regeneration *in vivo* of the nigrostriatal tract (Moon et al., 2001) and axons in the spinal cord (Bradbury et al., 2002), at least over short distances. Also, the implantation of Chondroitinase ABC soaked gel into the subarachnoid space has been shown to promote the regeneration dorsal spinocerebellar tract axons into grafts of peripheral nerve in spinal cord (Yick et al., 2000). These results appear to question the importance of the inhibitory domains in the core proteins of several CSPGs.

Whilst the receptor through which CSPGs exert their inhibitory effect has yet to be identified, it is known they are capable of activating RhoA in sensitive neurons (Monnier et al., 2003). The intracellular signaling pathway is not entirely clear, but protein kinase C (PKC) appears to be necessary for this process (Sivasankaran et al., 2004). Additionally, it has been reported that NG2, for example, can prevent the homophilic binding of the cell adhesion molecules N-CAM and L1 *in vitro* (Grumet et al., 1993). Such homophilic molecular interactions of cell adhesion molecules in the substrate with those in neurons are thought to be important for neurite outgrowth, not necessarily through their adhesive properties but through the activation of second messenger systems; there is evidence that *cis*-activation of the FGF receptor may participate in this process (reviewed by Walsh et al., 1997). However, regardless of the signaling mechanism, it is important to note that (i) regenerating peripheral axons can successfully extend through the distal stump of injured sciatic nerve, in which NG2 is strongly upregulated (Morgenstern et al., 2003; Jones et al., 2003; Rezajooi et al., 2004), and (ii) there is no sign of enhanced axonal regeneration in the injured CNS of NG2 null mutant mice (Anderson, unpublished observations).

There are two members of the tenascin family of proteins that have been implicated in the regulation of neurite outgrowth: Tenascin-C, and Tenascin-R (which is, in fact, a myelin-associated inhibitor of regeneration). Tenascin C has been reported to differentially regulate neurite growth depending on whether it is surface-bound, or soluble (Gotz et al.,

1996; Meiners and Geller, 1997), whilst Tenascin R has been shown to be inhibitory to the outgrowth of RGC fibres *in vitro* (Becker et al., 2000). Following spinal cord injury, Tenascin-C expression has been shown to be upregulated in and around the lesion site, and is probably synthesized by meningeal cells and reactive astrocytes (Zhang et al., 1997; Deller et al., 1997). Since Tenascin-C is strongly expressed in injury sites and the distal stumps of severed peripheral nerves, it is by no means obvious that its overall effects are inhibitory (Martini, 1994).

Cavity Formation

Cavitation frequently occurs in compression and contusion injuries, and - since the latter constitute the most common type of spinal cord injury in man - it is perhaps not surprising that the structural discontinuity imposed by cavitation and cyst formation often represent an additional barrier to axonal regeneration in the injured human spinal cord. Although the events that give rise to these structures have not yet been fully elucidated, it would appear that they are for the most part due to necrosis and apoptosis (Beattie et al., 2000). However, it should be noted that species-specific responses may be important; for example, in the rat spinal cord contusion model fluid-filled cysts are prominent, whereas in the mouse model cavities dense with connective tissue prevail (Inman and Steward, 2003). A plethora of cells have been detected within cavities including ependymal cells, macrophages, Schwann cells, and astrocytes (Wallace et al., 1987; Fitch et al., 1999). In contrast, GFAP-immunopositive reactive astrocytes are usually found bordering, but not within, the cavities (Farooque et al., 1995). Despite this, regenerating axons have been reported to enter the cavity, although their presence is inversely proportional to the severity of the lesion (Beattie et al., 1997).

Trophic Factor Deficiency in the Injured Mammalian CNS

Neurotrophic factors are secreted soluble proteins known to be important in nervous system development, plasticity and neurotransmission. Their actions range from promotion of cell survival, to axon outgrowth and control of cellular morphology. The term 'neurotrophic factor' is used widely to describe a number of different proteins or protein families, such as neurotrophins, glial derived neurotrophic factor family, ciliary

neurotrophic factor, transforming growth factor beta, platelet derived growth factor, and insulin-like growth factors. Only neurotrophins and their receptors will be discussed here.

Neurotrophins

Neurotrophins are so called since their biological activity is, for the most part, restricted to the nervous system. Members of this family of proteins share common structural features, and include nerve growth factor (NGF), brain derived neurotrophic factor (BDNF), neurotrophin-3 (NT-3), neurotrophin-4/5 (NT-4/5), neurotrophin-6 (NT-6), and neurotrophin-7 (NT-7) (Barde et al., 1982; Leibrock et al., 1989; Maisonpierre et al., 1990; Hallbook et al., 1991; Ip et al., 1992; Gotz et al., 1994; Lai et al., 1998).

The classic neurotrophic factor hypothesis, based primarily on findings concerning NGF and extrapolated to other family members, dictates that target-derived molecules undergo retrograde transport as internalized receptor-ligand complexes in neurotrophin-dependent CNS and PNS neurons and, ultimately, activate various proteins upon arrival in the cell body to elicit a biological response (Thoenen et al., 1988; DiStefano and Curtis, 1994). However, it has also become clear within recent years that neither BDNF nor NT-3 abide by this conventional hypothesis in that both are found to undergo anterograde transport in developing retinal ganglion cells and primary sensory neurons, are stored within vesicles in axon terminals, and can be released in an activity-dependent manner (von Bartheld et al., 1996).

Nerve Growth Factor (NGF/NTF1)

NGF, the first identified neurotrophin, was isolated from moccasin snake venom and then mouse sarcoma tissue more than five decades ago (Levi-Montalcini and Hamburger, 1951), and was soon shown to be crucial for the survival and maintenance of peripheral sympathetic neurons in neonatal rodents (Cohen, 1960). Similarly, it was later discovered that prenatal depletion of NGF through the administration of anti-NGF antibodies culminates in the loss of developing primary sensory neurons of the dorsal root ganglia (Johnson, Jr. et al., 1983). The mechanism of action underlying the role of

neurotrophins in sympathetic and sensory neuron development and survival has since become clear; it is now understood that excessive numbers of sympathetic and primary sensory neurons are present during development, and only those that successfully form connections with their target tissues and retrogradely transport target-derived neurotrophic factors, such as NGF, survive to maturity (Jones and Reichardt, 1990). Primary sensory neurons remain sensitive to NGF throughout their lifetime; although the molecule is not necessary for the survival of mature cells, it does stimulate neurite outgrowth (Lindsay, 1988).

In the adult rodent nervous system, strong expression of NGF transcripts and protein are detectable in the intact hippocampus and neocortex (Large et al., 1986); regions innervated by NGF-responsive cholinergic neurons of the basal forebrain. NGF is not expressed in the intact adult spinal cord (Korsching and Thoenen, 1985), but is upregulated by meningeal cells and some Schwann cells of nerve roots close to sites of compression or complete transection of thoracic spinal cord. Expression was found to peak at 1 day post operation (Widenfalk et al., 2001). In contrast, although NGF is not expressed by non-neuronal cells in intact adult peripheral nerve, there is no shortage of the molecule in lesioned adult peripheral nerves; NGF is strongly upregulated by Schwann cells in the distal stump soon after injury (Heumann et al., 1987). Intriguingly, these cells also upregulate $p75^{NTR}$ (Taniuchi et al., 1986). It has been suggested that NGF, and similar factors, may be temporarily bound and stored by $p75^{NTR}$-expressing Schwann cells as a stimulatory substrate for regenerating axons as they grow back through the distal stump towards their original targets (Sandrock, Jr. and Matthew, 1987).

It has been reported that continuous infusion of NGF to the dorsal spinal cord can promote the ingrowth of up to 37% of central processes from primary sensory neurons after dorsal root crush, by two weeks post operation (Oudega and Hagg, 1996). These ingrowing fibres are typically unmyelinated, small diameter fibres and are immunopositive for CGRP (i.e. they are consistent with the profile of a subpopulation of DRG neurons known to express the trkA receptor). Furthermore, they were observed growing up to a distance of several millimeters within the spinal white matter tracts. In

contrast, only 3% of primary sensory neurons were reported to penetrate the dorsal root entry zone in the untreated injured control animals. Similarly, others have reported that continuous intrathecal administration of NGF, or intraspinal injection of AAV expressing NGF, supports the regeneration of small diameter, unmyelinated, CGRP immunopositive fibres into the spinal dorsal horn following dorsal root crush (Ramer et al., 2000; Romero et al., 2001). Critically, none of these studies examined the effects of NGF administration after rhizotomy by transection; their employment of a crush model raises the possibility that some fibres may have been spared.

Autologous grafts of primary fibroblasts, that have been modified *ex vivo* to express high levels of NGF, have been shown to promote the growth of coerulospinal fibres and ventral motor axons, as well as CGRP immunoreactive primary sensory fibres when transplanted to the injured spinal cord. Injured corticospinal and raphaespinal fibres did not respond to the transplants (Tuszynski et al., 1996). Axons that successfully entered these grafts of NGF-secreting fibroblasts were not found to exit them; it has, therefore, been suggested that this arrested growth is perhaps due to the axons having arrived at the point where the concentration of growth factor is highest, and that a better strategy for spinal cord repair might be a system whereby the highest concentration of neurotrophin can be sequentially switched to sites downstream of the growing axons (Tuszynski et al., 1997; reviewed by Jones et al., 2001).

Brain Derived Neurotrophic Factor (BDNF/NTF2)

BDNF has been implicated in a plethora of physiological processes within the developing or mature CNS, including neuroprotection (Jones and Reichardt, 1990), chemotaxis (Ming et al., 2002), neurotransmission (Yang et al., 2002), long-term potentiation (Kovalchuk et al., 2002) and cortical inhibition (Huang et al., 1999). Of course, an important factor in nerve injury is cell survival, particularly of neurons; there is quite clear evidence that BDNF is one molecule that plays an important role in determining cell fate in the nervous system during development, in adulthood, and after injury. There is also circumstantial evidence that it may be involved in the progression of insidious neurodegenerative diseases.

Like NGF, BDNF has been shown to exert an anti-apoptotic effect on a subpopulation of developing primary sensory neurons; unlike NGF-dependent neurons, however, BDNF-dependent neurons never lose their dependence on this molecule which they themselves secrete to support their own survival in an autocrine manner (Acheson et al., 1995). Developing chick RGCs are also dependent on BDNF for their survival; *in vitro*, it has been established that these neurons begin to become dependent on BDNF at E6, becoming completely dependent by E11 (Rodriguez-Tebar et al., 1989). This timecourse corresponds to the onset and completion of target innervation *in vivo*, and the apoptosis of superfluous RGCs. Other cells that have been shown to be dependent on BDNF for survival, using the BDNF null mutant mouse, include vestibular and trigeminal sensory neurons and a subset of nodose-petrosal ganglion neurons (Conover et al., 1995). In the latter case, this would appear to include a subpopulation of afferent neurons that is involved in chemosensory regulation in the respiratory system since BDNF -/- mice exhibit a severely abnormal breathing pattern (Erickson et al., 1996). Additionally, some abnormalities in the morphology and physiology of serotonergic neurons has been observed in mice heterozygous for BDNF (Lyons et al., 1999).

Following transection or compression of the adult mammalian optic nerve, retinal ganglion cells undergo apoptosis with ~95% of the population dying within two months after injury. However, intravitreal administration of BDNF after complete transection of adult rat optic nerve has been reported to promote a 2.3fold increase in RGC survival at three weeks post operation. Unfortunately, this is not a prolonged effect and, by seven weeks, RGC survival is comparable to the levels observed in control animals (Mey and Thanos, 1993).

There is some circumstantial evidence that BDNF may be involved in at least two different neurodegenerative disorders. First, wild-type huntingtin protein has been reported to induce expression of BDNF within the cortex, whereas the mutant form of the protein – characteristic of Huntingdon's disease – does not (Zuccato et al., 2001). This could, in part, explain the degeneration of striatal neurons. Second, BDNF released from pre-synaptic terminals is known to be able to regulate the sensitivity of post-synaptic

target neurons to the effect of dopamine by controlling the expression of the D3 receptor in dopamine sensitive neurons (Guillin et al., 2001). Given the abnormal distribution of the D3 receptor in Parkinson's disease, it has been suggested that BDNF may be involved in the pathogenesis of the disorder.

In the adult brain, BDNF is expressed by neurons within the hippocampus, amygdala and neocortex; targets of the forebrain cholinergic neurons (Ernfors et al., 1990; Wetmore et al., 1990; Phillips et al., 1990). In spinal cord, it is found only in some neurons of lamina VII of the dorsal horn. A subpopulation of adult dorsal root ganglia neurons strongly expresses BDNF (Ernfors et al., 1990), and these appear to be of varying size. No obvious regulation of expression is detectable after compression or complete transection of the thoracic spinal cord (Widenfalk et al., 2001). Nonetheless, BDNF is one of the molecules that has been found to be upregulated in the spinal cord following treatment with the anti-Nogo-A function-blocking antibody, IN-1 (Bareyre et al., 2002). Transection of peripheral nerves elicits a strong upregulation of BDNF in the distal stump; however, the onset of expression commences after 3 days and peaks several weeks post injury (Meyer et al., 1992).

Continuous infusion of BDNF into the dorsal spinal cord after dorsal root crush has been reported to promote the growth of primary sensory axons into the ascending spinal white matter tracts (Oudega and Hagg, 1999). In contrast, others have found that continuous intrathecal infusion of BDNF does not enhance growth of primary sensory axons through the dorsal root entry zone, after dorsal root crush (Ramer et al., 2000).

Neurotrophin-3 (NT-3/NTF3)

NT-3 is both a survival and neurite-outgrowth inducing factor of neural crest and placode-derived neurons (Kalcheim et al., 1992). It also suppresses myelination within developing peripheral nerves, acting as an inhibitory modulator through the trkC receptor; myelination commences as expression of NT-3 declines (Cosgaya et al., 2002). NT-3 null mutant mice exhibit severe neurological and cardiac abnormalities, and die perinatally (Ernfors et al., 1994; Tessarollo et al., 1994; Donovan et al., 1996).

Subpopulations of primary sensory and sympathetic neurons were absent in the homozygous mutant. In fact, proprioceptive neurons, muscle spindles and Golgi tendon organs could not be found. Interestingly, in the heterozygote, muscle spindles were present at half the number found in wild-type controls; this is suggestive of a gene dosage effect (Ernfors et al., 1994). The causes of lethality in the homozygous mutant are the gross anatomical and functional abnormalities that it fosters in the development of the heart (Donovan et al., 1996). These include atrial and ventricular septal defects, and tetralogy of Fallot. This phenotype is compatible with a lack of survival or migration of cardiac neural crest cells.

NT-3 exhibits a very restricted pattern of expression in the adult brain; transcripts are primarily detected in the CA1 and CA2 neurons of the hippocampus (Ernfors et al., 1990). NT-3 mRNA is not detectable in adult spinal cord, either before or after compression or complete transection of the thoracic spinal cord (Widenfalk et al., 2001).

Importantly, NT-3 is the only neurotrophic factor that has to date been shown to promote the growth of injured corticospinal axons (Schnell et al., 1994; Grill et al., 1997). Also, it has also been shown to promote the ingrowth of primary sensory fibres after dorsal root crush (Oudega and Hagg, 1999).

Other Neurotrophins (NT-4/5, NT-6, and NT-7)

NT-4/5 has not been extensively studied, but is known to be widely expressed in the adult rodent CNS (Timmusk et al., 1993). It is also strongly upregulated in the distal stump of transected peripheral nerve at two weeks post injury (Funakoshi et al., 1993). NT-6 was isolated from *Xiphophorus* (Gotz et al., 1994), and NT-7 from both *Danio rerio* and *Cyprinus carpio* (Nilsson et al., 1998; Lai et al., 1998), but no mammalian orthologs of these family members have yet been identified.

High-Affinity Neurotrophin Receptors

Neurotrophin signaling occurs through three distinct tyrosine kinase receptors (Trks), the so-called high-affinity neurotrophin receptors. NGF binds to TrkA (Kaplan et al., 1991;

Klein et al., 1991a), BDNF to TrkB (Klein et al., 1991b), and NT-3 to TrkC (Lamballe et al., 1991); however, the latter exhibits some promiscuity. The dissociation constants of these receptor-ligand interactions are in the order of 10^{-11}nM, consistent with slow-on slow-off kinetics. However, all of these neurotrophins are also capable of binding the low-affinity neurotrophin receptor, $p75^{NTR}$.

TrkA

TrkA is a receptor for NGF (Kaplan et al., 1991; Klein et al., 1991a), as well as NT3 (Cordon-Cardo et al., 1991). However, $p75^{NTR}$ can form a receptor complex with trkA to increase the binding affinity for NGF, and also potentiate signal transduction (Hempstead et al., 1991). Ligand binding initially effects signal transduction by enhancing the phosphorylation of certain tyrosine residues within the intracellular domain of the Trk receptor; this mechanism is true for TrkA, B and C. Mutations in the *trkA* gene have been linked to congenital insensitivity to pain with anhidrosis (CIPA)(Smeyne et al., 1994; Indo et al., 1996; Mardy et al., 1999), and it has, therefore, been implicated in the anatomical and physiological development of neurons within the nociceptive and thermoregulatory circuits.

TrkB

Both BDNF and NT3, but not NGF, bind to TrkB (Squinto et al., 1991; Klein et al., 1991b). Using conditional knockouts, it has been revealed that TrkB is essential to the development of synaptic specializations of inhibitory GABAergic neurons in cerebellum (Rico et al., 2002), and that its absence in neurons of the forebrain results in impaired synaptic strengthening in complex learning tasks (Minichiello et al., 1999). The latter finding is indicative of an important role in synaptic plasticity and long-term potentiation.

TrkC

Cosgaya et al. (2002) found that $p75^{NTR}$ and TrkC have opposite effects on myelination in the peripheral nervous system: BDNF acts through $p75^{NTR}$ to enhance the process, whilst NT-3 acts through TrkC to inhibit it. Throughout myelination, the levels of expression of TrkC and $p75^{NTR}$ remain constant; however, the level of NT-3 gradually

diminishes, and the ongoing stimulation of $p75^{NTR}$ by BDNF prevails in its induction of the process. On completion of myelination, both neurotrophins and their respective receptors are downregulated.

The Low-Affinity Neurotrophin Receptor ($p75^{NTR}$/NGFR/TNFR16)

$p75^{NTR}$ is a member of the tumour necrosis factor receptor superfamily. Two isoforms of $p75^{NTR}$ are known to exist *in vivo*, both of which localize to the cell membrane. The full-length protein contains a 28αα signal peptide, four extracellular cysteine-rich repeat domains, a serine/threonine-rich region, a single transmembrane domain, and a 155αα cytoplasmic domain (Johnson et al., 1986). In comparison, the short-form lacks three of the four extracellular cysteine-rich repeat domains, but shares identical transmembrane and intracellular regions to the full-length form. The short-form is incapable of binding neurotrophins.

The uncleaved precursor to NGF (proNGF) binds to $p75^{NTR}$ with higher affinity than the mature cleaved form, whilst the opposite is true for binding to TrkA. Since the nature of the biological activity of the neurotrophins is dependent on their receptor interactions, it is clear that the extent of proteolysis of pro-neurotrophins in an important factor when considering the role of these proteins in any given context. Importantly, the binding affinity and selectivity of each of the neurotrophins to their preferred Trk receptor is enhanced with synergistic binding to $p75^{NTR}$ (Hempstead et al., 1991; Bibel et al., 1999). In addition to the neurotrophins, $p75^{NTR}$ has also been found to bind numerous other proteins including prion protein (Della-Bianca et al., 2001), the Aβ-peptide of amyloid precursor protein (Yaar et al., 1997), an envelope glycoprotein of the rabies virus (Tuffereau et al., 1998), and most recently Nogo receptor (Wong et al., 2002; Wang et al., 2002a), LINGO-1 (Mi et al., 2004), and Sortilin (Nykjaer et al., 2004).

$p75^{NTR}$ has been implicated in extraordinarily diverse biological processes including the induction of apoptosis and, paradoxically, the promotion of cell survival. In order to achieve these opposing effects, differential activation of intracellular signaling pathways is necessary. $p75^{NTR}$-dependent apoptosis occurs in response to proNGF binding, and

leads to the activation of nuclear factor kappa β (Carter et al., 1996). However, it has very recently been demonstrated that a $p75^{NTR}$ co-receptor, Sortilin, is necessary for the mediation of this response to proNGF binding (Nykjaer et al., 2004). The apoptosis of oligodendrocytes, following CNS injury, has been correlated with the expression of proNGF (Beattie et al., 2002). Similarly, corticospinal neurons, which express $p75^{NTR}$ soon after brain injury, also undergo proNGF induced $p75^{NTR}$-dependent cell death (Harrington et al., 2004). However, the expression of Sortilin in either the intact or injured nervous system has yet to be reported.

$p75^{NTR}$ also plays an important role in axonal growth through its interaction with Rho GTPase. It has been found that neurotrophin signaling through $p75^{NTR}$ decreases Rho activation (Yamashita et al., 1999). Conversely, ligand-bound Nogo Receptor signaling through $p75^{NTR}$ results in a strengthened interaction with the Rho-GDP dissociation inhibitor α (Rho-GDIα) and the subsequent activation of Rho GTPase (Yamashita and Tohyama, 2003). Likewise, the ganglioside receptor for MAG, GT1b, may also signal through $p75^{NTR}$ to increase Rho activation in a similar manner (Yamashita et al., 2002).

There are two different reported strains of $p75^{NTR}$ null mutant mice. One lacks exon 3 (Lee et al., 1992), and the other exon 4 (von Schack et al., 2001). Unfortunately, there are complications with both of these strains (reviewed by Barker, 2004). The $p75^{NTR}$ exon 3 null mutant has been reported to express a splice variant lacking the cysteine-repeat domains 2-4 (von Schack et al., 2001), and the $p75^{NTR}$ exon 4 null mutant continues to express a fragment of $p75^{NTR}$ which is capable of activating $p75^{NTR}$ signaling pathways (Paul et al., 2004). The $p75^{NTR}$ exon 3 null mutant mice were viable and fertile, but exhibited deficits in sensory and sympathetic innervation (Lee et al., 1992; Lee et al., 1994). In contrast, the mutant mice, with a deletion of exon 4, possessed a more severe phenotype with extensive developmental abnormalities in both the nervous system and vasculature (von Schack et al., 2001). Furthermore, the mutation proved lethal in up to 40% of homozygous knockouts. It is perhaps not surprising that experiments aimed at assessing the effect on axonal regeneration in these mutant animals have produced conflicting findings in various experimental models (Walsh et al., 1999;

Boyd and Gordon, 2001; Gschwendtner et al., 2003; Song et al., 2004). These are difficult to interpret in the light of what has been learned about the artifactual gene products in the respective strains.

Myelin-Mediated Inhibition of CNS Axonal Regeneration

The hypothesis that CNS myelin breakdown products were involved in the prevention of axonal regeneration in adult mammals was first posited by Berry (1982). He pointed out that non-myelinated axons in the CNS would regenerate after chemical ablation that did not damage nearby myelinated fibres, but not after mechanical axotomy, which always damaged some myelinated axons. Since damage to myelinated tracts resulted in the degeneration of myelin, he hypothesized that degeneration products of CNS myelin were inhibitory to axonal growth. Subsequently the ability of CNS myelin to inhibit neurite outgrowth was studied in detail by Schwab and Caroni.

NOGO

In a series of landmark papers Schwab and Caroni demonstrated that CNS myelin and oligodendrocytes were non-permissive to axonal growth (Schwab and Caroni, 1988; Caroni et al., 1988) and they extracted from CNS myelin, proteins of ~250kDa and ~35kDa that were both potent inhibitors of neurite outgrowth from both neonatal superior cervical ganglion cells and dorsal root ganglion cells. These proteins were termed NI-35 and NI-250 (Caroni and Schwab, 1988b). A monoclonal antibody IN-1, raised against NI-250, reacted with both NI-250 and NI-35 and blocked the inhibitory activity of these protein fractions and of myelin (Caroni and Schwab, 1988a). Unfortunately, the epitopes recognized by IN-1 have not been published and some doubt remains about the molecules with which it reacts (Fournier et al., 2002). IN-1 was subsequently used to induce regeneration of injured CNS axons *in vivo* (Schnell and Schwab, 1993; Schnell et al., 1994). Schwab's group eventually succeeded in microsequencing six peptides originating from the bovine homolog of NI-250, bNI220 (Spillmann et al., 1998) and subsequently used this information to search databases of mammalian genes and expressed sequence tags (ESTs), in order to identify a full-length mammalian form of the gene, incorporating all six homologous peptide sequences, which was termed *nogo* (Chen

et al., 2000). At the same time, the *nogo* gene was independently identified by two other groups (Grandpre et al., 2000; Prinjha et al., 2000). Recently, a leucine-rich, glycosylphosphatidylinositol (GPI) -linked cell surface protein of 473 amino acids has been identified as a receptor to Nogo (NgR) (Fournier et al., 2001). This molecule binds the Nogo-66 loop of the Nogo family of proteins with high affinity and its expression has been shown to be sufficient to confer sensitivity to Nogo-66 on otherwise insensitive cells (Fournier et al., 2001). Whilst it is clear that other powerful inhibitors of neurite outgrowth are present in the injured CNS (Dou and Levine, 1994; Canning et al., 1996; Davies et al., 1999; Zhang et al., 2001; Pasterkamp et al., 2001), investigations of NgR and its interactions have for the first time clearly elucidated the mechanisms limiting the sprouting and regeneration of some axons in the adult mammalian CNS.

The Nogo Gene

The human *nogo* gene has been localized to chromosome 2p13-14 by radiation hybrid mapping (Yang et al., 2000). Using crude *in silica* genomic mapping of the cDNA sequences of Nogo isoforms, it was found that the gene comprises at least 11 exons (Fig. 1.1) and putatively gives rise to at least seven different proteins by splice variation (Chapter 3; Hunt et al., 2002b) (Table 1.1). However, a detailed analysis of human and mouse *nogo* gene structure (Oertle et al., 2003a), in which 5′ capsite RACE PCR was undertaken to identify transcription start sites, revealed that the human gene is composed of 14 exons whereas the mouse gene is only composed of 11. The additional human exons were found to be redundant since they are spliced into mature mRNA transcripts to encode 5′ untranslated region (UTR); all of the mRNA isoforms, incorporating the newly discovered exons (termed 1D, 1F, and 1G), give rise to the same protein, Rtn-T (note that isoforms incorporating 1Aa and 1Ab also give rise to Rtn-T; however, these are not considered whole exons in their own right and are thought to form a single exon in conjunction with 1A). None of the transcripts incorporating exon 1D, 1F or 1G have been identified *in vivo* (Oertle et al., 2003a).

Nogo Protein

Nogo (RTN4) is a member of the Reticulon family of genes (the others being RTN1-3) - so called because their protein products are largely retained in the endoplasmic reticulum of cells. A conserved 3′ sequence is present in all forms of Nogo transcript and gives rise to the reticulon-type amino acid sequence. Interestingly, the Nogo-66 domain, which interacts with the Nogo receptor to cause growth cone collapse, is translated from this conserved region. Nogo also has a novel 5′ sequence where transcript variation arises through alternative splicing.

Of the seven different isoforms that are believed to arise from the *nogo* gene (Chapter 3; Hunt et al., 2002b; Oertle et al., 2003a), only three of these - termed Nogo-A, -B and -C (Fig. 1.2.), respectively – have been considered major isoforms expressed in the adult nervous system. Rtn-T is expressed in the testes (Zhou et al., 2002). The minor transcripts – none of which are referred to as Nogo - all have properly aligned open reading frames, but there is not yet any experimental evidence that the proteins corresponding to the minor transcripts are expressed *in vivo*.

Human Nogo-A, -B and -C proteins are 1192 amino acids (αα), 373 αα and 199 αα in length, respectively. Nogo-A appears as ~190-250kDa band after denaturing SDS-PAGE, whereas Nogo-B and -C appear as ~55kDa and ~25kDa bands, respectively. Their conformation (i.e. which parts of the molecule are likely to be exposed at the surface of cells) has considerable significance for their role as inhibitors of axonal regeneration but is still not entirely clear, particularly in the case of Nogo-A. Analysis of the primary sequence of Nogo-A, -B and-C reveals that none of the isoforms possesses an amino terminal signal sequence which would cause the protein to be directed towards the cell surface, whereas all forms of Nogo exhibit a dilysine endoplasmic reticulum (ER) retention signal (-KRKAE) within the conserved carboxy terminus (Hunt et al., 2002a).

Chen et al. (2000) reported that Nogo-A has seven N-glycosylation sites and many potential O-glycosylation sites. Glycosylation would be expected to be limited to cell surface molecules. However, whilst it is true that Nogo-A has multiple potential O-

glycosylation sites, and seven potential N-glycosylation sites, it should be noted that only five of the asparagine residues are positively predicted to bear N-glycosylations and, more importantly, because the protein lacks N-terminal signal sequence it will not necessarily be processed by the N-glycosylation machinery. The number of transmembrane domains determines which parts of Nogo are likely to be exposed at the cell surface and, therefore, available for interactions with receptors on other cells. Two transmembrane domains are strongly predicted within the conserved C-terminus of Nogo. Furthermore, it is generally accepted that Nogo assumes a topology such that the two most strongly predicted transmembrane domains are separated by the 66-residue extracellular or lumenal loop, called Nogo-66 (Grandpre et al., 2000; Chen et al., 2000; Prinjha et al., 2000). Nogo-66 has a specialized role in causing growth cone collapse (Fournier et al., 2001). Therefore, it is not surprising that recombinant Nogo-A and Nogo-C, which both contain the conserved Nogo-66 loop, have both been reported to cause growth cone collapse (Grandpre et al., 2000). The Nogo-A specific N-terminal sequence inhibits neurite outgrowth, and also prevents fibroblast spreading (Fournier et al., 2001). The active region is believed to be located in the middle of the Nogo-A specific domain (Prinjha et al., 2002). Whether the so-called Nogo-A specific domain passes through the cell membrane to have an extracellular domain is more contentious, but is of considerable significance for its availability to the growth cones of regenerating neurons. It is worth noting that Nogo-A does have a weakly predicted transmembrane domain in its unique amino terminal sequence (Hunt et al., 2002a).

Another feature thought to be present in both Nogo-A and -B is a proline-rich region (Hunt et al., 2002a), which would be a good candidate for involvement in interactions with other proteins (Kay et al., 2000). In addition, Oertle et al (2003) have recently identified consensus sequences for PEST domains (which can lead to rapid degradation of protein), SH3-ligands and WW-ligands (both involved in protein-protein interactions) within the so-called Nogo-A specific domain. Nonetheless, Nogo does not have the domain architecture of a conventional receptor protein.

Is Nogo Present at the Cell Surface?

Unless Nogo reaches the surface of cells, it is unlikely to be involved in growth cone collapse in non-degenerating tissue. The presence of a C-terminal dilysine ER retention signal (-KRKAE) does not mean that all of the protein is necessarily retained in the ER. There is growing evidence to show that proteins bearing such sequences are able to overcome their ER retention signals to reach the cell surface, despite also lacking a N-terminal signal sequence. As pointed out by (Chen et al., 2000), the myelin proteins PMP-22 and MAL also possess ER retention signal sequences and yet are able to reach the cell surface. The immunocytochemical identification of Nogo-A in oligodendrocyte membranes in white matter (Huber et al., 2002; Wang et al., 2002c) confirms that the molecule can be found at the surface of these cells, although much is likely to be retained in the ER. Of particular interest, is the finding that recombinant Nogo-A, and -B are always retained in the ER when transfected into COS cells (Grandpre et al., 2000; Chen et al., 2000). This suggests that there must be some cell-specific activity in the regulation of Nogo transport, at least in oligodendrocytes, perhaps involving the formation of complexes with other proteins that are targeted to the cell surface. Recently, (Pot et al., 2002) reported that axonal regeneration was inhibited in the peripheral nerves of transgenic mice expressing Nogo-A under the control of a P0 promoter. The significance of this study is that it is the first to demonstrate that Nogo-A is inhibitory to axonal regeneration *in vivo*, and that recombinant Nogo-A made by Schwann cells can become available to receptors on regenerating axons.

The Effects of Antibodies to Nogo on Axonal Regeneration In Vivo

The best evidence that Nogo is involved in limiting axonal regeneration *in vivo* comes from experiments with function-blocking antibodies, particularly IN-1 and its derivatives (Caroni & Schwab, 1988b; Rubin et al., 1994), produced by Schwab's laboratory. Most of these experiments involve the corticospinal tracts, whose cell bodies contain very high levels of mRNAs for *ngr*, *nogo-66* and *nogo-a* (Chapters 3 and 4; Hunt et al., 2002; Hunt et al., 2003). Also, most of these studies use antibodies produced by hybridomas implanted into the cerebral hemispheres and in every case the antibodies may have had access to the cell bodies as well as the growth cones of the corticospinal neurons. The

first such study (Schnell and Schwab, 1990) used a model in which the midthoracic spinal cord of young rats was injured, the dorsal and dorsolateral parts of the spinal cord being severed. The small ventral tract was presumably intact. Regenerating corticospinal axons were found up to 2.6 mm distal to the lesion in controls but up to 11 mm distal in IN-1 treated animals. Such axons were mainly in the position of the former corticospinal tract. The effects of IN-1 were later shown to be enhanced by implantation of foetal spinal cord at the lesion site (Schnell and Schwab, 1993) and more strongly enhanced by NT-3 treatment (Schnell et al., 1994) which led to axons apparently regenerating up to 20mm beyond the lesion. IN-1 treatment was subsequently shown to improve functional recovery after such lesions (Bregman et al., 1995), but both the effects on regeneration and on functional recovery were reduced if treatment was delayed until 8 weeks after lesioning (von Meyenburg et al., 1998). IN-1 also stimulated regeneration of corticospinal axons following pyramidotomy (Raineteau et al., 1999). In the later studies the regenerating axons were often found in the ascending dorsal columns, lateral columns and grey matter, rather than the former corticospinal tract. Although the partial lesion models used in these studies do not rule out the possibility that axons beyond the lesion are spared fibres or their sprouts (effects on collateral sprouting have been increasingly emphasized as the basis of functional recovery in studies using IN-1 *in vivo*- see below), the weight of evidence strongly suggests IN-1 can stimulate the regeneration of some corticospinal axons, mainly through intact tissue around incomplete transection lesions. It remains to be seen whether regenerated axons are responsible for any part of the functional recovery achieved by IN-1 treatment, and whether the antibody is effective following complete transections of the spinal cord or compression and contusion injuries which closely mimic the lesions found most often in man.

IN-1 has also shown effects on the regeneration of other types of CNS axon. First, it was shown that IN-1 treatment (via implanted hybridoma cells) increased the number of regenerating septohippocampal axons which re-entered the hippocampus following removal of the fimbria/fornix (Cadelli and Schwab, 1991). The axons in IN-1 treated animals grew for about 1.5- 4 mm in the hippocampus, significantly further than in control animals. However, the identification of the axons by cholinesterase staining, as

opposed to anterograde tracing, leaves some doubt about their origin. Septal nuclei are rare examples of neurons thought to regenerate in response to IN-1 although expressing very low levels of *ngr* mRNA (Chapter 3). It was subsequently shown that IN-1 together with BDNF increased regeneration in the visual pathway (after freeze/crush lesions of the intracranial optic nerve) of young rats (Weibel et al., 1994). However, the distance beyond the lesions at which regenerating axons were detected was only about 1.5 mm. Retinal ganglion cells in adult rats show strong *ngr* mRNA expression (Fournier et al., 2001; Hunt et al., 2002; Wang et al., 2002a). IN-1 has also been shown to enhance the regeneration of the central processes of spiral ganglion neurons in the CNS tissue of the auditory nerve, and to produce some functional recovery (Tatagiba et al., 2002). Once again, the number of axons regenerating was a small percentage of those injured and the distance the axons regenerated was limited to 1.5mm, although this allowed some to enter their former target nuclei. It is notable that some regeneration of the auditory axons beyond the lesion was seen even without IN-1 treatment.

Regeneration of the central processes of primary afferent (DRG) neurons *in vivo* does not seem to be affected by IN-1 (Oudega et al., 2000). The model used involved a peripheral nerve graft in the thoracic spinal cord (which is readily invaded by ascending dorsal column axons in animals with a conditioning sciatic nerve injury), so that the issue addressed was whether IN-1 could promote regeneration of the sensory axons from the graft into the rostral spinal cord. This did not happen. Most DRG neurons express *nogo* (Josephson et al., 2001; Huber et al., 2002; Hunt et al., 2002) but only a minority express *ngr* mRNA (Hunt et al., 2002; Josephson et al., 2002). Thus, although Nogo expression is widespread on both neurons and glia, the major effects of IN-1 on axonal regeneration *in vivo* appear to be on neurons which express NgR. However IN-1 does promote the regeneration of neonatal DRG neurons into CNS tissue (optic nerves) *in vitro* (Chen et al., 2000).

IN-1 and Axonal Sprouting

IN-1 has significant effects *in vivo*, other than on axon regeneration: it enhances the sprouting of some intact and injured axons and increases the expression of growth

associated genes by some neurons. Axonal regeneration implies the regrowth of an injured axon, usually in the general direction of its original projection. Sprouting involves the growth of branches from an axon, either injured or intact, but not the growth of such branches to a distant site. Obviously, for injured axons, axonal sprouting is a necessary precursor of regeneration. One of the most significant observations on the effects of IN-1 *in vivo* is that it increases sprouting rostral to lesions of corticofugal fibres, including ipsilateral corticobulbar and corticospinal axons rostral to a unilateral pyramidotomy, contralateral corticospinal axons caudal to a pyramidotomy (Bareyre et al., 2002) and corticostriate axons (Kartje et al., 1999). All of these fibres arise from neocortical neurons which strongly express NgR and Nogo-A (Chapters 3 and 4). Sprouting of corticospinal axons into abnormal territories was even observed in animals without axotomy (Bareyre et al., 2002). In the case of unilateral pyramidectomy, the recovery of function following IN-1 treatment was not abolished by relesioning the pyramid 1mm rostral to the original injury (Z'Graggen et al., 1998). Clearly, IN-1 induced plasticity, as opposed to regeneration, may be responsible for most of the effects of the antibody on functional recovery. Furthermore, IN-1 treatment increased the density of monoaminergic fibres in the spinal cord caudal to the lesions (Bregman et al., 1995; Bareyre et al., 2002). Serotonin has been shown to have important functions in motor control (Gerin et al., 1995; Nishimaru et al., 2000; Slawinska et al., 2000; Hains et al., 2001). In the cerebellum, IN-1 induces sprouting of uninjured Purkinje cell axons, within the cortical grey matter (Buffo et al., 2000). Together, these observations suggest that the control of axonal sprouting is an important physiological function of the molecule(s) detected by the IN-1 antibody.

IN-1 and the Control of Growth-Associated Gene Expression

Purkinje cells are renowned for their lack of response to axotomy (Rossi et al., 2001), and axotomized Purkinje cells upregulate very few of the growth-associated genes that are expressed in neurons that can successfully regenerate axons (Zagrebelsky et al., 1998; Chaisuksunt et al., 2000). Application of IN-1 to the cerebellum brings about upregulation in both intact and axotomized Purkinje cells of some genes normally associated with injury and regeneration in other cells, including the transcription factors

c-jun, P-Jun and JunD, and NADPH diaphorase (Zagrebelsky et al., 1998). Interestingly, granule cells were unaffected by IN-1, although they express NgR (but not Nogo) at least as strongly as Purkinje cells. IN-1 increased *gap-43* mRNA and protein in the spinal cord of rats (Bareyre et al., 2002), although it is not clear which neurons were affected. Spinal cord neurons express NgR weakly or not at all, but many express Nogo-66 strongly (Chapter 3; Hunt et al., 2002).

OLIGODENDROCYTE MYELIN GLYCOPROTEIN

Oligodendrocyte myelin glycoprotein (OMgp) is a GPI-linked CNS myelin protein which has also been shown to induce growth cone collapse and inhibit neurite outgrowth (Kottis et al., 2002; Wang et al., 2002b). OMgp was the first major peanut agglutinin-binding protein of adult human CNS white matter to be identified, more than a decade ago (Mikol and Stefansson, 1988). Its gene is one of three located on the reverse strand within the first intron of the neurofibromin gene (Viskochil et al., 1991), the others being EVI2A and EVI2B. A translocation event within the neurofibromin gene gives rise to a mutant form of the neurofibromin protein, which is no longer able to suppress mitogenesis and allows the development of the disease, neurofibromatosis type 1. Because of the unusual gene structure, it was considered that OMgp and neurofibromin expression and function could be closely related (Viskochil et al., 1991). Subsequently, it was demonstrated that OMgp, like neurofibromin, acts as a suppressor of mitogenesis when expressed in 3T3 fibroblasts (Habib et al., 1998a), apparently by blocking intracellular signalling pathways from the activated PDGFα receptor. Recently, Wang et al., (2002b) screened proteins released from CNS myelin by phospholipase treatment (i.e. GPI-linked cell surface proteins) for the ability to inhibit neurite outgrowth. The only inhibitory protein identified in this screen was OMgp.

The OMgp Gene

The human *omgp* gene spans ~3.0kb of genomic DNA, and is located on chromosome 17q11.2. The *omgp* gene is comprised of two exons (Fig. 1.1.), with the intron being present in the 5′ untranslated region (Mikol et al., 1990a; Mikol et al., 1993).

OMgp Protein

Human OMgp consists of 440αα, has a molecular weight of approximately 110-120kDa after post-translational modifications and is held at the cell surface by a GPI linkage. It bears an N-terminal signal sequence and a C-terminal hydrophobic stretch of residues incorporating a potential cleavage site, consistent with being GPI anchored. The protein appears to consist of a cysteine-rich N-terminal LRR flanking domain, followed by five LLR domains. Additionally, there is a predicted threonine rich region spanning, where post-translational O-glycosylation is likely to occur. Mikol et al. (1990b) reported the differential addition of the HNK-1 carbohydrate moiety to OMgp, depending on the tissue from which it was derived. Curiously, the HNK-1 antigen is also found on MAG and is associated with the preferential regeneration of motor axons in peripheral nerves (see below) (Low et al., 1994; Martini et al., 1994).

MYELIN-ASSOCIATED GLYCOPROTEIN (MAG)

MAG (otherwise known as siglec 4a) is a transmembrane protein of the immunoglobulin superfamily, found in both PNS and CNS myelin (Martini, 1994), where it plays a role in the formation and maintenance of myelin sheaths (Fruttiger et al., 1995; Carenini et al., 1997; Fujita et al., 1998; Marcus et al., 2002). It was originally shown to promote neurite outgrowth from neonatal dorsal root ganglion (DRG) neurons, but was subsequently found to inhibit neurite growth from adult DRG cells, cerebellar granule cells and many other types of neuron (McKerracher et al., 1994; Mukhopadhyay et al., 1994). It should be noted, however, that MAG has been found to stimulate, rather than inhibit neurite outgrowth from E17 mouse spinal cord neurons (Turnley and Bartlett, 1998) and even from neonatal cerebellar neurons in one study (Shimizu-Okabe et al., 2001). It may be that the effects of MAG, and possibly other inhibitors of neurite outgrowth, depend on how cells are isolated and cultured. There is evidence that the levels of cyclic AMP in neurons modulate the responses to MAG and are reduced in neurons when they become sensitive to MAG (Cai et al., 2001). Cyclic AMP levels are likely to be sensitive to differences in culture techniques. Although MAG is generally recognized as a potent inhibitor of axonal growth *in vitro*, the MAG knockout mouse exhibits little or no enhancement of axonal regeneration in the spinal cord (Bartsch et al., 1995; but see also

Li et al., 1996). However, the slow-degenerating mutant mouse provides some evidence that MAG can be inhibitory to axonal regeneration *in vivo*: regeneration is enhanced in the sciatic nerves of these mice if the *mag* gene is inactivated (Schafer et al., 1996). As the name siglec suggests, MAG is a sialic acid binding protein, which means that it has the potential to bind to a variety of sialylated cell surface molecules. Gangliosides GD1a and GT1b have been implicated as putative receptors mediating the neurite-inhibiting properties of MAG, but the evidence remains somewhat contradictory (Vinson et al., 2001; Liu et al., 2002; Domeniconi et al., 2002; Vyas et al., 2002). It has been speculated that the MAG-induced clustering of gangliosides into lipid rafts could activate RhoA to inhibit neurite growth (McKerracher, 2002). The evidence that the Nogo-66 receptor is part of one functional receptor complex for MAG on neurons is strong (see below).

The MAG Gene

The human *mag* gene consists of 12 exons (Fig. 1.1.), spanning nearly 22kb of genomic DNA, and is located on chromosome 19q13.1. Splice variation generates two isoforms of the protein (Salzer et al., 1987). Variant 1 (L-MAG) is transcribed from 11 exons (1-10 and 12) and translates to a protein of 626αα. Variant 2 (S-MAG) encompasses all 12 exons but gives rise to a shorter protein, of 582αα, due to introduction of an in-frame stop codon in exon 11, thus rendering exon 12 part of the 3′ UTR in this transcript.

MAG Protein

There is considerable experimentally-derived documentation of the secondary structure and conserved functional domains of the two human variants of MAG. Essentially, both proteins are known to retain the same secondary structure and topology, notwithstanding the slight variation in the cytoplasmic carboxy terminus. Briefly, MAG is known to possess five regions of internal homology that give rise to five immunoglobulin-like domains within its extracellular amino-terminus (Salzer et al., 1987). Toward the carboxy terminus, in the region of ~510αα – ~530αα is a single transmembrane domain. This is succeeded by different cytoplasmic carboxy termini, which may give rise to functional diversity between isoforms. It has been suggested that the modulation of linked carbohydrate moieties might occur during development as a means of regulating

the function of MAG in myelinogenesis (Pedraza et al., 1991). There is also evidence that the HNK-1 carbohydrate is linked to MAG in a highly differential manner in Schwann cells supporting motor and sensory nerves of adult mammals (Low et al., 1994). HNK-1 has, however, been associated with the enhanced regeneration of motor axons rather than growth inhibition (Martini et al., 1992). A soluble form of MAG, capable of inhibiting neurite outgrowth from P6 DRG neurons, is released from damaged CNS myelin (Tang et al., 2001); soluble MAG constitutes the great majority of the neurite-outgrowth inhibiting influence released from such myelin, suggesting that the release of Nogo from the cell surface is negligible.

NOGO-66 RECEPTOR

The Nogo-66 receptor (NgR) is a common receptor mediating growth cone collapse in response to at least three myelin proteins. Fournier et al. (2001) discovered the Nogo-66 receptor by transfecting COS-7 cells with clones from a cDNA library from adult mouse brain and screening to detect which clones bound a Nogo-66 alkaline phosphatase (AP) fusion protein. NgR, a GPI-linked cell surface protein, was shown to be sufficient to impart sensitivity to Nogo to otherwise insensitive cells: retinal ganglion cells from E7 chick embryos, which are otherwise insensitive to the growth-cone collapsing effects of Nogo-66, were rendered susceptible to its activity after transduction with a virus expressing NgR. The dissociation constant (Kd) of the Nogo-66 interaction with NgR expressing COS cells was calculated as 5nM, suggesting that it represents a physiological interaction.

Two groups (Liu et al., 2002; Domeniconi et al., 2002) have independently reported that NgR is also a functional receptor for MAG. Liu et al. (2002) set out to identify co-receptors for NgR by screening COS cells transfected with clones from a cDNA library with an AP-NgR fusion protein. Of the ten clones which were found to bind AP-NgR, six of them were NgR itself. This suggests that NgR may self-associate at physiological concentrations, although the Kd for this interaction was subsequently determined as ≥50 nM (Liu et al., 2002). This is considerably weaker than NgR-ligand interactions. The remaining four clones were all identified as MAG. Immunoprecipitation studies showed

that NgR does indeed precipitate MAG. Furthermore, gain of function studies demonstrated that MAG at nanomolar concentrations is capable of inducing growth cone collapse in neurons transfected with NgR. Domeniconi et al. (2002) identified a ~80kDa neuronal membrane protein, which they had previously shown to bind MAG, as NgR. They showed that the removal of neuronal GPI-linked proteins from rat P4 cerebellar granule cells protected them against MAG-mediated inhibition of neurite outgrowth. A MAG-Fc fusion protein bound to CHO cells expressing NgR and an AP-NgR fusion protein was shown to bind to CHO cells expressing MAG. Using AP-NgR and either MAG-expressing Chinese hamster ovary (CHO) cells, or immobilized MAG-Fc, a Kd of 8nM was calculated for this interaction (cf. Liu et al (2002) who calculated a Kd of approximately 20nM for interactions between AP-MAG ectodomain and NgR expressing COS cells). MAG-Fc was able to precipitate NgR from various lysates. However, Niederost et al. (2002) have recently reported that cerebellar granule cells cultured on polylysine respond to both a Nogo-A peptide and MAG even after phospholipase treatment. It is not easy to reconcile these apparently conflicting results.

Wang et al. (2002b) showed that NgR was also a functional receptor that allowed OMgp to cause growth cone collapse. They screened an expression library and identified NgR as a high-affinity OMgp-binding protein. Cleavage of NgR and other GPI-linked proteins from the cell surface rendered axons of DRG neurons insensitive to OMgp, whereas introduction of exogenous NgR conferred OMgp responsiveness on otherwise insensitive neurons. A Kd of 5nM was calculated for the interaction of AP-OMgp with NgR-expressing COS-7 cells.

The NgR Gene

The human *ngr* gene consists of two exons (Fig. 1.1), spanning ~27kb, on chromosome 22q11. There is no evidence of splice variation within this gene.

NgR Protein

Human NgR is a GPI-linked protein, of 473αα, detectable as a ~85kDa band following denaturing SDS-PAGE. NgR contains an N-terminal cysteine-rich LRR domain

(LRR-NT), followed by 8 LRR domains (the first of which is incomplete), and a C-terminal cysteine-rich LRR domain (LRR-CT). Wang et al. (2002b) deleted parts of the NgR molecule to identify regions important for interactions with Nogo-66 and OMgp. The LRR and LRR-CT domains of NgR were required for binding of OMgp, but the LRR-CT domain was both required and sufficient for binding of Nogo-66. Nonetheless, the OMgp and Nogo-66 competed to occupy their overlapping binding sites. However, Fournier et al. (2002) have provided evidence that all of the LRR domains as well as the LRR-CT and LRR-NT domains in NgR are apparently required for Nogo-66 binding. They also report that the unique C-terminal sequence is required for signal transduction, perhaps being involved in direct interactions with co-receptors, and that the GPI linkage facilitates efficient signal transduction. The GPI linkage apparently directs NgR to become localized in caveolin-positive lipid rafts.

MAG also competes with Nogo-66 for binding to NgR (Domeniconi et al., 2002), but the regions in NgR required for binding MAG have not yet been examined by domain deletion analysis. The competitive binding suggests that at least part of the LRR-CT domain of NgR required for Nogo-66 binding is also necessary for the binding of MAG. However, this speculation is complicated by the fact that the NgR antagonist peptide NEP1-40 (which competitively inhibits Nogo-66 binding and blocks growth cone collapse), does not compete with MAG (Liu et al., 2002). NEP1-40 corresponds to residues 1-40 of the Nogo-66 loop (and might better be thought of as Nogo-40). The most likely explanation for the absence of competition between MAG and NEP1-40 is that MAG competes for the active site on NgR which also recognises residues 41-66 of Nogo-66.

NgR Co-Receptors

$p75^{NTR}$

Since NgR is a GPI-anchored cell surface protein, it is incapable of transmembrane signal transduction. Therefore, it must interact with at least one other protein, a signal-transducing co-receptor. The first evidence that $p75^{NTR}$ could potentially be a co-receptor for NgR came from the work of Yamashita et al. (2002), who demonstrated that $p75^{NTR}$

was necessary for MAG-induced inhibition of neurite outgrowth from adult DRG neurons and postnatal cerebellar granule cells. Shortly thereafter, two groups reported that $p75^{NTR}$ could indeed function as a signal-transducing co-receptor for NgR (Wong et al., 2002; Wang et al., 2002a). The $p75^{NTR}$ signalling was shown to occur in response to NgR binding of Nogo-66, MAG or OMgp (Wang et al., 2002a). All regions of the NgR protein from the LRR-NT domain to the unique C-terminal region are necessary for binding $p75^{NTR}$.

The $p75^{NTR}$ null mutant mouse has now become a prime target for regeneration experiments. However, as described earlier, there is some doubt as to whether the two different strains of $p75^{NTR}$ null mutant mouse are complete knockouts. Nonetheless, an interesting study of the ability of axons to sprout in the CNS of one of these strains of animal was published before the relationship between $p75^{NTR}$ and NgR was known (Walsh et al., 1999). Transgenic mice were generated in which NGF was expressed by astrocytes in the CNS under the control of the GFAP promoter. Sympathetic axons sprouted into the brains of the mice, but many more axons grew into the brain if the *$p75^{NTR}$* gene was inactivated. It is particularly interesting that the sympathetic axons which sprouted into the brain were predominantly found in the white matter. It is not yet clear whether the sympathetic neurons which sprouted into the CNS expressed NgR. An intriguing possibility is that high concentrations of neurotrophins, which promote axonal sprouting and limited regeneration in the CNS (Zhang et al., 1998; Bradbury et al., 1999; Walsh et al., 1999), may act via neurotrophin-$p75^{NTR}$ interactions that block NgR signalling, rather than through the high affinity (trk) receptors. Neurotrophin binding to $p75^{NTR}$ is known to reduce its ability to activate RhoA (Yamashita et al., 1999). Alternatively, Trks activated by neurotrophin binding may sequester $p75^{NTR}$, thus effectively inactivating NgR. The structure and biological functions in the nervous system of $p75^{NTR}$ have been reviewed recently by Dechant and Barde (2002). A reason for caution in the interpretation of the role of $p75^{NTR}$ in NgR signalling is that $p75^{NTR}$ is differentially expressed by neurons. For example, it is difficult to detect on some classes of neurons, e.g. thalamic reticular nucleus neurons (Vaudano et al., 1998) and most neostriatal neurons (Sobreviela et al., 1994); its expression by other neurons is disputed,

e.g. adult retinal ganglion cells (Hirsch et al., 2000; Ding et al., 2001; but see also Sheedlo et al., 2002); and on DRG neurons there is a complete spectrum of strengths of $p75^{NTR}$ expression (Verge et al., 1992). It may be significant, however, that $p75^{NTR}$ is upregulated by several types of intrinsic CNS neurons after injury, including corticospinal neurons (Giehl, 2001) and Purkinje cells (Vaudano et al., 1998), neither of which has the capacity to regenerate axons into nerve grafts (Anderson et al., 1998).

LINGO-1

Recently, LINGO-1, a transmembrane LRR-containing protein, was also identified as being necessary for NgR signalling (Mi et al., 2004). The authors found that LINGO-1 co-immunoprecipitated with NgR and $p75^{NTR}$, and that the expression of all three proteins was necessary, in COS cells, for the activation of RhoA by Nogo-66, MAG or OMgp. Of course, this does not necessarily mean that the same is true of neurons.

Analysis of the tissue expression profile of LINGO-1, by northern blot, revealed that the transcript was restricted to nervous system tissue. RT-PCR of embryonic and postnatal rat brain demonstrated that LINGO-1 expression peaked at P1, and decreased thereafter. By *in situ* hybridisation, it was found that LINGO-1 transcript expression was confined to neurons within the nervous system. Likewise, immunohistochemistry was used to show that the protein was purely neuronal, and that in the cerebellum LINGO-1 is highly expressed in early postnatal cerebellar granule neurons, but that in adulthood it is predominantly expressed by Purkinje cells. Interestingly, 10 days after spinal cord injury in adult rats, LINGO-1 protein was detected in the injured descending axonal tracts rostral to the lesion. Also, RT-PCR of injured spinal cord tissue revealed a five-fold increase in LINGO-1 mRNA levels, 14 days post injury. There is only one other report of the expression pattern of LINGO-1 (aka LERN1) in the adult nervous system (Carim-Todd et al., 2003), which is broadly in agreement with the report of Mi et al. (2004). In this study, it was shown by *in situ* hybridisation, immunohistochemistry and northern blot of adult rat brain that LINGO-1 expression was largely restricted to neurons within the neocortex and limbic system, that very little expression was present in cerebellum, and that none was detectable in intact spinal cord.

NgR is not the Only Receptor for Nogo-A and MAG

NgR should be an important target for manipulations aimed at improving axonal sprouting and regeneration in the CNS, at least in the case of cortical projection neurons which express NgR strongly. Nonetheless, there is evidence that functional cellular receptors other than NgR exist for these axonal-growth inhibitory molecules. The interactions of MAG with gangliosides have been claimed to mediate the inhibition of neurite outgrowth (Vinson et al., 2001; Vyas et al., 2002; but see also Domeniconi et al., 2002), and MAG has trophic effects on oligodendrocytes (Gard et al., 1996), which have not yet been shown to express NgR. Of course, the other MAG receptors may mediate functions unrelated to growth cone collapse. The N– terminal region of Nogo-A, which does not bind to NgR, also has the ability to inhibit neurite outgrowth, as well as preventing the spreading of other types of cell (Grandpre et al., 2000; Fournier et al., 2001; Niederost et al., 2002; Prinjha et al., 2002). Presumably this is mediated by another receptor, which must be widely expressed. The possibility that gangliosides may also act as receptors for Nogo-A would explain why screening of expression libraries has so far failed to identify a receptor protein. Niederost et al. (2002) claim that phospholipase treatment, to remove NgR and other GPI-linked cell surface molecules, does not block all the inhibitory effects of Nogo-A or MAG on neurite outgrowth from cerebellar granule cells grown on polylysine (but the result for MAG contrasts markedly with the findings of Domeniconi et al. (2002) and Liu et al., (2002).

NgR Signalling

The first experiments on the intracellular signalling pathways involved in growth cone collapse in response to Nogo indicated that calcium release from intracellular stores was a critical factor (Bandtlow et al., 1993). MAG also induces a rise in intracellular calcium levels in neuronal growth cones (Wong et al., 2002). However, it is not clear whether these responses were mediated by NgR, since both Nogo and MAG may have additional receptors. More recently it has become widely accepted that pathways leading to growth cone collapse in response to CNS myelin converge on (activating) the RhoA GTPase (Lehmann et al., 1999; Dergham et al., 2002), and that some point on the pathway is susceptible to cyclic AMP levels (Cai et al., 1999; Cai et al., 2001; Cai et al., 2002).

Inhibition of Rac1, which has antagonistic effects on the cytoskeleton to RhoA, may also play a part in growth cone collapse (Niederost et al., 2002). How such pathways can be made compatible with a calcium response is not clear.

NgR Paralogs

Recently, three groups have reported the cloning of two paralogs of NgR, appropriately termed NgR2 and NgR3 (Pignot et al., 2003; Barton et al., 2003; Lauren et al., 2003). The expression profiles of these two paralogs are remarkably similar to that of NgR and, although their function remains unknown, it would not be surprising if they were found to be implicated in the failure of CNS axonal regeneration. However, the issue of whether the ligands of NgR also bind the NgR paralogs remains contentious; two groups have so far failed to demonstrate that Nogo-66, MAG or OMgp serve as ligands for either of the two paralogs (Pignot et al., 2003; Barton et al., 2003), but another group has recently presented data indicating that NgR2 binds MAG with greater affinity than NgR (Venkatesh et al., 2003). In addition, their data suggest that NgR2 does not bind to Nogo-66 or OMgp, but does to bind the NgR signal-transducing co-receptor, $p75^{NTR}$. They were not, however, able to demonstrate any interactions of the NgR ligands (Nogo-66, MAG, OMgp) or its co-receptor, $p75^{NTR}$, with NgR3.

HERPES SIMPLEX VIRUSES

Herpes simplex virus type-1 (HSV-1) is a member of the alpha herpesviridae family, and is known to principally underlie the pathogenesis of cold-sores. Its counterpart, HSV-2, with which it shares a significant degree of genetic homology, is predominantly responsible for the manifestation of genital-sores. Nonetheless, the two viruses and their associated pathologies are not mutually exclusive. HSV-1 is endemic within all populations, and it has been consistently estimated within recent years that ~65% of the American population (>12 years old) are seropositive for the virus (Oliver et al., 1995; Rosenthal et al., 1997; Langenberg et al., 1999; Xu et al., 2002). Owing to the propensity of the herpes simplex viruses to enter latency in the host organism, it is believed that infected individuals are incapable of immunological clearance of the virus and, thus, will

be carriers for life. Curiously, however, reactivation may occur repeatedly throughout the life-span of some infected individuals (recurrent symptomatic episodes), whilst not at all in others (life-long subclinical infections). There are many theories that seek to explain why this should be so, but these will not be discussed here (reviewed by Millhouse and Wigdahl, 2000).

Biology of HSV-1

HSV-1 is a nuclear replicating, dsDNA virus. Its genome comprises 152Kb (Roizman and Sears, 1996), and is composed of two unique regions: long (U_L), and short (U_S). Each of these possesses short inverted terminal repeat (ITR) sequences at both ends, which function to permit linear rearrangement of the genome by inversion between these two points. This gives rise to four potential linear arrangements of the HSV-1 genome (Jacob et al., 1979). However, during latency, the HSV-1 genome is believed to assume a circular episomal structure in which such rearrangements do not occur. Therefore, the inversion of the unique regions is believed to arise, for the most part, during the replication of the viral DNA when long linear concatamers of genomic DNA are synthesized.

HSV-1 consists of an icosahedral capsid, enclosing the viral genome, which is separated from a glycoprotein rich envelope by the tegument, a layer rich in proteins – particularly virion protein 16 (VP16) and virion host shut-off protein (vhs). Viral entry into the cell is achieved through interactions of the envelope glycoproteins, of which there are 12 (gB-gM), with cell surface receptors. Fusion of the viral and cellular membranes is followed by release of the viral capsid into the cytoplasm (Morgan et al., 1968). This is accompanied by the concomitant release of the tegument proteins, vhs and VP16. vhs acts immediately to induce host cell translational suppression via the activation of a pathway which results in the non-specific degradation of mRNA. In the mean time, the capsid is transported to the nucleus (Batterson and Roizman, 1983), where the viral DNA is deposited and sets about exploiting the host cell RNA polymerase II in order to effect transcription. By this time, VP16 will also have reached the nucleus where it assumes a role in transactivating the HSV-1 IE genes, and can facilitate the entry into a lytic life-

cycle – although this appears to be largely influenced by host cell-type. For example, the dichotomy is that: either, the virus will enter into a lytic life-cycle, in which it replicates to form new infectious viral particles; or, the virus will enter into a latent life-cycle, in which the viral DNA forms a circular nuclear episome and effectively remains dormant. Although the former is common in epithelial cells, the latter is typical in primary sensory neurons. Why this should be so is not yet clear.

In the classic model of primary HSV-1 infection, epithelial cells - especially those of non-keratinised mucous membranes - are the first to be infected by virus. In these cells, the HSV-1 rapidly undertakes a course of lytic replication. Newly formed infectious viral particles, released from lysed epithelial cells, infect the nerve terminals of primary sensory neurons that lie within close proximity to the lesion. The viral capsids are transported retrogradely along the axons, from the peripheral site of primary infection, until they reach the perikarya of the primary sensory neurons; these reside in the dorsal root ganglia (DRG).

Once the viral DNA has been deposited in the neuronal nucleus, the virus can either undertake another round of lytic replication or it can enter latency, as was mentioned earlier. However, HSV is renowned for its predilection to enter latency in primary sensory neurons and, although it can periodically reactivate and replicate, it is as a result of this property of establishing a life-long infection in these neurons that HSV is considered neurotropic.

Nonetheless, HSV-1 can infect a broad spectrum of cell-types both *in vivo* and *in vitro*. One issue of contention is the identification of those envelope glycoproteins that are necessary for membrane attachment to, and uptake by, a target cell. Whilst it is true that glycoprotein B (gB), gC and gD have all been implicated in the process, it seems unlikely that the same combination will be employed for attachment to all target cells. After all, the HSV-1 envelope bears at least 12 different glycoproteins, and in practical terms the virus is reasonably pan-tropic. Furthermore, whilst heparan sulfate has been shown unequivocally to interact with HSV-1 glycoproteins, enabling membrane attachment

(WuDunn and Spear, 1989; Shieh and Spear, 1991), there are three structurally unrelated protein families that serve as cellular entry receptors for HSV-1 (reviewed by Campadelli-Fiume et al., 2000).

HSV-1 Gene Activity in Lytic and Latent Cycles

HSV-1 gene activity can be broadly divided into *immediate early* (IE), *early* (E) and *late* (L). There are five IE genes giving rise to infected cell proteins (ICP) 0, 4, 22, 27 and 47; all of which have all been shown to cause cytopathic effects *in vitro* (Johnson et al., 1994).

The onset of IE gene expression is regulated by the tegument protein VP16, which is released into the cytoplasm alongside the capsid following the fusion of virus and cellular membranes. This protein subserves two important functions. First, VP16 is a late gene product which is incorporated into newly forming viral particles as an essential structural protein within the tegument. Second, upon infection of a target cell, the protein is released from the tegument into the cytoplasm and transported to the nucleus by Host Cell Factor (HCF) where it transactivates the HSV-1 IE genes (LaBoissiere and O'Hare, 2000).

VP16 mediated transactivation of IE genes is achieved via interactions with the cellular proteins HCF and Oct-1, both of which recognize and bind to TAATGARAT motifs within the promoter sequences of the IE genes. Oct-1 contains both a conventional homeodomain that enables DNA-binding at its carboxy terminus, and a bipartite DNA-binding domain, known as a POU domain, slightly n-terminal to the former. It is the POU domain that is responsible for Oct-1 binding of the TAATGARAT motif. The VP16/HCF complex does not dissociate, but binds to the TAATGARAT/Oct-1 complex (Preston, 2000), whereupon the c-terminal transactivating domain of VP16 contacts – and activates - the transcriptional pre-initiation complex at the TATA box.

As was mentioned earlier, VP16 is also a structural component of the tegument. The domains involved in this aspect of its function reside at the n-terminal of the protein.

Deletion of the structural domains renders the virus incapable of replication. Therefore, the n-terminal peptide must be preserved, or complemented *in vitro*, as it is an absolute requirement for the synthesis of infectious viral particles.

Successful transactivation of the IE genes results in the synthesis of five proteins (ICP 0, 4, 22, 27, and 47). With the exception of ICP47, these are all transcriptional transactivators which assist in driving the cascade of gene expression from IE through to L, during cycles of lytic replication.

ICP0 is a transactivator of IE, E and L genes. It is non-essential for growth *in vitro* but, if deleted, will reduce viral yields (Stow and Stow, 1986; Sacks and Schaffer, 1987). Its gene is located in the U_L region and is, therefore, present in two copies. ICP0 is a promiscuous transactivator of transfected genes (Roizman and Sears, 1996), and has also been shown to interact with elongation factor 1 delta and cyclin D3 (Kawaguchi et al., 1997a; Kawaguchi et al., 1997b).

ICP4 is a transactivator of E and L genes, and a repressor of IE genes. Its gene is present in both U_S regions, and is essential for replication *in vitro* (DeLuca et al., 1985). It is thought to bind directly to certain DNA motifs as a homodimer (Metzler and Wilcox, 1985), and brings about transcriptional activation through association with 'hi-jacked' cellular transcription factors TFIIB and either TFIID or the TATA-binding protein (Smith et al., 1993).

ICP22 is a transactivator of L gene expression, but is not essential for virus propagation *in vitro* (Poffenberger et al., 1993; Poffenberger et al., 1994; Rice et al., 1995; Leopardi et al., 1997; Bruni and Roizman, 1998).

ICP27 is a transactivator of L genes, and repressor of E genes. It is essential for replication *in vitro*. Also, the protein is known to prevent splicing of primary mRNAs (Bryant et al., 2001), favouring HSV-1 genes which for the most part do not contain

introns. In addition, ICP27 can interact with either ICP0 or ICP4 to trans-repress viral gene activity (Sekulovich et al., 1988; Mullen et al., 1995; Panagiotidis et al., 1997).

Unlike the other IE genes, ICP47 is not a transactivator of gene expression. Its principal role is in the prevention MHC presentation of HSV-1 antigens at the surface of infected cells. It does this by targeting the transporters of antigen processing (TAP). These proteins normally act by translocating peptide fragments across the ER membrane, but are retained inactive in the cytosol following binding by ICP47 (York et al., 1994; Fruh et al., 1995; Hill et al., 1995).

ICP6 is the large subunit of the viral ribonucleotide reductase (Preston et al., 1984; Bacchetti et al., 1984). It is a late stage IE gene, and is sometimes considered a hybrid IE/E gene. Its activation is independent of that of genuine IE genes. A null mutation in the ICP6 gene does not impair viral DNA synthesis or viral growth in dividing cells *in vitro*, but does significantly impair viral replication in non-dividing cells (Goldstein and Weller, 1988). Nonetheless, viruses lacking only ICP6 are capable of replicating *in vivo*, and will give rise to cutaneous lesions similar to those produced by inoculation with wild-type HSV-1 (Turk et al., 1989).

The E genes encode proteins that direct the replication of viral DNA, such as thymidine kinase, ICP8 (the major DNA binding protein) and DNA polymerase. The L genes encode proteins such as ICP34.5 (the neurovirulence factor), VP16, vhs and the envelope glycoproteins.

During viral replication, concatamers of viral DNA are formed. Inversions of the U_S and U_L sequence occur before the DNA is cleaved into genomic lengths and packaged into capsids. Tegument proteins accumulate around the capsid, which buds through the nuclear envelope and acquires envelope glycoproteins in doing so. Infectious viral particles are ultimately released by cell lysis.

After entering into latency, the HSV-1 genome persists in the nucleus of infected neurons as circular episomal elements (Mellerick and Fraser, 1987; Deshmane and Fraser, 1989). Whilst in latency, the genes required for the viral lytic cycle are switched off. The only transcripts produced at this stage of the viral life cycle are the Latency Associated Transcripts (LATS) which are encoded for by two identical regions found in the long terminal repeat sequences of the viral genome (reviewed by Latchman, 1990; Wagner and Bloom, 1997). The LATS are initially 8.5kb, before splicing gives rise to smaller RNAs (Wagner et al., 1988; Dobson et al., 1989).

The HSV-1 genome encodes in excess of 80 proteins, more than half of which are *essential* for viral propagation *in vitro*. The remaining genes are superfluous to virus growth *in vitro*, and have therefore been termed *non-essential* (Roizman and Sears, 1996).

HSV-1 as a Tool for Genetic Manipulation

Being neurotropic HSV-1 can, by definition, infect postmitotic cells which is one its most noteworthy advantages over other viral vectors commonly used for gene delivery, such as retroviruses and adeno-associated viruses (AAV). Unlike lentiviruses, which are also able to infect postmitotic cells, the HSV-1 genome does not integrate into the host-cell genome, thus eliminating the potential risk of insertional mutagenesis. Furthermore, the virus - with a 152Kb genome - can accommodate inserts of up to 35kb, enabling multiple-gene delivery. Also, HSV-1 can be grown to high titre as a wild-type virus. However, due to the virus' inherent ability to elicit an immune response, a number of gene deletions are necessary. Naturally, this procedure impedes viral replication and renders it more difficult to grow.

Wild-type HSV-1 is extremely cytotoxic, and can induce fatal encephalitis if administered in sufficiently high doses. For the purposes of gene delivery, a number of deletions of essential and non-essential genes are required to attenuate this toxicity. Deleting some of the immediate early genes reduces the pathogenicity of the virus. However, ICP4 and ICP27 are trans-activators of viral gene expression in both the early

and late stages. These, therefore, must be present *in trans* in a complementing cell line when growing the virus. Virion protein 16 (VP16), which induces IE gene expression after infection, can be inactivated by a 12bp insertion into its C-terminal transactivating domain, preventing it from exerting its transactivational effects over the immediate early genes (Ace et al., 1989). Yet, the structural function of VP16 is preserved, enabling it to retain its activity as a tegument protein. Also, non-essential genes, which play no part in replication can be deleted to reduce cytopathic effect, e.g. ICP34.5, a neurovirulence factor.

POST-TRANSCRIPTIONAL GENE SILENCING (PTGS) AND RNA INTERFERENCE (RNAi)

One of the great drawbacks of gene therapy, until recently, has been the limitation of its application to diseases which solely demand genetic supplementation. Unlike heritable monogenic disorders, which usually require delivery and expression of a functional gene to mask the effects of an inactivating mutation in an endogenous gene, some organic and acquired diseases require gene-suppression.

Historically, regulation of gene expression was believed to occur uniquely at the level of transcription, i.e. whether a gene is or is not transcriptionally active. It has long been recognized that DNA methylation, particularly of CpG sequences within promoter regions of tissue-specific genes, is one way by which efficient gene silencing can be achieved in eukaryotic cells (reviewed by Razin and Riggs, 1980). Originally, it was considered that such methylation patterns exert a local effect on chromatin structure, rendering the promoter region inaccessible and, therefore, inactive (reviewed by Cedar, 1988). However, there is now evidence to suggest that methylated DNA within promoter regions associates with nucleosomal repressor elements which induce such changes in chromatin structure and, thus, abrogate transcriptional activity (reviewed by Razin, 1998). This epigenetic process underlies genetic imprinting (whereby offspring may exhibit differential levels of gene activity on each copy of a given gene, dependent on the methylation pattern on that inherited from the mother and that of the father), and may be

responsible for some heritable genetic defects (reviewed by Holliday, 1987). However, so little was known about directing site-specific methylation of target sequences that attempts were never made to harness epigenetic manipulation for gene therapy in humans.

Almost a decade ago, molecular biologists attempting to enhance petunia flower-colour through the introduction of a homologous exogenous transgene reported, contrary to their expectation, that the resulting flowers were often completely or partially depigmented (Jorgensen et al., 1996). In plants, transgene-induced silencing of endogenous genes can be achieved transcriptionally by targeted gene-specific methylation, or post-transcriptionally through the targeted degradation of mRNA species (Jones et al., 1999). What was first termed co-suppression has ultimately led to the elucidation of the latter process, which is now known as post-transcriptional gene silencing (PTGS).

The molecular mechanism underlying this process did not start to become clear until Fire et al. (1998) reported that the injection of double-stranded RNA into *C.elegans* resulted in greater levels of silencing than was achieved with injection of either of the constituent single stranded RNAs alone. Indeed, so potent was the effect of this dsRNA, that the injection of only a few molecules per cell was found to be adequate to effect complete silencing of the target gene. Surprisingly, the authors also reported that the silencing effect was heritable, being transmitted to the first generation of offspring.

Having previously administered dsRNA by injection into the gut, the same group then determined that the same response could be achieved by feeding *C.elegans* with bacteria that had been genetically engineered to express dsRNA to the *C.elegans* unc-22 gene (Timmons et al., 2001). Even soaking the worms in solutions of dsRNA was found to successfully effect silencing (Tabara et al., 1998). The ease and simplicity of the latter has lead to the method becoming a hugely valuable functional genomic tool for the study of nematode worms.

Gene silencing, mediated by dsRNA delivery, is not restricted to C.elegans and has also been successfully applied to *D.melangastor* using a number of delivery methods. Indeed, some landmark discoveries about the mechanism of RNA interference (RNAi) were first made with *Drosophila* embryo lysates. Zamore et al. (2000) showed that not only is dsRNA processed to 21-23 nucleotide fragments, as was found earlier by Hamilton and Baulcombe (1999) in silenced plants, but also that the target mRNA is cleaved at similar intervals throughout the region that corresponds to the exogenous silencing dsRNA.

Although much remains unknown about the precise means by which dsRNA-mediated silencing occurs, considerable advances in understanding the process have been made over the past few years. At present, it is considered that RNAi can be divided into initiator and effector steps. In the former, dsRNA is first processively cleaved in an ATP-dependent fashion to 21-23 paired nucleotide fragments by the enzyme Dicer, a member of the type III family of ribonucleases which selectively degrade dsRNA. These short fragments of dsRNA are further processed to become short interfering RNAs (siRNAs), which typically consist of 19-21 paired nucleotides bearing dinucleotide 3′ overhangs.

The effector step entails the formation of the RNA-induced silencing complex (RISC), which is composed of the siRNA in association with numerous proteins. Targeting of homologous endogenous transcripts is accomplished through the ATP-dependent dissociation of the siRNA strands, with the antisense strand participating in contiguous base-pairing interactions with the target molecule. Cleavage occurs approximately 12bp from the 3′ terminus of the antisense siRNA strand (Nykanen et al., 2001), although the identity of the nuclease is not yet known. Interestingly, the stringency of the base-pairing of antisense siRNA strand and target mRNA is critical – a single base mismatch has been shown to dramatically reduce, if not completely abolish, silencing activity (Elbashir et al., 2001c).

Since PTGS is so potent in that the introduction of only a few molecules can be sufficient to completely silence gene expression within a single cell, and also in that its effects can

be heritable, one group has suggested that amplification of the siRNAs in Drosophila can occur through what they have termed "random degradative PCR" (Lipardi et al., 2001). This model is based on the notion that siRNAs could potentially act as primers, with target mRNA as template, and dsRNA as the product which would in turn be processively cleaved to form new siRNAs. However, this model requires the existence of an RNA-dependent RNA polymerase. Whilst such an enzyme is known to exist in *C.elegans*, for example, which could contribute to the potent activity of dsRNA reported by Fire et al. (1998), there is no obvious *in silica* evidence for an orthologous (homologous) gene in *Drosophila* – and, yet, for the theory of Lipardi et al. (2001) to be correct, a protein of the described function must exist.

The variety of organisms in which dsRNA has been shown to be active in inducing PTGS is indicative of its evolutionary importance, since it would appear to have emerged prior to the divergence of plants and animals. Why this mechanism evolved in the first instance, and why it is so well preserved throughout the eukaryotic kingdom today, remain something of a mystery. Nonetheless, it has repeatedly been suggested that this mechanism may have evolved as a primitive defence against RNA viruses or transposons, thus conferring a survival advantage (Cogoni and Macino, 2000; Hammond et al., 2001).

However, other researchers have posited a more plausible explanation – PTGS is integral to development. Evidence for this comes from the involvement of the *C.elegans* ortholog of Dicer, DCR-1, in generating 22 nucleotide small temporal RNAs (stRNAs) such as *lin-4* and *let-7* from larger stem-loop structures; these stRNAs prevent translation of certain proteins during development (Grishok et al., 2001; Hutvagner et al., 2001; Ketting et al., 2001). Similarly, another species of short RNA molecules termed microRNAs (miRNAs), which are typically 22 nucleotides in length, can also be generated from larger stem-loop structures through Dicer-mediated cleavage (Lee and Ambros, 2001); these too have been implicated in suppressing gene expression.

RNAi in Mammalian Cells

The PKR Response

Despite the preservation of PTGS across the eukaryotic kingdom, it has been somewhat more difficult to harness the potential for gene-specific dsRNA-mediated silencing in mammals owing to the recent evolutionary acquisition of a putative antiviral response. The introduction of dsRNA longer than approximately 30bp induces non-specific translational suppression through (i) the activation of dsRNA-dependent protein kinase (PKR), which in turn phosphorylates and inactivates the translation initiation factor, eIF2α, and (ii) the activation of RNase L, which non-specifically degrades single-stranded RNA (Lengyel et al., 1980). Together, these pathways function to shut-down all translational activity within an 'infected' cell, ultimately leading to cell-death. This, presumably, is beneficial to the host since it should in theory result in the elimination of a pathogen, such as an RNA virus, at an early stage.

siRNA

Since the introduction of dsRNA of less than 30 nucleotides in length does not activate the PKR response in mammalian cells, the obvious way to achieve gene silencing in mammals was through the introduction of siRNAs, instead of long dsRNA. Transfection of cultured mammalian cells with siRNAs revealed that, although complete gene silencing seems unattainable, at least 90% knockdown of mRNA and protein can be achieved with the best siRNAs (Elbashir et al., 2001a). However, the reason why so many siRNAs have been shown to be relatively inefficient, or indeed completely ineffective, in mammalian cells is not entirely clear. The most recent theory is that of strand bias, in which either the sense or antisense strand may preferentially associate with RISC (Schwarz et al., 2003; Khvorova et al., 2003). This process appears to be dependent on the nature of the nucleotide composition of the respective strands.

shRNA

It was, originally, convention to administer chemically synthesized siRNAs in gene silencing experiments. However, these proved to be expensive and relatively ineffective for *in vivo* delivery. The advent of commercially available kits for *in vitro* transcription

of siRNAs considerably lowered the cost of gene silencing experiments, but offered no improvement for *in vivo* delivery. For many researchers, this was a major impediment to their use. Nonetheless, it did not take long before several groups reported within a very short time-frame that a RNA polymerase III dependent promoter, either U6 or H1, could be manipulated for the generation of short-interfering RNAs either by transcription of short inverted repeat sequences from different RNA polymerase III dependent promoters (Miyagishi and Taira, 2002a), or by RNA polymerase III dependent promoter driven transcription of a single hairpin RNA structure (Lee et al., 2002; Paddison et al., 2002a; Paul et al., 2002a; Sui et al., 2002b; Yu et al., 2002b), termed short-hairpin RNA (shRNA) by Paddison et al. (2002a). These were reported to exhibit a similar level of activity to chemically synthesized siRNAs.

Virus-Mediated Delivery of shRNAs

More recently, numerous groups have reported successfully delivering shRNAs from a U6 or H1 promoter cassette within different viruses, including lentivirus (Abbas-Terki et al., 2002; Dirac and Bernards, 2003; Rubinson et al., 2003; Scherr et al., 2003; Stewart et al., 2003; Wiznerowicz and Trono, 2003; An et al., 2003) retrovirus (Brummelkamp et al., 2002b) and adenovirus (Shen et al., 2003).

Gene-Specific Methylation in Mammalian Cells

Recently, it has been shown that the gene-specific methylation that can arise in response to the introduction of complementary dsRNA in plant cells (Jones et al., 1999), also occurs in response to the introduction of siRNA targeted against CpG islands within the promotor of interest in mammalian cells (Kawasaki and Taira, 2004; Morris et al., 2004). This leads to the silencing of target gene expression at the transcriptional level, as opposed to the post-transcriptional gene silencing that is elicited by siRNAs designed against the target transcript sequence. Used in conjunction, siRNAs designed against the target transcript sequence as well as CpG islands within the target promoter, may result in enhanced silencing activity.

AIMS OF THIS STUDY

This thesis seeks to assess the likely role of the myelin associated inhibitors of regeneration (Nogo, MAG, OMgp) and their common receptor (Nogo Receptor) in the failure of axonal regeneration in the CNS. First, *in situ* hybridization was undertaken to record the expression mRNAs encoding *ngr*, *nogo-66* (i.e. all isoforms of nogo), *nogo-a* and *omgp* in the healthy and injured adult rodent nervous system. This descriptive anatomy was necessary to draw basic conclusions about the potential for NgR-ligand interactions *in vivo*, as well as determine whether these molecules would be amenable to HSV-1 based gene delivery.

Given the predominantly neuronal expression of *nogo-66* and *nogo-a* transcripts, an immunohistochemical study of Nogo-A protein expression in the healthy and injured adult rodent nervous system was also undertaken. This was necessary to establish (i) the extent to which Nogo-A protein is expressed by neurons in these models, and (ii) whether any correlation exists between neuronal expression of the protein and its regenerative capacity *in vivo*. During this study, an incidental observation of ATF3 upregulation by non-neuronal cells of transected adult rat sciatic nerve lead to a separate study of ATF3 expression by these cells in different models of peripheral nerve injury.

In an attempt to ultimately be able to assess the functional interaction of NgR with its ligands *in vivo*, a modified HSV-1 virus was constructed for the expression of a tagged-secreted form of the antagonist peptide to NgR, NEP1-40. This has previously been shown to disrupt the interaction of NgR with Nogo-66 *in vitro*, and to promote axonal regeneration *in vivo* (Grandpre et al., 2002). Since the authors reported that intrathecal infusion of NEP1-40 by mini-osmotic pump significantly augmented the regeneration of injured corticospinal tract axons, after dorsal hemisection of the adult rat thoracic spinal cord, it was considered that targeted HSV-1 mediated delivery of NEP1-40 may achieve comparable, if not better, regeneration in the injured spinal cord. Furthermore, it was thought that such a vector would be of value in the investigation of axonal regeneration in regions of the CNS where intrathecally infused peptide would not be expected to

penetrate sufficiently well to exert its effect, e.g. deep in the spinal cord of animals larger than rats.

In addition, with the recent developments in RNAi technology, it was decided that the development of an HSV-1 based platform for the delivery of short hairpin RNAs (shRNAs) should be attempted. These molecules can be generated by an RNA polymerase III dependent promoter in DNA vectors, and possess almost the same level of activity as chemically synthesized short interfering RNAs (siRNAs). The establishment of such a system in HSV-1 was deemed highly desirable, not least for the *in vivo* study of putative axon-inhibitory molecules and their receptors within the injured nervous system. In this study, an HSV-1 vector for the expression of shRNA against eGFP was first generated to establish proof of principle. The silencing activity of this vector was compared with that of another HSV-1 vector encoding long-hairpin RNA against eGFP, which was expected to by-pass the host cell dsRNA dependent protein kinase response owing to the function of the HSV-1 protein, ICP34.5. An HSV-1 vector for the expression of shRNA against NgR was also constructed, but this was only assessed *in vitro* for NgR silencing activity.

Figure 1.1.

The gene structure of human *nogo* (a), *omgp* (b), *mag* (c) and *ngr* (d), respectively. The chromosomal locations for these genes are denoted in brackets.

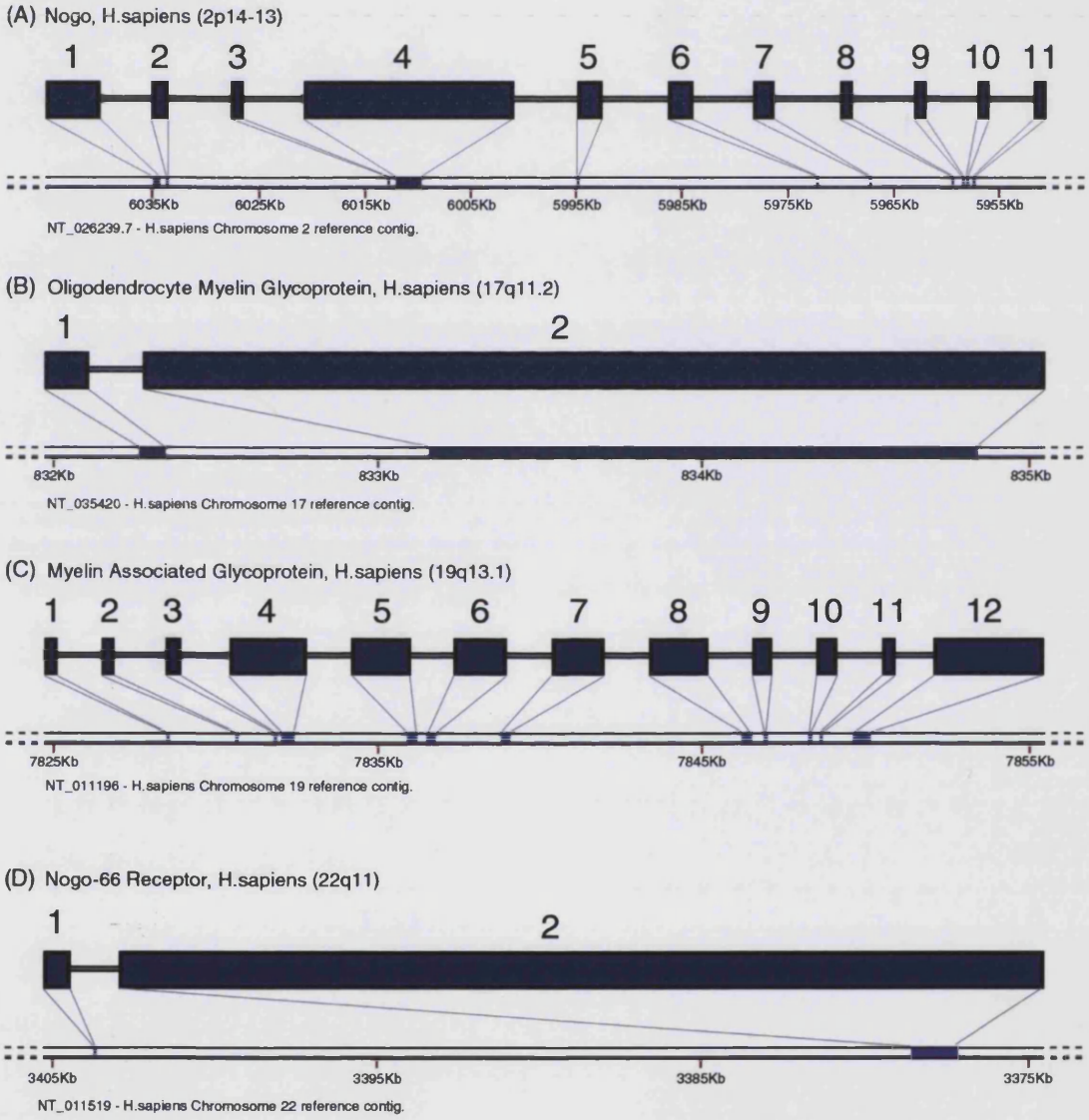

Figure 1.2.

The transcript structure of the three major isoforms of *nogo*. The 3′ striped segments denote exons 6-11, and are shared by all three major isoforms. The 5′ stippled segment (exon 1) is shared by *nogo-a* and *-b*. The white segments (corresponding to exons 3 and 4 of the *nogo* gene) are specific to *nogo-a*, but are also present in some minor Nogo transcripts (refer to Table 1.1). The black segment (exon 5) is specific to *nogo-c*. Evidently, only *nogo-a* and *-c* have specific sequence.

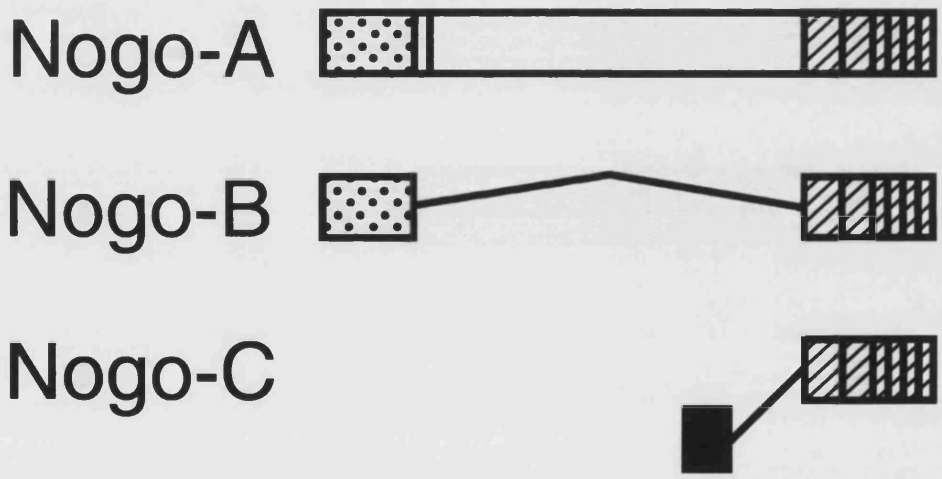

Table 1.1. Transcripts from the *nogo* (*reticulon 4*) gene

The human *nogo* gene consists of 14 exons and 8 introns, and gives rise to 12 mRNA isoforms which are translated into 7 different proteins. It originally appeared that there were 11 exons within the human *nogo* gene (Hunt et al., 2002) but recently it has been reported that there are 14 (Oertle et al., 2003). The mouse *nogo* gene contains only 11 exons. The table shows the seven isoforms of Nogo transcript that have been registered in Genbank, each of which encodes a different protein with a correctly aligned open reading frame. Oertle et al. (2003) have, however, shown that 10 mRNA isoforms, translating into 5 different proteins, are present in cDNA libraries from adult tissue. The numbers given beneath the exonic sequences correspond to their position within the human *nogo* gene (AY102285), registered in Genbank by Oertle et al. (2003).

* = Exons identified by Oertle et al,. (2003) using 5′ capsite RACE PCR. Currently, however, there are no independently submitted cDNA sequences nor dbEST submissions in Genbank incorporating these sequences.

** = Since the first exon of each of these mRNA isoforms encodes 5′ UTR (with the exon composition being otherwise identical), they all redundantly give rise to the same protein isoform, Rtn-T (986αα) (Zhou et al., 2002).

‡ = 1Aa and 1Ab are recently discovered exonic sequences (Oertle et al., 2003) that, together with 1A, constitute a single exon.

† = The first 832 bases of this exon are missing in the Brain my043 cDNA sequence, which was originally isolated from foetal brain tissue. It is possible that this cDNA sequence is incomplete.

The use of adult human brain, testis, and skeletal muscle cDNA libraries for 5′ capsite RACE PCR by Oertle et al. (2003) probably explains why they did not detect some Nogo mRNA isoforms that were originally isolated from foetal brain tissue (Brain my043 and Nogo-A short form cDNAs).

N.B. The human *nogo* gene has two major promoters; P1 gives rise to transcription starting at 1A or 1B; P2 gives rise to transcription starting at 1C. It has been suggested that 4 minor promoters also exist within the *nogo* gene (P3-6). These are thought to drive transcription of the testicular isoforms of Nogo, i.e. all those beginning with 1Aa, 1Ab, 1D, 1E, 1F or 1G.

Name	Genbank Accession Number	Exon																Predicted Protein length (αα)
		Hunt et al., 2002				2	-	-	3	4	5	6	7	8	9	10	11	
		-	-	1	-													
		Oertle et al., 2003																
		1Aa (3715-3827) ‡	1Ab (3946-4116) ‡	1A/1B (3999-4799) ‡	1D (4853-4986) *	1E (5346-5465)	1F (5918-5998) *	1G (7657-7727) *	2 (26322-26378)	3 (27057-29456)	1C (44188-44455)	4 (66846-67053)	5 (71892-72030)	6 (79807-79879)	7 (80704-80750)	8 (80950-81008)	9 (81373-82382)	
Nogo-A	AJ251383	N	N	Y	N	N	N	N	Y	Y	N	Y	Y	Y	Y	Y	Y	1192
Novel isoform 1**	AY123245	Y	N	N	N	N	N	N	Y	Y	N	Y	Y	Y	Y	Y	Y	986**
Novel isoform 2**	AY123246	N	Y	N	N	N	N	N	Y	Y	N	Y	Y	Y	Y	Y	Y	986**
Novel isoform 3**	AY123247	N	N	N	Y	N	N	N	Y	Y	N	Y	Y	Y	Y	Y	Y	986**
Testis Specific Rtn (Rtn-T)**	AF333336	N	N	N	N	Y	N	N	Y	Y	N	Y	Y	Y	Y	Y	Y	986**
Novel isoform 4**	AY123249	N	N	N	N	N	Y	N	Y	Y	N	Y	Y	Y	Y	Y	Y	986**
Novel isoform 5**	AY123250	N	N	N	N	N	N	Y	Y	Y	N	Y	Y	Y	Y	Y	Y	986**
Nogo-A short form	AF320999	N	N	Y	N	N	N	N	N	Y	N	Y	Y	Y	Y	Y	Y	960
Brain my043	AF063601	N	N	N	N	N	N	N	N	Y†	N	Y	Y	Y	Y	Y	Y	647
MGC clone:15807 IMAGE:3505850	BC016165	N	N	Y	N	N	N	N	Y	N	N	Y	Y	Y	Y	Y	Y	392
Nogo-B	AJ251384	N	N	Y	N	N	N	N	N	N	N	Y	Y	Y	Y	Y	Y	373
Nogo-C	AJ251385	N	N	N	N	N	N	N	N	N	Y	Y	Y	Y	Y	Y	Y	199

CHAPTER 2

Methods and Materials

MOLECULAR BIOLOGY

Laboratory Materials

Analytical grade laboratory chemicals were purchased from Boehringer Mannheim, Gibco-BRL Life Technologies, Merck and Sigma-Aldrich. Standard disposable laboratory plasticware was supplied by Greiner.

Custom-made primers for use in PCR primers were synthesized by either Gibco-BRL Life Technologies or Sigma-Genosys. All restriction- or modifying- enzymes, as well as dNTPs, were purchased from Promega or New England Biolabs.

RNA Extraction

Animal Tissue

The homogenisation of diced tissue was performed with a sonicating probe, set to full-power (3x20s, returning samples to ice for 1min between treatments). Samples were subsequently incubated for 5mins at room temperature on a shaking platform, before being centrifuged at 10 000 x g, 4°C, for 10mins to pellet unwanted cellular debris. The supernatant was collected and thoroughly mixed with 0.2 volumes of chloroform, before being centrifuged at 10 000 x g, 4°C, for 5mins in Phase-Lock tubes (Eppendorf). The aqueous layer was removed, mixed with 2 volumes of ice-cold isopropanol, and stored at -80°C for at least 1 hour. RNA was pelleted by centrifugation at 10 000 x g, 4°C, 30mins, then washed with ice-cold 70% ethanol made with DEPC-treated ddH_2O, and centrifuged at 10 000 x g, 4°C, for 5mins. The supernatant was discarded, and the pellet left to dry under cover at room temperature for 5mins. RNA was re-suspended in a suitable volume of DEPC-treated ddH_2O, aliquoted and stored at -80°C.

Mammalian Cell Lines

Cells cultured in 6- or 24-well plates were washed in 1xHBSS and subsequently lysed in an appropriate volume of Trizol reagent (Gibco-BRL Life Technologies). Total RNA was extracted as described previously, except that sonication was omitted.

DNaseI Treatment of Extracted RNA

Genomic DNA contamination was eliminated from extracted total RNA samples by treatment with DNaseI. A commercially available kit was used, as per the manufacturer's instructions (DNA-free; Ambion).

Assessment of RNA Integrity

1μg of each total RNA sample was resolved on 1%-TAE agarose gel made with DEPC-treated ddH_2O, and inspected by UV transillumination for the integrity of the ribosomal bands.

Mammalian Genomic DNA Extraction

Cultured cells

Genomic DNA was isolated from cultured cells using DNAzol (Gibco-BRL Life Technologies), as per the manufacturer's instructions. Briefly, the culture media was discarded and the cell monolayer washed in 1x PBS before an appropriate volume of DNAzol was added to lyse the cells. The reagent was collected and mixed by swirling with an equal volume of absolute ethanol. The precipitated DNA was washed twice in 70% ethanol and left to air-dry under cover for 5mins. Samples were resuspended in an appropriate volume of 8mM NaOH overnight on a vertical rotating wheel at 4°C. An appropriate volume of 0.1M HEPES was added to neutralise the NaOH, the DNA samples were aliquoted and stored at -20°C.

Reverse Transcription Polymerase Chain Reaction (RT-PCR)

Reverse Transcription (First-strand DNA synthesis)

First-strand DNA synthesis from total RNA was performed using avian myeloblastosis virus reverse transcriptase (AMV-RT; Promega, UK). Briefly, 1μg of total RNA was

mixed with either 500ng of Random primers (Promega, UK) or 1μg of oligo$(dT)_{15}$ primers (Promega, UK), and made up to a total volume of 12μl with DEPC-treated ddH_2O. This sample was incubated at 65°C for 10mins to permit the annealing of primers to RNA, and then snap-cooled on ice for 5mins. dNTPs, RNase inhibitor, AMV-RT buffer and AMV-RT were added to give a final volume of 20μl (1mg total RNA, 500ng random hexamers/1μg oligo$(dT)_{15}$, 1xAMV-RT buffer, 500μM dNTPs, 20-40U RNasin, and 20U of AMV-RT), and incubated at 42°C for 45mins. Samples were placed on ice, aliquoted and stored at -20°C for the longterm.

Polymerase Chain Reaction (PCR)

Each PCR amplification of DNA was performed in a total reaction volume of 50μl in a 0.2ml thin-walled Eppendorf tube. Products were amplified with either the proof-reading DNA polymerase, *Pfu* (template DNA, 400nM Forward Primer, 400nM Reverse Primer, 200μM dNTPs, 1x *Pfu* buffer, 1.5U *Pfu* DNA polymerase) or the non-proof-reading DNA polymerase, Taq (template DNA, 400nM Forward Primer, 400nM Reverse Primer, 200μM dNTPs, 1x $MgCl_2$-free Taq buffer, 1-4mM $MgCl_2$, 5U Taq DNA polymerase). In the latter, the optimal concentration of $MgCl_2$ was determined experimentally through the employment of a range of concentrations. *Pfu* was always used for cloning, and *Taq* for analytical PCR. Template DNA was (i) single-stranded DNA generated by reverse transcription from RNA (~50ng/reaction), (ii) plasmid DNA (1-10ng/reaction), or (iii) genomic DNA (~50ng/reaction). Polymerase chain reaction was performed in an Eppendorf Mastercycler using a hot-start protocol (i.e. enzyme was added following the denaturation of primers and DNA). Typical programme settings comprised denaturation at 95°C for 1m30s, annealing at 50-65°C (as appropriate) for 1m45s, and extension at 72°C (*Pfu*) or 74°C (*Taq*) for a suitable period of time (*Pfu* amplifies at 500b/min, and Taq at 1kb/min), for a total of 25-35 cycles.

A-Tailing of Pfu-Generated PCR Products

Pfu DNA polymerase is proof-reading enzyme (i.e. it possesses 3′→5′ exonuclease activity), which generates blunt-ended DNA products. In order to adapt *Pfu*-generated PCR products for cloning into the pGem T Easy PCR cloning vector (Promega, UK),

adenine-tails were added by *Taq* DNA polymerase. Briefly, PCR products were purified with GFX columns (Amersham, UK), and then incubated with Taq DNA polymerase (1x $MgCl_2$-free buffer, 2.5mM $MgCl_2$, 200μM dATP, 5U Taq DNA polymerase) for 20mins at 70°C.

Taqman® Quantitative PCR

Quantitative PCR was performed using an ABI7000 with Taqman® reagents (Applied Biosystems). The primers and probe for detection of rat *ngr* cDNA were custom-made by Applied Biosystems. The forward and reverse primers, CGT GGC TTG CAC AGT CTT GA and AGG TCC CGG AAG GCA TGT, respectively, were HPLC purified. The probe, CGT CTC CTC TTG CAC CAG AAC CAT GTG, possessed a 5′ 6-FAM Fluor label. The working concentrations of Taqman® primers and probes were first optimized (Fig. 2.1.A and B), as per the manufacturer's recommendations.

For sample analysis, total RNA was extracted from cultured postnatal rat cerebellar granule neurons with Trizol reagent, and treated with DNAfree (Ambion) to degrade contaminating genomic DNA. Reverse transcription was performed, as described earlier, using random primers. Each sample was analysed in triplicate. Reactions were each performed in a total volume of 50μl, containing 50nM of forward primer, 300nM of reverse primer, 50nM of 6-FAM-labelled probe, 25μl of 2x Universal PCR master mix (Applied Biosystems) and approximately 1ng of cDNA. No template controls, and standard curves were also included in each analysis. A predetermined assay reagent (PDAR) to detect the endogenous control, 18S rRNA, was used for sample normalisation. All reactions were singleplex.

Agarose Gel Electrophoresis

1% agarose-TAE gels were always used in resolving DNA samples. 1% w/v agarose was made up with 1x TAE buffer (0.4M Tris, 0.2M sodium acetate, 20mM EDTA, pH8.3) in a Duran bottle, boiled, and left to cool to approximately 50°C before ethidium bromide was added to a final concentration of 0.2μg/ml. The solution was poured to an appropriate depth in a gel tray containing a comb with suitably sized teeth, and left for

45mins to set. DNA samples were mixed with loading buffer (1x TAE, 50% v/v glycerol, 0.025% bromophenol blue) immediately prior to well-loading. For fragment size comparison, samples were run against 5µl of 1 kilobase DNA ladder (Gibco-BRL Life Technologies, UK).

Preparation of DNA Fragments

DNA Digestion by Restriction Endonuclease

DNA was incubated with the desired restriction endonuclease(s), diluted in a suitable buffer, for a minimum of 1 hour at the appropriate temperature. At least 2 units of (each) enzyme per microgram of DNA were used in these reactions. Care was taken to ensure that glycerol did not exceed 10% of the total reaction volume and, where appropriate, other measures were taken to prevent the 'star-activity' that is associated with some enzymes.

Generation of Blunt-Ended DNA

In the absence of compatible restriction sites for subcloning, 'sticky-ends' were blunted with the modifying enzyme T4 DNA polymerase (Promega, UK). This enzyme possesses 5′ to 3′ polymerase activity for filling-in 5′ overhangs, and 3′ to 5′ exonuclease activity for trimming back 3′ overhangs. DNA ends were modified in the presence of a suitable restriction endonculease buffer and 100nM dNTPs. 15 units of enzyme were added per µg of DNA. The reaction was incubated at room temperature for 10 mins before (i) heat inactivation at 80°C for 30mins, or (ii) purification of the DNA with GFX columns (Amersham), as per the manufacturer's instructions.

Isolation and Purification of DNA Fragments

Restriction endonuclease-digested, and/or end-modified, DNA samples were mixed with an appropriate volume of 6x loading buffer (30% glycerol, 0.25% bromophenol blue, 0.25% xylene cyanol) and resolved on a 1% agarose gel, containing 0.2µg/ml ethidium bromide. DNA fragments were visualized on a UV transilluminator, at a low power setting, and were quickly and carefully excised with a clean scalpel. The DNA fragment was subsequently extracted from the gel using the Gene Clean II Gel Extraction Kit (Bio

101, Vista, Ca, USA) or GFX columns (Amersham) as per the manufacturer's instructions. The purified DNA was ultimately eluted in an appropriate volume of autoclaved double-distilled water.

Annealing of DNA Oligonucleotides Encoding shRNA

In constructing vectors for the expression of shRNAs, it was necessary to order custom-made DNA oligonucleotides corresponding to the sense and antisense strands of the desired hairpin construct (see Chapter 8). PAGE purified and 5′ phosphorylated DNA oligonucleotides were purchased from Sigma-Genosys (Pampisford, Cambridgeshire, UK) and diluted in DEPC-treated ddH_2O to a stock concentration of 100mM. Adaptor DNA (i.e. annealed oligonucleotide DNA for ligation) was prepared by annealing the oligonucleotides at a final concentration of 100μM each in 1x annealing buffer (10x annealing buffer = 100mM Tris-HCl pH7.5, 1M NaCl, 10mM EDTA pH8.0). The annealing reaction was incubated in a water-bath at 65°C for 10mins, before being transferred to a beaker of 65°C water and left to cool slowly to room temperature. The quantity of double-stranded DNA per μl was calculated from the oligonucleotide data sheets, and a range of ligations performed in parallel (1-100ng of adaptor per ligation reaction). Samples of annealed oligonucleotide DNA were placed at -20°C for longterm storage.

DNA Ligations

Ligation reactions were performed in thin-walled 0.5ml Eppendorf tubes. Reactions consisted of an appropriate amount of linearized gel-purified vector (typically ~100ng), an appropriate molar ratio of gel-purified insert (between 1 to 3 copies of insert per copy of backbone), 1x T4 DNA ligase buffer and 3 units of T4 DNA ligase (Promega, Southampton, UK) made up to a final volume of 20μl with autoclaved double distilled water. Ligation reactions were either left at room temperature for several hours ('sticky-end' ligations), incubated at 4°C overnight (for optimal efficiency with the pGem T Easy PCR cloning vector system), or incubated in a thermal cycler ('blunt-end' ligations). The latter were performed in an Eppendorf Thermocycler, in which the samples were incubated at 16°C for 1min followed by 37°C for 1min, for 30 cycles. The final step

comprised 30mins incubation at 22°C. 10µl of the reaction product were used in the transformation of 200µl of competent *E. coli.*

Bacterial Propagation of Plasmid DNA

Bacterial Strains

A number of different bacterial strains of E. coli were used for plasmid cloning:

XL1-Blue (Stratagene Ltd., Cambridge, UK) – This is a standard strain of bacteria for the propagation of plasmid DNA. These cells were made competent using the calcium chloride method (described below) on the day of transformation, and were used extensively prior to the acquisition of the TOP10 strain of *E.coli.* Genotype = *recA1 endA1 gyrA96 thi-1 hsdR17 supE44 relA1 lac* [*F'proAB LacI*^{q} *ZΔM15, TN 10* (Tet^{r})]

TOP10 (Invitrogen, Paisley, UK) – This strain of bacteria can be made competent using the rubidium chloride method (described below), and subsequently stored longterm at -80°C. This was the preferred bacterial strain for routine cloning. Genotype = *F⁻ mcrA Δ(mrr-hsdRMS-mcrBC) Φ80lacZΔM15 ΔlacX74 deoR recA1 araD139 Δ(ara- leu)7697 galU galK rpsL (StrR) endA1 nupG*

GT116 (Invivogen, San Diego, CA, USA) – This strain of bacteria was used for the propagation of plasmids encoding shRNAs. It lacks the sbcC and sbcD proteins which are responsible for the recognition and cleavage of DNA hairpin structures (Connelly et al., 1998). Genotype = *F⁻ mcrA Δ(mrr-hsdRMS-mcrBC) Φ80lacZΔM15 ΔlacX74 recA1 endA1 ΔsbcC-sbcD*

BL21 (DE3) (Novagen, Merck Biosciences Ltd., Nottingham, UK) – This strain of bacteria was used for the expression of Nogo-66-$(His)_6$. It lacks the bacterial OmpT and Lon proteases, which can significantly impair the recovery of intact recombinant protein. Furthermore, it is a lysogen (i.e. has phage viral DNA integrated in its genome) of a modified λDE3 phage carrying a hybrid transgene encoding bacterial T7 RNA

polymerase under the control of the IPTG-sensitive *lacUV5* promoter. Genotype = *F⁻ ompT hsdS$_B$($r_B^- m_B^-$) gal dcm (DE3)*

Propagation of Bacteria

Master stocks of XL1-Blue and TOP10 *E. coli* were stored longterm in 15% glycerol at -80°C. Both strains of *E. coli* were grown in Luria Bertani media (LB media: 1% w/v Bacto®-tryptone, 1% w/v NaCl, 0.5% w/v Bacto®-yeast extract), which had been autoclaved at 120°C for 20mins at 10lb/square inch prior to use. Inoculates of untransformed bacteria from were initially grown in 5ml LB media in the absence of selective antibiotic agents at 37°C overnight in a Gallenkamp orbital shaker, set to 200rpm.

XL1-Blue *E. coli* were streaked across an LB Agar (2% Bacto®-Agar) plate, containing tetracycline at 12.5µg/ml, under sterile conditions. This plate was incubated overnight at 37°C, and stored for up to 1 month at 4°C. This served as master plate, from which individual bacterial colonies could be picked to make competent cells for transformation. In contrast, TOP10 bacteria were stored as ready-prepared aliquots of chemically competent bacteria at -80°C for up to one year (described later).

Preparation of Competent Bacteria

Calcium Chloride Method (used for XL1-Blue)

XL1-Blue *E. coli* were made competent using a protocol based on the calcium chloride method described by Sambrook and Russell (2001). In short, 100µl from the 5ml overnight culture of untransformed bacteria (described above), was used to inoculate 100ml of LB media, containing no antibiotic. This was grown to an optical density of 0.4-0.55 units at 580nm (OD_{580}), whereupon the bacteria were pelleted by centrifugation at 600 xg for 10mins at 4°C. The supernatant was then carefully removed, and the cells washed with 10mls of ice-cold 100mM $CaCl_2$. After 30mins on ice, the cells were again pelleted under the same centrifugal conditions, the supernatant was removed and the cells resuspended in ice-cold 100mM $CaCl_2$ to a final volume of 4mls. These competent bacteria were stored on ice for a maximum of three days.

Rubidium Chloride Method (used for TOP10 and GT116)

An overnight culture of bacteria was diluted 1:100 with 1 xLB and incubated at 37°C, 200rpm, until an $OD_{580/600}$ of 0.3-0.8 was obtained. The culture was kept on ice for 15mins, and then centrifuged at 600 xg, 4°C, for 10mins. Having discarded the supernatant, the pellet from 50ml of culture was re-suspended in 20ml of ice-cold RF1 (100mM $RbCl_2$, 30mM potassium acetate; 10mM $CaCl_2$, 50mM $MnCl_2$, 15% glycerol, titrated to pH5.8 with acetic acid), and left on ice for 15mins. The cells were centrifuged at 600 xg, 4°C, 10mins, the supernatant discarded, the pellet re-suspended in 2ml of ice-cold RF2 (10mM MOPS, 75mM $CaCl_2$, 10mM $RbCl_2$, 15% glycerol, titrated to pH6.5 with KOH) and left on ice for 15mins. Aliquots of 200µl were prepared, snap-frozen in liquid nitrogen, and stored at -80°C.

Transformation of Competent Bacteria

200µl of competent bacteria were transformed through the addition of an appropriate volume of extracted plasmid DNA or ligation reaction product. XL1-Blue or TOP10/GT116 *E. coli* were incubated with DNA on ice for 30mins, or 1 hour, respectively. These *E. coli* were subsequently heat-shocked at 42°C for 90 seconds, or 45 seconds, respectively. These cells were then incubated on ice for a further 2mins, or 5mins, respectively. 800µl of LB, pre-warmed to 37°C, was added to each transformation. These were then transferred to a Gallenkamp orbital shaker set to 37°C and 200rpm for 1hour, or 45mins, respectively. The transformed cells were subsequently pelleted by centrifugation at 600 xg, room temperature, for 10mins. Having carefully removed the supernatant, the cells were resuspended in 100µl of LB and plated onto LB Agar plates containing the appropriate antibiotic (100µg/ml ampicillin or 30µg/ml kanamycin, dependent on the resistance gene present in the plasmid DNA). Where detection of β-galactosidase activity was desirable, e.g. in using the pGem T Easy PCR cloning vector, LB Agar additionally contained a final concentration of 100µg/ml 4-chloro, 5-bromo, 3-indolyl-β-galactosidase (X-Gal, Insight Biotechnology, Ltd.), derived from a stock of 20mg/ml in dimethyl formamide.

Bacterial Growth on LB Agar Plates

Bacterial LB Agar plates were incubated at 37°C overnight, to support colony formation, and were then stored at 4°C until required.

Extraction of Plasmid DNA

Small Scale (Mini-Prep)

The "mini-prep" DNA extraction method is derived from the alkaline lysis method originally described by Birnboim and Doly (1979). Individual colonies of transformed bacteria were picked from antibiotic LB Agar plates and were each used to inoculate a single 5ml starter preparation of LB media, containing the appropriate antiobiotic selective agent (i.e. 100μg/ml ampicillin, or 30μg/ml kanamycin). Inoculates were incubated overnight at 37°C in a Gallenkamp orbital shaker, set to 200rpm. Cells were collected from 1.5ml of culture media by centrifugation at 600 xg for 1min, and supernatant was removed by aspiration. Pelleted cells were resuspended in 100μl of Solution 1 (50mM Tris-HCl pH7.5, 10mM EDTA pH8, 100μg/ml RNase A), lysed by addition of 200μl of Solution 2 (200mM NaOH, 1% v/v Triton X-100), and neutralized after 5mins by addition of 150μl of Solution 3 (3M NaOAc pH5.5). The lysate was centrifuged for 5mins at 600 xg, and the pelleted debris was removed with a hypodermic needle hooked at the tip. The DNA was precipitated by addition of 500μl of isopropanol, and pelleted by centrifugation for 5mins at 600 xg. The supernatant was carefully removed by aspiration and the DNA pellet was washed with 500μl of 70% ethanol. Having removed the wash solution, the pellet was left to air-dry under cover at room temperature. After approximately 10mins, the DNA pellet was resuspended in 20μl of double-distilled water and stored at -20°C.

Large Scale (Midi-Prep)

Midi-Prep plasmid DNA extractions were performed in order to obtain high grade DNA for cloning or transfection. Approximately 150ml of LB media, containing the appropriate antibiotic selective agent (i.e. 100μg/ml ampicillin, or 30μg/ml kanamycin), were inoculated with 150μl of the residual bacterial culture from one of the initial

overnight inoculates used in the mini-prep extraction of DNA for restriction digestion analysis. Innoculates were grown overnight at 37°C in a Gallenkamp orbital shaker, set to 200rpm. Cells from 100ml of culture were pelleted by centrifugation at 600 xg for 10mins, at room temperature. Plasmid DNA was subsequently isolated and purified using a commercially available Midi-Prep kit (Marligen), according to the manufacturer's instructions. DNA yields varied, dependent on the nature of the plasmid (i.e. whether it was a 'high copy number' vector), but typically ranged from 300ng-1μg/μl following resuspension in 200μl autoclaved double-distilled water.

Identification of Positive Bacterial Colonies

Analytical Digestion of Mini-Prep DNA by Restriction Endonucleases

Clonal analysis was usually performed by restriction endonuclease digestion of plasmid DNA obtained by Mini-Prep extraction. Typically, 10μl of Mini-Prep DNA were digested in a total volume of 20μl. 10 units of enzyme were included in the reaction with a suitable buffer, as indicated by the manufacturer; where two or more enzymes were used, care was taken to ensure that (i) a suitable buffer was used to achieve the highest enzymatic activity, and (ii) glycerol levels did not exceed 10%. Restriction endonuclease digestions were incubated at a suitable temperature for 1-2 hours. Samples were resolved on a 1% agarose gel containing 0.2mg/ml ethidium bromide, and visualized on a UV transilluminator.

Colony Transfer and Hybridisation with Radiolabelled DNA Probes

One particularly valuable method for the identification of positive clones, especially in the case of double blunt-end ligations in which the insertional efficiency is usually quite low, is to screen bacterial colonies with radiolabelled DNA probes.

Colony Transfer

Transfer of bacterial colonies was achieved by gently impressing a circular Hybond N nylon membrane on to the surface of an LB Agar plate, and leaving it in place for 2mins. A sterile hypodermic needle was used to make asymmetric puncture marks in the membrane, and the Agar plate was similarly marked with indelible ink; this served to

mark the orientation of the membrane on the plate such that it could be easily discerned later. The bacterial cells attached to the membrane were lysed are their DNA denatured by immersion in denaturing solution (1.5M NaCl, 0.5M NaOH) for 2mins. The filter were next immersed in neutralisation solution (2M NaCl, 1M Tris pH5.5) for 2mins, and washed in 2xSSC/0.1% SDS for 2mins. The filter then underwent two further washes in 2xSSC, for 2mins each, before being left to dry under cover for 20mins. The damp membrane was placed colony side up and cross-linked two times using a UV Stratalinker 2400.

Radiolabelling of DNA Fragments

All fragments of DNA to be used in the analysis of blotted nylon membranes were labelled with $\alpha[^{32}P]$dCTP by random primer labelling. The method employed was based on that originally described by Feinberg and Vogelstein (1983). All probes were labelled using Probequant (Amersham). In brief, the gel-purified DNA fragment was transferred to a screw-cap Eppendorf tube and heated to 100°C for 5mins, before snap-cooling on ice. Each tube in the Probequant kit contains a lyophilized bead of DNA polymerase large fragment (Klenow), buffer salts, random primers, dATP, dGTP and dTTP. These are resuspended on ice in a defined volume of double-distilled water, before a suitable quantity of the denatured DNA was added and mixed by pipetting. 50μCi of $\alpha[^{32}P]$dCTP were added to each reaction under conditions conforming to the UCL regulations for radioactivity usage. The reaction mixture was incubated at 37°C for 30mins and was then filtered through a G50 Sephadex column (Amersham, UK), according to the manufacturer's instructions, in order to remove unincorporated label. The radiolabelled DNA probe was heated for 5mins at 100°C and snap-cooled on ice for 2mins, immediately before addition to the hybridisation solution.

Hybridisation

The membranes were pre-hybridized for at least 1 hour at 65°C in Hybaid bottles containing 25mls of pre-heated hybridisation solution (6x SSC, 5x Denhardt's reagent [100x Denhardt's = 2% w/v bovine serum albumin, 2% Ficoll® (type 400), 2% w/v polyvinylpyrrolidone], 0.5% w/v SDS in double-distilled water containing 100μg/ml of

denatured sheared herring sperm DNA). An appropriate quantity of denatured α[^{32}P]dCTP-labelled DNA probe was added to the hybridisation solution, and left overnight at 65°C to hybridise. The membrane was washed with a series of pre-heated wash solutions for 20mins each (2x SSC, 0.1% SDS; 0.5x SSC, 0.1% SDS; 0.1x SSC, 0.1% SDS), before being wrapped in Saranwrap and exposed to film (Kodak X-OMAT) in a radioactivity cassette at -80°C. Where necessary, the membrane was re-washed in the third solution and again exposed to film.

Screening by PCR

Occasionally, large numbers of colonies were screened by PCR. This was advantageous when insertional efficiency was low, and mini-prep DNA extraction on such scale as was necessary to identify a positive clone would have been labour-intensive. In these instances, colonies were randomly picked from the desired LB Agar plate, and each mixed by pipetting in 50µl LB containing the appropriate selective agent. 1µl of each of these diluted clonal samples was used for PCR, each in a total reaction volume of 50µl.

Phenol:Chloroform:IAA Extraction and Purification of Plasmid DNA

High-purity DNA, free of protein contaminants, was prepared using the standard phenol:chloroform:isoamyl alcohol (IAA) method described by Sambrook and Russell (2001). This was performed routinely for all samples obtained by midi-prep DNA extraction, since it is a recommended treatment for samples that are to be sequenced, as well as for plasmids that are to be used in transfection. Linearized plasmids, for use in transfection or *in vitro* transcription of digoxigenin (DIG) labelled riboprobes, were also treated in this manner. DNA samples were diluted in 400µl of double-distilled water, and mixed thoroughly by inversion with an equal volume of phenol:chloroform:IAA (25:24:1), that had been made with pre-equilibrated phenol, pH7.5. Samples were centrifuged for 4mins at 10 000 xg, and the aqueous layer was carefully removed and retained. This aqueous solution was subject to further treatments with phenol where necessary, until no proteinaceous material could be observed at the interface between the aqueous and organic layers. The aqueous layer was subsequently mixed thoroughly by inversion with an equal volume of chloroform, and centrifuged at 10 000 xg for 4mins to

separate the aqueous and organic phases. Again, the aqueous layer was removed and retained, and subsequently mixed with 3M NaOAc (pH5.5) (0.1x total volume) and ice-cold absolute ethanol (2x total volume). The sample was mixed by inversion and placed at -80°C for 1 hour, to precipitate the DNA, before undergoing centrifugation at 10 000 xg, 4°C, for 20mins. The supernatant was removed, and the pelleted DNA sample washed with 70% ethanol. Finally, the wash solution was removed and the pellet left to air-dry, undercover at room temperature, for approximately 10mins before being resuspended in a suitable volume of autoclaved double-distilled water. Linearized plasmid for the synthesis of DIG-labelled riboprobes was resuspended in DEPC-treated autoclaved double-distilled water.

DNA Sequencing

All plasmid DNA samples for sequencing were subject to phenol:chloroform:IAA extraction and spectrophotometry, to ensure that they were submitted at sufficient purity (A_{260}/A_{280} greater than 1.8) and at the correct concentration (~100ng/ml). Samples were analysed using an ABI automated fluorescent dye sequencing facility (DNA Sequencing Facility, Department of Biochemistry, University of Cambridge, UK). SP6, T7 and T3 sequencing primers were provided by the DNA Sequencing Facility. All other sequencing primers were submitted at a concentration of 10pmol/μl, along with the relevant plasmid DNA samples.

Bacterial Expression of Recombinant Nogo-66-$(His)_6$

The sequence encoding the growth cone collapsing Nogo-66 loop sequence was amplified by RT-PCR from rat brain total RNA, using the primers CCC ATA TGA GGA TAT ATA AGG GCG TGA TC and CTC CTC GAG TCA GTG GTG GTG GTG GTG GTG CTT CAG GGA ATC AAC TAA ATC. The DNA product was subsequently digested with *Nde*I and *Xho*I, before in-frame ligation into the same sites within pET28a (Novagen). The sequence was verified by automated dye fluorescent sequencing, prior to transformation of BL21 λDE3 lysogen bacteria (Novagen). Postive bacterial clones were tested for expression of Nogo-66-$(His)_6$ by induction with 1mM IPTG for 3 hours. Total cellular protein of uninduced and induced cells from each colony was resolved by 20%

SDS-PAGE. Coomassie staining of the gel was used for comparison of protein fractions of uninduced and induced cells. Following identification of expressing colonies, one was selected to assess the fractional localization of the induced protein. This was performed according to the pET vector system manual (Novagen). Examination of the media, periplasmic, soluble and insoluble cytoplasmic fractions revealed that the majority of the protein was retained in inclusion bodies (in the insoluble cytoplasmic fraction), as is often the case with bacterially-expressed recombinant proteins. The inclusion bodies were solubilized in 6M urea for FPLC purification.

FPLC Purification of Recombinant Nogo-66-(His)$_6$

Histrap columns (Amersham), primed with nickel as per the manufacturer's instructions, were used in conjunction with an FPLC machine (Amersham) to purify Nogo-66-(His)$_6$. Briefly, 6M urea containing the induced Nogo-66(His)$_6$ from solubilized inclusion bodies was first passed through the nickel primed columns to capture the protein, which was ultimately eluted in a solution of 6M urea containing a rising concentration of imidazole (0 → 500mM) over the course of ten minutes. As the protein was eluted from the columns into 10 x 5ml fractions, at one minute intervals, continuous optical density measurements were recorded at an absorbance of 280nm. Samples of each eluted fraction, as well as samples of total cell protein from induced and uninduced transformed bacteria, were resolved by SDS-PGE. This was performed using a pre-made 12% Bis Tris NuPAGE® gel (Invitrogen) with MES buffer, and a broadrange pre-stained SDS-PAGE molecular weight standard (Bio-Rad). Bands of protein were visualized with Colloidal Coomassie® Stain (Invitrogen).

Extraction and Analysis of Recombinant HSV-1 genomic DNA

Extraction of Recombinant HSV-1 Genomic DNA

In order to obtain recombinant HSV-1 genomic DNA, complementing cells were transduced with replication-incompetent virus (strain = 1764/4-/27in/RL1+/pR19) at an MOI of 0.1, and cultured in the presence of 3mM HMBA. Upon observation of complete cytopathic effect, typically 48-72hrs after transduction, growth media was removed, the cell monolayer washed with HBSS and then lysed with DNAzol (Gibco-BRL Life

Technologies). Hereafter, the extraction of viral DNA was performed as described earlier.

Southern Blot Analysis of Recombinant Viral DNA

Sample Preparation and Gel Electrophoresis

Samples of DNAzol extracted recombinant viral DNA, as well as the source viral DNA (negative control), and the source shuttle plasmid (positive control) were digested by restriction endonucleases. Typically, 100ng of each viral DNA, and 20ng of midi-prep plasmid DNA, were digested with at least 10 units of each enzyme in a suitable buffer. The digestion reactions were made to a final volume of 50µl, and incubated overnight at a suitable temperature. Samples were loaded in alternate lanes of a 1% agarose-TAE gel and resolved alongside 5µl of 1kb DNA ladder (Gibco-BRL Life Technologies). The DNA ladder was visualized on a UV transilluminator and photographed against a fluorescent ruler for future reference.

DNA Transfer (Southern Blot)

The DNA was first 'nicked' by leaving the gel in place on the UV transilluminator for 2mins, at the highest setting. It was subsequently immersed for 45mins in denaturing solution (1.5M NaCl, 0.5M NaOH), briefly washed with double-distilled water, and then immersed for at least 30mins in neutralising solution (2M NaCl, 1M Tris pH5.5). An inverted gel tray was stood in a shallow tank of 20xSSC (150mM NaCl, 15mM sodium citrate pH8.0), and covered by a wick of 3mm Whatman paper (Whatman, Maidstone, Kent, UK). The gel was placed face-down on this platform and covered with a piece of Hybond N+ nylon membrane, pre-soaked in 6x SSC. Three pieces of 3mm Whatman paper, pre-soaked in 20x SCC, were layered on top and gently rolled with a plastic pipette to ensure the removal of any air bubbles. Several inches of dry paper towels were placed on top, followed by a sheet of glass and a weight. The blotting apparatus was left overnight for the DNA to migrate to the nylon membrane by capillary action. The membrane was washed briefly in 6x SSC, left under cover to dry for 20mins, and cross-linked twice with a UV Stratalinker 2400. Either the membrane was used immediately for radioactive analysis, or it was left under cover for a further 20mins to air-dry before

being placed in storage at 4°C, sandwiched between 3mm Whatman paper and sealed with Saranwrap.

Membrane Analysis

Radioactive analysis of the membrane with $\alpha[^{32}P]$dCTP-labelled DNA probes was performed as described previously.

Synthesis of DIG-Labelled Riboprobes for *In Situ* Hybridisation

In Vitro Transcription

The desired plasmid was first linearized using a suitable restriction endonuclease, and then phenol:chloroform:IAA-extracted as described earlier. Synthesis of digoxigenin-labelled riboprobe was performed using a commercial digoxigenin (DIG) labelling kit (Boehringer Mannheim), as per the manufacturer's instructions.

RNA Precipitation

The DIG-labelled riboprobe was precipitated by mixing the reaction product with a 0.1 volume of DEPC-treated 4M LiCl and 2 volumes of absolute ethanol (-20°C), before placing at -80°C for at least 1hour. The sample was centrifuged at 10 000 xg, 4°C, for 30mins to pellet the RNA. A single wash of the pellet was performed with 70% ethanol (-20°C) made with DEPC-treated ddH_2O. The sample was centrifuged at 10 000 xg, 4°C, for 5mins and the supernatant discarded. After 5mins of air-drying under cover, the RNA pellet was re-suspended in an appropriate volume of either (i) DEPC-treated ddH_2O with 1% v/v RNasin (Promega, Southampton, UK), or (ii) formamide. In the former case the sample was first incubated at 37°C for 30mins, prior to aliquoting and storing at -20°C.

Assessment of Riboprobe Integrity

1µl of riboprobe was mixed with 2x formaldehyde loading buffer (10% glycerol, 2mM EDTA pH8.0, 0.05% w/v bromophenol blue, 0.05% w/v xylene cyanol) and resolved on a 1% agarose-MEA gel (1% w/v agarose, 1x MEA [10x MEA = 200mM MOPS, 10mM EDTA, 50mM sodium acetate, titrated to pH7.2 with NaOH], 20% v/v formaldehyde) without ethidium bromide. Samples were resolved against a DIG-labelled riboprobe of

known size, for reference, and then transferred to a nylon membrane by northern blotting. With the exception of the UV nicking, denaturation and neutralisation steps this was essentially the same as described for Southern blotting. The UV cross-linked membrane was washed in buffer 1 (100mM Tris-HCl, 150mM NaCl pH7.5) for 15mins, blocked with modified buffer 2 (1% Boehringer blocking reagent, 0.5% BSA fraction V in buffer 1) for 30mins, incubated with alkaline phosphatase-conjugated anti-DIG antibodies diluted 1:5000 in modified buffer 2 for at least 30mins, washed in buffer 1 for 15mins, equilibrated in buffer 3 (100mM Tris-HCl, 100mM NaCl, 50mM $MgCl_2$ pH9.5) for 15mins, and developed in darkness for 15mins with buffer 3 containing 0.34mg/ml 4-nitroblue tetrazolium chloride (Boehringer), 0.175mg/ml 5-bromo-4-chloro-3s-indolylphosphate (Boehringer). The alkaline phosphatase catalysed reaction was quenched with buffer 4 (10mM Tris-HCl, 1mM EDTA, pH8.0) for 10mins. Only those samples that gave a single sharp band of the correct size were used for *in situ* hybridisation.

TISSUE CULTURE

Health and Safety Category 1 regulations were observed for all work undertaken with replication-incompetent HSV-1.

Tissue Culture Materials and Reagents

All tissue culture plastics were purchased from Nunc, CellStar or Sarstedt. Media, supplements and other common tissue culture reagents were purchased from Gibco-BRL Life Technologies unless otherwise stated.

Mammalian Cell Lines

Unless otherwise stated, full growth medium (FGM) was used in culturing cell lines. FGM comprises Dulbecco's modified Eagle medium (DMEM), 10% v/v foetal calf serum, and 100units/ml of penicillin and streptomycin. Serum free medium (SFM) was used during DNA transfection or viral transduction of cultured cells; it consists of DMEM and 100units/ml of penicillin and streptomycin.

Baby Hamster Kidney Cells (BHKs)

Baby Hamster Kidney Cells (clone 13) (Macpherson and Stoker, 1962) were obtained from the Imperial Cancer Research Fund, London, UK. These cells were cultured in FGM and incubated at 37°C in 5% CO_2. BHKs were passaged by trypsination (0.25% trypsin in versene at 37°C, 5% CO_2, for 2-3mins) after a single wash with Hank's Buffered Saline Solution (HBSS) at room temperature. The activity of the trypsin and versene solution was quenched by the addition of an appropriate volume of FGM, and the resultant cell suspension was used in seeding as desired.

27/12/M:4 (MAM49)

27/12/M:4 are complementing cells, derived from the BHK clone 13 cell line, which have been engineered to stably express ICP4 and ICP27 (Thomas et al., 1999). They are necessary for the propagation of those recombinant HSV-1 strains lacking functional copies of these genes. These cells were cultured in FGM containing 5% v/v tryptose phosphate broth, 800mg/ml neomycin (Gibco-BRL Life technologies, Paisley, UK) and 750mg/ml of zeocin (Cayla, Toulouse, France). 27/12/M4:4 cells were passaged as described for the BHK clone 13 cell line. Cells grown for viral infection were done so in the absence of neomycin and zeocin.

HT1080

The HT1080 human fibrosarcoma cell line (Rasheed et al., 1974) was obtained from ECACC (No. 85111505). These cells were cultured in FGM and incubated at 37°C, in 5% CO_2. Passaging was performed as described for BHK (clone 13) cells.

PC12

The PC12 cell line is derived from a rat adrenal phaeochromocytoma (Greene and Tischler, 1976), and was obtained from ECACC (No. 88022401). The cell line can be reversibly induced to differentiate into a neuronal morphology, characterized by the extension of axons, by incubation with the active 2.5S NGFβ subunit. PC12 cells were cultured in RPMI1640 media, with 10% foetal calf serum, 2mM glutamine and 1x penicillin/streptomycin. Cells were not routinely grown on collagen type IV coated

coverslips, but care was taken not to dislodge cells growing on electrostatically-charged TC plastic. To passage the cells, the media was replaced with a small volume of HBSS and the cells were dislodged by agitation. The cell suspension was used for seeding as desired.

Cell Line Storage

Following trypsination and neutralisation with FGM, cells were pelleted by centrifugation at 1 000 xg, for 10mins. The supernatant was discarded and the cells were resuspended in ice-cold DMEM containing 20% v/v FCS. A second ice-cold solution of DMEM containing 40% FCS and 16% dimethylsulphoxide (DMSO) was added in an equal volume. Typically, cells from a 175cm^2 flask were resuspended in a total volume of 10mls. The suspension of cells was immediately distributed as 1ml aliquots into pre-labelled ice-cold 2.0ml cryovials; these were quickly wrapped in paper towels, placed in a polystyrene container and stored at -80°C overnight. After 24hrs, the frozen cryovials were transferred to liquid nitrogen (-180°C) for longterm storage.

To defrost, aliquots of frozen cells were incubated at 37°C and immediately added to 10ml of FGM. This cell suspension was centrifuged at 1 000 xg for 10mins. The supernatant was discarded, and the cell pellet resuspended in 1ml FGM. Resuspended cells were seeded into a 25cm^2 flask and incubated at 37°C, in 5% CO_2, until confluent.

Transfection with Plasmid DNA

Transient Transfection

Transfections of plasmid DNA were based on the calcium phosphate method originally described by Stow and Wilkie (1976). All transfections were performed with phenol:chloroform:IAA extracted midi-prep DNA. Cells were cultured in 35mm wells such that they would reach 70-80% confluency at the time of transfection. For each transfection, two tubes were set up: the first containing 31µl 2M $CaCl_2$, 1µg plasmid DNA and 20µg of phenol:chloroform:IAA extracted sheared herring sperm DNA; the second containing 400µl HEBES transfection buffer (140mM NaCl, 5mM KCl, 0.7mM Na_2HPO_4, 5.5mM D-glucose, 20mM Hepes, titrated to pH7.05 with NaOH and sterilized

through a 0.2μm filter). The contents of the first tube were mixed by slow pipetting, and then added drop-wise to second tube whilst gently agitating to mix. The combined solution was left for 40mins at room temperature, allowing the DNA to precipitate. The FGM was removed from a 35mm well and replaced with transfection mixture. After 1 hour incubation at 37°C, in 5% CO_2, the well was over-layed with 1ml SFM and returned to incubation. 6 hours later all media was removed, the cell monolayer washed twice with 2ml FGM, and then shocked for 90s with ice-cold 20% v/v DMSO in HEBES. The cells were washed twice with 2ml FGM, and then over-layed with a final volume of 2ml FGM before being returned to incubation.

Stable Transfection (Construction of the eGFP-Expressing BHK Cell Line)

Stable transfection of plasmid DNA was necessary for the construction of the eGFP-expressing BHK cell line, termed 'clone 2B1'. The initial process was essentially the same as that described for transient transfection, except that linearized plasmid was used - peGFP-N1 (Clontech), linearized with *Apa*LI. Two days following the transfection of one 6-well of BHKs, the cells were trypsinized and seeded into 3x 15cm dishes (Sarstedt). Selection of transfected cells was achieved through the addition of neomycin to a final concentration of 750μg/ml (members of our laboratory have used killing curves to demonstrate that this is the minimum required dose to kill all untransfected cells). After a further two days of incubation at 37°C, in 5% CO_2, colonies were selected on the basis of uniformity and intensity of fluorescence under an inverted fluorescent microscope. Selected colonies were picked in a volume of 100μl using a P200 Gilson microtitre pipette, and were subsequently triturated in one well of a 96-well plate. Two 96-well plates of clones were grown for 2 days under standard incubation conditions and then screened by fluorescence microscopy to identify those clones with uniform expression of eGFP at moderate/strong intensity. Sixteen clones of cells were scaled up for growth in 6-well plates before one clone, termed 'clone 2B1', was ultimately identified as the most suitable for use in eGFP knock-down experiments. Aliquots of the clone 2B1 stable eGFP-expressing cell line were frozen in liquid nitrogen for longterm storage, using the method outlined earlier.

Production of Recombinant Replication-Incompetent HSV-1 vectors

Virus Strain

The replication-incompetent strain of HSV-1 described in this thesis, termed '1764/4-/27in/RL1+', was originally derived from the 17syn+ strain (Brown et al., 1973). The '1764' vector terminology refers to 17syn+ with deletions of both copies of ICP34.5 (Maclean et al., 1991) as well a 12bp inactivating mutation in the carboxy terminal transactivating domain of VP16, termed *in*1814 (Ace et al., 1989). The '4-' refers to the deletion of both copies of ICP4, whilst both the '27in' and the 'RL1+' refer to the historical deletion and replacement of functional copies of ICP27 and ICP34.5, respectively. In summary, this strain of virus lacks both copies of ICP4 and possesses an inactivating 12bp insertion in the transactivating domain of VP16, but otherwise has the full complement of HSV-1 genes.

This strain of HSV-1 was propagated on 27/12/M:4 cells grown in FGM supplemented with 3mM hexamethylene bisacetamide (HMBA). The 27/12/M:4 cells are complementing cell line that stably express ICP4 and ICP27. HMBA compensates for the inactivating mutation in the transactivating domain of VP16.

Homologous Recombination Transfections

Transfections were broadly performed as described above, except that 10-30μg of viral DNA was also included in the first tube. Transfected 27/12/M:4 cells were harvested by freeze-thawing after 5-7 days, when numerous plaques had become visible by light microscopy. Harvested cells were titred in 35mm wells, and the recombination efficiency was determined using fluorescence microscopy. Recombinant viral plaques appeared white under UV illumination, whilst non-recombinant plaques appeared green.

Purification of Viral Recombinants by Plaque Selection

Cells were seeded into six 35mm wells and cultured until ~80% confluent. The growth media was removed and harvested transfection product was serially diluted 1:2 with SFM, such that a final volume of 500μl could be applied per well. 500μl of undiluted harvested transfection product was added to the first well, with the five serial dilutions

being added to the remaining wells. After 1hour of incubation at 37°C, in 5% CO_2, the wells were overlayed with 2ml of media consisting of one part 1.6% w/v carboxymethycellulose and two parts FGM, with HMBA added to a final concentration of 3mM. The cells were incubated at 37°C, in 5% CO_2, for two days before recombinant plaques were identified and picked under the 520nm light wavelength of an inverted fluorescent microscope. When a pure recombinant population had been selected, i.e. when no eGFP-expressing cells could be identified, a single plaque was picked and used to infect a 35mm well of 80% confluent cells, as described above (except that no CMC was used in over-laying the cells, only FGM containing 3mM HMBA). After 3 days of incubation, under standard conditions, the well was harvested by freeze-thawing and retained as the master stock; a small volume was used for virus propagation, and the remainder was stored in liquid nitrogen.

Production of High Titre Stocks of Recombinant HSV-1

27/12/M:4 cells were cultured in a 35mm well until ~90% confluent, and were subsequently infected with an appropriate volume of virus from the master stock, as described previously. However, after the 1 hour incubation at 37°C, in 5% CO_2, the cells were over-layed with 2ml FGM containing 3mM HMBA. The cells were incubated until complete cytopathic effect (CPE) had been observed, typically 2-3 days post transduction, whereupon the cells were harvested by freeze-thawing. The propagation of the virus was gradually scaled-up in 25cm^2, 80cm^2 and 175cm^2 flasks. At least ten 175cm^2 flasks, infected at an MOI of 0.1, and harvested by freezing upon observation of CPE were used to obtain a high titre stock of virus. Their contents were pooled after defrosting, and were centrifuged at 600 xg, 4°C, for 45mins to pellet cellular debris. The supernatant was collected and filtered through 5.0μm (Whatman, Maidstone, UK) and 0.45μm filter disks (Gelman Life Sciences, Ann Arbor, Michigan, USA). The filtered virus-containing media was transferred to Beckman centrifuge bottles, and centrifuged at 12 000 xg, 4°C, for 2hrs. The supernatants were discarded and the virus pellets were resuspended under sterile conditions in no more than 500μl combined total volume. The virus suspension was transferred to an autoclaved glass sonicating vial, sealed, and subjected to sonication in a water bath (three 20s bursts were each interrupted by a 1min

incubation on ice). The virus suspension was subsequently aliquoted in 50µl to pre-labelled chilled cryovials, which were transferred to liquid nitrogen for storage. The virus titre was determined using the standard assay of virus titre, described below.

Assay of Viral Titre

27/12/M:4 cells were seeded into six 35mm wells and cultured until 70-80% confluent. A range of 1:10 serial dilutions of virus suspension in SFM were prepared in a 96 well plate, and those ranging from $1x10^{-9}$ to $1x10^{-4}$ml of the original virus suspension were used to infect each cell monolayer in a total volume of 500µl SFM. After 1 hour of incubation at 37°C, in 5% CO_2, the media was removed and the cells were over-layed with 2ml of media comprising one part 1.6% w/v carboxymethylcellulose (CMC) and 2 parts FGM (1:2), with HMBA added to a final concentration of 3mM. The cells were incubated for 48hrs at 37°C, in 5% CO_2, and the number of plaques per well, as determined by fluorescence microscopy, was used to calculate the viral titre of the original virus suspension. Titres are given as plaque forming units (pfu) per ml.

Primary Cultures of Mammalian Cells

Dissociated Cultures of Mouse/Rat Embryonic Cortical Neurons

The brains of four pups from each of three litters were carefully dissected to separate the cerebral cortices from the ganglionic eminence in artificial cerebral spinal fluid (ACSF: 25mM KCl, 2mM KH_2PO_4, 25mM HEPES, 37mM D-Glucose, 10mM $MgSO_4$, 175mM sucrose, 0.5mM $CaCl_2$, 1x penicillin-streptomycin, pH7.4). The cortices were incubated in 0.05% trypsin with 100ug/ml DnaseI in DMEM:F12 for 15 minutes at 37°C. Trypsinisation was quenched by addition of DMEM:F12 containing 10% FCS for 5mins at 37°C. The excised cortical tissue was then triturated with a fire-polished Pasteur pipette until no cellular aggregates were visible. The homogenous cellular suspension was subsequently pelleted by centrifugation at 1 000 xg for 3mins. The supernatant was discarded and the pellet was resuspended in growth media (DMEM:F12, 2mM L-glutamine, 1x penicillin-streptomycin, with 1:50 dilution of B-27). Cells were plated out on 13mm poly-L-lysine:laminin coverslips at a density of 1-2million cells per millilitre and left for 30 minutes at 37°C to attach. Following attachment, the cells were overlaid

with growth media, and incubated at 37°C with 5% CO_2. The media was changed daily. After 3 days *in vitro* (DIV), the cells were fixed in 4% paraformaldehyde (PFA) in PBS for twenty minutes, and rinsed in PBS prior to immunohistochemistry.

Preparation of Poly-L-Lysine:Laminin Coated Coverslips

13mm glass coverslips were immersed in concentrated chromic sulphuric acid overnight, rinsed in tap water for several hours, and stored in 70% EtOH. As required, these were place in 24-wells under sterile conditions, and left to dry in a tissue culture hood. 100µl aliquots of poly-L-lysine:laminin solution (10µg/ml:10µg/ml), made up in sterile ddH_2O, were added per coverslip. Having been left to dry out overnight in a tissue culture hood, the coverlslips were rinsed three times with sterile ddH_2O prior to use.

Dissociated Cultures of Rat Postnatal Cerebellar Granule Neurons

The cerebellar corices were carefully dissected from the brains of 6 P8 Sprague-Dawley rats and collected in a Petri-dish containing ice-cold HBSS, where the meninges were removed. The tissue was diced into smaller pieces and incubated in 0.05% trypsin with 100µg/ml DNaseI in DMEM:F12 for 15mins at 37°C. The solution was carefully removed by aspiration, and the segments of tissue washed with HBSS. A solution of DNaseI, pre-warmed to 37°C, was added (0.1% DNase I, 13.75mM glucose in BME) and trituration was performed with a fire-polished Pasteur pipette. The cellular suspension was diluted with 2 volumes of ice-cold HBSS, and then placed on ice for 5mins to allow the debris to settle. The supernatant was carefully layered on to an ice-cold Percoll cushion (40.5% Percoll in HBSS) and centrifuged at 1200 xg, 4°C, for 20mins to separate the neuronal and non-neuronal cell-types. The HBSS, the non-neuronal cells at the interface, and most of the Percoll was carefully aspirated, leaving the neuronal cell pellet in a small volume of residual Percoll. These cells were resuspended in HBSS and centrifuged at 80 xg, 4°C, for 10mins. The supernatant was discarded, the cell pellet re-suspended in culture medium (BME, 2mM glutamine, 1.5M glucose, 2M KCl, heat-inactivated FCS [57°C, 30mins], 1x penicillin and streptomycin), and the cellular suspension again centrifuged at 80 xg, 4°C, for 10mins. Finally, the cell pellet was again re-suspended in culture medium and the cellular density determined using a

haemocytometer. Cells were diluted appropriately and plated on poly-L-ornithine coated coverslips at a density of 1 x 10^6cells/13mm well. Cultures were incubated at 37°C, in 5% CO_2. After 24hrs, cytosine arabinoside was added to a final concentration of 10μM.

Preparation of Poly-L-Ornithine Coated Coverslips

13mm glass coverslips were removed from storage in absolute ethanol, placed in 24-wells under sterile conditions, and left to air-dry. The sterile stock solution of poly-L-ornithine (10mg/ml) was diluted to a final concentration of 10μg/ml in autoclaved dH_2O. 1.5ml of the working stock was added per 24-well, and incubated for 2 hours at 37°C. The poly-L-ornithine solution was subsequently removed and the wells washed twice with 1.5ml autoclaved dH_2O. The coverslips were then left to dry *in situ* in a sterile environment. Plates containing coated coverslips were either used on the day of preparation, or were stored at 4°C for up to three days.

Protein Extraction and Analysis

Standard Protein Extraction from Cultured Cells

Growth media was removed from cultured cells, and the monolayer washed twice with 1x PBS. Cells were lysed in an appropriate volume of 1x protein sample buffer (5% β-mercaptoethanol, 50mM Tris-HCl pH8.9, 6% v/v glycerol, 2% w/v SDS and 0.005% w/v bromophenol blue), heated to 95°C and snap-frozen at -20°C until required. Samples were again boiled prior to resolution by SDS-polyacrylamide gel electrophoresis.

SDS-PAGE

SDS-PAGE was essentially performed as described by Sambrook and Russell (2001). Gels were prepared in a vertical gel electrophoresis separation system, with resolving gel layer typically containing 20% acrylamide (20% acrylamide in 375mM Tris HCl pH 8.8, 0.1% w/v SDS, 0.1% ammonium persulphate, and 20μl TEMED in a total volume of 50mls), although this was dependent on the size of the protein of interest. The stacking gel contained 5% acrylamide (5% acrylamide in 0.125mM Tris pH6.8, 0.1% w/v SDS, 0.1% ammonium persulfate, and 10μl TEMED in a total volume of 10mls). Protein samples were mixed with sample buffer and resolved at a constant current (35mA per

gel), with variable voltage, in 1x running buffer (25mM Tris, 250mM glycine, 0.1% w/v SDS, pH8.3). Electrophoresis was continued until the proteins of interest had migrated to the middle of the resolving gel, as determined by reference to the Rainbow molecular weight markers (Amersham).

Staining of SDS-PAGE Gels with Coomassie R250

Gels were carefully removed from the electrophoresis system. The stacking gel was cut off with a sharp scalpel and discarded, whilst the resolving gel was immersed in solution 1 (2% w/v Coomassie Brilliant Blue R250, 25% v/v isopropanol, 10% v/v glacial acetic acid) and left under gentle agitation for 30mins. The gel was then transferred to solution 2 (2% w/v Coomassie Brilliant Blue R250, 10% v/v isopropanol, 10% v/v glacial acetic acid) and left under gentle agitation for at least an hour. Having been fixed and stained, the gel was then transferred to a de-staining solution (15% methanol, 7.5% glacial acetic acid) to remove the unbound dye. The gel was left under gentle agitation until bands of stained protein had become clearly visible against an unstained background, a process typically requiring at least four hours.

Transfer of Proteins to Nitrocellulose Membranes (Western Blot)

Resolved proteins were transferred from SDS-PAGE gels to Hybond C nitrocellulose membranes using the wet transfer method, originally described by Towbin et al. (1992). The SDS-PAGE gel, a nitrocellulose membrane and six appropriately sized pieces of 3mm Whatman paper (Whatman International Ltd., Maidstone, Kent, UK) were pre-soaked in transfer buffer (50mM Tris, 180mM glycine, 0.1% w/v SDS and 20% v/v methanol) and assembled in the Trans-Blot^{TM} apparatus (Bio-Rad, Hemel Hempstead, Herts, UK), as instructed by the manufacturer. The transfer was conducted at a constant ampage, with variable voltage, either (i) overnight at 20mA, 4°C, or (ii) for 2hrs at 70mA, 4°C.

Immunodetection of Proteins on Western Blots

Nitrocellulose membranes were incubated for 1hr with blocking solution (5% w/v Marvel in 1x PBS). Primary antibody, raised against the protein of interest, was diluted in the

blocking solution to suitable final concentration, and was incubated with the membrane for 2 hrs. Three 10min washes were performed with PBS-T (1xPBS, 0.1% Tween-20), before the horse radish peroxidase (HRP) conjugated goat anti-IgG secondary antibody (Dako) was applied (diluted 1:1000 in blocking solution). After 1 hour of incubation, the nitrocellulose membrane was again washed 3x 10mins with PBS-T. Enhanced Chemiluminescence reagent (ECL; Amersham) was used, as per the manufacturer's instructions. The membrane was quickly wrapped in Sarawrap and placed in a cassette under film (Kodak X-OMAT). Films were developed after varying exposure times (30s to 30mins) to visualise immunodetected proteins.

Equalisation of Protein loading in Western Blot Analysis

Sample protein concentrations were determined with RcDc reagent (Biorad), as per the manufacturer's instructions. The optical density of each sample was measured and compared against the values obtained from the standard curve (known concentrations of albumin), in order to calculate sample protein concentration. 20μg of sample protein was used for western blotting, unless stated otherwise.

Immunocytochemistry

27/12/M:4 cells and BHKs were grown on sterile uncoated 13mm glass coverslips, primary cultures of embryonic or postnatal cortical neurons on poly-L-lysine:laminin coated coverslips (prepared as described earlier), and primary cultures of post-natal cerebellar granule neurons on poly-L-ornithine coated coverslips.

Fixation of cells was performed by removing tissue culture media and adding an appropriate volume of 4% PFA in 0.1M phosphate buffer, prewarmed to 37°C. Cells were incubated with fixative at 37°C, in 5% CO_2, for 10mins, and then washed two times with an appropriate volume of 1x PBS. Coverslips were stored, immersed in 1x PBS, at 4°C. Immunoreaction was performed broadly in the same manner as described for slide-mounted tissue sections, except that coverslips were placed culture side up on strips of Parafilm mounted on glass slides.

Flow Cytometry

Cells cultured in 6-wells were trypsinized in 100µl 0.25% trypsin in versene for 5mins at 37°C, in 5% CO_2, before neutralisation with 400µl of the appropriate FCS containing growth media. Cells were pelleted at 1 000 xg, for 10mins at 4°C, and resuspended in 100µl ice-cold HBSS. Fixation was achieved by adding four volumes of fixative (4% PFA in 0.1M PB), and incubating for 5mins under standard conditions. Samples were again pelleted at 1 000 xg, for 10mins at 4°C, and resuspended in 400µl HBSS. Samples were transferred to FACs vials and stored on ice until analysed using a Beckton-Dickinson FACS Calibur.

ANIMAL EXPERIMENTATION

Animals

All animals were housed by UCL Biological Services in standard polypropylene cages, under an illumination cycle of 12 hours light and 12 hours darkness, with access *ad libitum* to food pellets and water.

Rats

Sprague-Dawley and Lewis rats were supplied by UCL Biological Services and Charles River, respectively. Adult rats, used in the experiments described herein, typically weighed 200-300g.

Mice

Balb/c mice were supplied by UCL Biological Services, as were ICR mice.

Animal Surgery

All animal surgery was performed under licence, and in accordance to the regulations of the UK Home Office and the UCL Animal Ethics Committee.

Sterilisation of Surgical Equipment

All Surgical instruments, drapes and swabs were routinely sterilized by autoclave, for 20mins at 120°C.

Anaesthesia

Anaesthesia was initially induced by delivery of 1.5% oxygen, 3% nitrous oxide and 4% Halothane (Fluothane, ICI) to an anaesthetic chamber. Subsequently, the animal was prepared for surgery and transferred to the operating area where anaesthesia was administered via a scavenging nose cone. The level of Halothane was reduced to 1.5-2% once the animal had become deeply anaesthetised, as indicated by the loss of toe-pinch reflex.

Animal Preparation

Veterinary hair clippers were used to shave the appropriate areas prior to surgery. These areas were also wiped clean with alcoholic swabs (70% EtOH) before the animals were rested on a heated pad in the operating bay. The scavenging nose cone for anaesthetic delivery was immediately attached, and the animal covered with a sterile drap.

Surgical Procedures

A Zeiss operating microscope was used in performing most surgical procedures.

Transection of the Rodent Corticospinal Tract

Animals were deeply anaesthetised and the skin incised along the midline of the neck. The trapesius muscles and postaxial musculature were separated along the midline and the vertebral column identified. A laminectomy of the C6 vertebra was performed with malleus scissors. The dura was opened and the dorsal columns severed with microsurgical forceps, as deep as the central canal, thus severing both the ascending dorsal columns and the dorsal corticospinal tracts. The musculature was repaired with silk sutures and the skin closed with Michel clips. N.B. This procedure was performed by Prof. P.N. Anderson.

Transection of the Rodent Sciatic Nerve

A skin incision, parallel and caudal to the femur, was made in the left thigh, and the underlying muscles were exposed. The muscles were separated by blunt diossection and the left sciatic nerve located. Transection of the nerve was performed at mid-thigh level with microsurgical scissors. The skin was closed with Michel clips. N.B. This procedure was usually performed by Prof. P.N. Anderson.

Transection of the Dorsal Root (Rhizotomy)

A left hemilaminectomy was performed at the L2 vertebra and the dura opened. The L3 and L4 dorsal roots were identified by their large diameter and transected with microsurgical scissors. The cut ends were reanastomosed with a single 10/O suture. The dura was closed with 10/O sutures, the musculature repaired with silk sutures and the skin closed with Michel clips. N.B. This procedure was performed by Prof. P.N. Anderson.

Crush of the Rodent Optic Nerve

The scalp of deeply anaesthetised Sprague-Dawley rats was opened along the midlne and the left orbit along its superor margin. The optic nerve was located in its dural sheath and the sheath opened with microsurgical sutures. The optic nerve was then crushed 1-2 mm behind the eye, avoiding damage to the ophthalmic artery. N.B. This procedure was performed by Prof. P.N. Anderson.

Autologous Graft of Peripheral Nerve to Rodent Thalamus

Adult female Sprague-Dawley rats, weighing 180-250g at the time of implantation, received peripheral (tibial) nerve grafts to the thalamus. The rats were anaesthetised with Halothane, nitrous oxide and oxygen mixture. The scalp was opened and a bur hole made in the left parietal bone and the dura opened. Segments approximately 1.5cm long of the left tibial nerve were removed and one end implanted through the craniotomy into the left thalamus, using a glass micropippette, to co-ordinates (2.3mm posteror to bregma, 2.6mm lateral to the midline and to a depth of 6mm) taken from the atlas of Paxinos and Watson (1986). The graft was fixed to the skull surrounding the craniotomy with

cyanoacrylate glue (Histoacryl, B. Braun, Germany). The distal end of the graft was left lying on the surface of the skull. The scalp was closed with Michel clips. This procerure was performed by Dr. G. Campbell and Prof. P.N. Anderson.

Autologous Graft of Peripheral Nerve to Rodent Cerebellum

These were performed in a similar manner to the grafts in thalamus, except that the bur hole was made in the left occipital bone and the graft implanted with its proximal end in the region of the cerebellar deep nuclei (co-ordinates: 11.3mm posterior to bregma, 3mm lateral to midline and 6mm deep). N.B. This procedure was performed by Dr. M.R.J. Mason.

Microinjection of Replication-Incompetent HSV-1

The cervical spinal cord of deeply anaesthetised Lewis rats was exposed as described above. An opening in the pia was made with a fine needle along the line of the dorsal root attachment point. A Hamilton needle approximately 300μm external diameter was lowered to a depth of 1.5 mm into the cord through the opening in the pia and allowed to sit in place for a minute. Two microlitres of HSV-1 suspension was then injected over a period of 15 minutes. The needle was withdrawn after a further 5 minutes, the dura closed and the wound closed in layers. N.B. This procedure was performed by Prof. P.N. Anderson.

Post-Operative Care

After surgery, animals were placed in an incubator, attended until they had regained full consciousness, and then transferred to cages.

Harvesting of Animal Tissues

All animals, operated or unoperated, were culled in accordance to Schedule 2 regulations of the UK Home Office. All animals were overdosed with Halothane, except those neo-natal animals used for establishing primary cultures; these were decapitated.

For RNA Extraction

Organs or tissues were immediately dissected, and removed to a sterile Petri Dish, containing ice-cold DEPC-treated 1xPBS, where they were first rinsed and then diced into small pieces with a sterile scalpel blade. Diced tissue was collected and immersed in an appropriate volume of ice-cold Trizol reagent (Gibco-BRL). RNA was subsequently extracted as described previously.

For In Situ Hybridisation

Organs were immediately removed, trimmed as necessary, and transferred to pre-labelled Peel-A-Way moulds (Polysciences, inc.) containing a small volume of Tissue-Tek. Organs were suitably oriented and then completely immersed in Tissue-Tek. Samples were quickly embedded in crushed dry-ice, and left to freeze. Fresh-frozen samples were wrapped in Parafilm, and stored at -20°C.

For Immunohistochemistry

Organs or tissues were usually prepared as described above for *in situ* hybridisation. However, it was sometimes necessary to transcardially perfuse a freshly killed animal with 4% paraformaldehyde (PFA) in 0.1M Phosphate Buffer (PB). After perfusion, organs and tissues were removed to 4% PFA in 0.1M PB to post-fix for an appropriate length of time (assumed tissue penetration of 2mm/hour). Organs and tissues were cryoprotected by immersion in 30% sucrose in 1x PBS, 4°C, at least overnight or until no longer buoyant.

HISTOCHEMISTRY

Non-Radioactive *In Situ* Hybridisation

The greatest effort was taken to ensure that all solutions and glassware used up to and throughout the high-stringency washing phase remained RNase-free. Solutions were either treated with DEPC (0.1% v/v DEPC overnight, and then autoclaved) or made using DEPC-treated ddH_2O and molecular-grade reagents. Glassware was always washed with a strong detergent, such as D90, and rinsed with DEPC-treated ddH_2O prior to use.

Preparation of Silanised Slides

Twinfrost slides were distributed in racks and immersed in 10% D90 in tap water for 2 hours, before they were washed with tap water for 20mins, followed by distilled water for several minutes. The slides were treated with acid-alcohol for 15mins, washed in distilled water for several minutes, autoclaved at 120°C, and later placed in an oven at 60°C until completely dry. Once removed, and left to cool to room temperature, the slides were immersed for 5mins in a solution of 6% 3-aminopropyltriethoxy-silane made up with 100% acetone. Immersions of 2x 2mins in 100% acetone and 2x 2mins in distilled water were performed. Having been left to air-dry, the slides were stored in closed containers until required.

Fixation and Permeabilisation of Tissue

10μm fresh-frozen sections were cut, using a Bright cryostat, and thaw-mounted onto silanised slides. These were placed in Coplin jars containing fixative (4% PFA in PBS), and stored overnight at 4°C. Three 5min washes in 1xPBS (made from DEPC-treated 10x PBS) were performed, and the sections were subsequently immersed in 70% ethanol for 5mins. For longterm storage at 4°C, sections were sequentially dehydrated in 80% ethanol for 5mins, followed by absolute ethanol in which they remained; for processing, these sections were sequentially rehydrated using the same concentrations of ethanol in descending order. The 70% ethanol was removed, the sections washed 2x 5mins in DEPC-treated ddH_2O, immersed in 0.1M HCl for 10mins, washed 2x 10mins in 1xPBS, immersed in 0.1M triethanolamine (pH8.0) containing 0.25% acetic anhydride for 20mins, and again washed 2x 5mins in 1x PBS. Finally, sections were sequentially dehydrated in ascending concentrations of ethanol (70%, 80%, and 95%) for 5mins each, before being removed and allowed to air-dry for several minutes.

Pre-Hybridisation

PAP grease-pen (Dako) was used to encircle all of the sections on each of the slides, before they were transferred to an incubation chamber humidified with PBS:Formamide (1:1) soaked strips of 3mm Whatman paper (Whatman, Maidstone, Kent, UK). Equal volumes of prehybridisation buffer and de-ionised formamide (Fluka) were mixed (50%

formamide, 25mM EDTA, 50mM Tris HCl pH7.6, 2.5X Denhardt's reagent, 0.25mg/ml tRNA, 20mM NaCl) and applied to sections. The incubation chamber was sealed with parcel tape and incubated at 37°C on a level platform for at least 5 hours, if not overnight.

Hybridisation

Equal volumes of hybridisation buffer (20mM Tris-HCl pH7.5, 1mM EDTA, 1x Denhardt's reagent, 0.5mg/ml tRNA, 0.1mg/ml poly A RNA, 0.1M DTT, 10% dextran sulphate) and deionised formamide were mixed, and the relevant cRNA probe added at an appropriate concentration (typically 2-6µl/ml). The solution was mixed thoroughly by inversion and incubated in a waterbath at the desired hybridisation temperature (55-65°C). One at a time, the slides were removed from the incubation chamber and the pre-hybridisation solution was replaced with pre-warmed hybridisation solution. The incubation chamber was sealed with parcel tape and incubated overnight at the desired hybridisation temperature, on a level platform.

High-Stringency Washing

The slides were loaded into a Coplin jar and immersed in room temperature 0.2x SSC (diluted from 20x SSC) for 2mins. Subsequently, the slides were washed 3x 20mins with 0.1xSSC/50% formamide, pre-heated to an appropriate temperature (55-60°C). For the duration of the high-stringency washes, the Coplin jar was incubated in a waterbath at the same temperature. Finally, the slides were rinsed in room temperature 0.2xSSC for 10mins.

Development

Buffer 1 (100mM Tris-HCl, 150mM NaCl pH7.5; diluted from 10x buffer 1) was used to equilibrate the sections for 10mins. They were then blocked in modified buffer 2 (1% Boehringer blocking reagent, 0.5% BSA fraction V in buffer 1) for 30mins. In the meantime, alkaline phosphatase conjugated anti-DIG monoclonal antibody was diluted 1:1500 in an appropriate volume of modified buffer 2. One at a time, the slides were placed in an incubation chamber and overlayed with the antibody-containing solution. The chamber was sealed with parcel tape and incubated overnight at 4°C on a level

platform. The slides were loaded into a Coplin jar, washed 2x 15mins in buffer 1, and equilibrated for 2mins in buffer 3 (100mM Tris-HCl, 100mM NaCl, 50mM $MgCl_2$ pH9.5). Slides were replaced in the incubation chamber and overlayed with buffer 3 containing 0.34mg/ml 4-nitroblue tetrazolium chloride (Boehringer), 0.175mg/ml 5-bromo-4-chloro-3s-indolylphosphate (Boehringer), and 0.25mg/ml levamisol (Sigma). The incubation chamber was sealed and the sections left to develop in darkness and at room temperature for at least 12 hours. Upon microscopic visualisation of the cellular accumulation of the chromogen, the alkaline phosphatase catalysed reaction was quenched by 10mins immersion of the slides in buffer 4 (10mM Tris-HCl, 1mM EDTA, pH8.0). These were washed in distilled water for several minutes, and then left under cover in a slide rack to air-dry overnight. The slides were immersed 2x 2mins in Histoclear and subsequently mounted in DPX under glass coverslips.

Note that, for all new riboprobes, a range of conditions were tested beginning with low hybridisation temperature and excess probe. The temperatures were gradually increased and the quantity of probe reduced, until the best results were achieved. At the same time, the specificity of each antisense probe was verified by comparison to its respective sense probe, which was hybridized under identical conditions. No signal, above the background level observed in sections hybridized with antisense probe, was observed in sections hybridized with sense probe.

Radioactive *In Situ* Hybridisation (Radiolabelled DNA Oligonucleotides)

Radiolabelling of 45-mer DNA Oligonucleotides

45-mer antisense and sense DNA oligonucleotides were labelled with ^{35}S (Dupont NEN) using terminal deoxytransferase (Promega). Levels of probe radioactivity were measured with a scintillation counter to ensure counts were greater than 200 000 disintegrations per million (DPM) per 400pg of ^{35}S-labelled DNA oligonucleotide. Labelled DNA oligonucleotides were stored at -20°C, in 20mM DTT.

Slide-Mounted Tissue Preparations

Tissue sections for radioactive *in situ* hybridization were cut, mounted, fixed, and dehydrated as described for the non-radioactive ISH procedure.

Hybridisation

Two nanograms of labelled probe were used per milliliter of hybridization buffer (50% formamide, 4x SSC, pH 7, 25mM sodium phosphate pH 7, 1mM sodium pyrophosphate, 5x Denhardt's solution, herring sperm DNA, 0.1 mg/ml polyadenylic acid, 0.1 g/ml dextran sulfate, 20mM DTT). For competitive cold controls, unlabelled 45-mer oligonucleotides were added to a concentration of 200 ng/ml hybridization buffer, inclusive of 2 ng/ml of the respective radioactive probe. One hundred microliters of hybridization mixture containing relevant probes was added per slide. Incubation of slides was carried out in sealed chambers moistened with 2x SSC and 50% formamide. Hybridization was performed at 42°C overnight.

High-Stringency Washing and Exposure to Radiographic Film

Four times 30-min high-stringency washes of the sections were performed using 1x SSC at 58°C. The sections were subsequently rinsed in 0.1x SSC at room temperature, before being dehydrated in 70% ethanol and 95% ethanol, for 1 min each. Sections were air-dried for 30 min and exposed to Biomax MR film (Kodak) for 3-6 days.

Emulsion Dipping

Slides were dipped in a 1:1 ratio of K.5 emulsion (Ilford) and 0.5% glycerol at 42°C and allowed to dry. Slides were transferred light-tight boxes, containing silica gel, and stored at 4°C for 14 days, before undergoing development. Slides were developed for 2mins in D19 (Kodak), rinsed in water, and fixed in Hypam (Ilford) for 4mins. The slides were then immersed in water for several hours before being stained with thionine, dehydrated, immersed in Histoclear, and coverslipped with DPX.

Immunohistochemistry

Slide-Mounted Tissue Preparations

20μm fresh-frozen sections were cut with a Bright cryostat and thaw-mounted on to Superfrost Plus slides.

Post-Fixation

As a preliminary examination of antigen sensitivity to fixation, different methods of tissue-section fixation were employed for newly-acquired antibodies: 30s immersion in –20°C methanol; 10mins immersion in -20°C methanol:acetone (1:1); 25mins immersion in 95% ethanol/5% acetic acid at 4°C; ~45mins immersion in 4% PFA in 1xPBS. Some sections were also processed without fixation. However, unless stated otherwise, tissue sections were post-fixed with 4% PFA.

Immunochemistry

Sections were immunoreacted in an incubation chamber, containing strips of 3mm Whatman paper moistened with 1x PBS. A PAP-grease pen was used to outline slide-mounted sections before they were rinsed several times in 1x PBS prior to incubation for 30mins at RT in blocking solution (0.1M PBS, 5% NGS, 0.5% Triton-X 100). The samples were then incubated with primary antibodies, diluted appropriately in blocking solution, overnight at RT. Several washes with 1x PBS were performed, and the sections incubated with fluorophore-conjugated secondary antibodies, diluted in 1x PBS, for two hours at RT. Again, several washes with 1x PBS were performed, and the sections stained with bisbenzimide (2.5μg/ml) for 7 minutes. Several more washes with 1x PBS were performed, and the sections coverslipped under DABCO medium (90% glycerol, 10% 0.1M PBS, 2.5% DABCO (Sigma)) and sealed with nail-varnish. Control sections, which were not incubated with primary antibodies, were used to ensure signal specificity. Slides were stored in darkness at 4°C.

Primary Antibodies

Details of the primary antibodies that were used in this thesis are listed in Table 2.1.

Secondary Antibodies

Tetramethylrhodamine-conjugated goat anti-mouse IgG monoclonal antibody (Molecular Probes) and Alexa-Fluor conjugated goat anti-rabbit IgG monoclonal antibody (Molecular Probes) were each used at a dilution of 1:400 in 1x PBS. Secondary antibodies were applied either alone or together in 1x PBS, as necessary. Both secondary antibodies were adsorbed against rat serum before being applied to primary antibody-treated sections of rat tissue; briefly, the diluted secondary antibodies were incubated in 10% rat serum (Sigma) at 37°C, 30mins, and then passed through a 0.45μm filter disk prior to application.

Digital Image Capture and Analysis

Immunohistochemically reacted samples were excited, viewed and photographed under a Zeiss Axioplan II microscope, and also a Leica TCS SP confocal laser scanning microscope where appropriate. Prior to image-capture with the confocal microscope, the power of the laser, pinhole, offset and gain were optimized to eliminate cross-talk. A sequential series of images was captured, with those from a single optical plane being compared directly for the assessment of antigen co-localisation. Standard light microscopy for the alkaline phosphatase reacted BCIP-NBT chromogen was undertaken with the Zeiss Axioplan II. Digital images captured with the Zeiss Axioplan II microscope were initially processed with Openlab image analysis software. All images were finally processed in Adobe Photoshop 5.0.

Figure 2.1.

The optimisation of concentrations of Taqman® primers to *ngr* (A), and Taqman® 5' 6-FAM labelled probe to *ngr* (B), for their subsequent use in quantitative PCR.

A

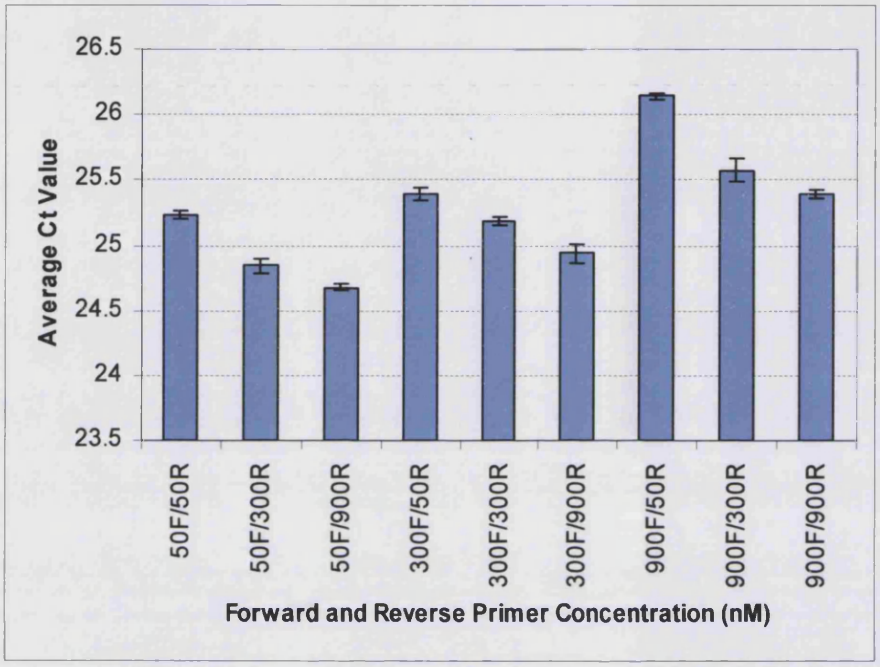

B

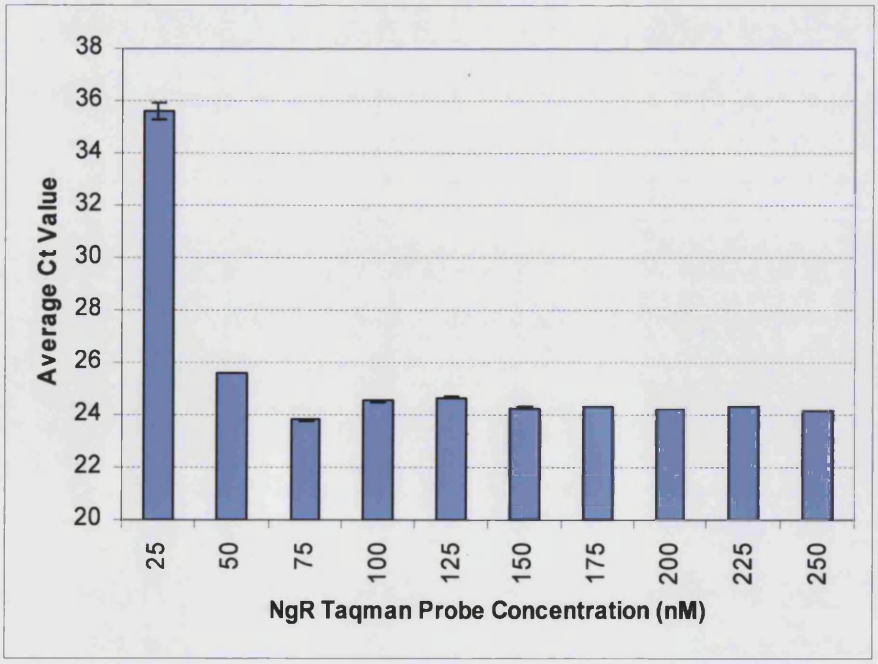

Table 2.1.

Details of the primary antibodies that have been used in work reported in this thesis.

Antibody Name	Type	Working Dilution	Supplier
anti-Nogo-A, clone 6D5	Mouse monoclonal IgG (raised against purified recombinant Nogo-A specific peptide)	1:20	Kindly provided by Dr.R.K. Prinjha, Glaxosmithkline plc., Harlow, UK.
anti-Neurofilament 200KDa	Rabbit polyclonal	1:20	Sigma
anti-NG2	Rabbit polyclonal	1:10 000	Kindly provided by Dr. W.B. Stallcup, The Burnham Institute, La Jolla, California, USA.
anti-GFAP	Rabbit polyclonal	1:400	Dako
anti-GFAP	Mouse monoclonal	1:600	Dako
anti-ATF3	Rabbit polyclonal	1:800	Santa Cruz
anti-S100	Mouse monoclonal	1:3000	Sigma
anti-$p75^{NTR}$	Mouse monoclonal	1:100	Sigma

CHAPTER 3

Expression of mRNA for the Nogo-66 Receptor and its Ligand, Nogo-66, in the Intact and Regenerating Nervous System

INTRODUCTION

The hypothesis that myelin breakdown products could be inhibitory to axonal regeneration was first posited by Martin Berry following the observation that mechanical, but not chemical, ablation of axons prevented regeneration (Berry, 1982). In the late 1980s, his theory was substantiated by Pico Caroni and Martin Schwab, who successfully isolated two fractions of myelin, NI-250 and NI-35, that were inhibitory to DRG and SCG neurite outgrowth *in vitro* (Caroni and Schwab, 1988b). They subsequently raised a monoclonal IgM antibody against NI-250, popularly termed IN-1, which recognized both NI-250 and NI-35 (Caroni and Schwab, 1988a). This antibody was successfully used in numerous *in vivo* studies to enhance axonal regeneration from different types of injured CNS neurons (Schnell and Schwab, 1990; Cadelli and Schwab, 1991; Weibel et al., 1994; Bregman et al., 1995; Merkler et al., 2001; Tatagiba et al., 2002). However, more than a decade elapsed before the gene encoding the inhibitory components of these fractions was independently identified by three different groups (Grandpre et al., 2000; Chen et al., 2000; Prinjha et al., 2000); Schwab's group micro-sequenced fragments of the bovine ortholog of NI-250, bNI-220 (Spillmann et al., 1998), and used the derivative degenerate nucleotide sequences to screen databases of gene sequences and expressed sequence tags (ESTs) to identify the gene, which they ultimately termed *nogo*.

The *nogo* gene was originally thought to give rise to three major isoforms through alternative splicing; Nogo-A, -B and -C. The carboxy termini of the Nogo isoforms are conserved and share significant sequence identity, as well as predicted structural identity, with a family of proteins known as Reticulons (the others being RTN1-3). Nogo is also

known as Reticulon 4 (RTN4). Although the function of this family of proteins remains largely unknown, they have earned their name through their propensity to localize in the endoplasmic reticulum (ER); all isoforms of Nogo possess a dilysine ER retention signal in their conserved carboxy termini. Although the precise topology of Nogo-A remains a contentious issue, it is widely agreed that the conserved carboxy termini of the Nogo isoforms contain two large transmembrane domains and a unique 66-residue lumenal/extracellular loop structure (termed Nogo-66).

Fournier et al. (2001) used alkaline-phosphatase tagged Nogo-66 to screen for potential receptors by expression cloning of a cDNA library in COS cells. A positive clone encoding a protein of 473 amino acids was identified. Sequence analysis revealed that the protein was predicted to be GPI-linked, with seven leucine rich repeat (LRR) domains, a carboxy terminal LRR domain (LRR-CT) and a unique carboxy terminal sequence. Importantly, it was demonstrated that the transduction of naïve E7 chick retinal ganglion cells with recombinant HSV-1, for the expression of NgR, was necessary and sufficient to confer sensitivity to Nogo-66 in both neurite outgrowth inhibition and growth cone collapse assays.

In addition to the Nogo-66 loop, it has been shown that myelin associated glycoprotein (MAG) and oligodendrocyte myelin glycoprotein (OMgp) are also functional ligands of NgR (Liu et al., 2002; Domeniconi et al., 2002; Wang et al., 2002b). The mechanism of NgR-activated transmembrane signalling is not yet entirely clear, but may in part occur through the recruitment of the low affinity neurotrophin receptor, $p75^{NTR}$ (Wong et al., 2002; Wang et al., 2002a). However, owing to obvious discrepancies in the expression profiles of NgR and $p75^{NTR}$, as well as the absence of enhanced axonal regeneration in the injured descending and ascending spinal tracts of the $p75^{NTR}$ null mutant mouse (Song et al., 2004), it is widely believed that another signal-transducing co-receptor for NgR may exist. Very recently, it has been reported that a novel transmembrane protein, LINGO-1, potentiates NgR-activated signal transduction through $p75^{NTR}$; LINGO-1 is apparently incapable of signal transduction in the absence of $p75^{NTR}$, but is markedly upregulated following CNS injury (Mi et al., 2004).

This chapter details the expression pattern of *ngr* mRNA in the intact and injured adult rodent nervous system, as well as that of the various *nogo* transcripts which encode the Nogo-66 ligand. Autologous peripheral nerve grafts to thalamus and cerebellum were performed in order to determine whether there was a correlation between the intrinsic ability of different classes of CNS neurons to extend axons into a peripheral graft and *ngr* mRNA expression.

Within the nervous system, the expression of *ngr* mRNA was found to be neuron-specific; however, it is differentially expressed by specific classes of neurons. In comparison, *nogo-66* mRNA is expressed by both neurons and glia within the intact CNS, but is expressed more widely by neurons than *ngr*. No correlation could be found between the ability of CNS neurons to extend axons into peripheral nerve grafts and *ngr* mRNA expression.

SUMMARY OF METHODS

Animals

Twelve unoperated female Sprague-Dawley rats and 2 unoperated C57 black mice were used in these experiments. Sixteen operated rats were also used. In 7 rats, a segment of autologous tibial nerve was grafted to the thalamus. These animals were killed at 3 (n=1), 14 (n=4), and 16dpo (n=2). In 3 rats, an autologous tibial nerve was grafted to the cerebellum, with the proximal end in the region of cerebellar deep nuclei. These animals were killed at 3 (n=1) and 28dpo (n=2). In 6 rats, the left sciatic nerve was transected. These animals were all killed at 3dpo.

Non-Radioactive *In Situ* Hybridisation

Cloning of Mouse Ngr

5' and 3' segments of mouse *ngr* (GenBank Accession No. AF283462) were cloned by PCR from a mouse single-stranded DNA library, using the proofreading polymerase *Pfu*. For the 5' segment (bases 135–561), the primers ATC G**CT CGA G**GA AGC CGC TTC CAG TGC CCG AC and ACT G**AA GCT** TGC CGT GGA ACG TGG TAG GGT CC

incorporating a *Xho*I and *Hin*dIII restriction endonuclease site, respectively, were used. For the 3' segment (bases 784–1760), the primers ATC G**CT CGA** GAG TCT TGA CCG CCT CCT CTT and ACT G**AA GCT** TCC CGG AAC CCT GTA AAC ATG incorporating a *Xho*I and *Hin*dIII site, respectively, were used.

Cloning of Rat Nogo-66

The *nogo-66* domain of rat *nogo-a* (GenBank Accession No. AJ242961; bases 3328–3525) was cloned from a rat single-stranded DNA library by PCR using *Pfu* polymerase. The primers ATC G**CT CGA** GAG GAT ATA TAA GGG CGT GAT C and ACT G**AA GCT** TCT TCA GGG AAT CAA C TA AAT C incorporating a *Xho*I and *Hin*dIII site, respectively, were used.

Cloning of Rat 3' Nogo Region

The 3' region of rat *nogo-a* (GenBank Accession No. AJ242961; bases 3222–3801) was cloned from a rat single-stranded DNA library by PCR using *Pfu* polymerase. The primers ACT G**CT CGA** GGG TGG TTG GTG CCA GCT TAT and ATC G**AA GCT** TCA CCC CCG TAA TCA AGT GAG incorporating a *Xho*I and *Hin*dIII site, respectively, were used. All PCR products were ligated into the pSP72 vector (Promega) in the same orientation between the *Xho*I and *Hin*dIII sites. Sequences were verified using the ABI prism system.

Synthesis of DIG-Labelled Riboprobes

In all cases, *Xho*I-linearized plasmid was used in conjunction with T7 RNA polymerase for the *in vitro* transcription of antisense DIG-labelled riboprobes. Conversely, *Hin*dIII-linearized plasmid was used with SP6 RNA polymerase for the synthesis of the sense DIG-labelled riboprobes. Antisense and sense cRNA probes labelled with DIG were generated according to the manufacturer's recommendations using an RNA labelling kit (Boehringer Mannheim, Germany).

Radioactive *In Situ* Hybridisation

The antisense and sense 45-mer DNA oligonucleotides to *nogo-66*, TGA ATG GGT GGC CTT CAT CTG ATT TCT GGA TAG CCT GGA TCA CGC and GCG TGA TCC AGG CTA TCC AGA AAT CAG ATG AAG GCC ACC CAT TC, respectively, were used in the radioactive *in situ* (as described in Chapter 2).

RESULTS

The two distinct non-overlapping DIG-labelled sense riboprobes to mouse *ngr* mRNA gave no signal (Fig. 3.1.A), whilst the complimentary antisense riboprobes generated an identical expression profile (Fig. 3.1.D,E). Furthermore, this pattern of expression was found to be the same in both mouse and rat tissue. Confirming the previous report (Fournier et al., 2001), *ngr* mRNA was found to be expressed exclusively in grey matter.

***ngr* mRNA Expression in the Unoperated Nervous System**

All layers of the neocortex showed strong staining, including large cells consistent with being pyramidal projection neurons (Fig. 3.1.B). No signal was detected in the neostriatum, despite strong expression in the adjacent neocortical tissue (Fig. 3.1.C and Fig. 3.2.A). *ngr* was strongly expressed in neurons of the hippocampus, dentate gyrus, piriform cortex and amygdala (Fig. 3.1.C). In the diencephalon, strong expression was observed in the medial habenular nuclei and dorsal thalamic nuclei (Fig. 3.1.C-E). There was no detectable *ngr* mRNA expression in thalamic reticular nuclei (TRN), hypothalamus, or ventral lateral geniculate nuclei (Fig. 3.1.C and E). In the midbrain, moderate expression was found in the red nucleus (Fig. 3.1.F). There was weak expression in the substantia nigra pars compacta, and apparently very little in the substantia nigra zona reticularis (Fig. 3.1.F). Weaker expression was observed in the septal nuclei and basal forebrain neurons (Fig. 3.1.G).

In the cerebellum, the granule cell layer exhibited the strongest expression of *ngr* mRNA (Fig. 3.2.B,C). Purkinje cells exhibited weak/moderate signal, but were best visualized in oblique sections through cerebellar cortex (Fig. 3.2.C). Moderate signal was detected in

the deep cerebellar nuclei, and brainstem nuclei (including reticular nuclei, pontine nuclei, nucleus prepositus hypoglossi and vestibular nuclei) (Fig. 3.2.B).

In the spinal cord, there was only low expression of *ngr* mRNA (Fig. 3.2.D). However, expression was comparatively greater in the motor neurons of the ventral horn than the secondary sensory neurons of the dorsal horn. Also, there appeared to be a subpopulation of 20-30% of DRG neurons that showed low/moderate levels of expression (Fig. 3.2.E); the remaining DRG neurons did not express *ngr*. Similarly, the superior cervical ganglion exhibited a similar pattern of expression to DRG, i.e. *ngr* was only expressed by a minority of neurons, and the signal was weak/moderate (not shown).

The thymus was negative for *ngr* mRNA expression, whilst the heart exhibited relatively strong expression (not shown). This is in agreement with previous published findings (Fournier et al., 2001). Curiously, in the distal colon, moderate/strong expression of *ngr* was detectable in neurons of the myenteric plexus (Fig. 3.3).

ngr mRNA Expression Following Peripheral Nerve Graft Implantation

Grafting of tibial nerve to thalamus failed to induce expression of *ngr* mRNA within neurons of the TRN, which are particularly adept at innervating nerve grafts (Fig. 3.2.F). With the exception of a very slight upregulation of *ngr* in the dorsal thalamic neurons of one animal, this class of neuron also failed to show any consistent change in expression. Likewise, implantation of tibial nerve grafts to cerebellum brought about no change in baseline expression in the various classes of cerebellar neuron. Deep cerebellar nuclei, which have a well documented ability to regenerate axons into nerve grafts (Chaisuksunt et al., 2000a), and neurons within the cerebellar cortex, which do not regenerate under such conditions, both maintained the moderate levels of *ngr* expression observed in the healthy adult rodent.

Expression of _nogo-66_ mRNA

Two antisense DIG-labelled riboprobes (to the *nogo-66* sequence itself; and to the 3' *nogo* sequence, encompassing *nogo-66*, and adjacent flanking regions conserved

throughout all known *nogo* mRNA species) and one ^{35}S-labelled 45-mer DNA oligonucleotide probe set (to the 5' end of the *nogo-66* sequence) gave very similar patterns of expression (Fig. 3.4.A,D,F). The respective complementary sense probes, and competitive cold controls, gave no signal (Fig. 3.4.B,C,E,F).

Contrary to previous reports, transcripts encoding *nogo-66* were found to be more strongly expressed in grey matter than white (Fig. 3.5.A). Neocortex, hippocampus and thalamic nuclei expressed *nogo-66* mRNA most strongly (Fig. 3.5.C,D). Neurons of the TRN were positive (Fig. 3.5.C). *nogo-66* was expressed throughout the neostriatum, but most prominently in the larger neurons whose size and distribution matches that of the cholinergic interneurons (Fig. 3.5.A,B). *nogo-66* mRNA was also detected in septal and vestibular nuclei (Fig. 3.5.E). Moderate expression was detectable in the red nucleus, substantia nigra pars compacta and zona reticularis (not shown). In the cerebellum, strong expression was detected in Purkinje cells and deep cerebellar nuclei, but not in the cerebellar granule cell layer (Fig. 3.5.E,F).

In spinal cord, signal was detected in most neurons, especially in the motor neurons of the ventral horn (Fig. 3.6.A,B). There was also sporadic low level expression within the white matter of the spinal cord, particularly in the dorsal horns. Strong signal was detected from most neurons of the DRG (Fig. 3.6.C). Within the visual system, the retinal ganglion cell layer, the outer nuclear layer and the inner nuclear layer all displayed moderate to strong expression (Fig. 3.6.E). In the uninjured optic nerve, *nogo-66* transcripts were sporadically present at low/moderate levels in the non-neuronal cells (Fig. 3.6.D). Whilst no expression was found in the undamaged adult rat sciatic nerve, a clear upregulation of mRNAs encoding Nogo-66 was found in scattered non-neuronal cells in the distal stump of the axotomized sciatic nerve, at 3dpo (Fig. 3.7.A-G). This upregulation was of greatest intensity in the cells closest to the severed end of the distal stump (Fig. 3.7.B). RT-PCR was used to confirm upregulation of *nogo-66* transcripts in the distal stump, 3dpo (Fig. 3.7.H).

Expression of *nogo-66* transcripts was examined in animals with thalamic grafts. In two animals, mild but clear upregulation of these transcripts was found at the graft/brain interface (Fig. 3.7.I). However, there was no apparent regulation of expression in any defined classes of neuron such as the TRN, which remained positive for *nogo-66* transcripts. Unfortunately, owing to poor cellular preservation of structure in the nerve grafts in fresh-frozen sections, it was impossible to discern any regulation of *nogo-66* expression within the graft itself.

DISCUSSION

It has been assumed that Nogo is expressed primarily by oligodendrocytes and that the interaction of NgR with its ligands can explain the general failure of axonal regeneration in the CNS (reviewed by Filbin, 2003). In this study of the *in situ* expression of transcripts encoding NgR and Nogo-66, it has become clear that *nogo-66* transcripts are predominantly expressed by neurons and that the NgR-ligand interaction cannot universally explain the failure of axonal regeneration in the CNS.

Nogo-66 Receptor

Although the pattern of *ngr* mRNA expression within the CNS in this study was broadly found to concur with that reported by Fournier et al (2001), there is one major difference. Cerebellar Purkinje cells gave low to moderate signal for *ngr*, whilst cerebellar granule cells gave decidedly stronger signal. In contrast, Fournier et al (2001) described strings of strongly staining Purkinje cells, with little or no signal from cerebellar granule cells. Strangely, these results are very similar to those obtained in this study when probing for Nogo-66 encoding transcripts in the cerebellum. The initial *in situ* hybridisation (ISH) studies for *ngr* carried out by Fournier et al (2001) were not exhaustive, which perhaps explains why they also did not document the differential expression of *ngr* in other parts of the brain. For example, they did not comment on the striking lack of expression of *ngr* mRNA within the neostriatum nor the low levels in the spinal cord. In their ISH experiments, Fournier et al (2001) used a single ~1Kb 5' DIG labelled riboprobe. In this study, two DIG labelled riboprobes were employed; ~0.5Kb 5' and ~1Kb 3' probes were

generated from distinct non-overlapping sequences. The results obtained from the ISH with these two different probes were very similar, implying that the correct profile of *ngr* mRNA expression has been recorded.

Within the nervous system, *ngr* expression was found to be purely neuronal, being strongest in neocortical and hippocampal neurons. This is compatible with studies demonstrating that administration of function-blocking antibody against Nogo (mAb IN-1) after spinal cord injury in postnatal rats results in augmented sprouting and/or axonal regeneration of corticospinal axons (Schnell and Schwab, 1990; Schnell and Schwab, 1993; Bregman et al., 1995; Raineteau et al., 1999; Bareyre et al., 2002). Conversely, *ngr* is very poorly expressed, if at all, in secondary sensory neurons of the spinal cord. Adult DRG neurons - of which only a subpopulation are positive for *ngr* (20-30% in adult rat DRG) - are refractory to treatment with mAb IN-1 following injury to their central processes. Attempts to enhance axonal regeneration after injury to the dorsal columns (i.e. DRG axons) with mAb IN-1 have proved unsuccessful (Oudega et al., 2000). However, up to 60% of cultured embryonic DRG growth cones collapse upon exposure to soluble Nogo-66; this discrepancy between *ngr* expression and sensitivity to Nogo-66 may be explained by (i) addition of selective trophic agents which alter the phenotype of the primary culture (ii) species from which the DRG were obtained (iii) age of DRG (iv) a potentially unreliable assay (in so much as growth cones can collapse very easily, even in the complete absence of collapsing agents). Interestingly, Purkinje cells exposed to mAb IN-1 have been shown to sprout and upregulate growth-associated genes c-Jun, JunD, and NADPH Diaphorase (Zagrebelsky et al., 1998; Buffo et al., 2000), which is compatible with their expressing NgR, albeit at modest level.

If the interaction of NgR with the Nogo-66 domain of the Nogo family of proteins is an absolute determinant of the success of axonal regeneration within the CNS, then one would imagine that many classes of neuron devoid of *ngr* or which only express it at low levels, such as primary and secondary sensory neurons, should be capable of a very robust regenerative response within CNS tissue given an adequate trophic environment. However, there is no evidence to suggest for example, that neostriatal neurons (which

show no expression of *ngr*) are especially good at regenerating axons following injury - although there is evidence of increased neurite outgrowth following grafting of smooth muscle to the neostriatum (Tew et al., 1998). With this in mind, it seems likely that there are other factors that have as great or greater a role than NgR ligands in the inhibition of axonal regeneration in the injured CNS. Indeed, more likely than not, the success of CNS axonal regeneration is likely to be determined multifactorially.

Nogo Family of Proteins

Nogo-66 encoding transcripts were detected by three different probes: ^{35}S-radiolabelled 45-mer DNA oligonucleotides against the Nogo-66 sequence; DIG labelled riboprobe against Nogo-66 sequence; DIG labelled riboprobe against Exons 6-11of the *reticulon 4* gene (termed 3' Nogo, which encompasses the Nogo-66 sequence – refer to Table 3.1). The profiles obtained using each of these probes were identical. Having performed an extensive search of the National Institutes of Health National Centre for Biotechnology Information (NCBI) database, seven different Nogo-66 encoding transcripts were identified by Open Reading Frame. It is impossible to say which of these isoforms have been detected in these ISH experiments, given that the 3' region (Exons 6-11) is perfectly conserved throughout all seven transcripts. In spite of this, any of these isoforms should in theory be capable of inducing growth-cone collapse through the interaction of their identical Nogo-66 domains with NgR (Fournier et al., 2001), provided that the subcellular localisation of each is such that this would be mechanically feasible.

Overall, the findings reported herein for the expression of Nogo-66 encoding sequences are similar to those of Josephson et al (2001); *nogo* transcripts were found to be expressed in neurons as well as glia – but, on balance, the expression was predominantly neuronal. This is in contrast to earlier reports by Chen et al. (2000), GrandPre et al (2000), and Prinjha et al. (2000). Nonetheless, Schwab's group has since published a paper on their ISH and immunohistochemical findings for Nogo expression within the nervous system, which described high levels of both *nogo-a* mRNA and protein in some classes of neuron (Huber et al., 2002).

In addition to the work already published by Josephson et al (2001), in which *nogo* expression was examined in the spinal cord and forebrain, this study has also examined *nogo-66* in both cerebellum and injured peripheral nerve as well as after peripheral nerve graft to thalamus. Curiously, whereas Josephson et al (2001) reported no change in *nogo* regulation following weight drop injury to spinal cord, a moderate but clear upregulation at the rim of a peripheral nerve graft to thalamus was observed at 16dpo in this study. Naturally, such an upregulation of *nogo-66* has the potential to deter NgR-expressing neurons from extending axons into the peripheral nerve graft. Neurons from the TRN, which are known to grow axons into segments of peripheral nerve grafted to thalamus, show no sign of *ngr* expression but do, however, express *nogo* transcripts.

Grafting of Peripheral Nerve to Brain

ngr mRNA is strongly expressed by corticospinal and hippocampal neurons – both of which demonstrate little if any ability to regenerate into peripheral nerve grafts implanted into the brain (Anderson and Lieberman, 1999). Even when stimulated to regenerate with NT-3, corticospinal neurons will not extend axons into peripheral nerve grafts (Blits et al., 2000). Likewise, in double transgenic mice overexpressing GAP-43 and L1, axons from Purkinje cells turn away from peripheral nerve grafts (Zhang et al, unpublished observations). Together, these findings infer that peripheral nerves may harbour molecules inhibitory to some types of CNS neuron. Conversely, neurons of the TRN – which are devoid of *ngr* - have a high propensity to extend axons into grafted peripheral nerve (Benfey et al., 1985; Morrow et al., 1993; Vaudano et al., 1998) and neurons of the substantia nigra pars compacta and basal forebrain, which exhibit only low levels of *ngr* mRNA expression or none at all, are also capable of innervating grafted peripheral nerve (Woolhead et al., 1998).

However, there is often no correlation between *ngr* transcript expression and potential to regenerate axons into peripheral nerve grafts. For example, the deep cerebellar nuclei, which innervate peripheral nerve grafts very successfully, show moderate to strong expression of *ngr* mRNA (Vaudano et al., 1993; Vaudano et al., 1998; Chaisuksunt et al., 2000b); though, it is not yet known whether these neurons express the NgR co-receptors,

$p75^{NTR}$ and LINGO-1, which are necessary for signal transduction. Similarly, most neurons of the neostriatum and lateral geniculate nucleus, which do not express *ngr* mRNA, are very poor at regenerating axons into peripheral nerve grafts in the brain (Vaudano et al., 1995; Woolhead et al., 1998). That complete absence of *ngr* mRNA expression does not correlate with successful innervation of peripheral nerve grafts, implies that other factors have a significant role to play in axonal regeneration and that the NgR-ligand interactions alone are not the absolute determinant of regenerative success.

Examination of peripheral nerve grafts for expression of *nogo-66* was not conclusive, owing to the poor quality of the graft in fresh-frozen tissue. However, the observation that *nogo-66* transcripts are upregulated by non-neuronal cells of the distal stump of axotomized peripheral nerve at 3dpo is intriguing, but not unprecedented. Tenascin C (Martini, 1994), chondroitin-sulphate proteoglycans (Zuo et al., 1998a; Morgenstern et al., 2003; Rezajooi et al., 2004), Sema3A and Sema3F (Scarlato et al., 2003) are also upregulated in the injured peripheral nerve. Although the injured peripheral nerve regenerates very well, it is clear that the environment in which it achieves this exhibits an abundance of inhibitory factors. Why these inhibitory factors are unable to exert a greater suppressive influence is not immediately obvious, but is most likely to be due to an as yet undefined mechanism of 'override' initiated by the presence of large quantities of neurotrophins and neurotrophic factors, or indeed by the presence of supportive extracellular matrix molecules such as laminin. It is equally plausible that the receptors for these ligands in some instances are either absent or downregulated in the regenerating neurons.

It should also be noted that, whilst Josephson et al (2001) have failed to detect *nogo* transcripts in uninjured peripheral nerve by *in situ* hybridization, as was the case in this study, Martin Schwab's group has claimed on two occasions to have detected *nogo-b* transcripts by Northern blot in uninjured sciatic nerve (Chen et al., 2000; Huber et al., 2002) but closer inspection reveals that the bands presented in both Northern blots are, in

fact, one and the same. This contrasts with the findings of GrandPre et al (2000), who were unable to detect any *nogo* transcripts in uninjured peripheral nerve by Northern blot.

Neuronal Co-Expression of mRNA Encoding NgR and Nogo-66

The co-expression of *ngr* and *nogo-66* by many types of neuron, including neocortical neurons, is quite intriguing. Similarly, a range of human neural and non-neural cell lines have been found to express both *nogo* and *ngr* mRNA by RT-PCR (Satoh and Kuroda, 2002). All evidence for Nogo-66 based induction of growth cone collapse comes from a gain-of-function experiment in which naïve embryonic retinal ganglion cells (RGCs), transfected with HSV-1 to express NgR, are rendered sensitive to the effects of Nogo-66 (Fournier et al., 2001). Considering that adult RGCs express both *ngr* and *nogo-66* transcripts without any obvious abnormalities in neurite outgrowth or growth-cone function *in vitro*, it seems unlikely that the above growth cone collapse observations should be correct. That is, at least, until the subcellular location of the proteins is taken into consideration; as a GPI anchored protein, NgR localizes to lipid-rafts within the membranes of the axons and growth cones (Fournier et al., 2001); whilst Nogo, on the other hand, appears to localize primarily to the endoplasmic reticulum owing to its carboxy-terminus dilysine ER-retention signal, though a very small fraction of the protein has been reported to be expressed in the cell membrane of oligodendrocytes (Oertle et al., 2003b). Such a distribution of ligand and receptor within the same neuron would be expected to limit any interaction intra-neuronally, but not inter-neuronally. Thus, exists the possibility that the Nogo-66-NgR interaction has a role, not so much in neurite outgrowth inhibition in the injured nervous system, but more so as an axon guidance mechanism employed in tract formation during development. Some evidence for this is perhaps provided by studies in which the development of corticospinal tract axons in early postnatal rats was disrupted by the administration of the IN-1 function-blocking antibody (Schwab and Schnell, 1991). Likewise, the intrathecal administration of NEP1-40, which antagonizes Nogo-66 binding to NgR, results in significantly enhanced axonal outgrowth following corticospinal tract injury; though, more interestingly, these regenerating axons appear to navigate 'blindly' through the white and grey matter of the spinal cord, having lost affinity to their tract of origin (Grandpre et al., 2002). This

phenomenon could potentially be ascribed to the blocking of the proposed 'Nogo-66-NgR axon guidance mechanism' described above. A similar theory has been further expounded by Raisman, who believes that these interactions could serve as a directional influence on axonal elongation, enhancing the growth and regeneration of axons in a longitudinal projection (Raisman, 2004). Preliminary evidence for this comes from experiments in which E15 mouse hippocampal explants were cultured on substrates of Nogo-66 or Nogo-A. It was found that increased fasciculation of outgrowing axons occurred on both substrates, but that it was more extensive on a substrate of Nogo-A (Mingorance et al., 2004).

The Function of NgR and the Nogo Family of Proteins

Most of the recent findings concerning Nogo and NgR suggest that the initial understanding of the Nogo-66-NgR mechanism was hugely oversimplified. The attractive model of Nogo functioning principally as a potent myelin associated inhibitor of axonal regeneration through its interaction with neuronal NgR has undergone much revision, owing to the emergence of numerous lines of evidence which collectively indicate a much broader biological role. For example, Nogo-66 encoding transcripts are expressed so widely throughout human tissues (Table 3.1) that it seems implausible that the various Nogo isoforms do not have diverse functions. Indeed, the Nogo-66 domain, which binds NgR, has been shown through yeast-two hybrid studies to interact with three mitochondrial proteins (Hu et al., 2002); Nogo-B has been shown to possess pro-apoptotic activity (Li et al., 2001) and to interact with ASYIP, otherwise known as Reticulon 3 (Qi et al., 2003); Nogo-B has also been implicated in vascular remodeling (Acevedo et al., 2004); a testis-specific form of Nogo, Rtn-T, which is the only known transcript to contain exon 2, is thought to play a role in testicular development (Zhou et al., 2002); and, there is also some evidence that Nogo-A interacts with CASPR at CNS paranodes to regulate potassium channel localization during development (Nie et al., 2003).

In the nervous system, mRNA transcripts encoding Nogo-66 localize predominantly to neurons (Josephson et al., 2001; Huber et al., 2002; Hunt et al., 2002b), which is

indicative of a function quite distinct from that of myelin-mediated inhibition of axonal regeneration. Interestingly, these transcripts are only moderately upregulated in a few cells at the borders of a site of injury (this study; Hunt et al., 2002b). Other studies have reported that mRNAs encoding Nogo family members show no, or only moderate, signs of regulation following spinal cord injury (Josephson et al., 2002; Wang et al. 2002). In this study, it was also found that Nogo-66 encoding transcripts are upregulated in non-neuronal cells of the distal stump of axotomized sciatic nerve, especially at the point of severance, where clearly they fail to prevent axonal regeneration. However, another group has reported that they could not detect any upregulation in the distal stumps of transected adult rodent nerve by *in situ* hybridization (Kim et al., 2003b). From preliminary quantitative PCR studies on intact and injured adult rat sciatic nerve, it appears that all three major isoforms of *nogo* are expressed in the intact sciatic nerve – in which they are not detectable by *in situ* hybridization – and that some of these are upregulated in the distal stumps of injured sciatic nerve within several days of injury (J Fabes, Department of Anatomy and Developmental Biology, UCL - personal communication). Studies in which either Nogo-A or Nogo-C have been overexpressed by Schwann cells in transgenic mice have shown marginally impaired peripheral nerve regeneration (Pot et al., 2002; Kim et al., 2003b); therefore, one would imagine that at least a small percentage of the endogenously expressed Nogo isoforms would reach the cell surface where they would be capable of exerting an inhibitory effect on the regenerating peripheral axons, assuming of course that they are expressed by Schwann cells.

Northern blot analysis of intact sciatic nerve has produced conflicting results. Whilst Schwab's laboratory has on two occasions published the same blot demonstrating *nogo-b* expression in intact adult rat sciatic nerve (Chen et al., 2000; Huber et al., 2002), Strittmatter's laboratory has not detected any expression of the *nogo* isoforms (Grandpre et al., 2000). By *in situ* hybridization, at least three groups have failed to detect the expression of any of the *nogo* isoforms in intact nerve (this study; Josephson et al., 2001; Hunt et al., 2002b; Kim et al., 2003b). However, as stated earlier, preliminary

quantitative PCR appears to show that all three major isoforms of *nogo* are expressed to some extent in intact sciatic nerve.

Somewhat surprisingly, *ngr* is not regulated after autologous peripheral nerve graft to brain (this study; Hunt et al., 2002b) or spinal injury (Josephson et al., 2002). Its expression does not correlate with the intrinsic ability of CNS neurons to extend axons into grafted peripheral nerve, which indicates that it is not an absolute determinant of successful axonal regeneration (this study; Hunt et al., 2002b). The strong expression of *ngr* in other tissues, such as heart (Fournier et al., 2001; Wang et al., 2002c; this study), imply that it too is likely to participate in functions unrelated to axonal regeneration. The expression of *ngr* by myenteric neurons also raises some interesting questions, since there is no myelin in the enteric system and enteric neurons have no projection to the CNS. However, these cells have also been found to express both *nogo-a* transcripts and protein (Chapter 4; Osborne et al., 2004). Whether the two molecules are capable of interacting in this system, and what their function may be, remains unknown.

The *ngr* null mutant mice have so far proved to be something a disappointment. A preliminary report suggested neither major phenotypic abnormalities, nor enhanced CST regeneration after spinal cord injury (Kim et al., 2003). This perhaps is not surprising given that both MAG and Nogo-A can signal in the absence of NgR (Niederost et al., 2002). However, a slight enhancement in the sprouting of serotonergic fibres in the spinal cord was described. It was also reported that the *ngr* null mutant mice performed worse than wild-type control littermates on a Rotarod test, which is used to measure learning ability. This is interesting in light of an earlier report which demonstrated regulation of hippocampal *ngr* expression during learning exercises (Josephson et al., 2002). The most recent report on the *ngr* null mutant mice claims that corticofugal plasticity and the recovery of motor function are enhanced in models of stroke (Lee et al., 2004).

Summary

There is no direct correlation between neuronal expression of *ngr* mRNA in the CNS and ability to regenerate axons into peripheral nerve grafts to brain. Nonetheless, the results from experiments in which the function-blocking antibody IN-1 was administered to the CNS seem to be completely compatible with the findings of this study on the distribution of *ngr* mRNA, as the cells which responded to IN-1 are those which have been found to express *ngr*. Furthermore, it seems increasingly unlikely that the original view of the Nogo-66-NgR signaling mechanism being a specific oligodendrocyte-neuron interaction is entirely correct. At present, the evidence is suggestive of an additional role in inter-neuronal signalling, which could potentially have a very important role in axon guidance and tract formation during development. In any event, whilst *ngr* expression is not the absolute determinant of success of axonal regeneration within the injured CNS, Nogo is still arguably the most potent *in vivo* inhibitor of axonal regeneration presently known and NgR one of the most important gateways for the induction of growth cone collapse and neurite outgrowth inhibition. On this premise alone, approaches to knock down Nogo/NgR expression or to otherwise disrupt the Nogo-66-NgR interaction should be sought and, further, combined with other measures – such as the provision of supplementary neurotrophins - to achieve optimal levels of axonal regeneration of some classes of neuron (e.g. corticospinal) within the injured CNS.

CONCLUSION

The distribution of *ngr* mRNA *in situ*, both before and after injury, is not consistent with its being an absolute determinant of the success of axonal regeneration. Likewise, the expression profile of transcripts encoding the NgR ligand, Nogo-66, is indicative of an as yet undefined role in neuronal function; that is, in addition to its known role as a myelin-associated inhibitor of axonal regeneration.

Figure 3.1.

A. Cerebellum of adult mouse reacted with sense 3' *ngr* probe. No signal can be seen; compare with Fig 3.2.B. Scale bar = 250μm.

B. Neocortex from an adult mouse hybridized with 5' *ngr* probe. The pattern of *ngr* signal is very strong in neurons of all layers, but not in glia of the molecular layer or subcortical white matter. Scale bar = 500μm.

C. Coronal section through the forebrain of an adult mouse, hybridized for *ngr* (3' probe). Strong *ngr* signal can be seen in the neocortex and hippocampal formation, amygdaloid nuclei (asterisk), medial habenular nucleus (arrow) and in the dorsal thalamus (T). The hypothalamus (H) and the small region of neostriatum visible (S) show little or no *ngr* signal. *ngr* signal is absent from white matter. Scale bar = 1mm.

D,E. Sections through the hippocampal formation and dorsal thalamus (T) from adult mice, hybridized with the 5' probe (in D) and the 3' probe (in E). The pattern of *ngr* signal obtained with the two probes is identical. Strong signal can be seen in the hippocampus and dentate gyrus and medial habenular nuclei, and in the dorsal thalamus, but not in the TRN (between arrows in E) or subcortical white matter. Scale bar = 500μm.

F. Transverse section through the crus cerebri of an adult rat hybridized with the 3' *ngr* probe. Neurons in the red nucleus (asterisk) show moderate levels of *ngr* signal but those in the substantia nigra pars compacta (arrows) show only very weak signal. Scale bar = 500μm.

G. Section through the basal forebrain of an adult rat hybridized with the 3' *ngr* probe showing only background levels of signal. The anterior commisures are denoted by asterisks. Scale bar = 500μm.

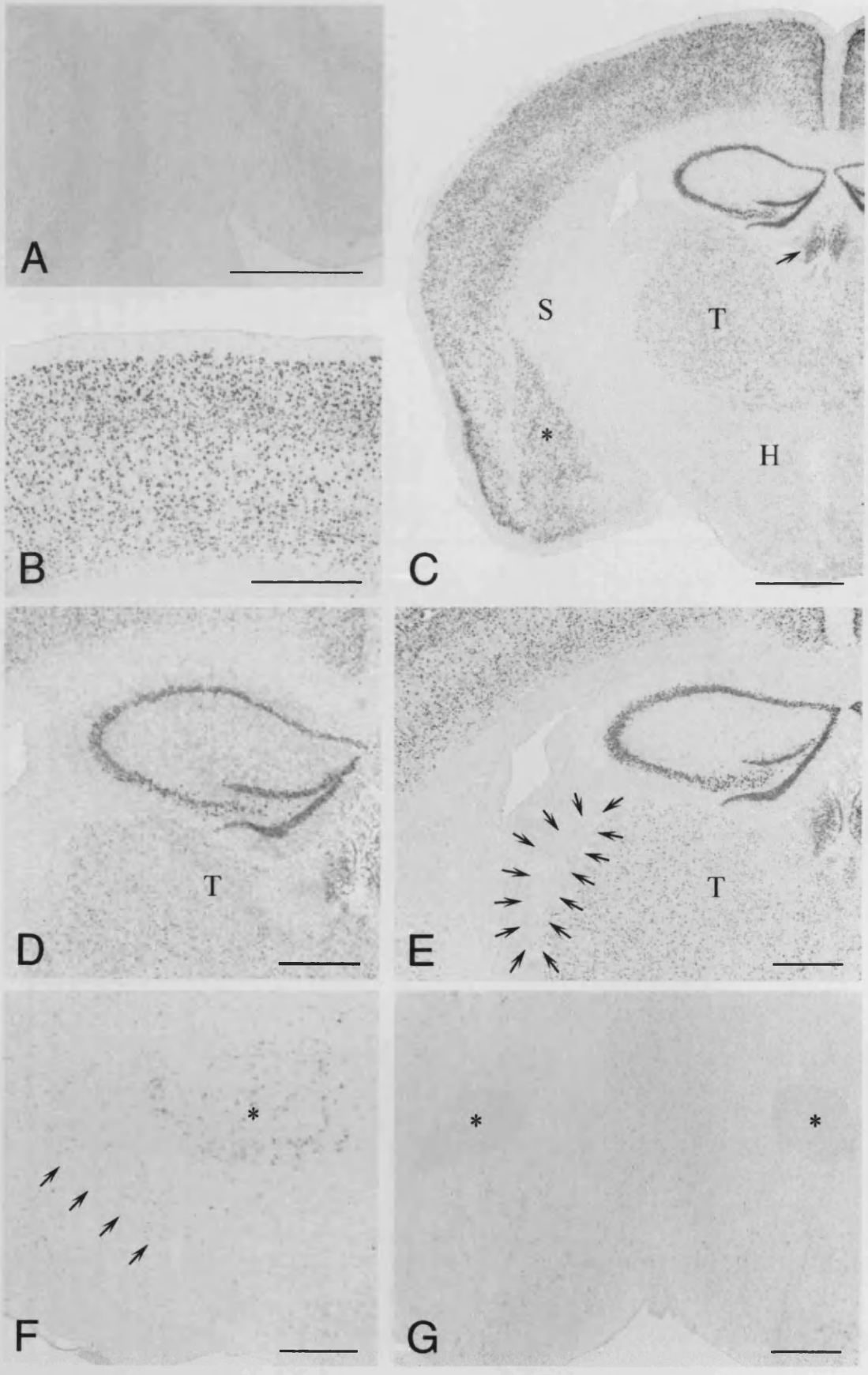
A
B
C
S
T
H
D
T
E
T
F
G

Figure 3.2.

A. Section through neocortex and neostriatum of an adult rat, hybridized with 3' probe Note the virtual absence of *ngr* signal from the caudatoputamen (asterisk) and the subcortical white matter, in contrast to the strong signal from the neocortical neurons. Scale bar = 500μm.

B. Section through the cerebellum from an adult rat hybridized with 3' *ngr* probe. Note the strong signal from the granule cell layer (G) and moderate signal from neurons in the deep nuclei (asterisk). Scale bar = 500μm.

C. Higher power image of a section through rat cerebellar cortex. The oblique section through the cortex allows *ngr* signal from the Purkinje cells (arrows) to be seen, although it is always weaker than that from the granule cell layer. Scale bar = 500μm.

D. Transverse section through the cervical spinal cord from an adult rat hybridized with the 3' *ngr* probe. There is generally little *ngr* mRNA detectable in the spinal cord although motor neurons (arrows) show a distinct but weak signal. Scale bar = 500μm.

E. L5 DRG from an adult rat hybridized with the 3' *ngr* probe. A subpopulation of primary sensory neurons (e.g. at arrows) shows *ngr* signal. Scale bar = 250μm.

F. Coronal section through the thalamus from a rat 3 days after the implantation of a tibial nerve graft (G). Neurons in the TRN (between arrows) still show no *ngr* signal although they are known to regenerate into such grafts. Scale bar = 500μm.

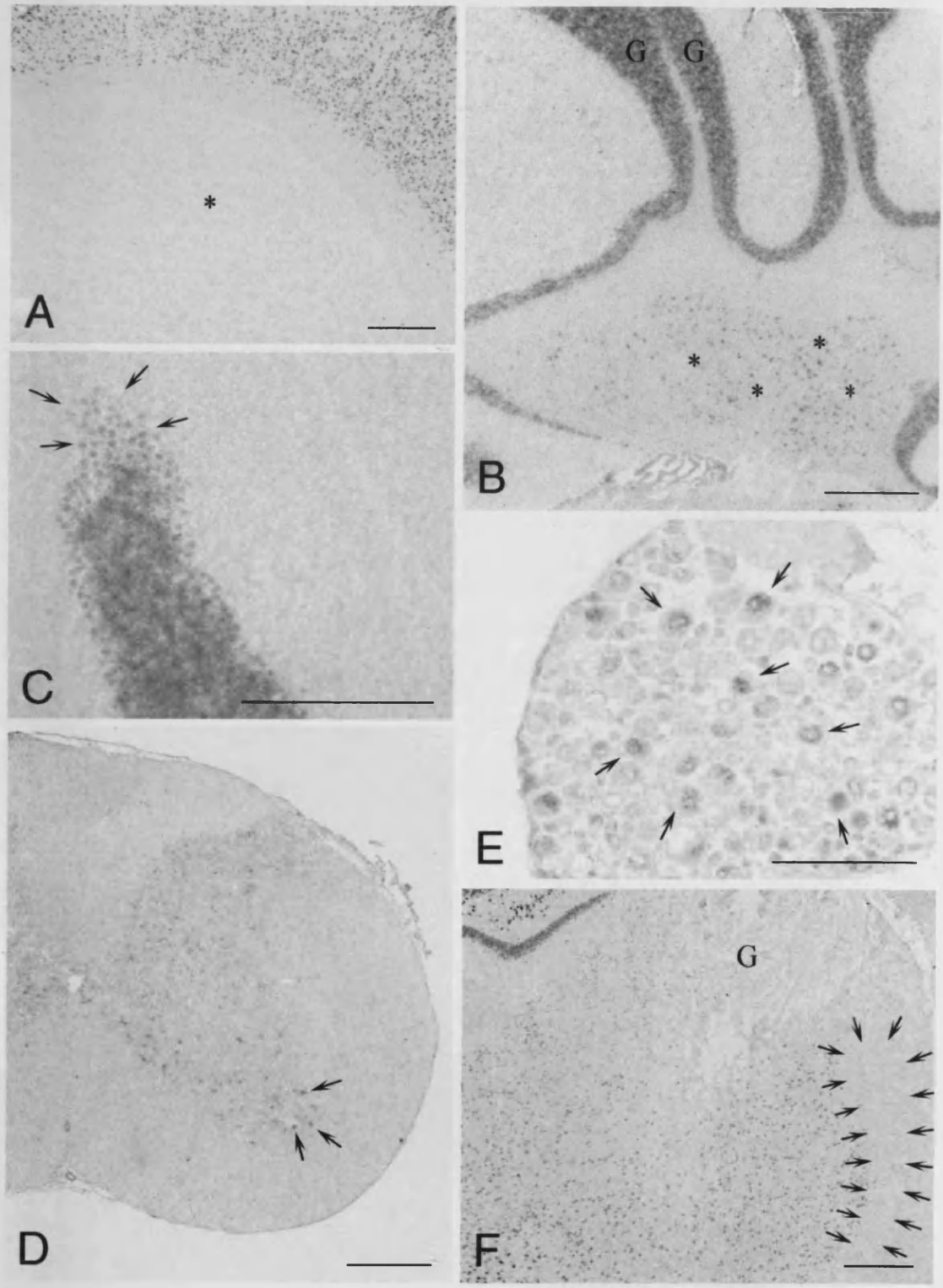
A
B
G G
C
D
E
F
G

Figure 3.3.

Longitudinal section of distal colon from adult rat. A and B, Moderate signal for *ngr* is exhibited by neurons of the myenteric plexus. Scale bar = 200μm. This tissue was sectioned, reacted and photographed by J. Mills.

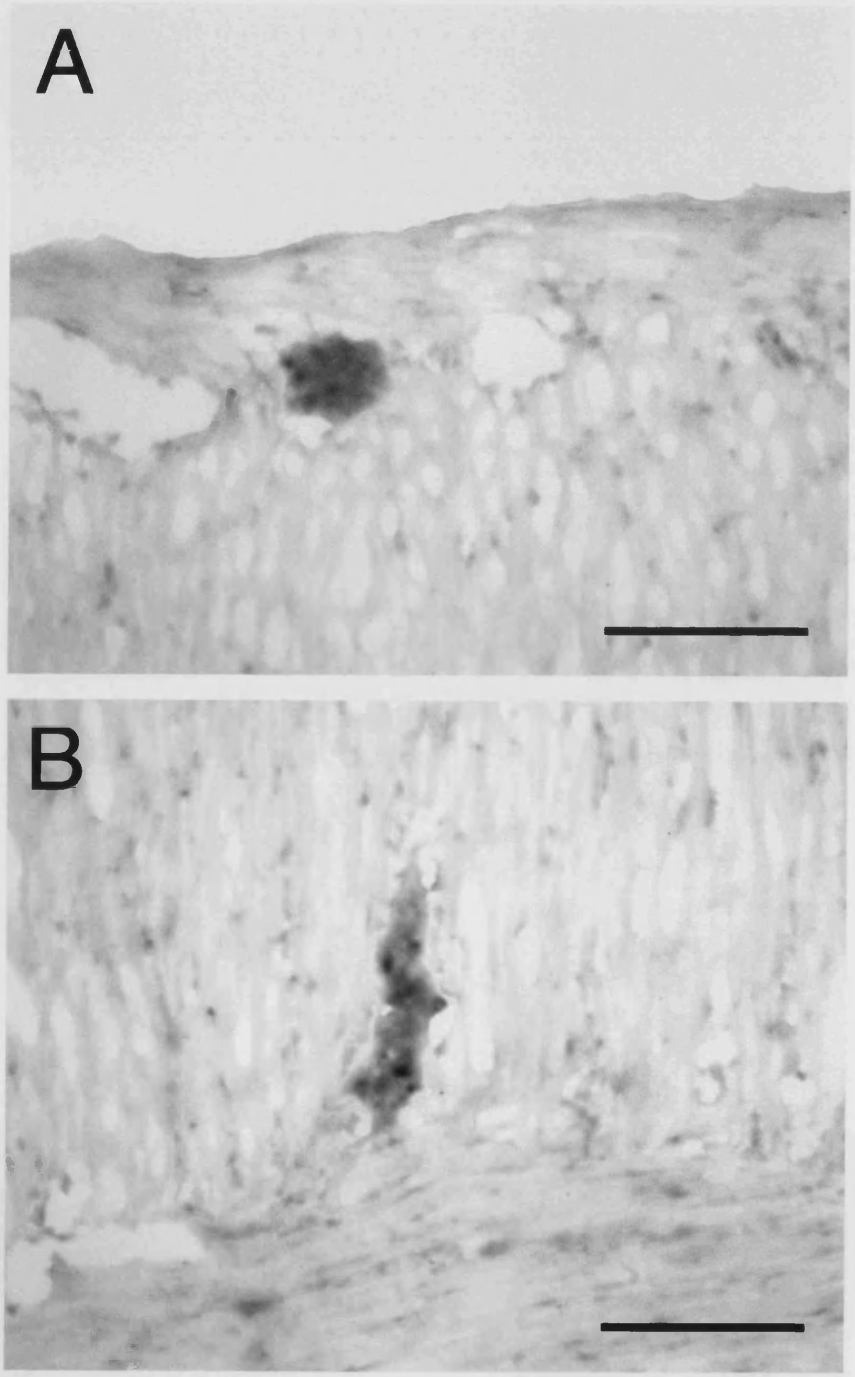
A
B

Figure 3.4.

Specificity of *nogo* probes. Sections through the hippocampal formation and dorsal thalamus reacted with 3 antisense probes, and their controls. In A and B sections were probed with ^{35}S-labelled antisense Nogo-66 DNA oligonucleotides and viewed with dark field illumination. There is strong signal from the labelled probe in A but in B excess unlabelled probe has been added as a competitive control to detect non-specific binding. In C, ^{35}S-labelled sense probe has been used and viewed with dark field illumination. There is no signal from either of the control sections. In D and E sections were reacted with antisense (D) and sense (E) DIG-labelled *nogo-66* riboprobes. The section treated with sense probe (E) shows no signal. In F and G, sections were reacted with antisense (F) and sense (G) DIG-labelled 3' *nogo* riboprobes. Strong signal is present in the section treated with antisense riboprobe (F), but none is present in that treated with the sense probe (G). Scale bar = 500μm.

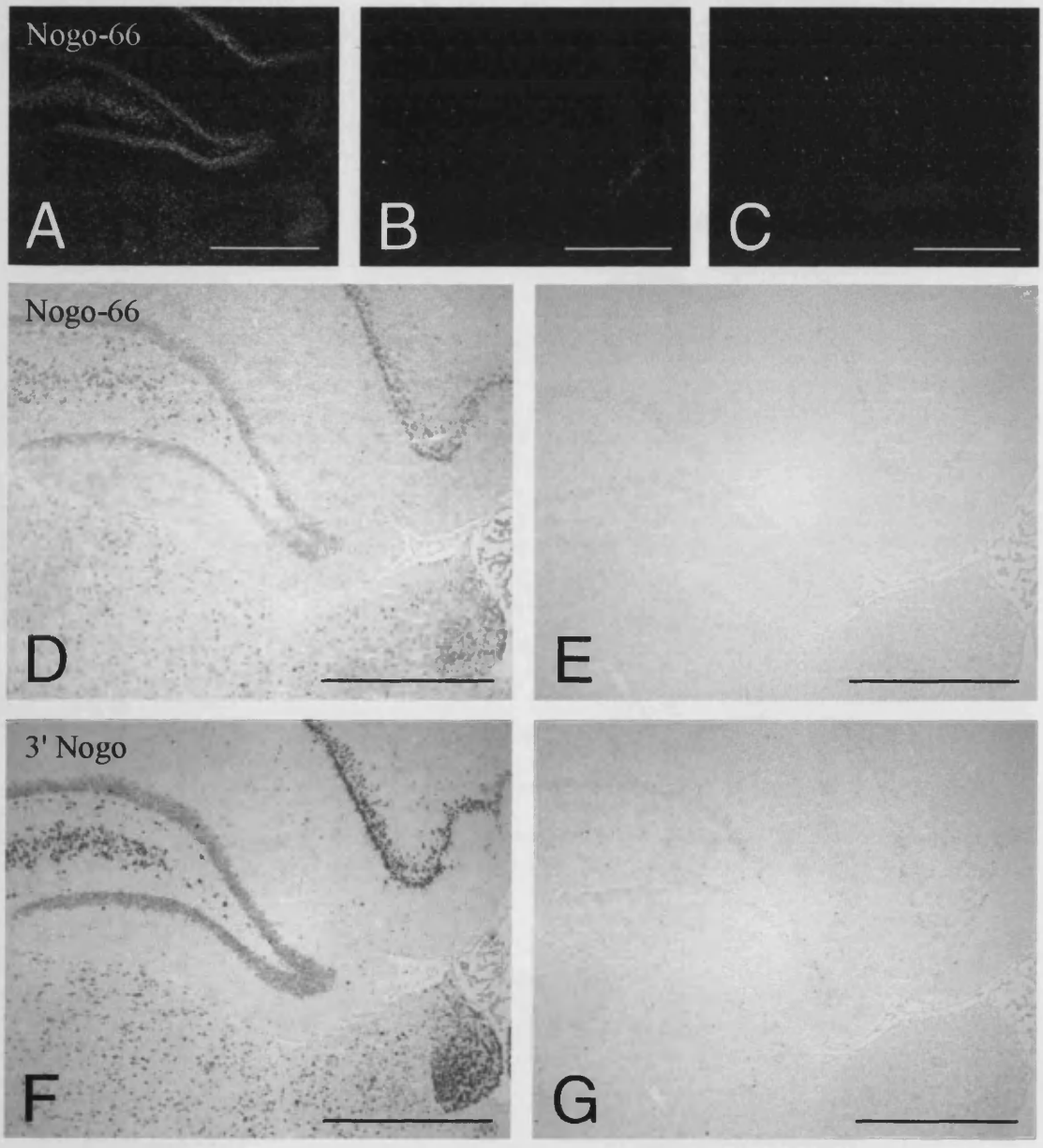
Nogo-66
A
B
C
Nogo-66
D
E
3' Nogo
F
G

Figure 3.5.

A. Coronal section through neostriatum from adult rat, reacted with probe for 3' region *nogo*. There is strong signal from many neurons in the neocortex (C) and neostriatum (S). There is much weaker signal from the cells in the subcortical white matter (W). Scale bar = 500μm.

B. Neostriatum of adult rat reacted with probe for 3' region *nogo*, showing the strong signal from striatal projection neurons and a scattered population of predominantly large diameter striatal neurons (arrows). Scale bar = 250μm.

C. Section through the hippocampal formation and thalamus of an adult rat hybridized for 3' region *nogo*. There is strong signal in the hippocampal formation, medial habenular nucleus (H), some dorsal thalamic nuclei, and the TRN (indicated by arrows). Scale bar = 250μm. Insert shows TRN from adult rat exhibiting strong signal for *nogo-66* using the radioactive oligonucleotide probe. Scale bar = 500μm.

D. Part of the neocortex from an adult rat, hybridized for 3' region *nogo*. Note the strong signal from neurons in layers 2-6. There is very week signal in the molecular layer (M) and weak signal in the subcortical white matter (W). Scale bar = 250μm.

E. Section through the cerebellum and brainstem of an adult rat reacted with the probe to 3' region *nogo*. Strong signal can be detected from Purkinje cells, neurons in the deep cerebellar nuclei (D) and vestibular nuclei (V). Scale bar = 1mm.

F. A higher power image of cerebellar cortex from adult rat reacted with the probe to 3' region *nogo*. A line of Purkinje cells (arrows) showing strong signal for *nogo* can be seen, with weak signal from cells in the granule cell layer and background levels in the molecular layer (asterisk). Compare with *ngr* expression in Fig 3.2.B. Scale bar = 250 μm.

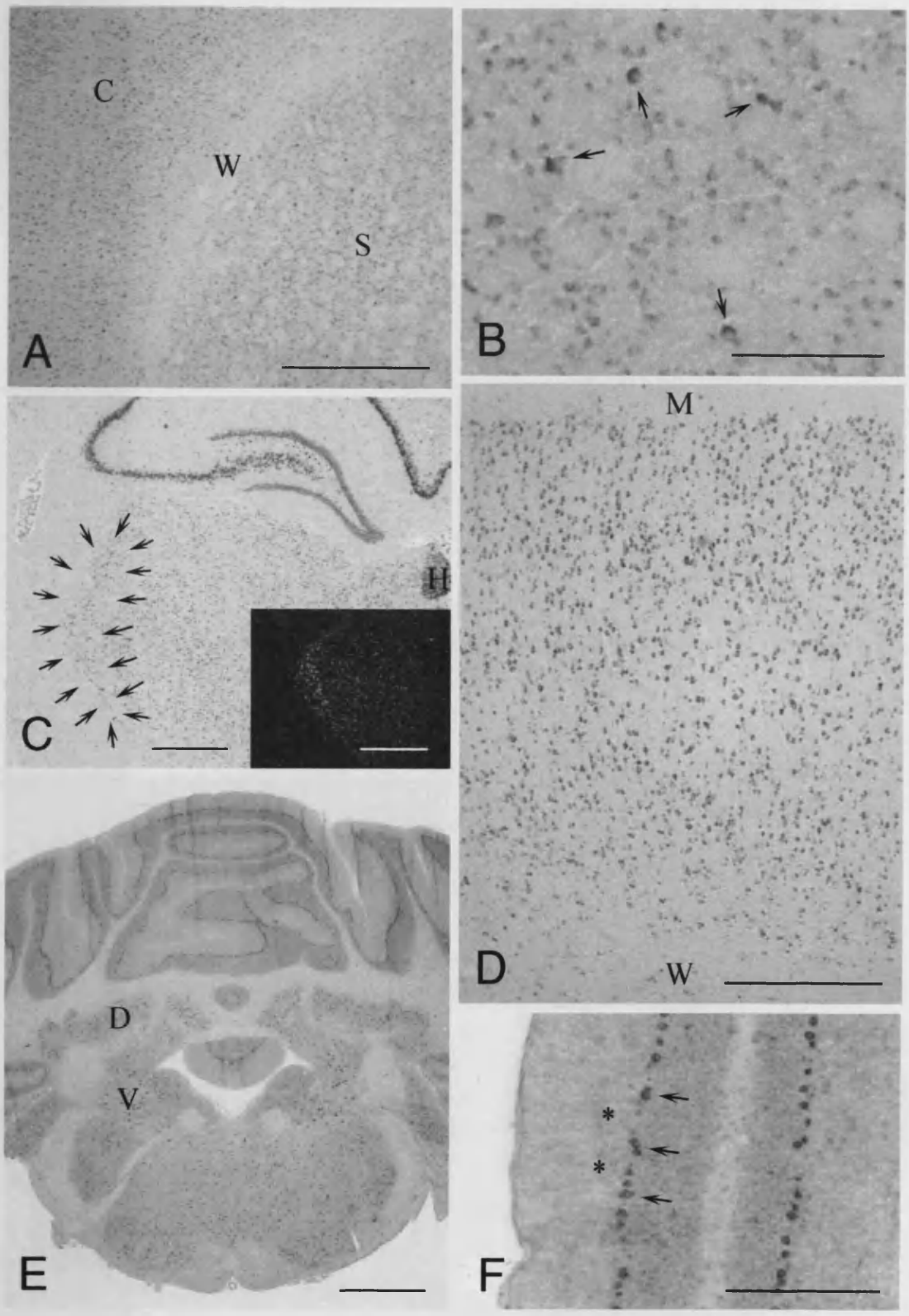
C
W
S
A
B
H
C
M
D
W
D
V
E
*
*
F

Figure 3.6.

A. Cervical spinal cord from adult rat reacted with the probe to 3' region *nogo*. Signal can be seen in many neurons in the grey matter, but is strongest in motor neurons. At this magnification it is difficult to resolve any signal in white matter. Scale bar = 500μm.

B. Higher power image of cervical spinal cord from adult rat reacted with the probe to 3' region *nogo*. Signal can be seen in many neurons in the grey matter, but is strongest in motor neurons (arrowed). Distinct signal is also present in the white matter of the dorsal columns (asterisk). Scale bar = 500μm.

C. Lumbar dorsal root ganglia reacted with probe to 3' region *nogo*. Very strong signal is present in primary sensory neurons but not in the Schwann cells. Scale bar = 500μm.

D. Optic nerve from adult rat, reacted with the probe to 3' region *nogo*. Weak signal can be detected in scattered glial cells (arrowed). Scale bar = 100μm.

E. Retina from adult rat, reacted with the probe to 3' region *nogo*. Strong signal can be seen from the ganglion cell layer (R), inner nuclear layer (INL) and the outer nuclear layer (ONL). Scale bar = 100μm.

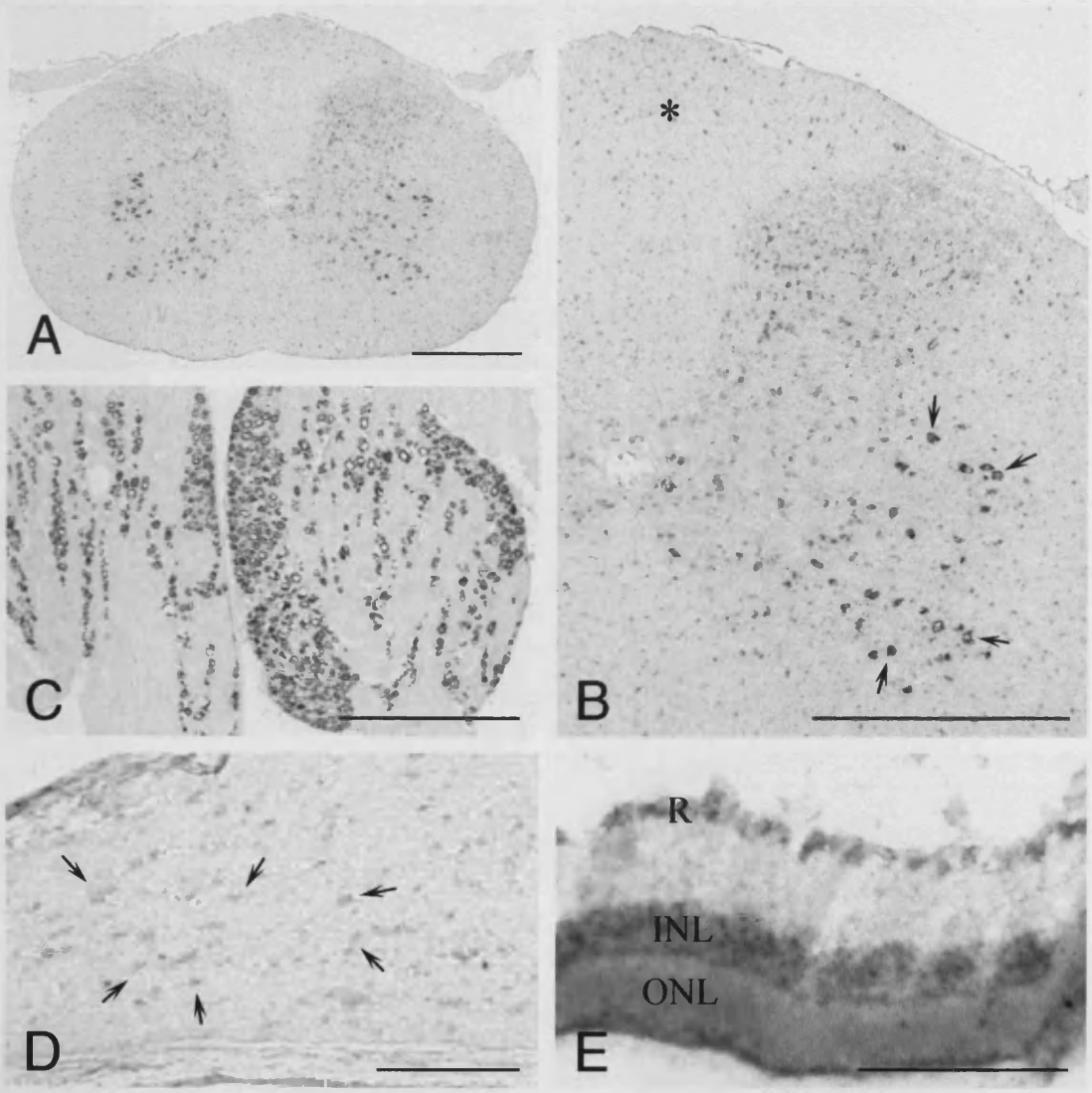
A
B
C
D
E
*
R
INL
ONL

Figure 3.7.

Detection of *nogo* in adult rat peripheral nerve.

A,B. Dark field images of distal stump of sciatic nerve 3 days after transection, reacted with the radioactive Nogo-66 probe. A low level of signal is present from many cells but is strong on scattered cells, particularly near the cut end of the nerve (B). Scale bar = 500μm.

C. Bright field image of the section seen in Fig 3.7.A. Some cells showing highest levels of signal are arrowed. Scale bar = 250μm.

D. Bright field image of contralateral (uninjured) sciatic nerve. No signal for Nogo-66 is detectable. Scale bar = 250μm.

E,F. Bright field images of sections of sciatic nerve 3 days after injury (E) and contralateral to the injury (F), reacted with the probe to 3' region *nogo*. Strong signal can be seen from scattered cells in the injured nerve (arrows) but not in the intact nerve (F). Scale bar = 100μm.

G. Film, after 3 days exposure, showing sections of sciatic nerve from adult rat treated with the radioactive probe to Nogo-66. Strong signal is apparent from sections of the distal stump of the injured nerve (DS) 3 days after transection, but not from sections of the intact nerve (C) which are consequently undetectable in the figure.

H. RT-PCR for *nogo-66* from RNA extracted from the distal stump of adult rat sciatic nerve, 3 days after transection. A single strong band for Nogo-66 (~0.2Kb) is present after 35 PCR cycles. Sample was run against a 1Kb DNA molecular weight marker (Gibco BRL) on a 1% agarose gel.

I. *In situ* hybridization with the probe to 3' region *nogo* on a section of the thalamus of an adult rat 16 days after the insertion of a peripheral nerve graft (G). Increased signal can be seen from cells in the thalamus near the graft/brain interface (arrowed). Scale bar = 500μm.

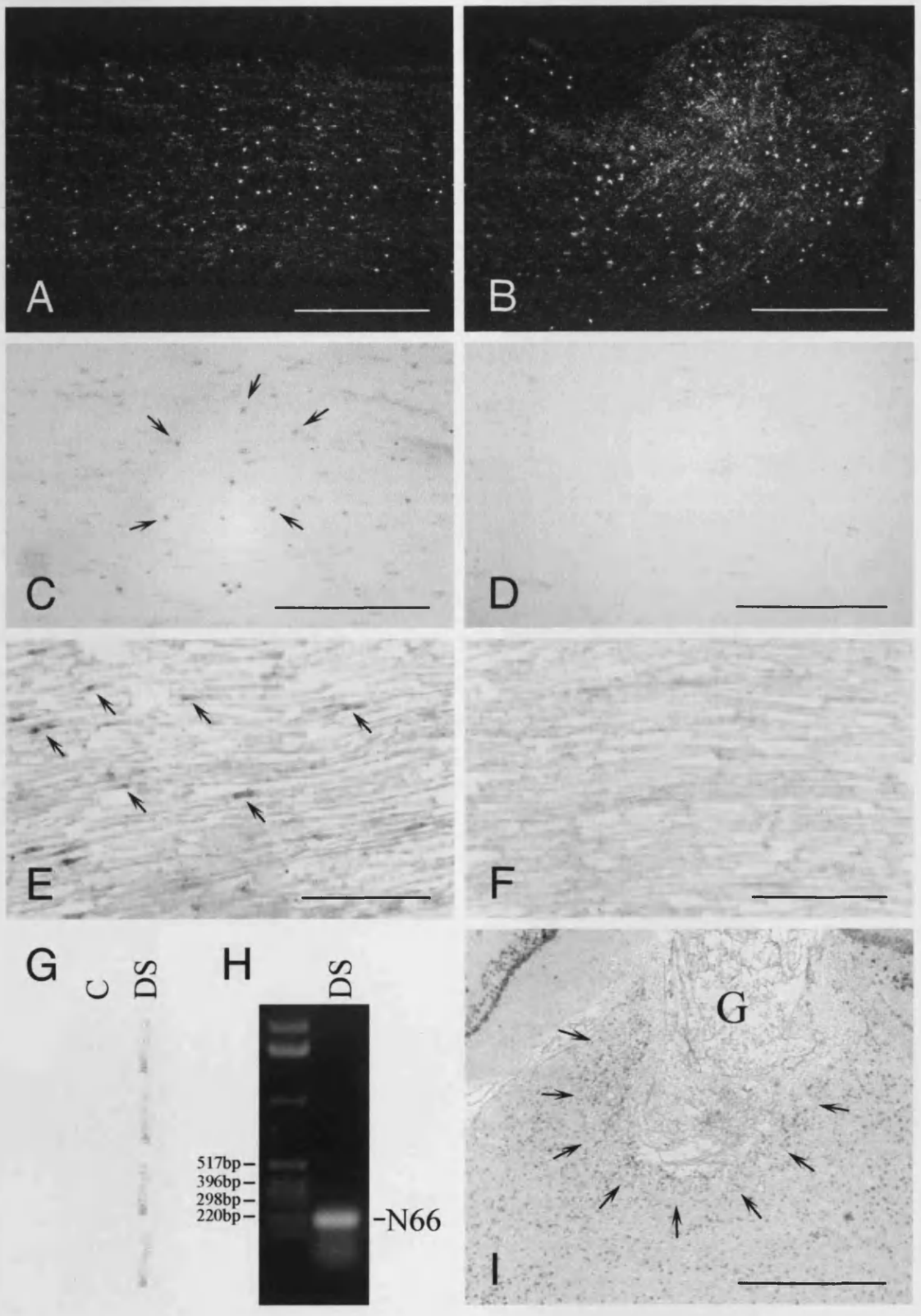
A
B
C
D
E
F
G
C
DS
H
DS
517bp
396bp
298bp
220bp
-N66
G
I

Table 3.1.

Splice variants of *reticulon 4* containing the *nogo-66* coding sequence.

The human *reticulon 4* gene has been mapped to chromosome 2p14→13 (Yang et al, 2000). It comprises 11 known exons and is spread over nearly 80Kb of chromosomal DNA. Differential splicing of the gene gives rise to at least seven different mRNAs containing the *nogo-66* coding sequence. For some of these molecules there are multiple encoding sequences deposited in the NCBI database with variations confined to the first and last exons – probably because the sequencing process does not reliably read the ends of the transcripts. The dilysine ER retention signal, -KRKAE, is found at the C-terminus (Exon 11) of all spice variants. The *nogo* probes we have used for *in situ* hybridization, to the *nogo-66* coding sequence located within exons 6 and 7, and the 3' *nogo* region spanning exons 6-11 have the capacity to detect any of the splice variants listed.

Splice variants containing the *nogo-66* coding sequence are widely expressed in normal and neoplastic human tissues, implying that this gene is multi-faceted and has functions other than inducing neuronal growth cone collapse. Nogo A has a specific domain (encoded by exons 3 and 4) which also displays neurite outgrowth inhibitory activity, through an unknown mechanism. However, the testis specific reticulon (Rtn-T) is translated from a transcript containing these two exons and has been postulated to play a role in testicular development.

NIH-MGC: National Institutes of Health - Mammalian Gene Collection project.

NSP – Neuroendocrine Specific Protein

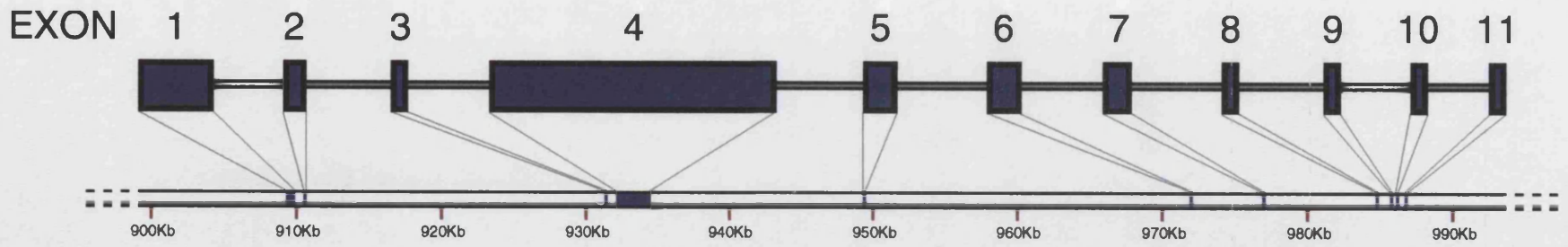

Name	Genbank Accession Number	Exon 1	Exon 2	Exon 3	Exon 4	Exon 5	Exon 6	Exon 7	Exon 8	Exon 9	Exon 10	Exon 11	mRNA length	Amino acid length	Sequence submitted by	Source (human tissue)
Nogo-A	AJ251383	Y	N	Y	Y	N	Y	Y	Y	Y	Y	Y	3579	1192	Prinjha et al	None specified
Reticulon 4a	AF148537	Y	N	Y	Y	N	Y	Y	Y	Y	Y	Y	4632	1192	Zhou et al	None specified
KIAA0086	AB020693	Y	N	Y	Y	N	Y	Y	Y	Y	Y	Y	4053	1192	Ohara et al	Adult male brain
Rtn-xL	AB040462	Y	N	Y	Y	N	Y	Y	Y	Y	Y	Y	4166	1192	Eguchi et al	Foetal brain
Testis Specific Rtn (Rtn-T)	AF333336	N	Y	Y	Y	N	Y	Y	Y	Y	Y	Y	3491	986	Sha et al	Adult testis
Nogo-A short form	AF320999	Y	N	N	Y	N	Y	Y	Y	Y	Y	Y	2883	960	Jin and Ju	None specified
Brain my043	AF063601	N	N	N	Y	N	Y	Y	Y	Y	Y	Y	2481	647	Mao et al	Foetal brain
MGC clone:15807 IMAGE:3505850	BC016165	Y	N	Y	N	N	Y	Y	Y	Y	Y	Y	1784	392	NIH-MGC	Kidney: renal cell adenocarcinoma
Nogo-B	AJ251384	Y	N	N	N	N	Y	Y	Y	Y	Y	Y	1122	373	Prinjha et al	None specified
Reticulon 4b	AF148538	Y	N	N	N	N	Y	Y	Y	Y	Y	Y	2235	373	Zhou et al	None specified
ASY cell death-inducing gene	AB015639	Y	N	N	N	N	Y	Y	Y	Y	Y	Y	2052	373	Yutsudo	Fibroblast
Foocen-m	AF132047	Y	N	N	N	N	Y	Y	Y	Y	Y	Y	2276	373	Ito and Schwartz	Placenta
Rtn-xS	AB040463	Y	N	N	N	N	Y	Y	Y	Y	Y	Y	1709	373	Eguchi et al	Foetal brain
MGC clone:10125 IMAGE:3901353	BC010737	Y	N	N	N	N	Y	Y	Y	Y	Y	Y	1485	373	NIH-MGC	Pancreas: epitheloid carcinoma
MGC clone:13655 IMAGE:4082756	BC012619	Y	N	N	N	N	Y	Y	Y	Y	Y	Y	1654	373	NIH-MGC	Brain: glioblastoma
Nogo-C	AJ251385	N	N	N	N	Y	Y	Y	Y	Y	Y	Y	600	199	Prinjha et al	None specified
Reticulon 4C	AF087901	N	N	N	N	Y	Y	Y	Y	Y	Y	Y	1617	199	Zhou et al	None specified
NSP C Homolog	AF077050	N	N	N	N	Y	Y	Y	Y	Y	Y	Y	1785	199	Song et al	Pituitary
NSP C Homolog	AF125103	N	N	N	N	Y	Y	Y	Y	Y	Y	Y	1798	199	Zhang et al	CD34+ve haematopoietic stem/progenitor cells
SP1507 Unknown mRNA	AF177332	N	N	N	N	Y	Y	Y	Y	Y	Y	Y	1700	199	Gu et al	None specified
MGC clone:1239 IMAGE:3139770	BC001035	N	N	N	N	Y	Y	Y	Y	Y	Y	Y	1160	199	NIH-MGC	Placenta: choriocarcinoma
MGC clone:14766 IMAGE:4291127	BC007109	N	N	N	N	Y	Y	Y	Y	Y	Y	Y	1079	199	NIH-MGC	Skeletal muscle
MGC clone:24257 IMAGE:3933041	BC014366	N	N	N	N	Y	Y	Y	Y	Y	Y	Y	1698	199	NIH-MGC	Brain

CHAPTER 4

Nogo-A Expression in the Intact and Injured Nervous System

INTRODUCTION

Nogo-A is widely considered one of the most inhibitory proteins to axonal regeneration. In addition to the Nogo-66 domain, which is present in all Nogo isoforms and has been shown to exert neurite outgrowth inhibition through the Nogo-66 Receptor (NgR) (Fournier et al., 2001), Nogo-A possesses a unique amino terminus which is also a potent inhibitor of neurite outgrowth (Grandpre et al., 2000; Prinjha et al., 2000). This 'Nogo-A specific' domain is active in the absence of NgR (Niederost et al., 2002). However, whilst studies to elucidate a Nogo-A specific receptor have so far proved fruitless, there have been numerous studies implicating the Nogo family of proteins, including Nogo-A , in ever broader biological processes (Li et al., 2001; Hu et al., 2002; Acevedo et al., 2004).

Within the nervous system, *in situ* hybridisation studies using pan-*nogo* antisense riboprobes have revealed a widespread distribution of *nogo* transcripts, both in oligodendrocytes and neurons (Chapter 3; Josephson et al., 2001; Huber et al., 2002; Hunt et al., 2002b). Furthermore, *nogo-a* transcripts are also expressed by these cell types (Josephson et al., 2001; Huber et al., 2002). That neurons should express *nogo-a* is not in keeping with the notion that Nogo-A functions solely as a myelin associated inhibitor of axonal regeneration within the nervous system. Intriguingly, Nogo-A protein has been reported to be extensively expressed by CNS and PNS neurons within the developing nervous system, prior to the emergence of oligodendrocytes and the onset of myelination (Tozaki et al., 2002). It has also been found to be strongly expressed in developing muscle (Wang et al., 2002c).

In situ hybridisation and immunohistochemistry were performed to elaborate on Nogo-A expression, particularly by neurons, in the adult rodent nervous system before and after injury. Furthermore, localisation of the protein was compared with that in cultured embryonic neocortical and adult DRG neurons. Some preliminary observations, regarding Nogo-A expression in the developing nervous system and muscle, were also made.

SUMMARY OF METHODS

Animal Models

Twenty operated adult Sprague-Dawley rats were used in these experiments. In 3 rats, autologous segments of the left tibial nerve were grafted to the left thalamus. These animals were killed at 14 days post operation (dpo). In 8 rats, the left sciatic nerve was transected in the thigh, and 2-3mm of the nerve resected to create a gap between the proximal and distal stumps. These animals were killed at 4 (n=2), 8 (n=3) and 16dpo (n=3). In 6 rats, the dorsal columns of the spinal cord were transected at C6, using microsurgical scissors. These animals also underwent a left sciatic nerve transection to stimulate the sprouting of dorsal column axons into the lesion site, and were killed at 4 (n=2), 8 (n=2) and 16dpo (n=2). In 3 rats, the left optic nerve was crushed with watchmaker's forceps. These animals were killed at 4 (n=2) and 14dpo (n=1) days. Three unoperated adult Sprague-Dawley rats, and two unoperated P14 male Balb/c mice were also used in these experiments. For dissociated adult DRG cultures, three unoperated adult Lewes rats were killed. For dissociated embryonic cortical cultures, three pregnant ICR mice were killed by dislocation of the neck at 13.5 days post conception (E13.5), and three pregnant Sprague-Dawley rats were each killed at 17 days and 19 days post conception (E17 and E19). N.B. All observations of Nogo-A expression *in vivo* were derived from Sprague-Dawley rats or Balb/c mice.

Immunohistochemistry

20μm fresh-frozen sections were cut with a Bright cryostat and thaw-mounted on to Superfrost Plus slides. As a preliminary examination of antigen sensitivity to fixation,

different methods of tissue-section fixation were employed: 30s immersion in –20°C methanol; 10mins immersion in -20°C methanol:acetone (1:1); 25mins immersion in 95% ethanol/5% acetic acid at 4°C; ~45mins immersion in 4% PFA in 1xPBS. Some sections were also processed without fixation. For all double-labelling immunohistochemistry, fixation with 4% PFA was the preferred method. Immunohistochemistry was performed as described in Chapter 2.

The following primary antibodies were used in this study: mouse anti-Nogo-A monoclonal antibody (clone 6D5; RKP et al., manuscript in preparation; Dupuis et al., 2002); rabbit anti-neurofilament 200kDa polyclonal antibody (Sigma); rabbit anti-NG2 polyclonal antibody (kind gift of Dr. W.B. Stallcup, The Burnham Institute, La Jolla, California); rabbit anti-bovine glial fibrillary acidic protein (Dako); rabbit anti-ATF3 (Santa Cruz). Two secondary antibodies were used: monoclonal tetramethylrhodamine conjugated goat anti-mouse (Molecular Probes); monoclonal Alexa-Fluor conjugated goat anti-rabbit (Molecular Probes). Both secondary antibodies were adsorbed against rat serum prior to use. Control sections, which were not incubated with primary antibodies, were used to ensure signal specificity.

SDS-PAGE and Western Blotting

Freshly isolated P8 Sprague-Dawley rat cerebellar granule neurons (a kind gift from Laura Facci; prepared as described by Ginham et al., 2001) were homogenized by boiling in Laemmli sample buffer ($1x10^6$ in 200µl). 10µl of lysate was run on a 7.5% Tris-glycine polyacrylamide gel (BioRad) adjacent to Rainbow markers (RPN-800, Amersham Pharmacia) at 75V. Proteins were electroblotted onto PVDF (BioRad) at 30V overnight. The filter was blocked using 5% milk powder (Marvel) in PBS for 90 mins. Anti-Nogo-A monoclonal 6D5 conditioned medium was diluted 1 in 20 in 5% milk and incubated with the filter for 90 mins. After washing (3x 5mins) with PBS the filter was incubated with goat anti-mouse-HRP (BioRad) diluted 1 in 3000 for 90 minutes. The filter was washed with four changes of PBS (5 mins each) and then visualized using ECL onto Hyperfilm ECL (Amersham Pharmacia). This work was performed by Dr. Rabinder Prinjha, Glaxosmithkline plc.

In Situ Hybridisation

Cloning of Rat Nogo-A Fragment

A 499bp fragment of Genbank sequence AJ242961 (bases 1517-2015, which correspond to part of the 'Nogo-A specific domain') was obtained by RT-PCR from adult rat brain total RNA. Primers incorporating the internal restriction endonuclease sites *Xho*I and *Hin*dIII were used in the amplification (ACT G*CT CGA G*AG GAT GCT TCT TTC CCC AGT and ATC G*AA GCT T*AA AAC TGG TGA CGG AGT TGC, respectively). The purified DNA product was ligated between these sites in the pcDNA3 vector (Invitrogen), and the insert sequence was verified using an automated fluorescent-dye sequencing system (Applied Biosystems, UK).

Generation of DIG-Labelled Riboprobes

Antisense probes were generated by linearisation of the pcDNA3 plasmid with *Xho*I, followed by *in vitro* transcription with T7 RNA polymerase. Conversely, sense probes were generated by linearisation with *Hin*dIII, followed by *in vitro* transcription with SP6 RNA polymerase. Antisense and sense cRNA probes labelled with DIG were generated according to the manufacturer's recommendations using an RNA labelling kit (Boehringer Mannheim, Germany). *In situ* hybridisation was performed as described in Chapter 2.

RESULTS

Western Blot of P8 Rat Cerebellar Granule Cells with anti-Nogo-A mAb (Fig. 4.1)

Immunoblotting of P8 Sprague-Dawley rat cerebellar granule cell lysate, with the anti-Nogo-A monoclonal antibody 6D5, revealed a single strong band of 180KDa. Additionally, immunoblotting of cos cell lysate, following transfection with a DNA expression vector encoding human Nogo-A, enabled the detection of the same band (not shown; RKP et al., in preparation).

***nogo-a* mRNA Expression in the Intact Nervous System (Table 4.1)**

nogo-a transcripts were expressed widely throughout the nervous system in both white and grey matter. In the neocortex many neurons including large pyramidal cells were found to express *nogo-a*, as were many small cells whose morphological appearance resembled oligodendrocytes (Fig. 4.2.A). Similarly, cells within the subcortical white matter also expressed high levels of *nogo-a* mRNA. In the neostriatum, cells whose large size and scant distribution was consistent with being cholinergic interneurons were found to strongly express the transcript. Lower levels were detectable in many other smaller cells within this region (Fig. 4.2.B). In the hippocampus, moderate levels of *nogo-a* expression were found in the CA1-CA4 cells and neurons of the dentate hilus. Very little or only background expression was evident in the dentate gyrus (Fig. 4.2.C). Moderate levels of *nogo-a* were present in the red nucleus and substantia nigra pars compacta (SNpc) (Fig. 4.2.D).

In the cerebellum, *nogo-a* transcripts were moderately expressed by small cells within the white matter and granule cell layer whose appearance was consistent with being oligodendrocytes. Strong expression was also evident in neurons of the cerebellar deep nuclei. Interestingly, many Purkinje cells strongly expressed *nogo-a*, yet some others exhibited no expression (Fig. 4.2.E). Only background levels were discernible within the granule cell layer, notwithstanding a few larger cells – thought to be non-granule cell neurons – and smaller presumptive glia. Very strong expression of *nogo-a* was found in neurons of the pontine nuclei (not shown).

In the spinal cord, *nogo-a* transcripts were most strongly expressed by neurons throughout the grey matter, especially within the large motor neurons of the ventral horn (Fig. 4.2.F). However, neurons of the superficial dorsal horn exhibited notably lower levels of expression. Transcripts were highly expressed by neurons of the dorsal root ganglia (DRG), but no discernable expression was observed in either the satellite or other non-neuronal cells of the DRG (Fig. 4.2.G). Similarly strong expression was observed in neurons of the superior cervical ganglion (Fig. 4.2.H). In the retina, strong expression of *nogo-a* transcripts was readily detectable in the retinal ganglion cell neurons (Fig. 4.2.I).

In the distal colon of adult rat, neurons of the myenteric plexus were also found to express *nogo-a* mRNA (Fig. 4.3).

Nogo-A Protein in the Intact Nervous System (Table 4.1)

Since it has previously been reported that different methods of tissue post-fixation affect the immunohistochemical detection of Nogo-A (Huber et al., 2002), numerous post-fixation methods were examined to verify this claim. Fresh-frozen tissue sections were post-fixed with paraformaldehyde, methanol, methanol:acetone (1:1), or acid alcohol, or were not post-fixed at all. The pattern of Nogo-A immunohistochemical detection was very similar in terms of distribution and relative intensity for all forms of post-fixation (as well as none at all), except with acid alcohol. Paraformaldehyde produced the lowest background level of signal, whilst methanol or methanol:acetone (1:1) produced the strongest cellular signal. In contrast, acid alcohol greatly enhanced white matter immunofluorescence and simultaneously decreased the perikaryal signal from both neurons and glia. All tissue sections labelled only for Nogo-A were routinely fixed with methanol:acetone (1:1), but double-labelled sections were post-fixed with paraformaldehyde for compatibility with other examined antigens.

In the neocortex of adult rat, most neurons were only weakly immunoreactive for Nogo-A whilst presumptive oligodendrocytes were strongly immunopositive (Fig. 4.4.A). In the neostriatum of adult rat, presumptive glia were strongly immunopositive for Nogo-A, but moderate immunoreactivity was also detected in large neurons (perikarya $\geq$ 20μm in diameter) whose distribution was consistent with being cholinergic interneurons (Fig. 4.2.B, inset). No discernable Nogo-A expression was observed in the perikarya within the granule cell layer of the hippocampal formation, but neurons of the dentate hilus were immunoreactive for Nogo-A (Fig. 4.2.C, inset). In the cerebral peduncles, both presumptive oligodendrocytes and axons were immunopositive for Nogo-A (Fig. 4.4.B).
In the cerebellum of adult rat, strong immunoreactivity for Nogo-A was detected in the neuronal perikarya of the deep nuclei, and in most but not all Purkinje cell perikarya and their dendrites (Fig. 4.4.C). Nogo-A could not be detected in the axons of Purkinje cells. No obvious nuclear signal for Nogo-A in Purkinje cells, or spinal motor neurons, was

observed (cf. Jin et al., 2003), but its presence at a lower level than that in the cytoplasm could not be definitively excluded. Intriguingly, some Purkinje cell perikarya did not exhibit any discernible immunoreactivity for Nogo-A (Fig. 4.4.D). Strong expression of the protein was found in numerous other neuronal perikarya throughout adult rat brain, including those of the habenular nuclei, the pontine nuclei and the mesencephalic nucleus of V (not shown).

In the lumbar spinal cord of adult rat, strong Nogo-A immunoreactivity was detectable in neurons throughout the grey matter, especially in motor neurons of the ventral horn (Fig. 4.4.E). Interestingly, the axons of motor neurons were also found to be Nogo-A immunopositve. In cervical spinal cord, some motor neurons in the ventral horn did not express Nogo-A (not shown). Strong expression of Nogo-A was observed in the presumptive glia, distributed throughout the grey and white matter of both lumbar and cervical spinal cord. No co-localisation with NG2 could be demonstrated at either level, suggesting that this population of glia does not include oligodendrocyte precursor cells (OPCs) (Fig. 4.5.A-C). In the SCG, the perikarya of postganglionic sympathetic neurons were strongly immunoreactive for Nogo-A, as were their axons (Fig. 4.4.F). Likewise, strong expression of the protein was detected in the perikarya and axons of DRG neurons (Fig. 4.4.G). In the intact sciatic nerve of adult rat, immunofluorescent signal for Nogo-A was detected in apparently all myelinated axons (Figs. 4.5.D-F), but was particularly prominent in bundles of unmyelinated axons (Fig. 4.4.H).

High levels of Nogo-A protein expression were detected in the retinal ganglion cells of adult rats (Fig. 4.6.A). However, their axons were much less readily immunoreactive, both in the retinal nerve fibre layer and the optic nerve (Fig. 4.6.B-C). Strong expression of Nogo-A was found in the perikarya and axons of the ciliary ganglion neurons (Figs. 4.6.C and D).

Nogo-A Expression in the Embryonic and Early Postnatal Nervous System

Nogo-A was found to be expressed throughout the telencephalic wall of embryonic mouse forebrain. At E13.5, the protein appeared to be present in the perikarya of radial

glia, their processes, as well as tangentially aligned axon-like structures (Fig. 4.7.A). However, immunofluorescent signal for Nogo-A did not co-localize with that of calretinin, a calcium-binding protein, expressed by preplate neurons. At E17.5, structures reminiscent of radial glia within the cortical plate (CP) were immunopositive for Nogo-A, as were corticofugal and corticopetal fibres in the intermediate zone (IZ) (Fig. 4.7.B). Sections through E14 rat hindlimb immunoreacted for Nogo-A and neurofilament revealed that developing peripheral nerve, as well as skeletal muscle, express high levels of Nogo-A (Fig. 4.8.A-B).

In the neocortex of P14 mouse, Nogo-A was not obviously expressed by neurons, but was by presumptive oligodendrocytes (Fig. 4.7.C). In the neostriatum of these animals, Nogo-A was not detected in any neuronal perikarya. However, presumptive oligodendrocytes, often closely associated with bundles of axons, were strongly immunoreactive for the protein (Fig. 4.7.D).

Nogo-A Expression in Cultured Neurons

Dissociated cultures of adult Lewis rat DRG neurons (3 days *in vitro*; DIV), foetal (E13.5) ICR mouse cortical neurons (3DIV) (Fig. 4.6.E-G) and foetal Sprague-Dawley rat E17 and E19 cortical neurons (3DIV) (not shown) exhibited strong perikaryal Nogo-A immunoreactivity. Within the neurites, Nogo-A expression was most marked in the growth cones (Figs. 4.6.F-H) and axonal varicosities. Strong expression was also often present at branch points or at sites where axons crossed (Fig.s 4.6.E-H). Intriguingly, Nogo-A immunofluorescent signal tended to be detected more distally within the neurites than was that of neurofilament (Fig. 4.6.F). Indeed, in the growth cones, most of the signal for Nogo-A was localized to the central domain and rarely to the periphery (Fig. 4.6.H); however, it was occasionally detected in some filopodia.

Nogo-A Expression after Peripheral Nerve Injury

Transcripts for *nogo-a* were not detected in intact adult rat sciatic nerve, nor the proximal and distal stumps of transected sciatic nerves at 4, 8 and 16 days post operation (dpo) (Figs. 4.9.A-B). However, strong immunofluorescent signal for Nogo-A was present in

the axons within the proximal stumps at all timepoints. At 4 dpo, axonal sprouts were observed at the severed end of the proximal stump (Figs. 4.10.A-B) and, by 8 and 16dpo, these were found to have extended distally with many axons having entered the distal stump (Figs. 4.10.C-D and 4.11.A-B). The majority of sprouting and regenerating axons, identified by neurofilament immunoreactivity, were Nogo-A immunopositive at all timepoints after transection. However, the relative expression was variable: the fibres which were most prominently immunoreactive for Nogo-A were not always strongly immunoreactive for neurofilament, and vice versa (Figs. 4.5.G-I). In fact, the regenerating axons exhibited a more patchy immunoreactivity for Nogo-A than they did for neurofilament. This was such that the Nogo-A-defined axons were often slightly different in shape compared to the neurofilament-defined axons. Clearly, the tips of many regenerating axons expressed signal for Nogo-A, but not for neurofilament (Figs. 4.10.C-F). It would seem, therefore, that Nogo-A may serve as a suitable immunohistochemical marker for most regenerating axons in injured peripheral nerve.

At 16dpo, in the tissue bridge between proximal and distal stumps, spontaneously generated small striated muscle fibres were found amid the regenerating axons. Interestingly, these ectopic muscle fibres were always strongly Nogo-A immunoreactive (Figs. 4.11.A-D), and were often observed in contact with regenerating axons which had grown along their surface (Figs. 4.11.E-F). Those axons which had come into contact with these Nogo-A immunopositive muscle cells exhibited varying degrees of immunoreactivity for the protein, but many were found to express high levels of Nogo-A. No discernible regulation of Nogo-A expression by axotomized motor or DRG neurons, themselves identified by ATF3 immunoreactivity in their nuclei, was observed at 4dpo (not shown).

Nogo-A Expression After Peripheral Nerve Implantation into the Thalamus

At 16dpo, *in situ* hybridisation revealed a strong expression of *nogo-a* mRNA in a ring of cells bordering the tip of a autologous tibial nerve graft in thalamus (Fig. 4.9.C). No such pattern of expression was detected contralateral to the graft. Transcripts for *nogo-a* were abundant in the neurons of the thalamic reticular nucleus - which is the source of the

majority of regenerating axons following peripheral nerve graft to thalamus – on both the grafted and contralateral (i.e. non-regenerating) sides. There was no obvious regulation of *nogo-a* mRNA expression in these regenerating intrinsic CNS neurons.

Nogo-A Expression After Spinal Cord Injury

Dorsal column transection and concomitant sciatic nerve conditioning lesions were performed on adult Sprague-Dawley rats to assess transcript and protein expression at different timepoints after injury. At 8dpo, a mild upregulation of *nogo-a* mRNA expression was observed in cells bordering a lesion to the dorsal columns of adult rat spinal cord (Figs. 4.9.D-E). However, there were far fewer *nogo-a*-expressing cells within the lesion site itself compared to the surrounding spinal cord tissue. In contrast, immunohistochemical analysis of Nogo-A expression after dorsal column injury revealed a markedly different picture. As early as 4dpo, there was a considerable increase in Nogo-A immunoreactivity. This was predominantly detected in neurites at the borders of the lesion, especially in axons in the ascending dorsal columns, and also in some scattered perikarya. The lesion site was for the most part devoid of Nogo-A immunoreactivity (Fig. 4.12.A). Nonetheless, by 8 and 16dpo, Nogo-A could be observed in swollen axons within the ascending dorsal columns caudal to the injury, as well as in fibres penetrating the lesion site (Figs. 4.12.B and D). Most of these fibres were also immunoreactive for neurofilament (Fig. 4.12.C), indicating that these were indeed axonal sprouts. No colocalisation of Nogo-A with GFAP or NG2 immunoreactive structures could be found (Figs. 4.12.E-F), demonstrating that these penetrating fibres were not the processes of astrocytes or NG2 immunopositive glia. Within the lesion site, some in-growing Nogo-A positive processes terminated with large rounded neurofilament negative structures which were consistent with being retraction bulbs. In some instances, confocal microscopic analysis of a single optical plane revealed that axons, both in the ascending dorsal columns caudal to the lesion as well as in the lesion itself, were immunoreactive for neurofilament and Nogo-A (not shown). At later timepoints, some Nogo-A immunoreactive perikarya were identified within the lesion sites (not shown), usually near the borders. Similarly, strong upregulation of Nogo-A was detected in some neuronal perikarya in the grey matter at the lesion borders.

Nogo-A Expression After Optic Nerve Crush

At 4dpo, the lesion site could clearly be defined by the relative absence of Nogo-A and GFAP immunoreactivity. Conversely, the proximal and distal boundaries of the lesion site were further enhanced by an upregulation of Nogo-A expression (Fig. 4.12.G). The perikarya of small cells, consistent with being oligodendrocytes, strongly expressed Nogo-A. No axonal labelling was readily discernible in the proximal stump of the crushed optic nerve, owing to the high level of background signal presumably due to the presence of large amounts of myelin (Fig. 4.12.H). Nonetheless, axonal sprouts, identified by their neurofilament immunoreactivity, had entered the lesion site from the proximal stump. Some of these invading neurites weakly expressed Nogo-A, which was visible because of the lower background signal within the lesion site. However, some putative axonal sprouts were found to express Nogo-A, but not neurofilament (not shown).

DISCUSSION

This study has confirmed many previous reports that Nogo-A is expressed by numerous types of neuron. As well as confirming that the protein is expressed by presumptive oligodendrocytes, but not astrocytes, it was also demonstrated that it is not expressed by NG2 immunopositive glia. Additionally, it was shown that Nogo-A is extensively expressed throughout the intact and regenerating axons of the peripheral nervous system. Nogo-A is very strongly expressed by unmyelinated axons in peripheral nerves, but appears to be expressed with varying degrees of intensity by most, if not all, peripheral nerve axons. *In vitro* dissociated cultures of E13.5 mouse, as well as E17 and E19 rat, neocortical neurons and adult rat DRG neurons exhibited strong expression of Nogo-A, most notably in the neuronal perikarya, axonal varicosities and growth cones. *In vivo*, following the transection of adult rat sciatic nerve, regenerating axons were found to contain large amounts of Nogo-A, as were ectopic striated muscle fibres that arise spontaneously in the tissue bridge between proximal and distal stumps amid the regenerating Nogo-A immunoreactive axons.

In adult rats, which had undergone a dorsal column transection and a concomitant sciatic nerve conditioning lesion, many axons sprouting into the spinal dorsal column lesion site were found to contain Nogo-A and, moreover, represented the major source of the protein within the lesion. In short, a strong expression of axonal Nogo-A appeared to correlate well with the ability to regenerate.

Expression of *nogo-a* mRNA vs. *nogo-66* mRNA in the CNS

Transcripts encoding the Nogo-66 ligand are most strongly expressed by neurons, are found in presumptive oligodendrocytes and are upregulated around sites of injury to the CNS and in distal stumps of peripheral nerves (Chapter 3; Hunt et al., 2002a). *In situ* hybridisation for *nogo-a* mRNA reveals a broadly similar distribution in the intact nervous system, which is consistent with previous reports (Josephson et al., 2001; Huber et al., 2002). Nonetheless, it has become clear that the relative expression of *nogo-a* mRNA and *nogo-66* mRNA by neurons and glia is different: for example, *nogo-a* expression by glia is much more obvious, and its expression by neurons – especially neocortical neurons – is less marked than for *nogo-66*. This implies that neocortical neurons express *nogo-b* or *–c* as well. The finding that *nogo-a* mRNA is expressed by myenteric plexus neurons of the distal colon is in keeping with previously reported immunohistochemical findings, and is highly suggestive of a neuron-specific function of the protein.

Nogo-A Protein Expression in the CNS

This study has confirmed previous reports of Nogo-A expression by many CNS neurons (Huber et al., 2002; Tozaki et al., 2002). Nonetheless, there is a clear disparity between transcript and protein expression patterns, which is best illustrated by adult rat neocortical neurons in which the mRNA is strongly expressed but the protein only weakly so. It may be that this phenomenon can be explained by post-transcriptional regulation, or perhaps by rapid export of the protein into the axons from the neuronal perikarya. However, there is little evidence for the latter since the axons do not appear to contain an abundance of Nogo-A. In fact, although in these experiments the corticofugal axons were not specifically immunolabelled for Nogo-A expression, only very weak expression was

evident at best in axons within the cerebral peduncles and dorsal corticospinal tract of the spinal cord. Similarly, throughout the whole of the CNS, it was found that intrinsic CNS neurons which express Nogo-A in the perikarya show very weak if any labelling of their axons. It seems unlikely that this is the result of higher background levels of signal detected throughout the CNS, since axons are very easily identifiable in the peripheral nervous system (see below). One example of this comes from Purkinje cells, most of which show strong perikaryal expression of Nogo-A, as well as weak to moderate immunoreactivity in their dendrites but little or no signal in their axons. That Nogo-A is expressed strongly in the perikarya of many Purkinje cells, but very weakly or not at all in others is also quite intriguing. Several other genes are known to give rise to unusual patterns in the cerebellar Purkinje cells, typified by *zebrin* (Hawkes and Leclerc, 1989; Brochu et al., 1990; Gravel and Hawkes, 1990) which is expressed in rows by a series of parasagittal stripes. Indeed, this finding warrants further investigation. Contrary to an earlier report (Jin et al., 2003), no obvious Nogo-A immunoreactivity was observed in the nuclei of Purkinje cells, nor of spinal motor neurons, but this does not exclude the possibility that the protein was expressed at much lower levels than were present in the neuronal cytoplasm. The glial cells that were found to express Nogo-A did not include either NG2+ cells, or astrocytes. The former is noteworthy since oligodendrocyte precursors are known to express NG2, whilst mature oligodendrocytes are known to express Nogo-A, thus indicating that the onset of Nogo-A expression can be listed with other changes in gene expression which mark the phenotypic maturation of this cell lineage. This finding has recently been confirmed by Mingorance et al. (2004).

Nogo-A Protein Expression in the PNS

Unlike intrinsic CNS neurons, the majority of neurons which have axons projecting into peripheral nerves express high levels of Nogo-A transcripts and protein in their perikarya as well as large amounts of the protein in their axons. This is true of spinal motor neurons of the ventral horn (wherein Nogo-A is clearly visible even in the intraspinal segments of their axons), DRG neurons, postganglionic sympathetic neurons and ciliary ganglion neurons. It seems that Nogo-A is expressed at varying degrees in all neurofilament-labelled axons of the intact peripheral nerve, although the most intense

immunofluorescent signal for Nogo-A is found in bundles of unmyelinated axons; these would include DRG c-fibres and postganglionic sympathetic fibres. In time, Nogo-A may paradoxically prove to be a useful marker of peripheral axons. Nonetheless, the role of Nogo-A within neurons of the peripheral nervous system remains something of a mystery, not least since it has been reported to be expressed by another type of peripheral neuron: that of the colonic myenteric plexus (Osborne et al., 2004).

Nogo-A Expression in the Embryonic and Early Postnatal Nervous System

It was difficult to discern any Nogo-A positive neuronal perikarya within the E13.5 or E17.5 mouse cortex. Immunoreactivity for calretinin, which is expressed by preplate neurons at these developmental timepoints, did not clearly coincide with that of Nogo-A. The apparent expression of Nogo-A by radial glia, lately considered a neuronal progenitor cell (reviewed by Goldman, 2003), within the embryonic telencephalic wall of mouse forebrain requires further investigation and, unfortunately, could not be definitively confirmed in this study owing to a lack of appropriate antibodies. Similarly, it was impossible to confirm whether the axon-like structures running tangentially through the E17.5 mouse telencephalic wall were indeed corticofugal and corticopetal axons, but morphologically they appeared to be such. In the event that these preliminary observations should prove correct, it would raise some interesting questions as to the nature and extent of Nogo-A involvement in the developing nervous system. This potentially commands even greater significance, given the absolute absence of CNS myelin throughout this period of cortical development.

Nogo-A Expression in Cultured Neurons

In dissociated cultures of adult Sprague-Dawley rat DRG neurons, and E13.5 ICR mouse neocortical neurons – as well as E17 and E19 Sprague-Dawley rat neocortical neurons – similar patterns of Nogo-A expression were observed. The strongest expression was detected in the perikarya. However, the axons were also rich in Nogo-A, although the distribution was somewhat uneven with an obvious accumulation of the protein in axonal varicosities, at branch points, at places where axons crossed and in growth cones. This pattern is perhaps suggestive of a role in axon growth, guidance and perhaps synapse

formation (which may account for the very large number of axonal varicosities which were observed in these cultures of neocortical neurons). The Nogo-A immunoreactivity did not co-localize precisely with that of neurofilament; for example, Nogo-A was prominent in the terminal elements of the neurites, including the growth cones, where there was little or no signal for neurofilament. This finding may is in agreement with the observations made on the expression profiles of regenerating axons *in vivo* (see below). In the cultures of adult DRG neurons, Nogo-A was clearly visible in the central domain of large growth cones, as has been previously reported (Tozaki et al., 2002), and was reminiscent of the expression pattern of SCG10 - a growth-associated neuronal protein which controls microtubule dynamics and enhances neurite outgrowth – which is also localized for the most part to growth cones and perikarya (Di Paolo et al., 1997; Riederer et al., 1997; Lutjens et al., 2000). It is important that the extent to which Nogo-A is present at the cell surface in neurons, if at all, be investigated thoroughly since this is likely to yield some vital clues about the function of neuronal Nogo-A.

Nogo-A Expression after CNS Injury

In this study, three models of CNS injury were examined in adult Sprague-Dawley rats: transection of the spinal dorsal columns, autologous tibial nerve graft in thalamus and optic nerve crush. *In situ* hybridisation was performed on injured spinal cord and grafts in thalamus. In both cases *nogo-a* transcripts were obviously upregulated in some cells bordering the lesion sites. Immunohistochemistry was performed on injured spinal cord and crushed optic nerve, where it was found that signal for Nogo-A was considerably higher at the margins, and much lower within the substance, of the lesions.

The finding that Nogo transcripts are downregulated within the lesion site of injured spinal cord is congruent with earlier reports (Josephson et al., 2001; Huber et al., 2002; Wang et al., 2002c). However, the observation that Nogo expression is increased in some cells at the margins of spinal injury sites remains contentious, since only Wang et al. (2002) have reported a similar finding whilst Josephson et al (2001) and Huber et al (2002) were unable to detect any sign of upregulation of the transcripts around contusion and transection sites, respectively. There is no simple explanation for this discrepancy.

However, in the present study, the protein was also found to be upregulated by some neuronal perikarya at the borders of the lesion site.

The ingress of large numbers of Nogo-A immunopositive axons to the spinal cord lesion site at 8-16dpo was somewhat unexpected. Most of the penetrating axonal sprouts, as identified by neurofilament immunoreactivity, were found to be Nogo-A immunopositive. Given that these animals also underwent a conditioning peripheral nerve lesion, which is known to enhance the sprouting of ascending axons of DRG neurons into a dorsal column lesion site, it is likely that many of these Nogo-A positive axons are indeed those of sensory DRG neurons. The strongest immunofluorescent signal for Nogo-A was detected in dorsal column axons close to the lesion, which is perhaps indicative of the molecule undergoing fast anterograde axonal transport. This process often results in an axonal accumulation of protein proximal to the lesion site (Banks et al., 1969; Anderson et al., 1978). Some of the axons which had entered the lesion sites did not express Nogo-A, and may have been those of local spinal neurons. It is certainly true that some types of neuron express little or no Nogo-A. Also, the uneven distribution of Nogo-A throughout the axonal shafts in cultured neurons may explain why some segments of regenerating axons *in vivo* were not found to express Nogo-A. In any event, the meshwork of Nogo-A positive processes, which may have consisted of fine axonal sprouts and/or oligodendrocyte processes, at the lesion borders could pose a considerable inhibitory barrier to regenerating axons. This is potentially further compounded by presence of significant numbers of interweaving NG2-expressing processes. The few Nogo-A positive non-neuronal cells that appeared within the lesion site at 16dpo were most probably mature oligodendrocytes, which presumably had formed from their precursors which do not express Nogo-A. Surprisingly, at all timepoints, the major source of Nogo-A within the lesion sites was always the ingrowing Nogo-A-expressing axonal sprouts. What bearing this has on the inhibition of axonal regeneration in the injured spinal cord, if any, remains to be seen.

Autologous tibial nerve grafts in thalamus were employed as a model of regeneration, since it is well establish that axons of certain classes of intrinsic CNS neurons, e.g. the

thalamic reticular nucleus (TRN), are particularly adept at regenerating their axons into such grafts. In the intact state, or whilst undergoing regeneration, TRN neurons were found to express *nogo-a* transcripts. Clearly, this implies that their expression of *nogo-a* is not detrimental to the regeneration of their axons into grafts of peripheral nerve. Those cells which upregulate *nogo-a* at the borders of a peripheral nerve graft in thalamus have yet to be identified, but some exhibited a neuronal morphology. Interestingly, those neurons of the dorsal thalamus which successfully regenerate their axons into peripheral nerve grafts are usually located within close proximity to the graft. However, it seems quite unlikely that all the cells which were seen to upregulate *nogo-a* around the graft were successfully regenerating neurons.

In the experimental model of optic nerve crush, the lesion site was almost completely devoid of Nogo-A by 4dpo, which was comparable with spinal cord lesion sites at the same timepoint. The increased expression of Nogo-A at the borders of the optic nerve lesions may have been in oligodendrocytes or axons. The axonal sprouts found within these lesion sites expressed less Nogo-A than was found in sprouting axons in spinal cord lesions, and much less than was found in regenerating peripheral axons. This is probably because many of the axons that sprout into spinal lesions, following conditioning peripheral nerve injuries, are ascending central processes of DRG neurons. These neurons strongly express Nogo-A.

Three *nogo-a* null mutant mice which have been described (Zheng et al., 2003; Simonen et al., 2003; Kim et al., 2003c), and the corticospinal tracts of each of these has been reported to respond differently to injury. In two of these mutants, regeneration is enhanced by varying degrees (Simonen et al., 2003; Kim et al., 2003c), and in the other there appears to be no improvement (Zheng et al., 2003). The overt lack of conformity between phenotypes is a little troublesome, although some attribute it to the different genetic manipulations that were employed and the potential for differential 'genetic compensation'. The initial examination of intact corticospinal tracts in one of these knockout models has revealed no obvious anatomical abnormalities (Simonen et al., 2003). This is surprising in the light of an earlier report that administration of the IN-1

antibody to postnatal rats disrupts the anatomical development of these tracts (Schwab and Schnell, 1991). On the whole, these mutants have been of little assistance in clarifying the role of Nogo-A in axonal (re-)growth. One hypothesis must be that oligodendrocyte and neuronal Nogo-A have antagonistic effects. In this vein, the generation of a conditional neuronal Nogo-A null mutant might yield some interesting data.

Nogo-A Expression After Peripheral Nerve Injury

At 4 days after nerve transection, apparently all sprouting axons were Nogo-A immunopositive. At 8 and 16dpo, Nogo-A was present in many regenerating axons but the intensity of expression was variable. For example, some of the fibres which were most strongly immunoreactive for neurofilament, were not for Nogo-A, and vice versa. These Nogo-A positive fibres were likely to be axons, not Schwann cell processes, because (i) all were emanating from the proximal stump, (ii) some were neurofilament positive, (iii) some were myelinated, (iv) no Nogo-A positive cell bodies were identified in the outgrowth from the proximal stump, and (v) no *nogo-a* mRNA signal was detected in the proximal stump of injured nerves. Given the pattern of Nogo-A and neurofilament in the axons of cultured neurons (see above), it is quite probable that the Nogo-A positive but neurofilament negative structures observed at the forefront of the outgrowth from the proximal stump were in fact growth cones. That a significant number of neurofilament-positive regenerating axons appeared to express little or no Nogo-A is somewhat intriguingly, since apparently all axons within the intact nerve express the protein. However, in cultures of neurons (see above) the pre-terminal neurites were often found to express little Nogo-A – except at axonal varicosities or points of axonal contact – lending a possible explanation to what has been observed *in vivo*. Of course, it is equally plausible that these regenerating neurofilament-positive but Nogo-A-negative axons may be representative of a subpopulation of neurons that is capable of downregulating Nogo-A expression in axons following injury. However, in the present study, no obvious downregulation of Nogo-A was observed in any DRG neurons or spinal motor neurons of the ventral horn, following transection of the peripheral nerve.

The most important question to arise from this work is whether the Nogo-A expressed by peripheral axons has any role in their ability to regenerate. A knowledge of the subcellular distribution of the protein, i.e. whether it is present at the axonal surface, as well as its topology is likely to assist in answering this. However, it is worth noting that regenerating peripheral axons have been shown to be sensitive to the effects of Nogo-A, when overexpressed by Schwann cells in peripheral nerves (Pot et al., 2002). This is important, since only a subpopulation of motor and sensory neurons express *ngr* transcripts and relatively weakly at that, implying that these neurons may express other presently unidentified receptors for Nogo-A (Prinjha et al., 2002).

Considering that increased expression of Nogo-A in adult muscle has been implicated in the development of amyotrophic lateral sclerosis (ALS) (Dupuis et al., 2002), it is somewhat surprising that ectopic striated muscle fibres - arising in the tissue bridge between the proximal and distal stumps of injured peripheral nerve - were strongly immunoreactive for Nogo-A. However, since axonal sprouting also occurs in ALS (Stalberg et al., 1986) it is possible that these ectopic muscle fibres were responding to axonal sprouting by expressing Nogo-A. During development, skeletal muscle has also been reported to express Nogo-A (Tozaki et al., 2002; Wang et al., 2002c) but its temporal pattern of expression has yet to be correlated with innervation by the developing peripheral nervous system. The hypothesis of relationship between excessive axonal sprouting and muscular expression of Nogo-A is supported by a recent report that denervated muscle also upregulates Nogo-A in wild-type rodents (Magnusson et al., 2003). However, Dupuis et al. (2002) did not detect any upregulation of Nogo-A in the denervated muscles of wild-type animals.

Summary

The present study has confirmed that *nogo-a* mRNA is expressed by many different classes of neuron, but that perikaryal protein expression is not directly proportional, e.g. neocortical pyramidal neurons express moderate levels of transcript but relatively little protein. After injury, Nogo-A is upregulated by some intrinsic CNS neurons around the lesion site. Most, if not all, uninjured neurons with axons in peripheral nerve express

Nogo-A in both their perikarya and axons. After injury, the majority of regenerating peripheral axons are clearly Nogo-A positive. This is also true of axons sprouting into CNS lesion sites. There appears, therefore, to be a correlation between axonal expression of Nogo-A and high regenerative ability. Despite being considered an inhibitor of axonal growth, there remains the possibility that Nogo-A has an alternative role in neurons, especially within their axons, that is beneficial to vigorous axonal regeneration.

CONCLUSION

In addition to its well documented expression in oligodendrocytes, Nogo-A is also expressed by numerous classes of neuron within the CNS and PNS, both in the intact and regenerating nervous system. Although Nogo-A is widely detectable in neuronal perikarya, its expression in intrinsic CNS axons of adult mammals is very limited. However, the expression of Nogo-A in axons correlates well with axonal regenerative potential, and the majority of axons in peripheral nerves continue to express the molecule whilst undergoing regeneration.

Table 4.1.

Neuronal expression of *nogo-a* mRNA and protein.

Key:-

-	not detectable
-/+	very weak
+	weak
++	moderate/strong
+++	very strong
NE	not examined
*	some, but not all, neocortical neurons were weakly immunoreactive for Nogo-A
**	strongest neuronal expression in well-dispersed, large diameter neurons (indicative of cholinergic interneurons)
†	most, but not all, Purkinje cells were found to express Nogo-A
††	all motor neurons in the lumbar spinal cord expressed *nogo-a* mRNA and protein, but some motor neurons in the cervical spinal cord were not immunoreactive for Nogo-A (N.B. *in situ* hybridization was not performed on comparable sections of cervical spinal cord)
‡	although no immunoreactivity was detected in perikarya in either the inner or outer nuclear layers, weak expression was present in both the inner and outer plexiform layers, presumably in axon terminals (see Fig. 4.6.A)

	nogo-a mRNA	Nogo-A protein
Adult rat (Sprague-Dawley)		
Neocortex	++	+*
Neostriatum	++**	+**
Hippocampal formation:-		
CA1-4	+	+
Dentate gyrus	-/+(very weak)	-
Hilus of dentate gyrus	++	++
Amygdala	+	-
Piriform cortex	+	+
Habenular nucleus	+++	+++
Thalamic reticular nucleus	++	+
Other thalamic nuclei	++	+
Tuberomammillary nucleus	++	++
Other hypothalamic nuclei	+	++
Substantia nigra	++	+
Oculomotor nucleus	++	++
Red nucleus	++	++
Cerebellum:-		
Purkinje cells	++†	++†
Granule cell layer	-	-
Molecular cell layer	-	-
Deep cerebellar nuclei	++	++
Mesencephalic nucleus V	NE	++
Pontine nuclei	+++	++
Spinal motor neurons	++††	++††
Retina:-		
Retinal ganglion cells	+++	+++
Inner nuclear layer	-/+(very weak)	-‡
Outer nuclear layer	-	-‡
Superior cervical ganglion	+++	+++
Ciliary ganglion	NE	+++
DRG	+++	+++
Adult rat (Lewis)		
Dissociated DRG neurons *in vitro* (3DIV)	NE	+++
P8 rat (Sprague-Dawley)		
Cerebellar granule neurons (western blot)	NE	+++
E17 and E19 rat (Sprague-Dawley)		
Dissociated cortical neurons *in vitro* (3DIV)	NE	+++
P14 mouse (Balb/c)		
Neocortex	NE	-
Neostriatum	NE	-
E13.5 mouse (ICR)		
Dissociated cortical neurons *in vitro* (3DIV)	NE	+++

Figure 4.1.

Western blot of P8 Sprague-Dawley rat cerebellar granule neurons. Protein was separated on a 7.5% gradient gel and detected with the anti-Nogo-A monoclonal antibody 6D5. The position of Rainbow molecular weight markers is shown on the left. A single strong Nogo-A band of 180kDa is detectable. N.B. Nogo-A was not detected in cerebellar granule cells of adult rats by immunohistochemistry, but such cells do express Nogo-A in the neonate (Huber et al., 2002).

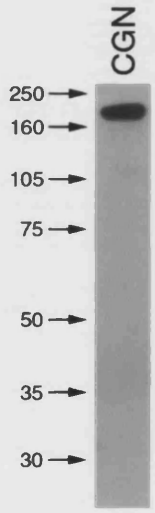

Figure 4.2.

In situ hybridization for *nogo-a* mRNA in adult Sprague-Dawley rat tissues.

A. Coronal section through part of the forebrain showing cerebral cortex (asterisk) and corpus callosum (cc). Strong signal for *nogo-a* can be seen in cells of varying sizes in most of the cortex, except the molecular layer (m), in the corpus callosum and the underlying fimbria/fornix. V indicates lateral ventricle. Scale bar = 200μm.

B. Forebrain, showing the deep layers of cerebral cortex (c), underlying white matter (w) and neostriatum (asterisk). Although the level of expression is generally lower in the neostriatum than in cortex, scattered large striatal cells (arrows) express very strong signal for *nogo-a* mRNA. Scale bar = 200μm. Inset: immunohistochemistry for Nogo-A in adult rat striatum. Scattered, large neuronal perikarya - resembling cholinergic interneurons – express the Nogo-A protein. Scale bar = 50μm.

C. Part of the dentate gyrus (asterisk) shows very low or background levels of signal but scattered neurons (arrowheads) in the hilus express moderate or strong signal for Nogo-A mRNA. Scale bar = 100μm. Inset: immunohistochemistry for Nogo-A on adult rat dentate gyrus. Scattered neuronal perikarya in the hilus of the dentate gyrus express the Nogo-A protein, whilst the granule cells of the dentate gyrus do not. Scale bar = 25μm.

D. Coronal section through part of the midbrain showing strong *nogo-a* mRNA expression in the substantia nigra (indicated by arrows) and red nucleus (asterisk). Scale bar = 200μm.

E. Part of cerebellar cortex showing strong signal for *nogo-a* mRNA from some Purkinje cells (arrowheads) but not from others (regions indicated by arrows). The molecular layer (m) shows no signal and the granule cell layer (g) shows background levels except for scattered cells of various sizes which may be oligodendrocytes and ectopic Purkinje cells. W indicates white matter. Scale bar = 200μm.

F. *nogo-a* mRNA is strongly expressed in motor neurons in the ventral horn of the lumbar spinal cord. Scale bar = 200μm.

G. Neurons in the L5 DRG express strong signal for *nogo-a* mRNA. The non-neuronal cells in the attached dorsal root (r) show no signal. Scale bar = 100μm.

H. Sympathetic neurons in the superior cervical ganglion show strong signal for *nogo-a* mRNA. Scale bar = 200μm.

I. Section through retina showing strong signal for *nogo-a* mRNA from cells in the ganglion cell layer (arrowheads). Scale bar = 100μm.

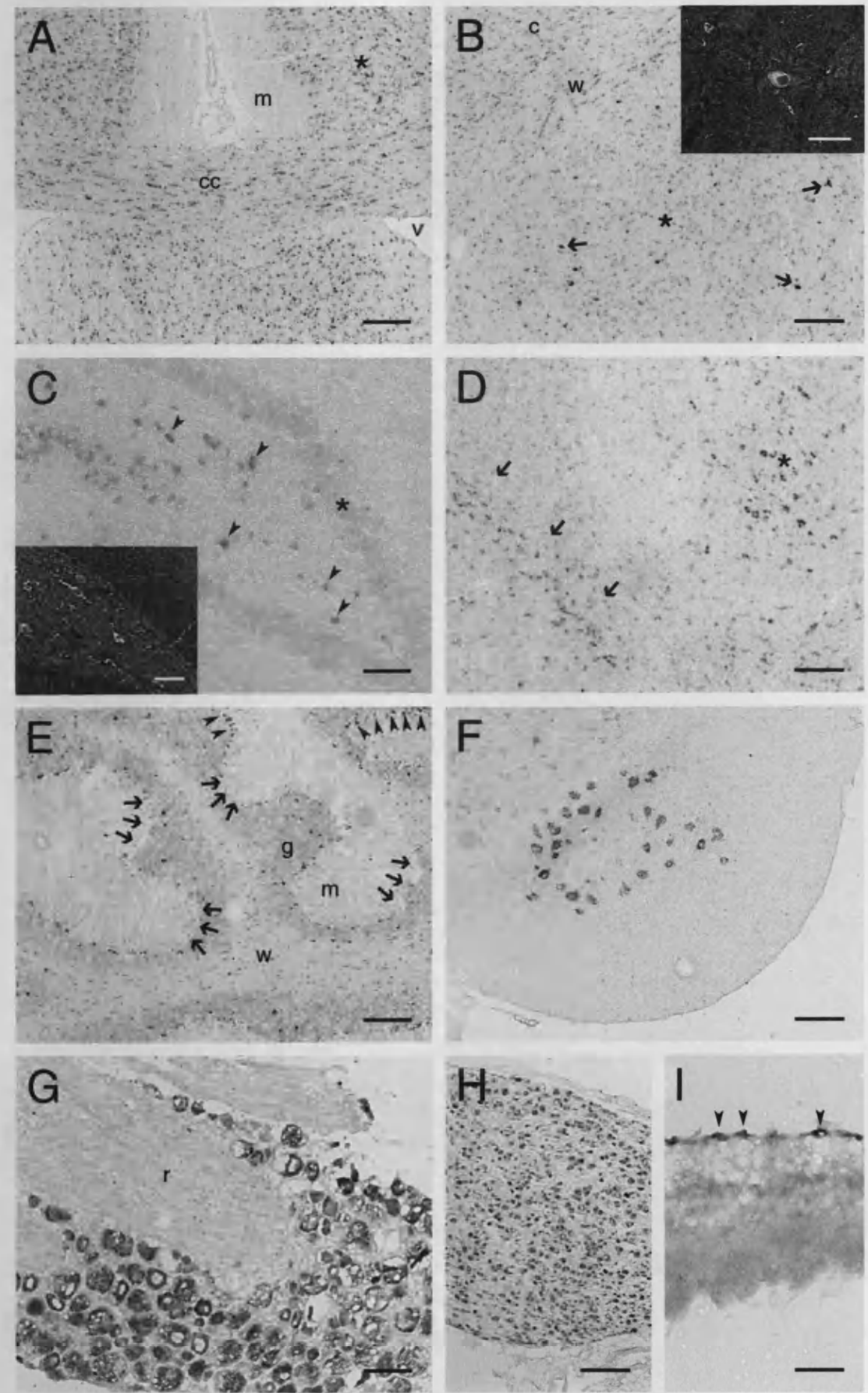
A
m
cc
v
B
c
w
C
D
E
g
m
w
F
G
r
H
I

Figure 4.3.

A-B *nogo-a* transcript expression in neurons of the myenteric plexus (arrows). Scale bars = 200μm. These sections were prepared and reacted by J. Mills.

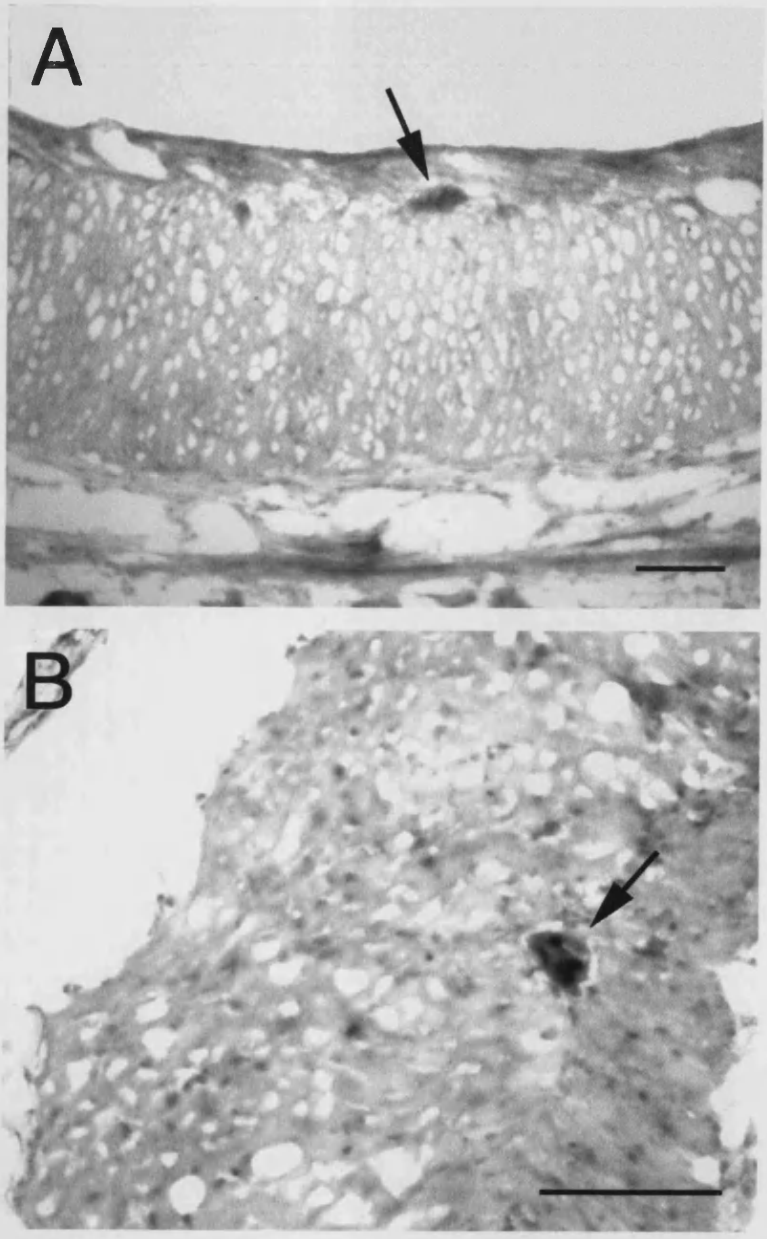
A
B

Figure 4.4.

Immunohistochemuistry for Nogo-A in adult Sprague-Dawley rat tissues.

A. Part of motor cortex showing strong Nogo-A immunoreactivity in presumptive oligodendrocytes (arrowheads) and weak expression in neurons (arrows). Scale bar = 100μm.

B. Transverse section through the cerebral peduncle (containing corticofugal axons). Nogo-A immunoreactivity can be seen in axons and some presumptive oligodendrocytes. Scale bar = 20μm.

C. Cerebellar cortex showing Nogo-A expression in many Purkinje cells and scattered small presumptive oligodendrocytes in the granule cell layer (g). The dendrites of Purkinje cells (arrowheads) extending into the molecular layer (m) are also labelled. Scale bar = 100μm.

D. Higher power image of section through cerebellar cortex, parallel with the Purkinje cell layer, showing some Purkinje cell perikarya expressing Nogo-A and others (arrows) lacking Nogo-A. Presumptive oligodendrocytes in the granule cell layer (g) are indicated by arrowheads. Scale bar = 100μm.

E. Ventral horn of lumbar spinal cord showing strong Nogo-A expression in motor neurons and smaller, presumptive oligodendrocytes. Axons in the ventral white matter are also Nogo-A positive. Scale bar = 100μm.

F. Superior cervical ganglion showing strong Nogo-A expression in neuronal perikarya, as well as axons. Scale bar = 100μm.

G. L5 DRG showing strong Nogo-A expression in all sensory neurons, most larger cells displaying a reticular pattern, with the smaller cells exhibiting the most intense immunoreactivity. Sensory axons also contain Nogo-A . Scale bar = 100μm.

H. Sciatic nerve in longitudinal section. Although all axons express Nogo-A (see also Fig. 4.5.D-F), the bundles of non-myelinated axons (arrows) are the most strongly immunoreactive. Scale bar = 50μm.

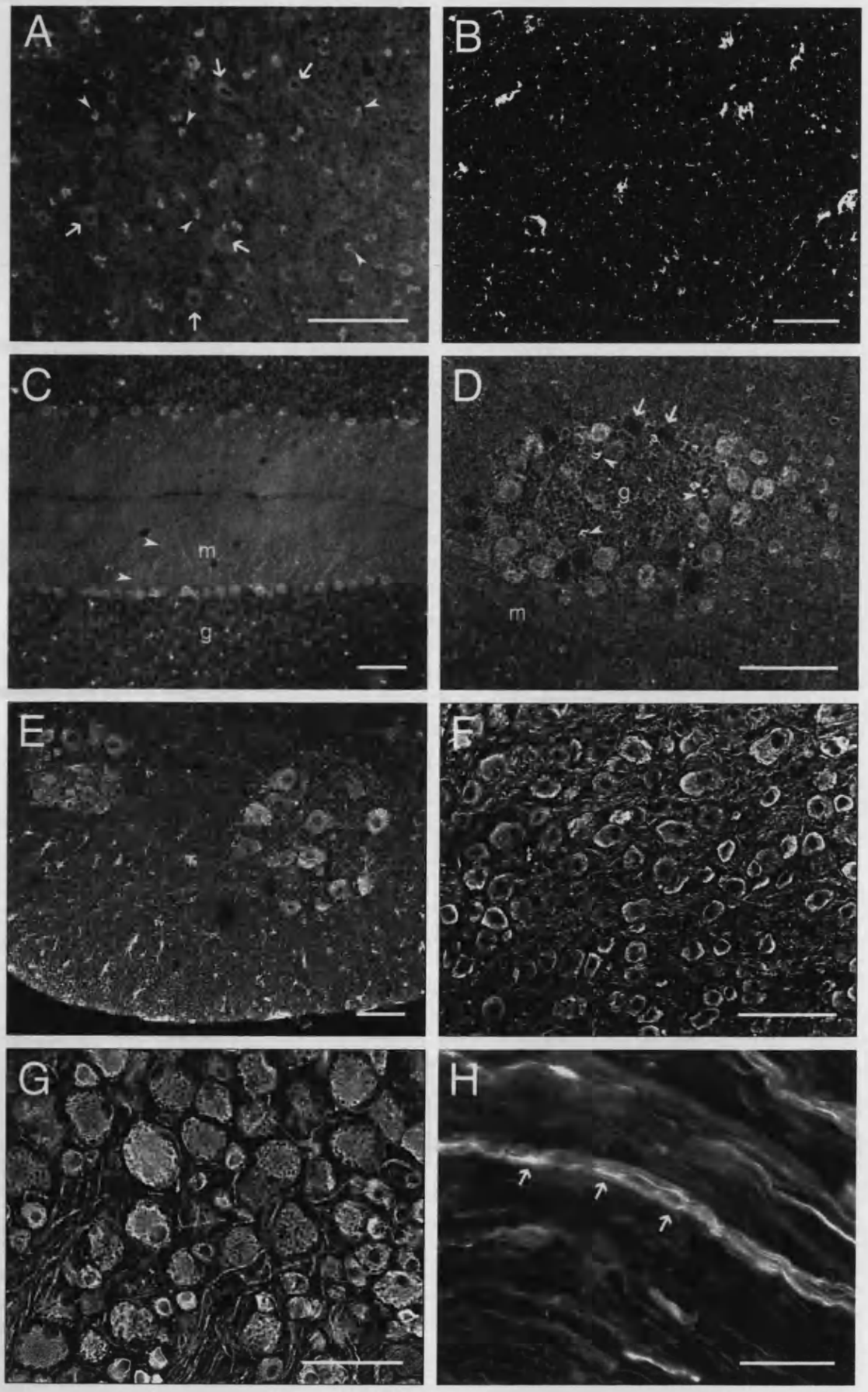
A
B
C
m
g
D
g
m
E
F
G
H

Figure 4.5.

Confocal microscope images of single optical planes of spinal cord white matter (A-C), intact sciatic nerve (D-F) and regenerating sciatic nerve (G-I) to show the extent of colocalisation of NG2 and Nogo-A (A-C) and neurofilament protein and Nogo-A (D-I). All images were taken from adult Sprague-Dawley rats. Nogo-A is red.

A. Nogo-A positive cells and fibres in the dorsal column white matter of adult rat spinal cord. Scale bar =20μm, applies also to B and C.

B. NG2 positive cells and processes in the same optical section.

C. Superimposed images show that although the NG2 positive structures are often close to the Nogo-A positive structures, the antigens were never colocalized.

D. Nogo-A immunoreactivity in sciatic nerve. Scale bar =20μm, applies also to E and F.

E. Neurofilament immunoreactivity in the same optical section.

F. Superimposed images show that although apparently all neurofilament positive structures are immunoreactive for Nogo-A, Nogo-A is strongly expressed by bundles of non-myelinated axons which are neurofilament negative (arrows in D,E,F).

G. Nogo-A immunoreactivity in regenerating sciatic nerve, 16dpo. Scale bar = 20μm, applies also to H and I.

H. Neurofilament immunoreactivity in the same optical section.

I. Superimposed images show that although all neurofilament positive structures are immunoreactive for Nogo-A to varying degrees, a few Nogo-A positive structures (red) are not immunoreactive for neurofilament.

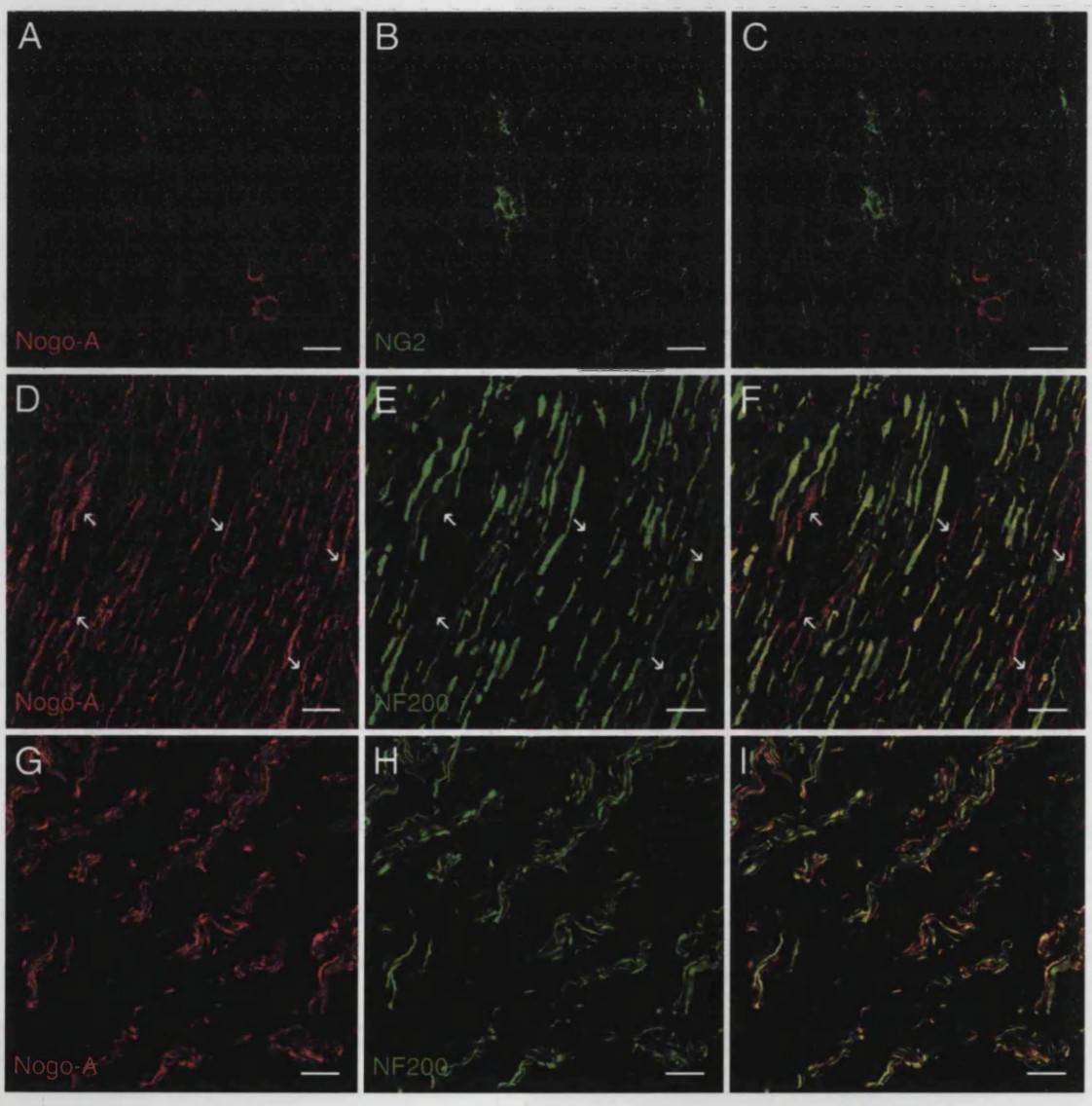
A
B
C
Nogo-A
NG2
D
E
F
Nogo-A
NF200
G
H
I
Nogo-A
NF200

Figure 4.6.

Nogo-A immunofluorescence in adult Sprague-Dawley rat retina and associated nerves (A-D) and in cultured neurons (E-H).

A. Section through retina showing strong Nogo-A expression in the ganglion cell layer (RGL) (arrowheads) (cf. Fig. 4.2.I). Weak immunoreactivity for Nogo-A is present in the inner and outer plexiform layers (IPL and OPL, respectively), but no expression can be detected in perikarya of the inner and outer nuclear layers (INL and ONL, respectively). Scale bar = 100μm.

B. Higher power of section through the ganglion cell layer and optic fibre layer, double stained for Nogo-A (red) and neurofilament protein (green). The retinal ganglion cell axons are strongly immunoreactive for neurofilament and weakly Nogo-A positive, whereas the ganglion cell bodies (some arrowed) are strongly Nogo-A positive but neurofilament negative. Scale bar = 100μm.

C. In the optic nerve (Op), retinal ganglion cell axons are difficult to distinguish using Nogo-A staining but some presumptive oligodendrocytes can be seen. The perikarya of neurons in the adjacent ciliary ganglion (asterisk) are strongly Nogo-A positive. Scale bar = 100μm.

D. Axons (mainly non-myelinated) in the ciliary nerves are strongly Nogo-A positive. Scale bar = 50μm.

E. Cultured neurons from E13.5 ICR mouse cerebral cortex, immunoreacted for Nogo-A (red) and neurofilament protein (green), and stained with bisbenzimide to show cell nuclei (blue). Nogo-A is concentrated in neuronal cell bodies, sites where neurites cross (arrowhead) and axonal varicosities. Scale bar = 50μm.

F. Cultured neurons from E13.5 ICR mouse cerebral cortex, immunoreacted for Nogo-A (red) and neurofilament protein (green), and stained with bisbenzimide, showing Nogo-A at growth cones at the ends of neurites (arrowheads) and branch points (arrows). Scale bar = 50μm.

G. Higher magnification images of cultured neurons from E13.5 ICR mouse cerebral cortex, showing Nogo-A concentrated at a neurite branch point (arrowhead) and in varicosities (arrows). The neurites are not evenly stained for Nogo-A and one of the processes arising at the branch point has virtually no label. Scale bar = 10μm.

H. Phase contrast/immunoflouresence image of the terminal parts of a neurite in a culture of adult Lewis rat DRG neurons (3DIV). Nogo-A is concentrated in the growth cones and branch points. This culture was prepared, immunoreacted and photographed by Dr. G. Campbell. Scale bar = 10μm.

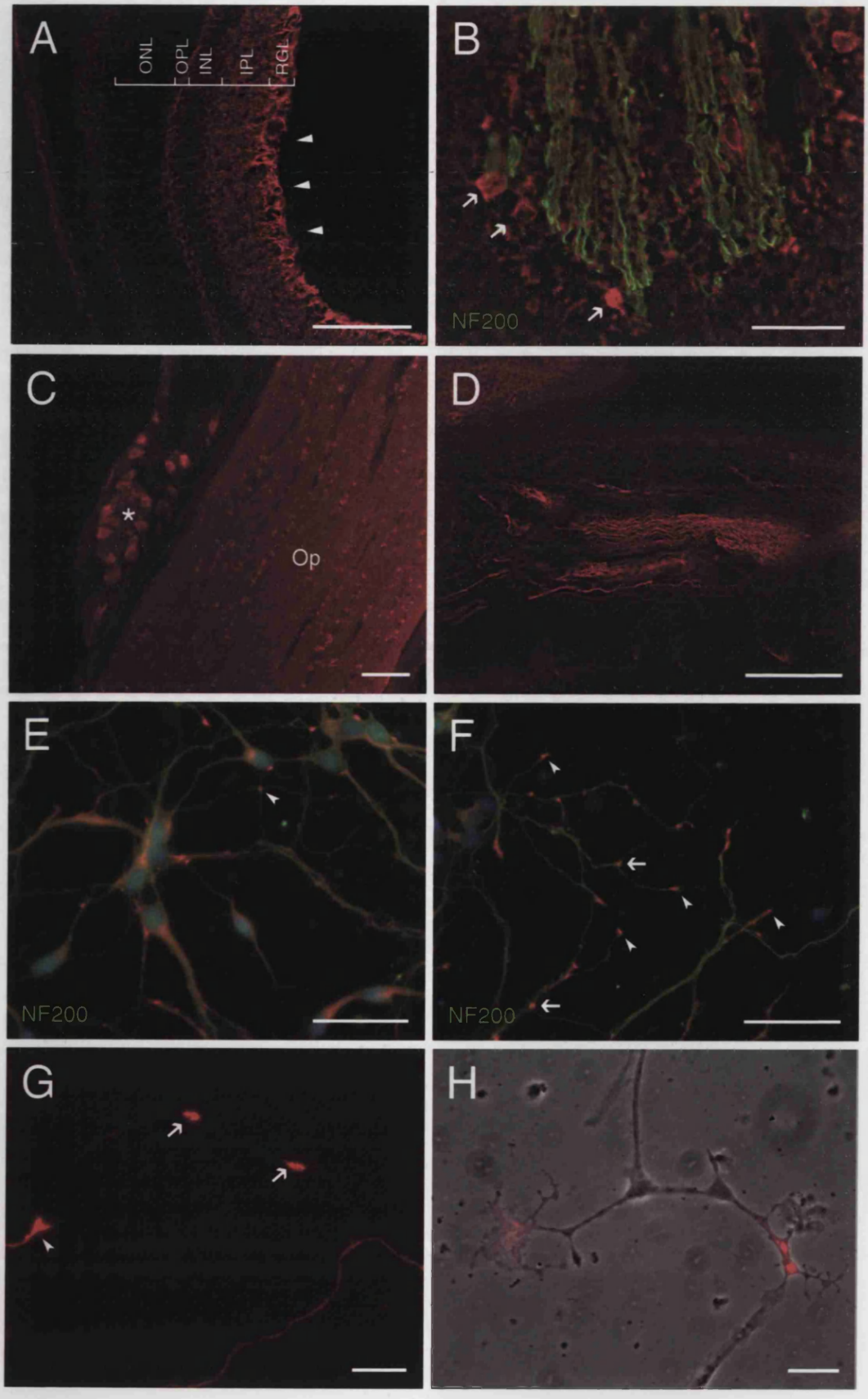
A
ONL
OPL
INL
IPL
RGL
B
NF200
C
Op
D
E
NF200
F
NF200
G
H

Figure 4.7.

Nogo-A expression in embryonic (A-B) and postnatal (C-D) mouse forebrain.

A. Nogo-A is expressed in the ventricular zone (VZ), in radial glia cells (arrows), as well as in the preplate layer (PPL), in early fibres (arrowheads) of the developing cortex at E13.5. Note that there is no colocalisation of Nogo-A in calretinin (CalR) positive preplate cells (green). Scale bar = 100μm.

B. Nogo-A expression in the fibre systems of the developing cortex at E17.5. LI – layer I; CP – cortical plate; SP – subplate; IZ – intermediate zone. Scale bar = 100μm.

C. Nogo-A is expressed in oligodendrocytes, but not neurons, in P14 neocortex. Scale bar = 20μm.

D. In P14 striatum, immunofluorescent signal for Nogo-A was detected exclusively in presumptive oligodendrocytes and their processes amid the bundles of myelinated axons. Scale bar = 50μm.

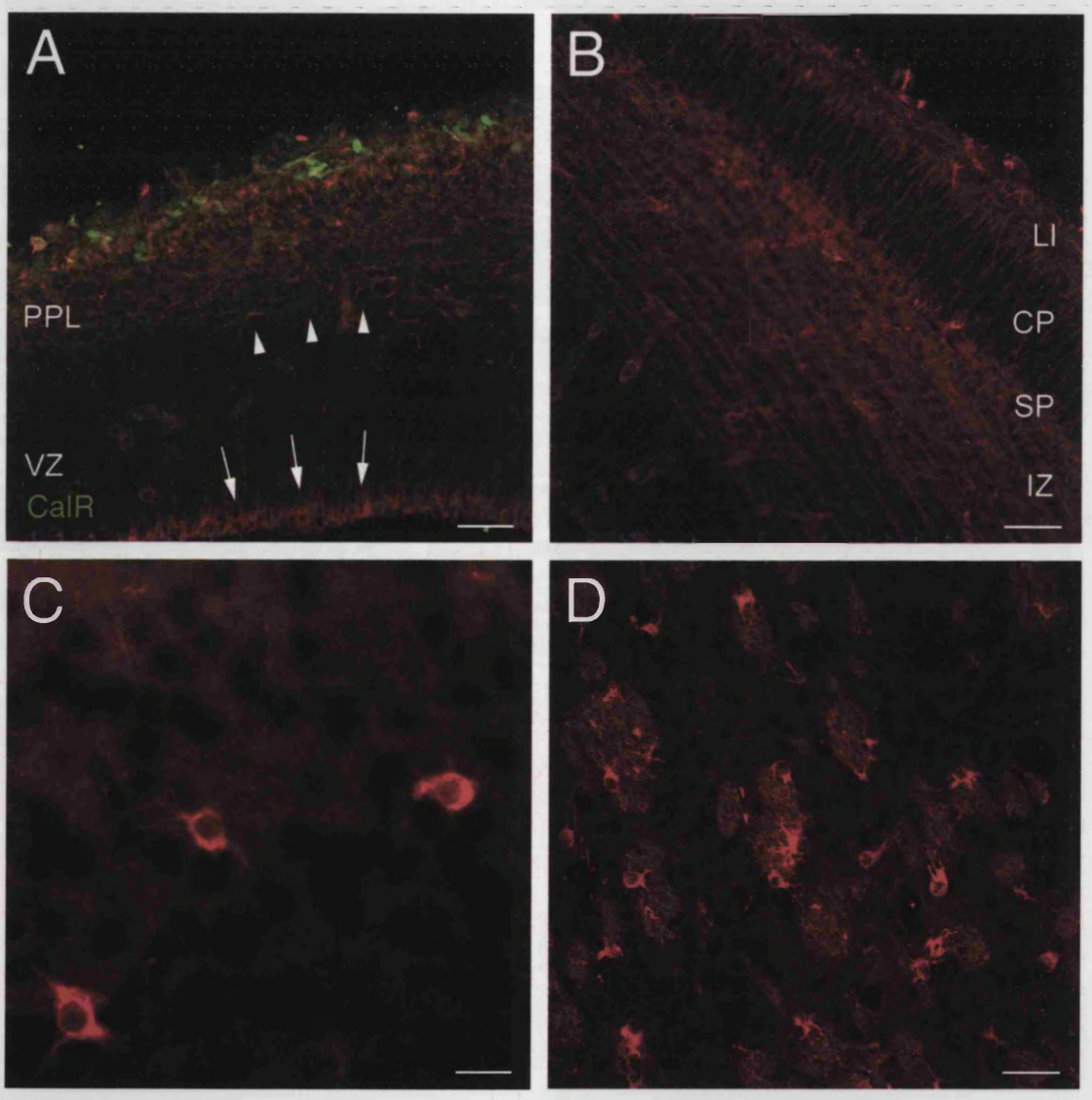
A
PPL
VZ
CalR
B
LI
CP
SP
IZ
C
D

Figure 4.8.

Nogo-A expression in E17 rat hindlimb.

A. Immunofluorescent signal for Nogo A (red) was observed in developing rat sciatic nerve (n), as well as developing skeletal muscle (m). Scale bar = 200μm.

B. Same field as A, with immunofluorescent signal for neurofilament (green) in developing rat sciatic nerve. Scale bar = 200μm.

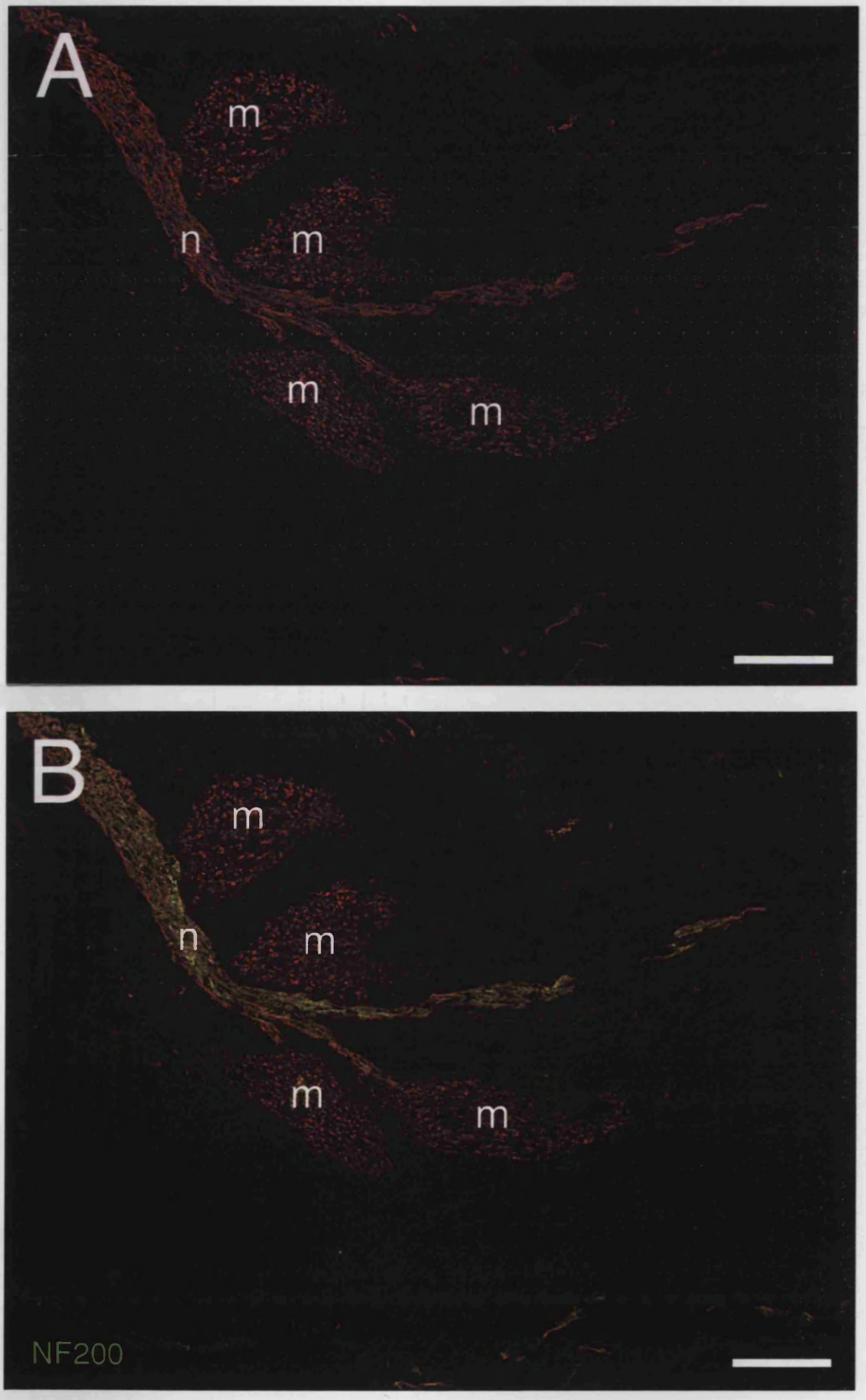
A
m
n
m
m
m
B
m
n
m
m
m
NF200

Figure 4.9.

In situ hybridization for *nogo-a* mRNA in injured nervous tissues of adult Sprague-Dawley rats.

A and B. Show the absence of signal in the proximal (A) and distal (B) stumps of a sciatic nerve 4 days after transection. Scale bar = 50μm.

C. Section through a peripheral nerve graft (g) in the thalamus, 14 days after implantation. *nogo-a* mRNA has been upregulated by cells in the thalamus bordering the graft. C indicates a small cavity in the CNS tissue caused by the grafting procedure. Scale bar = 200μm.

D. Horizontal section through transected dorsal columns of cervical spinal cord, 8dpo. A slight/moderate upregulation of *nogo-a* transcript expression is observed at the border of the lesion (L) by cells within the injured dorsal columns (arrows). Scale bar = 500μm.

E. Parasagittal section through transected cervical dorsal columns spinal cord, 8dpo. A slight/moderate upregulation of *nogo-a* mRNA expression is detected near the borders of the lesion (L) at the level of the dorsal columns (arrows), but not elsewhere. Scale bar = 500μm.

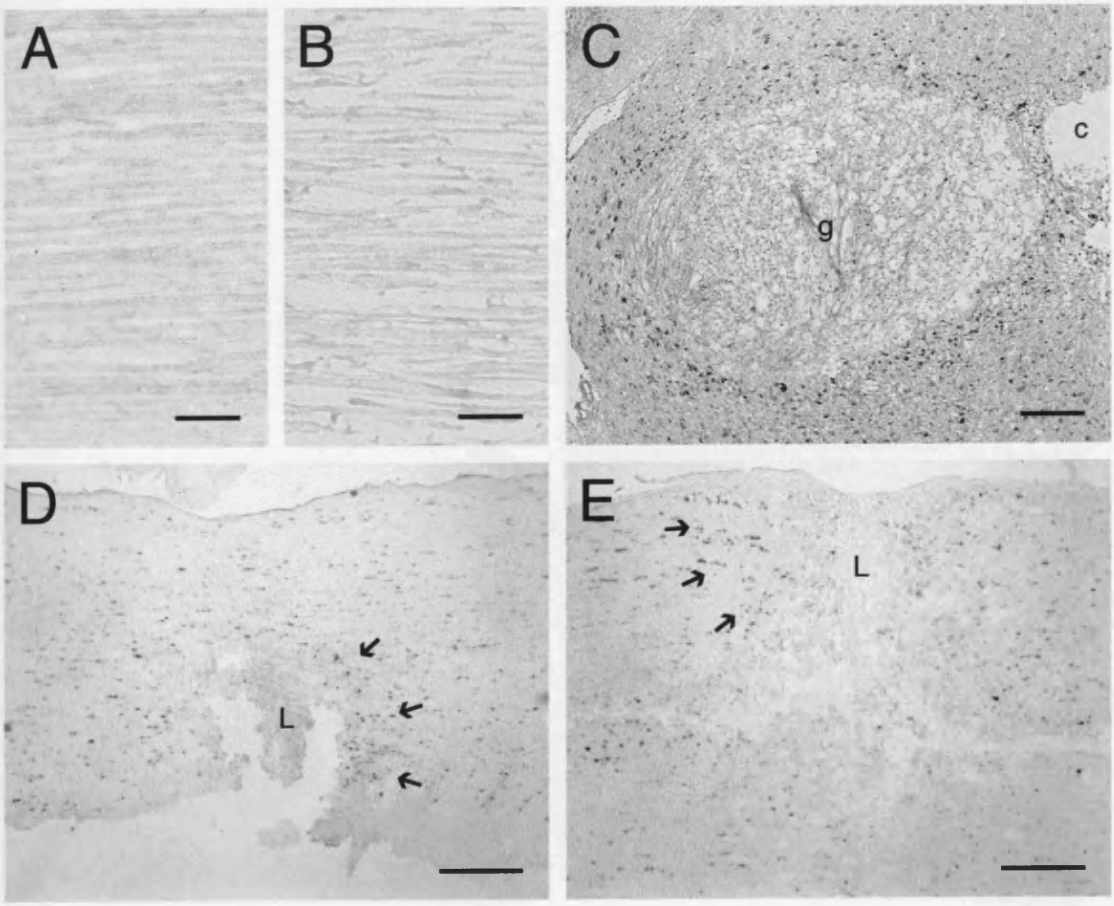
A
B
C
c
g
D
L
E
L

Figure 4.10.

Severed sciatic nerves, from adult Sprague-Dawley rats showing the proximal stump and/or regenerating axons immunoreacted for Nogo-A (red) and neurofilament protein (green). The proximal stump is to the left of the image in A-D.

A. Many Nogo-A positive axons are present in the proximal stump at 4dpo, when regeneration into the lesion site (L) is minimal. Scale bar = 100μm.

B. At higher magnification it can be seen that Nogo-A positive axons which run parallel in the proximal stump (at the left of the image) have sprouted into the lesion site, where some end at Nogo-A positive varicosities. Scale bar = 100μm .

C. Nogo-A positive axons regenerating from the proximal stump towards the distal stump across the gap, 8dpo. Scale bar = 100μm , also applies to D.

D. The same field immunoreacted for neurofilament protein. Although the images in C and D both show large numbers of regenerating axons, many fibres that are neurofilament positive contain little Nogo-A and vice versa.

E. Axons at the edge of the outgrowth from the proximal stump 8dpo, immunoreacted for Nogo-A. Scale bar = 20μm , also applies to F.

F. The same field immunoreacted for neurofilament protein and Nogo-A, clearly shows that some axons are nogo-A positive but neurofilament negative.

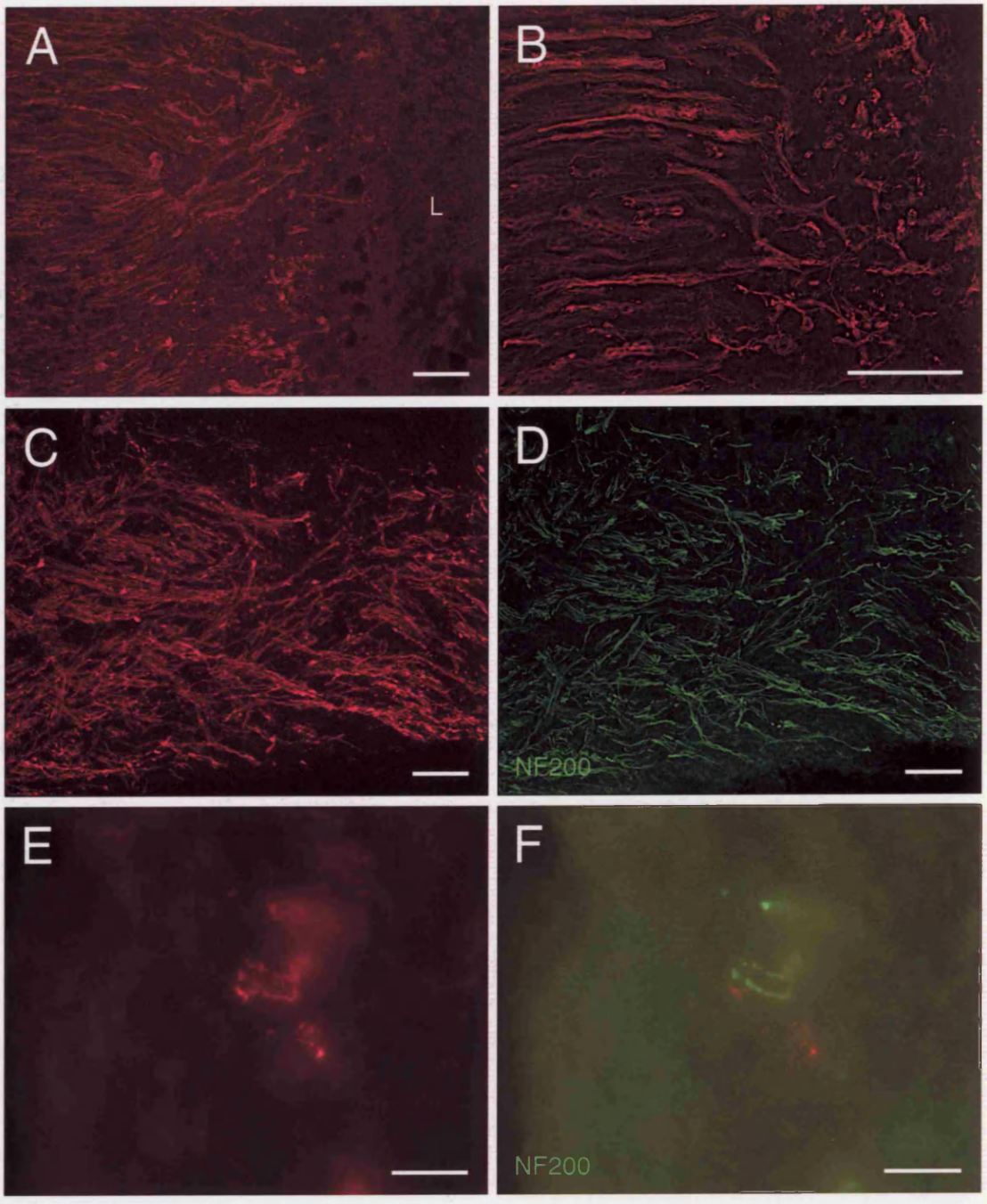
A
L
B
C
D
NF200
E
F
NF200

Figure 4.11.

Outgrowth from severed sciatic nerves of adult Sprague-Dawley rats immunoreacted for Nogo-A (red) and neurofilament protein (green), 16dpo. The proximal stump is to the right of the image.

A. Bundles of Nogo-A positive axons regenerating towards the distal stump have a few Nogo-A positive ectopic muscle fibres (asterisk) developing in their midst. Scale bar = 100μm also applies to B.

B. The same field, double stained for Nogo-A and neurofilament protein. Although many regenerating axons are immunoreactive for both Nogo-A and neurofilament the antigens are not precisely colocalized within the axons.

C. At higher magnification, Nogo-A positive axons can be seen among and at the surface of the muscle fibres (asterisk). Scale bar = 50μm also applies to D.

D. The same field, double stained for Nogo-A and neurofilament protein. Some axons are Nogo-A positive but neurofilament negative (arrows).

E. An ectopic muscle fibre (asterisk) is Nogo-A positive and is approached by Nogo-A positive axons (arrows). Scale bar = 20μm also applies to F.

F. The same field, double stained for Nogo-A and neurofilament protein. It can be more clearly seen that the expression of Nogo-A and neurofilament protein is variable between axons. Some axons (arrowheads) are running along the surface of the Nogo-A positive muscle fibre.

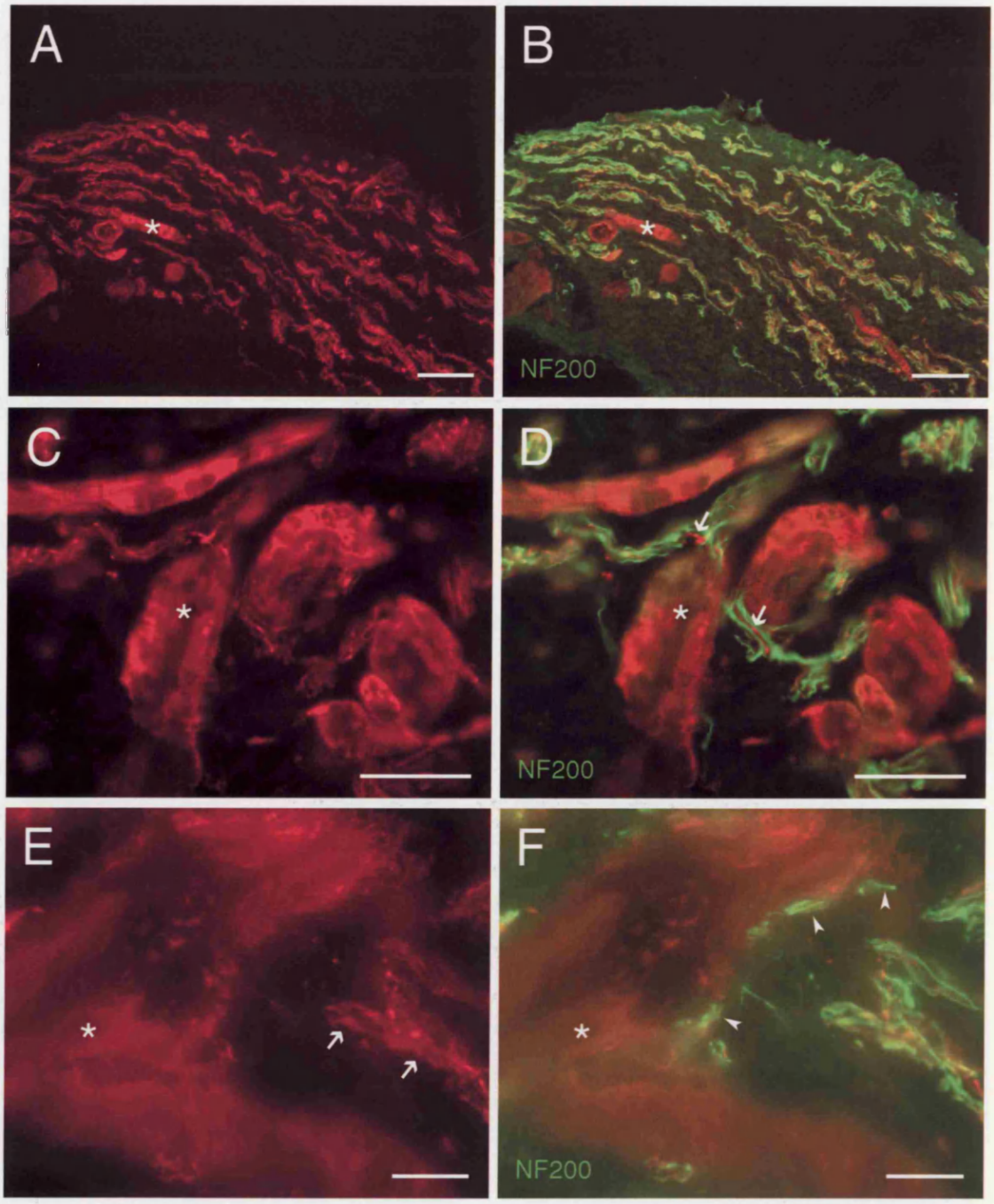
A
B
NF200
C
D
NF200
E
F
NF200

Figure 4.12.

Transection injuries of the dorsal columns of the spinal cord (A-F, caudal to the right) and crush injuries to the optic nerve (G,H, proximal to the left) of adult Sprague-Dawley rats.

A. At 4dpo in a horizontal section stained for Nogo-A, the lesion site (L) lacks significant Nogo-A expression but there is some increased immunoreactivity at the borders of the lesion. Scale bar =100μm.

B. By 8dpo there is a further increase in Nogo-A in the injured dorsal column (arrow) caudal to the lesion (L), particularly in swollen axons. Some Nogo-A positive fibres are present in the lesion. Scale bar =100μm.

C. At higher magnification the lesion site (L) at 8dpo contains many neurofilament positive fibres, presumably including sprouts from the injured dorsal column axons. Scale bar =100μm, also applies to D.

D. The same field as C, immmunoreacted for Nogo-A, shows many Nogo-A positive fibres in the lesion site (L) which are not always co-localized with neurofilament protein.

E. At the edge of a lesion in the spinal cord, 16dpo, a meshwork of Nogo-A positive fibres (arrowheads) and NG2 positive fibres is present in the grey matter, but the two antigens are not co-localized. Scale bar =100μm.

F. At the edge of a dorsal column lesion in the spinal cord, 8dpo, some GFAP positive processes (green) have extended into the lesion site (L) but they are distinct from the red Nogo-A positive fibres. Scale bar =100μm.

G. The crush site of an optic nerve 4dpo, immunoreacted for Nogo-A. There is a modest increase in Nogo-A at the boundaries of the lesion (L). Scale bar =100μm.

H. At higher magnification, Nogo-A positive fibres can be seen sprouting into the lesion site (L) of an optic nerve 4dpo. Scale bar =50μm.

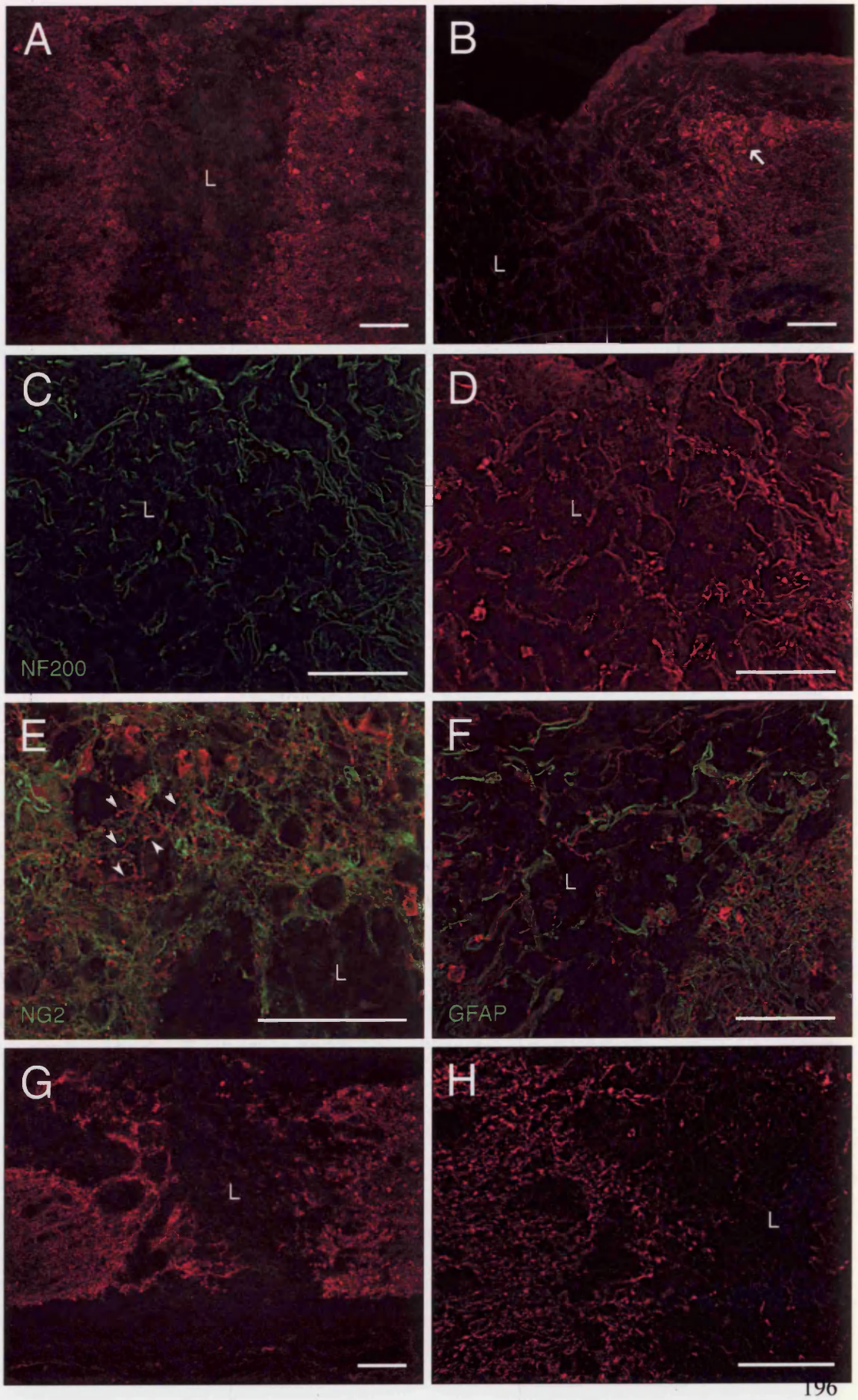
A
L
B
L
C
L
NF200
D
L
E
L
NG2
F
L
GFAP
G
L
H
L

CHAPTER 5

Expression of ATF3 by Glial Cells during Wallerian Degeneration: Differential Response of PNS and CNS Glia

(N.B. Although unrelated to the Nogo-66 Receptor and its ligands, the work reported within this chapter stemmed from a fortuitous observation of ATF3 upregulation by non-neuronal cells of injured sciatic nerve; the discovery was made whilst using the anti-ATF3 antibody as a comparative control for assessing changes in Nogo-A protein expression by peripherally axotomized DRG neurons. In addition to contralateral DRG, which was immunoreacted for direct comparison, sections of intact and injured sciatic nerve were also immunoreacted as negative controls).

INTRODUCTION

Wallerian degeneration is the process by which the nervous system responds to injury (Waller, 1850). It occurs in both the PNS and CNS, but differs in numerous respects. After transection of a peripheral nerve, Schwann cells within the distal stump rapidly begin to proliferate, and haematogenous monocytes infiltrate the damaged tissue. The latter differentiate into macrophages, and are responsible for the phagocytotic removal of cellular debris and extracellular matrix. This clearance permits the ultrastructural remodeling of injured nerve, in that Schwann cell columns (i.e. the bands of Bungner) are prepared to receive regenerating axons. The response of non-glial cells in the proximal stump of a severed peripheral nerve is somewhat attenuated. Naturally, these proscribed cellular responses are governed by significant changes in gene expression (Kubo et al., 2002; Costigan et al., 2002). Indeed, integral to such changes in gene activity is a class of proteins known as transcription factors. These bind directly to specific DNA sequences, typically lying within a gene promoter region, and regulate its transcription.

Often, a single active transcription factor will promote the transcription of a number of downstream target genes, some of which may also encode transcription factors; in other words, the activity of one transcription factor may regulate the expression of another. In the glial cells of the distal stump of injured peripheral nerve, it is known that the transcription factors c-jun, c-fos, krox-20 and scip are themselves transcriptionally upregulated (Pyykonen and Koistinaho, 1991; Stewart, 1995; Zorick et al., 1996; Soares et al., 2001). It is, of course, of particular interest to know which cascades of gene expression come under the control of these transcription factors, since it appears that it is the response of Schwann cells to nerve injury that enables them to recapitulate their ability to promote axonal regeneration. In contrast, their counterparts in the CNS (i.e. oligodendrocytes) do not undertake comparable programmes of gene expression during Wallerian degeneration, and many of these cells initially die before they repopulate from precursors, which may partly explain their failure to promote axonal regeneration after injury. Indeed, whereas implanted segments of peripheral nerve, suspensions of autologous Schwann cells and synthetic axon guidance channels lined with Schwann cells are all known to promote axonal regeneration of some classes of CNS neurons (reviewed by Jones et al., 2001), oligodendrocytes are believed to be inhibitory to axon outgrowth (reviewed by Yiu and He, 2003). Additionally, the process of Wallerian degeneration in the CNS is further complicated by the fact that other types of CNS glia (e.g. reactive astrocytes, oligodendrocyte precursor cells, meningeal cells and activated microglia), which are abundant in the injured CNS, are also thought to inhibit axonal regeneration (Liu et al., 1998; reviewed by Fawcett and Asher, 1999; Chen et al., 2002). At the moment, very little is known about the transcriptional control of these cellular processes; but, intriguingly, a number of different transcription factors are strongly upregulated by peripheral glia, but not CNS glia, during Wallerian degeneration.

ATF3 belongs to the bZip leucine zipper family of transcription factors that bind to cAMP and phorbol ester responsive promoters at cAMP response element (CRE) and activator protein-1 (AP-1) binding sites (reviewed by Hai and Hartman, 2001). However, ATF3 expression is reminiscent of that of c-Jun in injured neurons (Tsujino et al., 2000), and has been shown to form functional heterodimers with c-Jun *in vitro* (Pearson et al.,

2003). In contrast to ATF3 homodimers, ATF3/c-Jun heterodimers tend to activate rather than suppress gene expression through an AP-1-like transcription factor binding site (Nilsson et al., 1997).

In the study described here, the expression of ATF3 during Wallerian degeneration in the PNS and CNS was examined. Intriguingly, ATF3 was found to be upregulated by PNS glia, but not CNS glia, during Wallerian degeneration. Schwann cells in degenerating distal stumps of transected peripheral nerve strongly upregulated ATF3; and downregulation did not occur if axonal regeneration was prevented by ligation of the proximal stump.

SUMMARY OF METHODS

In 20 adult Sprague-Dawley rats the left sciatic nerve was transected in the thigh, and 2-3mm of the nerve resected to create a gap between the proximal and distal stumps. These animals were killed at 1 (n=4), 4 (n=3), 8 (n=3), 16 (n=3) and 30dpo (n=4). In three of the animals with resected nerves the proximal stump was ligated and turned aside to prevent axonal regeneration into the distal stump. These rats were killed at 30dpo. In 9 rats the left sciatic nerve was transected and reanastomosed with 10/O sutures to allow rapid axonal regeneration into the distal stump. These rats were killed at 4 (n=3), 16 (n=3) and 30dpo (n=3). In 8 rats the left L3-6 dorsal roots were cut using microsurgical scissors. The animals were killed at 1 (n=3) and 8 (n=3) and 30dpo (n=2). In 6 rats the left optic nerve was crushed with watchmakers' forceps 2mm from the eyeball. These rats were killed at 4 (n=2), 8 (n=2) and 30dpo (n=2). In 6 P1 rat pups the left sciatic nerve was transected. The animals were killed after 4 (n=3) and 7 dpo (n=3).

Immunofluorescencce Histochemistry

Primary antibodies: rabbit polyclonal anti-ATF3 (Santa Cruz); mouse monoclonal anti-neurofilament 200kDa (Sigma); rabbit polyclonal anti-c-Jun (a kind gift of Dr. A. Behrens, Cancer Research UK, London, UK); mouse monoclonal anti-bovine glial

fibrillary acidic protein (Sigma); mouse monoclonal anti-S100 (Sigma); mouse monoclonal anti-p75 (Sigma).

Secondary antibodies: monoclonal tetramethylrhodamine conjugated goat anti-mouse (Molecular Probes); monoclonal Alexa-Fluor-conjugated goat anti-rabbit (Molecular Probes).

In Situ Hybridisation

In three adult rats, in situ hybridisation was performed on the proximal and distal stumps of resected sciatic nerve, as well as a comparable segment of the uninjured contralateral sciatic nerve, 8dpo. Dr. M.R.J. Mason undertook this work using digoxygenin-labelled antisense and sense riboprobes for *ATF3* (Mason et al., 2003).

Statistical Analysis

All sections of injured sciatic nerve for statistical analysis were immunoreacted for ATF3, and stained with bisbenzimide (which labels all nuclei). The percentage of ATF3 immunopositive nuclei were calculated from comparable fields, photographed using a x20 objective, from each of three adjacent sections of injured sciatic nerve, per animal. These data were collated with those from at least two other animals, depending on the injury model and timepoint (see above). The sample mean and the standard error of the mean were subsequently calculated. Graphs were generated in Microsoft Excel.

RESULTS

ATF3 Expression in Peripheral Glia

Uninjured Sciatic Nerve

ATF3 immunoreactivity could be detected neither in contralateral sciatic nerves, nor in those of unoperated control rats.

Resected Sciatic Nerve

The resection of adult rat sciatic nerve, in which a 2-3mm segment was excised at the level of the thigh, was performed to slow the course of regeneration. In this model, ATF3 immunoreactive cells had appeared in the distal stump as early as 1dpo, but not in the proximal stump. At all time points, the ATF3 immunopositive endoneurial cells within the distal stump exhibited strong immunoreactivity peaking at 16dpo (Figs.5.1.B,D,F,H and Fig.5.2.B); by 30dpo, the number of ATF3 immunoreactive cells showed considerable variability from one animal to another, perhaps reflecting critical differences in the extent of regeneration that had occurred. In contrast, the temporal pattern of expression of ATF3 by cells within the proximal stump was quite different, but expression also peaked at 16dpo (Figs.5.1.A,C,E,G and Fig.5.2.A). Additionally, in comparison to the distal stump, ATF3 immunoreactivity in the proximal stump was much weaker at any given timepoint (Fig.5.1.A-H and Fig.5.2.A-B).

The size and shape of ATF3 immunoreactive cells was not entirely homogenous, suggestive of a mixed population. Furthermore, although there were very rarely any immunoreactive cells within the perineurium, a few cells within the epineurium were immunoreactive for ATF3 and appeared most often to be associated with the tunica adventitia of blood vessels. However, the density of cells within the endoneurium of the distal stump, as measured by staining with bisbenzimide, increased on average between 2 and 3 fold from 4dpo to 16dpo; a period when ATF3 immunoreactivity increased from 51.41% to 64.37% (Fig. 5.2.B).

ATF3 immunopositive endoneurial cells were often found in contact with regenerating axons at later timepoints (Figs. 5.3A, and 5.3B), suggesting that it is not the direct loss of axonal contact *per se* that induces the upregulation of ATF3. Nonetheless, the percentage of ATF3 immunoreactive nuclei within the distal stump of resected peripheral nerve appears to be inversely correlated with the extent of axonal regeneration (Fig. 5.3C).

Transection & Reanastomosis vs. Transection & Ligation

To further investigate whether the degree of regeneration could explain the wide variation in the percentage of ATF3 immunopositive cells in the distal stump of resected nerve at 30dpo, transected & reanastomosed as well as transected & ligated sciatic nerve were examined.

Reanastomosis of the proximal and distal stump of a transected peripheral nerve is beneficial to axonal regeneration. In the transected and reanastomosed adult rat sciatic nerve, a small number of neurofilament immunopositive regenerating axons could be detected entering the distal stump as early as 4dpo. By 16dpo, there was extensive axonal regeneration into the distal stump, although most of these fibres would not have re-innervated their original target tissues. By 30dpo, the density of axons within the distal stump was very similar to that observed at 16dpo; however, many of these fibres were probably completely regenerated. In comparison to the distal stump of resected nerve (Fig. 5.2.B), the percentage of ATF3 immunoreactive endoneurial cells in the distal stump of transected and re-anastomosed sciatic nerve was notably lower at each successive time-point (Fig. 5.2.C and 5.3.D). The proximal stumps contained very few ATF3 immunopositive cells in this model (not counted), and these tended to be close to the site of reanastomosis.

Ligation of the proximal stump, following transection of the sciatic nerve prevented any axonal regeneration. By 30dpo, the percentage of ATF3 immunopositive cells remained consistently high (67.92%; Fig. 5.2.C) with average levels exceeding those observed at 8dpo or 16dpo in the distal stumps of resected sciatic nerve (63.93% and 64.37%, respectively; Fig. 5.2.B).

ATF3 mRNA Expression in Resected Sciatic Nerve

Signal for *ATF3* mRNA was detected in the distal stumps of resected sciatic nerves at 8dpo (Fig. 5.3.F), but not in contralateral intact sciatic nerves (Fig. 5.3.E).

Transected Neonatal Sciatic Nerve

To investigate whether the upregulation of ATF3 by peripheral glia in response to Wallerian degeneration was age-specific, the sciatic nerve was transected in P1 rat pups and examined at 4 and 7dpo. At both time points, large numbers of endoneurial cells within the distal stump were immunoreactive for ATF3 (Fig. 5.4). However, the intensity of expression was slightly lower than that observed in lesioned adult sciatic nerve.

Schwann Cells Upregulate ATF3 During Wallerian Degeneration

The majority of ATF3 immunoreactive cells within the distal stump were also immunoreactive for the Schwann cell marker, S100 (Fig. 5.5.A). Furthermore, most ATF3 immunopositive cells also expressed $p75^{NTR}$ (Fig. 5.5.B), which is known to be strongly upregulated by Schwann cells during Wallerian degeneration. By phase contrast microscopy, ATF3 immunoreactive could be observed within the bands of Büngner adjacent to macrophages laden with myelin debris (Fig. 5.5.C). The endothelial cells and pericytes of endoneurial blood vessels were very rarely immunoreactive for ATF3 in injured adult nerve, except at 1dpo when a small number of these cells were found to be weakly positive. The ATF3 immunoreactive cells found at the periphery of epineurial blood vessels were thought to be Schwann cells, since they also expressed S100.

ATF3 Expression in CNS Glia

Transection of the Dorsal Root (Rhizotomy)

Rhizotomy was performed to establish whether upregulation of ATF3 is common to both peripheral and CNS glia during Wallerian degeneration. Within each dorsal rootlet is a small cone of CNS tissue, termed the dorsal root entry zone (DREZ), from which GFAP immunopositive astrocytic processes extend following rhizotomy. These processes project into the injured adjoining rootlet, and constitute the first CNS tissue to be encountered by regenerating primary sensory afferents. Indeed, very few of the axons regenerating along the dorsal rootlets actually manage to grow back into the spinal cord; the majority arrest at the DREZ, and some axons turn back on themselves (Chong et al., 1999; Zhang et al., 2001).

By 1dpo, ATF3 immunoreactive cells were present close to the site of transection. By 4 and 8dpo, when long GFAP immunopositive astrocytic processes were observed extending out from the DREZ into the adjoining dorsal rootlets, ATF3 immunoreactive cells were present throughout the whole segment of peripheral nerve from the site of transection up to the border of the DREZ (Fig. 5.5.D and E). Both the DREZ and the rostral spinal dorsal column, which were undergoing Wallerian degeneration, were devoid of immunoreactivity for ATF3.

Expression of c-Jun during Wallerian Degeneration

The pattern of c-Jun immunoreactivity closely resembled that of ATF3 in all injury models examined. For example, c-Jun was strongly upregulated by large numbers of endoneurial cells in the distal stump of lesioned sciatic nerve, following a similar temporal course as ATF3. Also, c-Jun immunopositive cells were present in the distal segment of peripheral nerve up to the border of the DREZ following rhizotomy (Fig. 5.5.F); no c-Jun immunopositive CNS glia were observed either in the DREZ or the degenerating rostral spinal dorsal column.

Optic Nerve Crush

There is a considerable degree of axonal sprouting in the proximal stump of adult rat optic nerve following crush injury (Zeng et al., 1994), but very little axonal regeneration (Campbell et al., 1999).

At all time points examined (4, 8 and 30dpo), both the lesion site and the meninges contained some strongly ATF3 immunopositive cells. However, throughout the proximal and distal stumps, there were a few very weakly ATF3 immunoreactive cells (Fig. 5.5.G); although, this could be the result of non-specific binding of the rabbit antiserum. Many putative retinal ganglion cells ipsilateral to the lesion, but not contralateral, were ATF3 immunopositive at all time-points (Fig. 5.5.H) consistent with a previous study (Takeda et al., 2000).

DISCUSSION

The evidence presented here for the upregulation of ATF3 in the distal stump of transected sciatic nerve of adult rat is supported by a previous study (Nagarajan et al., 2002), in which the distal stump of transected sciatic nerve of adult mouse was examined for changes in gene expression using gene chip technology. Analysis of their raw microarray data, made publicly available for downloading, shows that ATF3 was significantly upregulated. In addition, numerous other genes, already known to be upregulated, were also detected in this analysis (Table 5.1).

ATF3 Expression in Schwann Cells in the Injured Peripheral Nerve

ATF3 expression is induced in many endoneurial cells in the injured sciatic nerve, including Schwann cells in the distal stump. The duration of expression is prolonged by ligation of the proximal stump after transection (30dpo = 67.92%), but reduced by reanastomosis of the proximal and distal stumps after transection (30dpo = 3.64%). Intermediate values were recorded after resection (30dpo = 31.80%), which slows the course of regeneration and leads to a more variable outcome. Intriguingly, it would appear that glial expression of ATF3 is negatively regulated by signals derived from completely regenerated axons, not by contact of Schwann cells with regenerating axons *per se*. Evidence for this comes from the distal stumps of transected & reanastomosed nerve; by 16dpo and 30dpo there was little difference in axonal density, yet ATF3 immunopositive cells were widespread and often in contact with axons in the former (16dpo = 21.10% vs. 30dpo = 3.64%). Similarly, in the distal stump of resected nerve at 30dpo (31.80%) the axonal density was variable, reflecting the slowed rate of regeneration, and many ATF3 immunoreactive cells – some in contact with axons - could be observed.

It is unlikely that the upregulation of ATF3 is a general response to injury, since it is neither upregulated in perineurial cells, nor endothelial cells of the endoneurial or epineurial blood vessels which would also have been damaged. That the number of cells upregulating ATF3, and the strength of expression, was markedly higher in the distal stump than the proximal stump at all timepoints is also indicative of a genuine molecular

process occurring during Wallerian degeneration. Also, given that the ATF3 immunoreactive nuclei within the distal stump are for the most part found within S100 or $p75^{NTR}$ immunopositive structures, it is reasonable to suggest that the molecule is principally expressed by Schwann cells. However, the homogenous appearance of ATF3 immunoreactive nuclei - in terms of shape, size and intensity of signal – does not preclude the involvement of other cell types.

Differential Expression of ATF3 in PNS and CNS Glia

Rhizotomy elicited ATF3 expression by peripheral glia in the segment of peripheral nerve from the site of transection up to the border of the DREZ. In contrast, the CNS glia in the DREZ and rostral spinal dorsal column did not express ATF3, despite undergoing Wallerian degeneration in response to the death of the very same axons. These differences in glial response were strikingly obvious in sections of the ipsilateral DREZ. However, direct trauma to the CNS, in the form of an optic nerve crush, evoked a somewhat different response. Although strongly immunoreactive cells were detected in the lesion site, as well as in the meninges, only very weakly immunoreactive cells could be observed in the proximal and distal stumps at any survival time. It is possible that this weak immunoreactivity is due to non-specific binding of the rabbit antiserum. Nonetheless, the pattern of immunoreactivity is distinct from that observed in the injured PNS and strongly suggests that ATF3 is not upregulated in a program of gene expression associated with the CNS glial response during Wallerian degeneration. It may, however, be upregulated strongly in a few cells at the lesion site and in the meninges as a result of direct trauma.

ATF3 and c-Jun Exhibit a Similar Pattern of Expression in Injured Peripheral Nerve

Although no double-labelling experiments were performed owing to the lack of compatible antibodies, the pattern of ATF3 expression was very similar to that of c-Jun in all models of injury examined. In lesioned peripheral nerve, strong expression of c-Jun was observed in endoneurial cells of the distal stump. Likewise, following rhizotomy, c-Jun expression was observed in PNS glia residing in the distal segment of the transected peripheral nerve root, but not in CNS glia residing in the respective DREZ or

degenerating spinal dorsal column, all of which were undergoing Wallerian degeneration in response to the loss of the same axons. In the injured optic nerve, it is known that c-Jun is not upregulated during Wallerian degeneration (Vaudano et al., 1998). It is enticing to think that ATF3 and c-Jun may be forming functional heterodimers in peripheral glia; ATF3 homodimers tend to be involved in the repression of transcription, and ATF3/c-Jun heterodimers in activation. It is not yet clear which genes can be regulated by these homo- and/or hetero-dimers but, not surprisingly, it is known that their consensus binding sites are slightly different.

Is ATF3 Expression in Schwann Cells Linked to Axonal Regeneration?

Wallerian degeneration is different in PNS and CNS glia and, perhaps with the exception of olfactory ensheathing glia (OEG), Schwann cells are the most permissive for axonal regeneration. Therefore, it is quite plausible that one of the key reasons why axonal regeneration fails in most parts of the CNS is simply because oligodendrocytes, astrocytes and microglia do not respond appropriately to injury.

In injured peripheral nerve, there are many changes in gene expression in the distal stumps (Kubo et al., 2002). For example, cell adhesion molecules such as N-CAM, L1 and CHL1 are all upregulated and thought to be beneficial to regeneration (Tacke and Martini, 1990; Hillenbrand et al., 1999). Similarly, $p75^{NTR}$ is upregulated by Schwann cells and is believed to assist in the process of regeneration by storing neurotrophic factors, such as NGF and BDNF, which are also upregulated (Funakoshi et al., 1993). Extracellular matrix molecules such as laminin, tenascin-C and collagens are upregulated (Eather et al., 1986; Martini et al., 1990; Siironen et al., 1992; Doyu et al., 1993), as well as various cytokines (Rotshenker et al., 1992; Curtis et al., 1994; Subang and Richardson, 2001), although there is some debate about the extent in which these molecules assist in regeneration. On the other hand, myelin-associated molecules such as P0 and MAG are downregulated (Poduslo, 1984; Gupta et al., 1990); the latter having long been implicated in axonal regenerative failure within the CNS. However, it should not be overlooked that Schwann cells within the distal stump of transected peripheral nerve also upregulate molecules that are believed to be highly inhibitory to axonal regeneration in the injured

CNS - such as Sema3A, Nogo and NG2 (Hunt et al., 2002b; Scarlato et al., 2003; Rezajooi et al., 2004) . Yet, these do not seem to be detrimental to regeneration within the peripheral nervous system. There are, of course, a number of potential explanations, one of them being that the activity of co-expressed permissive molecules overrides that of inhibitory molecules.

ATF3 and Transcriptional Control

ATF3 is also upregulated by many axotomized neurons, and was at first considered to be a neuron-specific marker of injury in the nervous system (Tsujino et al., 2000). *In vitro*, it has been shown to act through HSP27 to confer resistance to apoptosis and to promote neurite outgrowth (Nakagomi et al., 2003). These are, of course, desirable responses in injured neurons; but, protection from apoptosis would presumably be of equal benefit to Schwann cells during Wallerian degeneration. That ATF3 and c-Jun share a similar pattern of expression in both neurons (Takeda et al., 2000) and Schwann cells following axonal injury is suggestive of their controlling molecular responses common to both cell types, possibly through the formation of heterodimers. Indeed, CHL1 and GAP43 are upregulated by axotomized neurons as well as Schwann cells (Verge et al., 1990; Hall et al., 1992; Chong et al., 1994; Zhang et al., 2000). Likewise, $p75^{NTR}$ - which is strongly expressed by Schwann cells during Wallerian degeneration - is also upregulated by axotomized motorneurons (Gschwendtner et al., 2003). Whether these changes in gene expression are linked to the activity of upregulated ATF3, either as a homodimer or as a heterodimer in conjunction with c-Jun, remains to be seen. Although, in the case of GAP-43, it would appear that overexpression of c-Jun alone is insufficient to drive transcription of GAP-43 (Carulli et al., 2002), even though its promoter contains an AP-1 transcription factor binding site (Weber and Skene, 1998).

Summary

ATF3 is widely upregulated by Schwann cells distal to a peripheral nerve transection. Its temporal expression pattern appears to be regulated by axonal regeneration and reinnervation of target organs: transection & ligation, which prevents peripheral nerve regeneration, leads to prolonged ATF3 expression whereas transection & reanastomosis,

which expedites regeneration, leads to a shorter course of expression compared to transection & resection models, which are designed to slow the course of regeneration. Curiously, in contrast to peripheral Schwann cells, CNS glia do not appear to upregulate ATF3 during Wallerian degeneration. This differential transcriptional response to axotomy may, in part, explain why Schwann cells are one of the most highly supportive cell-types for axonal regeneration and are fundamental to the success of regeneration in the peripheral nervous system. In time, a fuller understanding of the molecular mechanisms that make them so will doubtless prove hugely valuable to the study and treatment of CNS nerve injury.

CONCLUSION

Schwann cells, but not CNS glia, express both ATF3 and c-Jun during Wallerian degeneration. These transcription factors may participate - perhaps through the formation of heterodimers - in regulating cascades of gene activity which ultimately render Schwann cells supportive for axonal regeneration.

The principal observation reported in this chapter, that ATF3 is upregulated in the endoneurial cells of axotomized peripheral nerve, was also independently discovered by M.K.Hossain-Ibrahim. Figure 5.2 incorporates our collective data on the temporal expression profile of ATF3 in various models of peripheral nerve injury.

Figure 5.1.

Resection of adult rat sciatic nerve. ATF3 immunoreactive nuclei (green) are shown in the proximal (A,C,E,G) and distal (B,D,F,H) stumps at 4,8,16 and 30dpo, respectively. ATF3 expression is stronger and more widespread in the distal stump, than in the proximal stump at all timepoints. The main image in C, and the inset image, show segments of proximal stump and distal stump, respectively, photographed under standardized conditions (exposure, gain and offset). The perineurium (P) is devoid of ATF3 immunoreactivity. Scale bars: A,B = 200μm; C-H = 50μm.

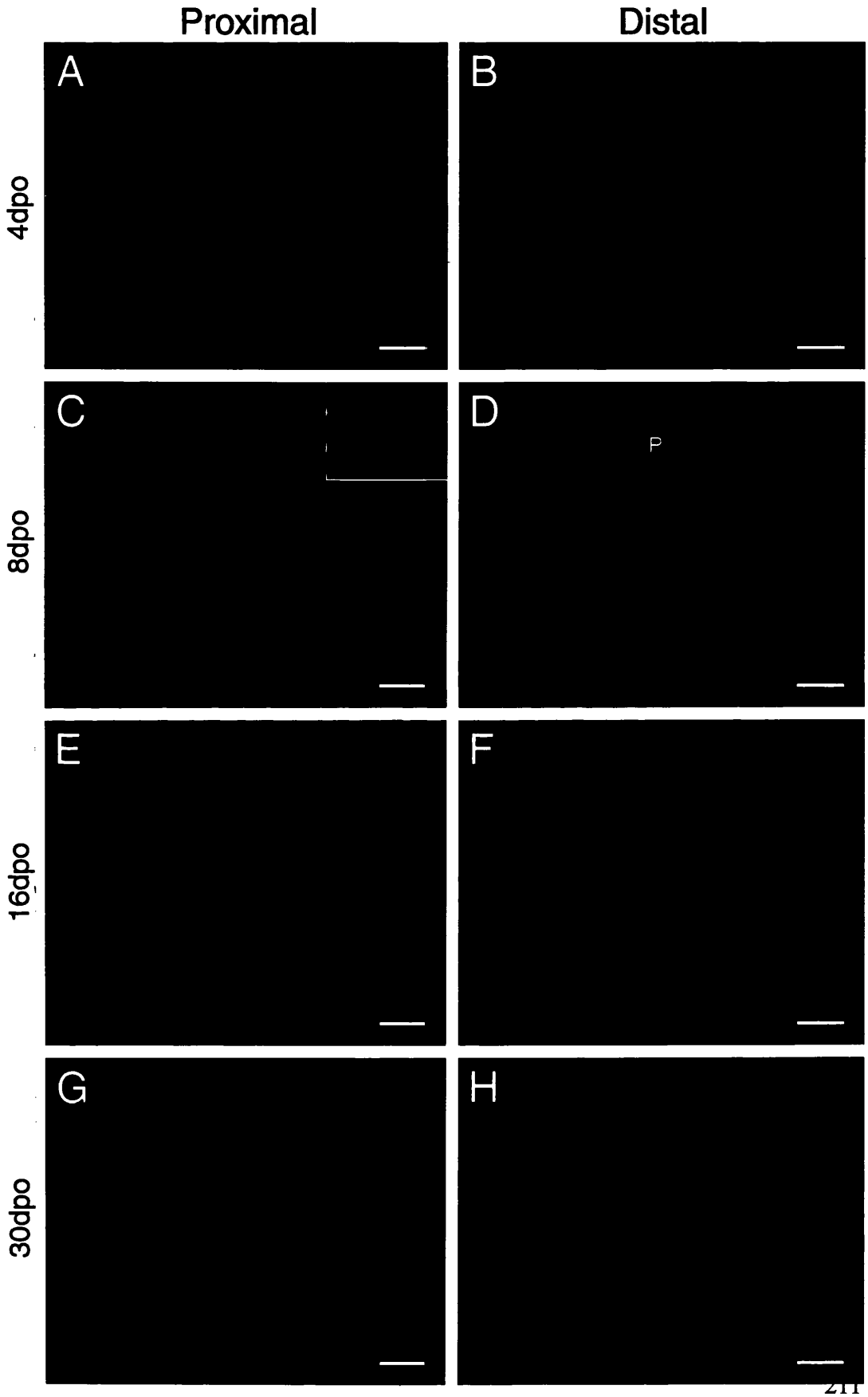
Proximal
Distal
A
B
4dpo
C
D
P
8dpo
E
F
16dpo
G
H
30dpo

Figure 5.2.

Histograms showing the percentage of ATF3 immunopositive nuclei in the proximal (A) and distal stumps (B,C) of injured adult rat sciatic nerves. In the proximal stump after resection (A), not only were the number of ATF3 immunopositive nuclei less numerous but also more weakly immunoreactive than in the distal stump (B). There is no bar for 4dpo in A, because so few nuclei were ATF3 immunopositive (<1%). In C, the course of ATF3 expression in the distal stump after cut and reanastomosis (C&R) at 8,16 and 30dpo is compared with cut and ligation (C&L) of the sciatic nerve at 30dpo. In contrast to resection (B), in which regeneration is slowed, C&R permits rapid axonal regeneration which is associated with a faster downregulation of ATF3 in the distal stump. However, when regeneration is prevented by C&L, ATF3 expression in the distal stump remains high.

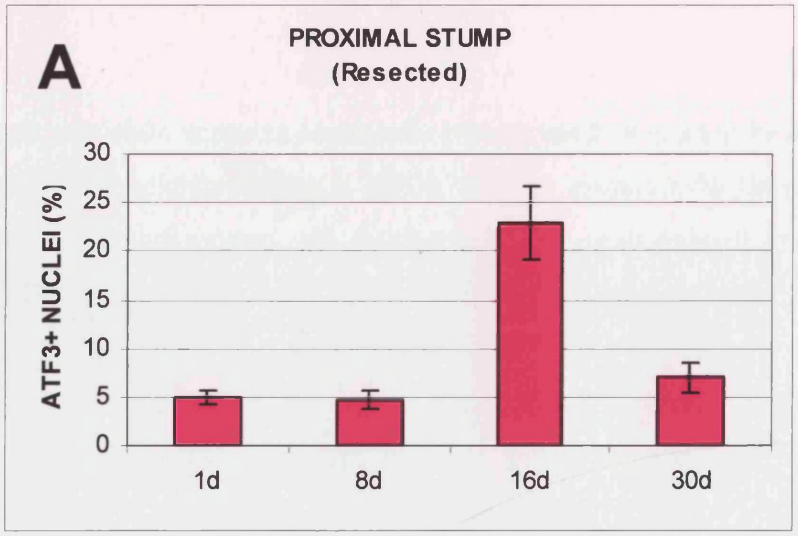
A
PROXIMAL STUMP
(Resected)
ATF3+ NUCLEI (%)
30
25
20
15
10
5
0
1d
8d
16d
30d

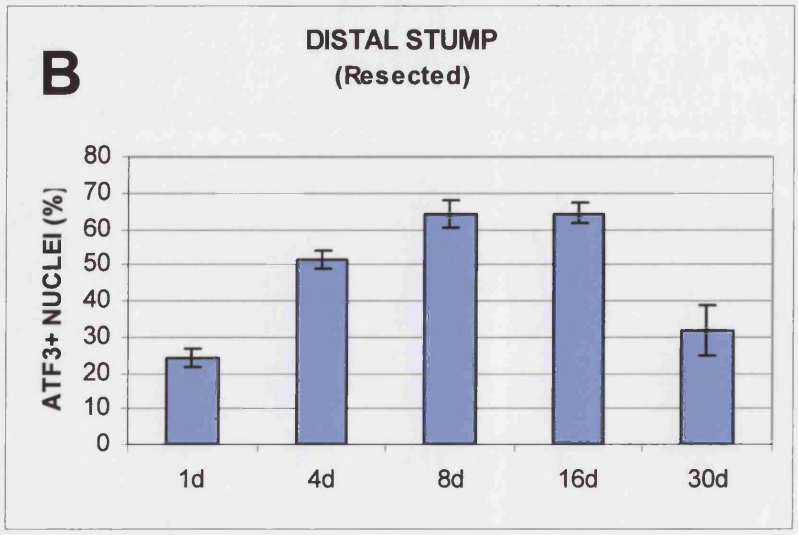
B
DISTAL STUMP
(Resected)
ATF3+ NUCLEI (%)
80
70
60
50
40
30
20
10
0
1d
4d
8d
16d
30d

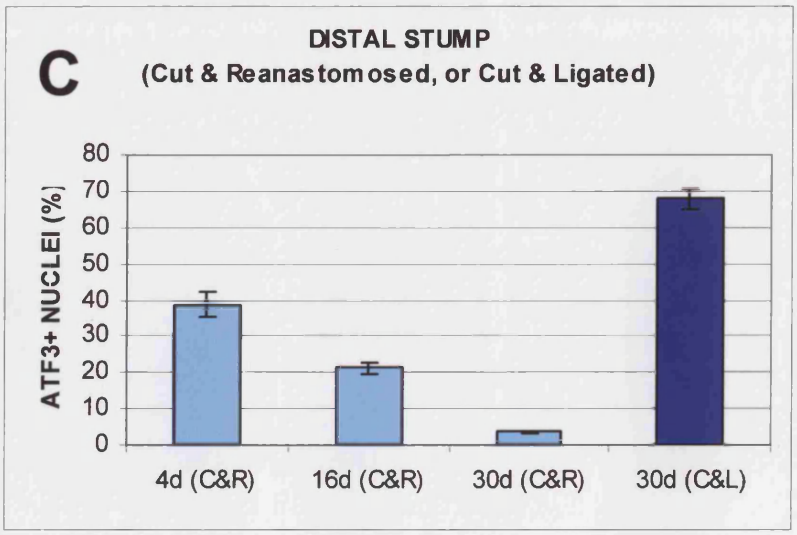
C
DISTAL STUMP
(Cut & Reanastomosed, or Cut & Ligated)
ATF3+ NUCLEI (%)
80
70
60
50
40
30
20
10
0
4d (C&R)
16d (C&R)
30d (C&R)
30d (C&L)

Figure 5.3.

Sciatic nerves from adult rats. In distal stumps of resected nerves at 30dpo (A, B, and C), a considerable degree of variation in both ATF3 immunoreactivity (green) and the quantity of axonal regeneration (as determined by heavy chain neurofilament immunoreactivity; red) is evident. In some instances, ATF3 immunopositive nuclei and regenerating axons are found in close association, suggesting that the presence of regenerating axons in the distal stump is not alone sufficient for the immediate downregulation of ATF3. In D, the distal stump of cut and reanastomosed sciatic nerve is shown at 30dpo, when axonal regeneration is extensive and ATF3 expression has declined. By *in situ* hybridisation, *ATF3* mRNA is undetectable in intact sciatic nerve (E), but upregulated in the distal stump of resected nerve 8dpo (F). Scale bars = 50μm. The sections shown in E and F were prepared and reacted by Dr. M.R.J. Mason.

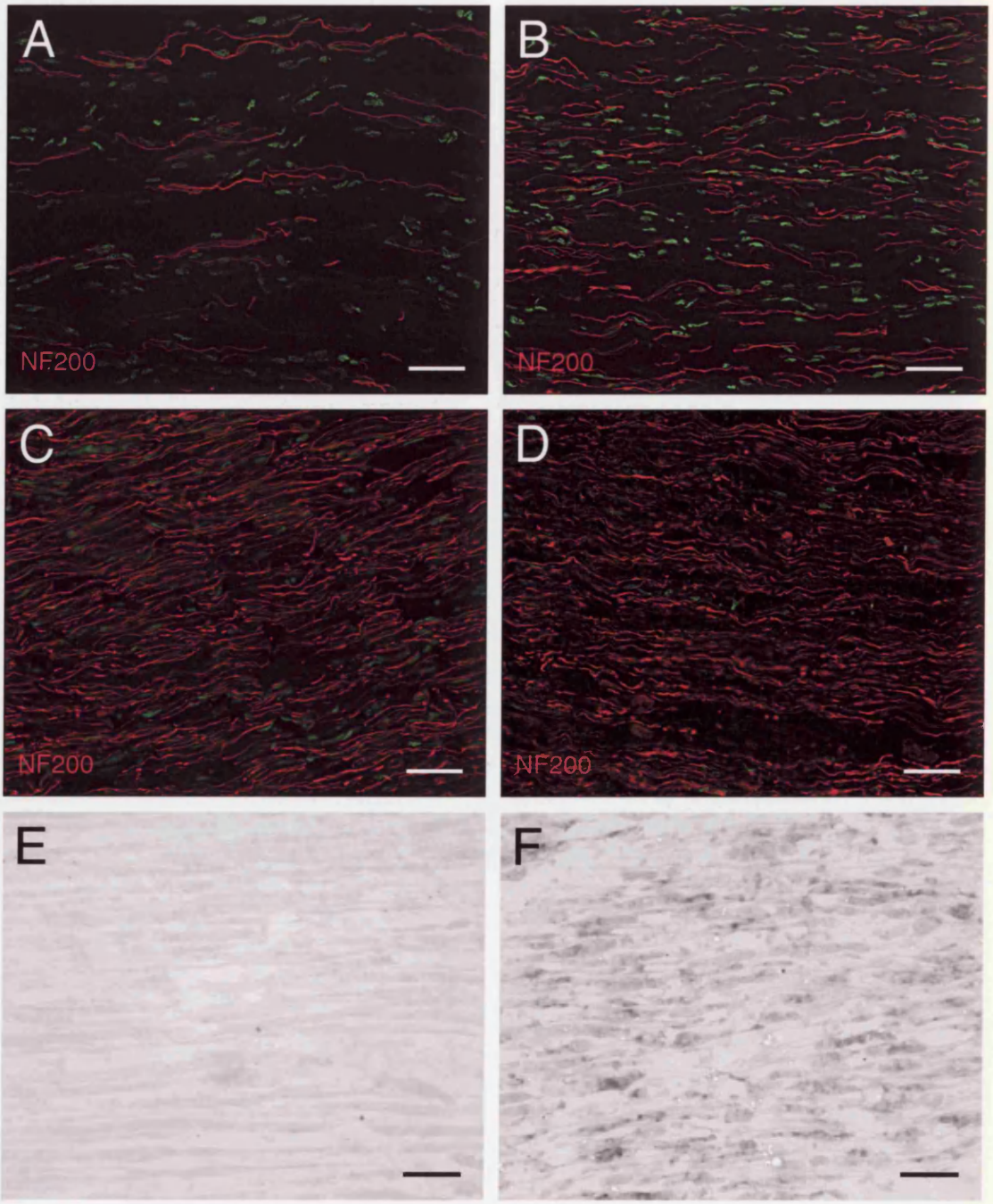
A
NF200
B
NF200
C
NF200
D
NF200
E
F

Figure 5.4.

The distal stump of a sciatic nerve from a neonatal rat, 5dpo. The nerve was resected at P1. Similar to adult rat sciatic nerve, many endoneurial cells strongly express ATF3. Scale bar = 50μm.

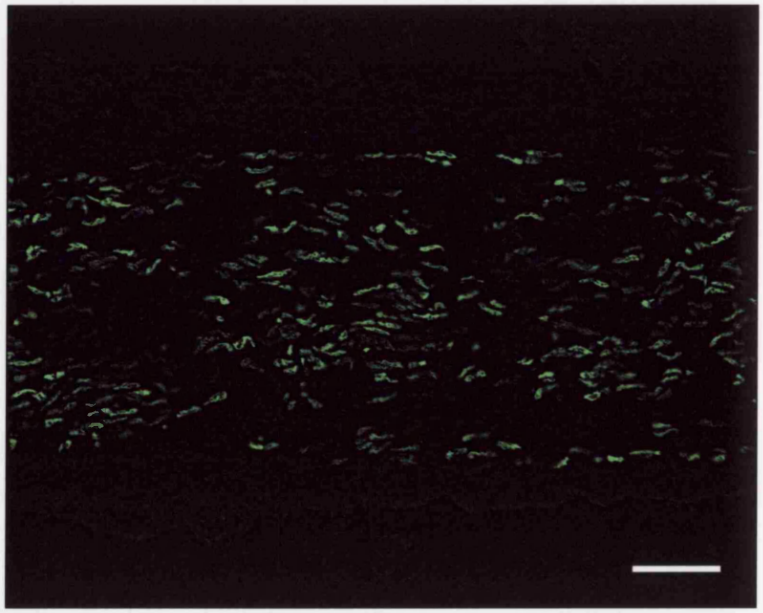

Figure 5.5.

PNS glia, but not CNS glia, express ATF3 during Wallerian degeneration. ATF3 (green) is expressed in S100 (red in A) and $p75^{NTR}$ (red in B) immunopositive cells in the distal stumps of resected sciatic nerves of adult rat (A = 30dpo; B = 8dpo). C is a double exposure showing a phase contrast image and ATF3 immunofluorescence (green) of the distal stump of a resected nerve, 4dpo. The ATF3 nuclei are found between the debris-laden macrophages (asterisk) inside the bands of Büngner (indicated by arrows). D and E show the dorsal rootlets of adult rat sciatic nerve, immunoreacted for ATF3 (green) and GFAP (red) 8 days after dorsal rhizotomy. The GFAP immunopositive astrocytes which characterise the dorsal root entry zone (d) of the spinal cord have long processes projecting into the peripheral segment of the rootlets (asterisk). For the most part, ATF3 expression is confined to the peripheral segment of the rootlets in which Schwann cells reside. F shows a dorsal rootlet, 1 day after dorsal rhizotomy, immunoreacted for c-Jun (green) and GFAP (red). Note that c-Jun expression is confined to the Schwann-cell containing part of the rootlet (asterisk), as is ATF3 (compare with E). G and H are images of optic nerve and retina from the same animal, 30 days after a left optic nerve crush injury. Both have been immunoreacted for ATF3 (green) and GFAP (red). In G, reduced GFAP immunolabelling marks the crush site (L) which also contains some ATF immunopositive nuclei. Additionally, some nuclei proximal and distal to the lesion are ATF3 immunoreactive, but these are much less numerous and more weakly labelled than in injured peripheral nerves. H shows the retina ipsilateral to the optic nerve crush site, in which strongly ATF3 immunopositive nuclei are visible in the ganglion cell layer (arrowheads). Op = optic nerve head. Scale bars: A-C = 25μm; D = 100μm, E = 50μm; F = 100μm; G = 50μm; H = 50μm.

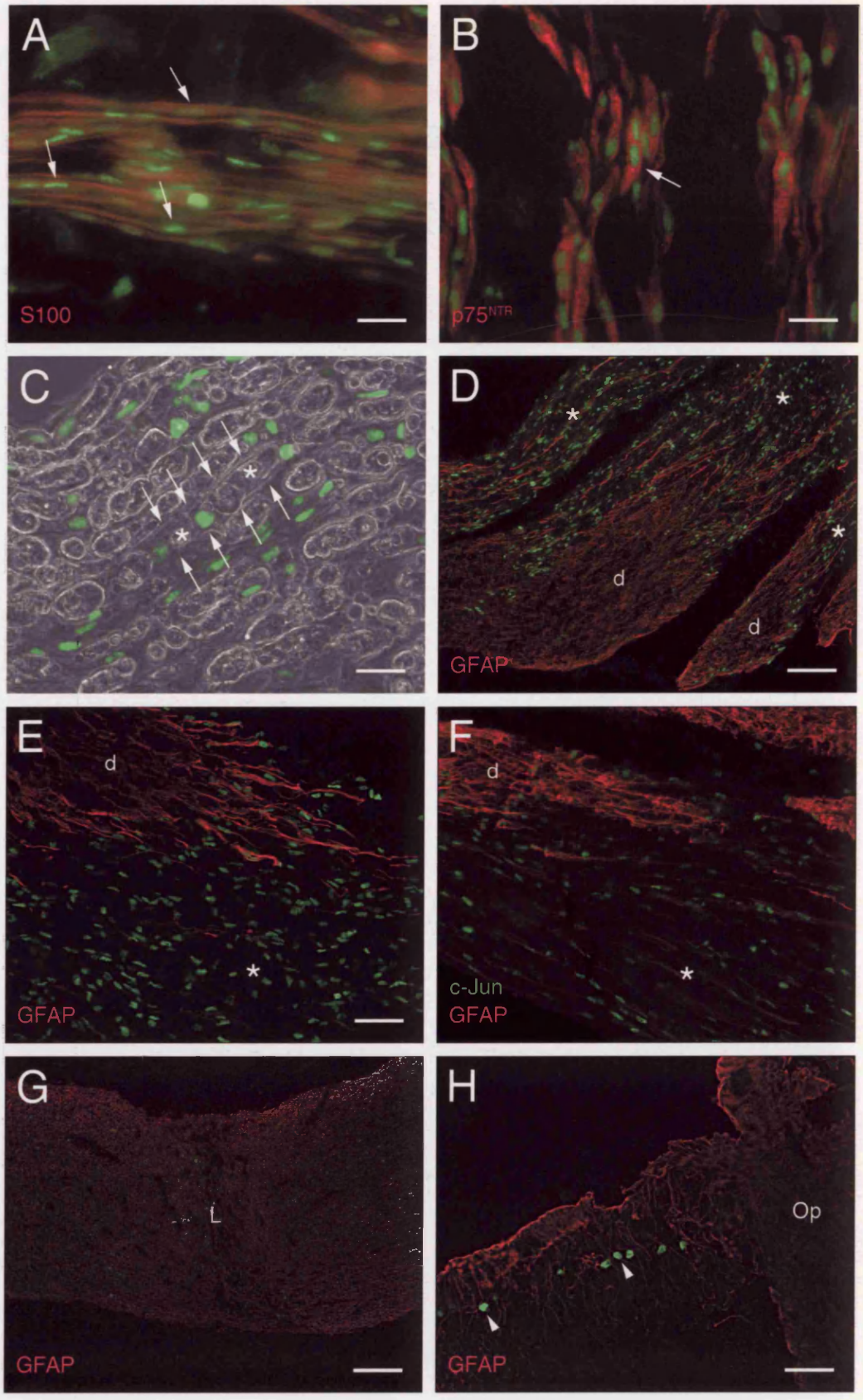
A
S100
B
p75NTR
C
D
d
d
GFAP
E
d
GFAP
F
d
c-Jun
GFAP
G
L
GFAP
H
Op
GFAP

Table 5.1.

Some of the genes which appear to be upregulated more than five-fold in the distal stump of adult rat sciatic nerve at 14d, or 28d, after transection (calculated from the raw microarray data made available for downloading by Nagarajan et al. 2002).

Gene name	Supporting Evidence
Jun oncogene	Stewart, 1995
Tenascin C	Martini et al., 1990
Insulin-like growth factor 1	Cheng et al., 1996
ATF3	Hunt et al., 2004
Neuropilin	Scarlato et al., 2003
Lectin, galactose binding, soluble 3 (a.k.a. galectin-3/MAC-2)	Reichert et al., 1994
GAP-43	Curtis et al., 1992

CHAPTER 6

omgp mRNA Expression in the Intact and Injured Nervous System

INTRODUCTION

Oligodendrocyte myelin glycoprotein (OMgp) was first identified in a screen of adult human CNS white matter for peanut agglutinin-binding proteins (Mikol and Stefansson, 1988). It is a GPI-linked leucine rich repeat (LRR) protein that is subject to differential post-translational modification with the HNK-1 carbohydrate (Mikol et al., 1990b). The function of the molecule remained something of a mystery until recently, when it was identified as a functional ligand for the Nogo-66 Receptor (Wang et al., 2002b). Shortly afterwards, it was also reported to be the main neurite-outgrowth inhibitor in 'arretin', a protein fraction extracted from bovine myelin (Kottis et al., 2002).

As its name suggests, OMgp is believed to be a myelin protein. However, there is some evidence that it may in fact be predominantly expressed by neurons (Habib et al., 1998c), not only by oligodendrocytes as had initially been thought (Mikol and Stefansson, 1988). Furthermore, the transient expression of OMgp in 3T3 fibroblasts was found to suppress mitogenesis by blocking intracellular signalling pathways from activated PDGFα receptor (Habib et al., 1998a). Together, these two studies are suggestive of another role for OMgp, possibly as part of a receptor complex on neurons.

Since there is now irrefutable evidence that many of the isoforms of Nogo are expressed by adult neurons (Josephson et al., 2001; Huber et al., 2002; Hunt et al., 2002b), and also that Nogo-A and NgR are expressed in neurons throughout embryonic development (Huber et al., 2002; Josephson et al., 2002; Tozaki et al., 2002; Lauren et al., 2003; Meier et al., 2003; Mingorance et al., 2004), it seems plausible that neuron-neuron signalling may be occurring through the NgR-ligand interactions. OMgp, being a GPI anchored cell surface protein, is of course well located for such cell surface interactions, in contrast to

the Nogo family of proteins which all contain a carboxy terminal ER-retention signal. Since it is also possible that OMgp is a receptor in its own right, interneuronal NgR-OMgp interactions could potentially result in two-way signalling.

The finding of *omgp* expression by neurons has been given very little attention, especially in the context of OMgp-mediated inhibition of axonal regeneration (Wang et al., 2002b; Kottis et al., 2002). This is an important issue, not least because NgR is the only protein with which OMgp has, to date, been shown to bind. Naturally, there may be other proteins with which OMgp interacts; in fact, it would be surprising if there were not, as it can alter intracellular signalling in cells in which it is overexpressed. If this finding is correct, OMgp would require a signal transducing co-receptor and, presumably, at least one ligand. One possibility would be that the soluble form of NgR, cleaved from the cell surface by a zinc metalloproteinase (Walmsley et al., 2004), could act as such a ligand for OMgp. Though what the function of such a system would be is difficult to say.

Since very little is known about OMgp, it was felt that an investigation of its expression pattern in the adult rodent nervous system, by *in situ* hybridisation, was warranted, not least, because the previous report of *omgp* expression by neurons had yet to be confirmed. Furthermore, because the protein appears to modulate PDGFα signalling in fibroblasts, it could be of considerable importance in neuronal physiology. In this study, *in situ* hybridisation using both DIG-labelled riboprobes and ^{35}S-labelled 45-mer DNA oligonucleotides was performed.

SUMMARY OF METHODS

Animal Models

Seven unoperated adult Sprague-Dawley rats, and one unoperated Balb/c mouse, were used in these experiments. The Balb/c mouse brain, and one Sprague-Dawley rat brain, were used for the extraction of total RNA. Three Sprague-Dawley rats received autologous peripheral nerve grafts to thalamus, and were culled after 16 days. The remaining three rats were used unoperated for *in situ* hybridisation.

Cloning of the Rat *omgp* Coding Sequence

Rat genomic DNA was isolated from adult Sprague-Dawley rat brain using DNAzol, as described in Chapter 2. PCR was performed with the forward and reverse primers, GGC TTT GAT GGA ATA TCA G and TAG CAG CAA GTA CCA AGA CA, using the proof-reading DNA polymerase, *Pfu* (Promega). The amplicon was ligated into the PCR cloning vector, pGem T Easy (Promega). Two clones were sequenced by automated fluorescent dye sequencing.

***In Situ* Hybridisation with DIG-Labelled Riboprobes**

A 540bp fragment of mouse *omgp* (bases 1096-1635 of Genbank sequence NM_019409) was cloned by PCR from total RNA extracted from adult Balb/c mouse brain, using the forward primer ACT GCT CGA GTA GTA GCA CTG ATA GGG CTG and the reverse primer ACT GAA GCT TGC AAG TAC CAA GAC ATT GTG. The amplicon was ligated into pcDNA3 using the *Xho*I and *Hin*dIII restriction sites, which were also contained in the forward and reverse primers, respectively. *Hin*dIII-linearized plasmid was used for the synthesis of DIG-labelled sense riboprobes in conjunction with SP6 RNA polymerase. Conversely, *Xho*I-linearized plasmid was used for the synthesis of DIG-labelled antisense riboprobes in conjunction with T7 RNA polymerase. *In situ* hybridisation was carried out as described in Chapter 2. The sense riboprobe produced no signal.

Radioactive *In Situ* Hybridisation

A ^{35}S-labelled 45-mer DNA oligonucleotide, ACT CAT TCC ATC CTG GAG GTG AAT AGT TAG AGT TGC AGC TGC TGC (bases 1042-1086 of Genbank sequence AY316298), was used for radioactive *in situ* hybridisation as described in Chapter 2. The specificity of binding of this antisense *omgp* probe was verified by 'competitive control', in which a mixture of radiolabelled and unlabelled oligonucleotide (in a ratio of 1:100) was applied to sections. The absence of radioactive signal in competitive control sections was indicative of the high specificity of the antisense probe.

RESULTS

Cloning of Rat *omgp*

In order to perform *in situ* hybridisation with radiolabelled 45-mer DNA oligonucleotides on rat tissue, it was first necessary to obtain the rat *omgp* coding sequence (CDS) in order to design exact-matching probes. At the time that this work was undertaken, the rat *omgp* CDS had not yet been cloned, sequenced and registered in Genbank. Unfortunately, the early build of the rat genome, which was publicly accessible through the National Centre for Biotechnology Information (NCBI) website (www.ncbi.nih.gov), was fraught with sequencing errors. Using the Basic Local Alignment of Sequence Tool (BLAST) to align the Genbank approved mouse *omgp* CDS against the draft rat genome, it became apparent that there was a frame shift in the draft rat genomic *omgp* CDS, and numerous nucleotide mismatches (Fig. 6.1). Furthermore, there were no matching rat expressed sequence tags (ESTs) deposited in dbEST, therefore preventing the extrapolation of a consensus sequence from overlapping ESTs. The cloning of the rat *omgp* CDS was, therefore, required to ensure the design of perfectly complementary 45-mer oligonucleotide antisense sequences for radioactive *in situ* hybridisation. Also, given the growing significance of OMgp in axonal regeneration and the common usage of rats as experimental models, it was felt that the cloning of the rat *omgp* CDS and the submission of its sequence to a publicly accessible database, such as Genbank, would be of wider benefit.

BLAST alignment of the full-length mouse *omgp* sequence against the draft rat genome sequence revealed that the gene structure of *omgp* is the same in both mouse and rat. That is to say that the *omgp* gene consists of two exons, with the intron being located in the 5′ untranslated region (UTR) and the CDS being located entirely within the second exon. Having obtained the rat genomic sequence corresponding to the mouse *omgp* CDS, a correction was made for the obvious frame-shift, due to the omission of an A at position 169, to provide a rough prediction of the correct rat *omgp* CDS.

Regions of complete homology between the mouse full-length *omgp* cDNA and rat genomic sequences, overlying the start codon and flanking the stop codon of the CDS,

were selected for PCR primer design. Using total RNA extracted from adult Sprague-Dawley rat brain tissue, RT-PCR was performed, and the 1.5Kb amplicon cloned into pGem T Easy PCR cloning vector (Promega, Southampton, UK). Two clones were subsequently submitted for automated fluorescent-dye sequencing, both of which were identical (Fig. 6.2).

The cloned sequence was compared by BLAST with the draft rat genomic *omgp* CDS (Fig. 6.3). A single nucleotide mismatch was detected at position 713 (T→C), in addition to the obvious sequencing errors in the draft rat genomic *omgp* CDS. However, alignment of the sequencing results with the mouse and human full-length *omgp* cDNA sequences revealed that, in these sequences, the base at position 713 was also T (not shown). It was, therefore, assumed that the mismatch was most likely to be due to a sequencing error in the draft rat genome database, and not a genuine point-mutation arising from RT-PCR. The cloned rat *omgp* CDS was deposited in Genbank (Accession number AY316298). Recently, an updated build of the rat genome has been made publicly available, and the replacement genomic contig (Accession Number NW_47336.1), which spans the *omgp* gene, shares 100% sequence identity with the cloned rat CDS that was submitted to Genbank as part of this study (Fig. 6.4).

At the level of the nucleotide sequence, the rat *omgp* CDS is 95% homologous to that of mouse, and 90% homologous to that of human. The same percentage homologies apply at the level of the amino acid sequence for OMgp (Fig. 6.5).

omgp mRNA Expression in the Intact Adult Rodent Nervous System

By radioactive *in situ* hybridisation, it was grossly apparent from the radiographic film that *omgp* was strongly expressed in the neocortex, pyriform cortex, hippocampal formation, habenular nucleus, some brainstem nuclei, spinal cord grey matter and dorsal root ganglia (DRG) (Fig. 6.6.A-F). Moderate signal was also observed in the cerebellar cortex (Fig. 6.6.D). Unfortunately, due to a technical problem, silver granule precipitation was not achieved and the cellular expression could not be examined microscopically.

However, using a DIG-labelled antisense riboprobe to *omgp*, it was found that both neurons and glia expressed *omgp* transcripts in the neocortex. However, expression of the transcript by large pyramidal projection neurons was less prominent than in smaller neurons throughout the full thickness of the cortex (Fig. 6.7.A). The overall level of expression of *omgp* by neocortical neurons appeared weaker and less extensive relative to *nogo-a*, *nogo-66* and *ngr* (Fig. 6.7.B-D), but many smaller putative glial cells appeared to express the transcripts at low to moderate levels throughout the cortex. Additionally, weak to moderate signal for *omgp* was detected in the glial cells of the subcortical white matter. In the neostriatum, *omgp* mRNA was detectable in both neurons and glia, but much more weakly than in neocortex (not shown). In the hippocampal formation, strong signal for *omgp* was observed in the CA1-CA4 pyramidal neurons, and the granule neurons of the dentate gyrus (Fig. 6.8.A). In the cerebellar cortex, Purkinje cells were the only class of neuron to strongly express *omgp*, but very weak signal was also observed in the granule cell layer (Figs. 6.8.B and C). Strong expression was also observed in neurons of the vestibular nuclei (Fig. 6.8.B). Weak expression of *omgp* by glia was also observed throughout the cerebellar white matter.

In the spinal cord, *omgp* was strongly expressed by neurons in both the dorsal and ventral horns (Fig. 6.8.D). Only very weak signal was detectable in glial cells of the spinal white matter. Moderate to strong expression was observed in different subpopulations of dorsal root ganglia (DRG) neurons (Fig. 6.8.E). The same was true of the postganglionic sympathetic neurons of the superior cervical ganglion (SCG) (Fig. 6.8.F). Intact sciatic nerve did not appear to express *omgp* (not shown).

Autologous Peripheral Nerve Graft in Thalamus

No obvious regulation of *omgp* expression was observed 16d post implantation of autologous tibial nerve graft to thalamus, except in one of three animals. In this rat, the ventral blade of the dentate gyrus, ipsilateral to the graft, was no longer found to express *omgp* (Fig. 6.9). No other differences were noted.

DISCUSSION

In Situ Hybridisation for *omgp* mRNA in the Intact Adult Rodent Nervous System

In the present study, *in situ* hybridisation was performed to map *omgp* mRNA expression in the intact adult rodent nervous system, using both DIG-labelled riboprobes and ^{35}S-labelled DNA oligonucleotides. It was confirmed that expression of *omgp* mRNA is predominantly neuronal (Habib et al., 1998b). Expression was generally higher in the spinal cord than brain, with the strongest expression being detected in neurons of the spinal grey matter. On the whole, *omgp* mRNA did not appear to be regulated after CNS injury, although this was only assessed using DIG-labelled riboprobes.

Exposure to film of slides hybridized with ^{35}S-labelled DNA oligonucleotides revealed a pattern of *omgp* expression which was grossly consistent with that obtained using DIG-labelled riboprobes. However, owing to a technical problem with the process of silver granule precipitation, it was not possible to determine the precise cellular expression of *omgp* transcripts using radioactive *in situ* hybridisation on this occasion. The relatively long exposure to film and alkaline-phosphatase development times required with the radioactive and DIG approaches, respectively, would seem to indicate that the mRNA is likely to be relatively lowly expressed throughout the adult rodent nervous system compared to other species of mRNA.

The findings presented herein were broadly consistent with those of a previous study of *omgp* expression, by Habib *et al.* (1998b) who performed *in situ* hybridization (ISH) using radio-labelled riboprobes. That is to say that the more prominent transcript expression was detected in pyramidal neocortical neurons, neurons of pyriform cortex, pyramidal neurons of the hippocampus, cerebellar Purkinje cells, brainstem nuclei, and spinal cord grey matter, as was reported by Habib *et al.* (1998b). However, in this study, *omgp* expression in the hypothalamic nuclei could only be described as moderate at best. In addition to the tissues examined by Habib *et al.* (1998b), DRG and SCG were also examined. Neurons within these ganglia were found to express *omgp* at moderate to strong levels, which presumably reflected different subpopulation expression profiles. Furthermore, intact sciatic nerve was not found to express the mRNA.

omgp mRNA Expression Following Grafting of Peripheral Nerve to Thalamus

No regulation of *omgp* expression could be detected in CNS neurons following the grafting of an autologous segment of tibial nerve to thalamus, except in one animal. In this rat, 16dpo, signal for *omgp* was absent from the ventral blade of the dentate gyrus. This was not found in the other two rats, also 16dpo, which may be suggestive of some experimental anomaly.

OMgp Protein Expression in the Nervous System

Unfortunately, the absence of a commercially available anti-OMgp antibody meant that immunohistochemistry could not be performed as part of this study. However, Habib *et al.* (1998b) have performed immunohistochemistry with an affinity-purified polyclonal anti-OMgp antibody, which revealed strong staining of the plasma membrane of Purkinje cell bodies and of the dendrites projecting into the molecular layer. No staining of the cerebellar granule cells was observed, although immunoreactive Purkinje cell axons were detected in the granule cell layer and underlying white matter. The perikarya of hippocampal pyramidal cells were strongly immunoreactive for OMgp, as were corticotectal tract fibres. Some hypothalamic nuclei expressed OMgp protein. Widespread immunoreactivity was found in the neocortex, with the strongest labelling in layer V. Since these results were at odds with their previous finding using a less specific polyclonal antibody (Mikol and Stefansson, 1988), that there was strong OMgp immunoreactivity in white matter, Habib *et al.* (1998b) sought to verify the expression of OMgp in oligodendrocytes. They demonstrated OMgp protein was expressed by primary cultures of mouse oligodendrocytes but concluded, on the basis of their comprehensive immunohistochemical and complementary ISH studies, that expression of OMgp is predominantly neuronal within the murine CNS.

Neuronal Expression of OMgp

The available evidence thus suggests that OMgp is principally a neuronal protein with a limited amount of OMgp being expressed by oligodendrocytes. The functions of neuronal OMgp have not been explored. As with neuronal Nogo, the possibility that these ligands interact with neuronal NgR in *cis* (i.e. at the surface of the same cell)

remains open but, considering that OMgp over-expression in NIH3T3 cells suppresses mitogenic signalling (Habib et al., 1998a), it is hard to imagine that OMgp does not participate in some regulatory signalling mechanism in neurons.

Summary

The predominantly neuronal expression of *omgp* does not preclude a role for the protein as a myelin-associated inhibitor of axonal regeneration, since putative oligodendrocytes were also found to express *omgp*, albeit weakly, throughout the CNS white matter. However, this function of OMgp has only been demonstrated *in vitro* and, based on the expression profile, it is unlikely to constitute the sole function of the protein. Another as yet undetermined role for OMgp, possibly in neuron-neuron signalling, cannot be excluded. Unfortunately, an *omgp* null mutant mouse has not yet been reported. Such an animal would be expected to yield some important information regarding the likely function of OMgp. However, it has been found by quantitative PCR of postnatal rat brain (Vourc'h et al., 2003a), and also by both northern and western blot of postnatal mouse brain (Habib et al., 1998b), that *omgp* expression is developmentally regulated and peaks during the late stages of myelination. Furthermore, it has been reported that primary cultures of oligodendrocytes exhibit a similar pattern of *omgp* expression, prompting the authors to suggest that OMgp may have roles *in vivo* in the arrest of oligodendrocyte proliferation, the arrest of myelination or the compaction of myelin (Vourc'h et al., 2003a). The same group has also detected a coding single nucleotide polymorphism in the human *omgp* gene (OMGP62), which apparently impairs the transport of the protein to the cell membrane. This polymorphism was reported to be present in both autistic and control populations, but was associated with a lower developmental quotient in the autistic subjects (Vourc'h et al., 2003b). Intriguingly, this may be linked to the finding that the *ngr* null mutant mice have impaired learning skills (Kim et al., 2003a).

CONCLUSION

The predominantly neuronal expression of *omgp* mRNA in the adult rodent nervous system raises important questions about the role of OMgp *in vivo*. This has been

somewhat overlooked in its recent description as a myelin-associated inhibitor of axon regeneration (Wang et al., 2002b). Whilst it is possible that oligodendrocyte OMgp does modify axon growth and regeneration through the NgR/p75^{NTR}/LINGO-1 receptor complex *in vivo*, it seems unlikely that this is its main physiological role. Indeed, OMgp-NgR signalling in a neuron-neuron model is also plausible. Ultimately, however, further consideration should be given to the evidence suggesting that OMgp is capable of acting as a receptor in its own right.

N.B. Part of the work report in this chapter was carried out in collaboration with an MSc student, J. Mills, working under my supervision. In particular, Ms Mills prepared and reacted the sections shown in Figs. 6.8.D-F. She also assisted with the cloning of the rat *omgp* CDS.

Figure 6.1.

Alignment of the mouse *omgp* cDNA sequence against the draft rat genome. Using genomic BLAST, available via the NCBI website, the full-length mouse *omgp* cDNA sequence (Genbank Accession No. BC024757) was used to identify the corresponding *omgp* sequence within the draft rat genome (on contig NW_042664). Numerous single base mismatches were apparent, many of which were expected to be evolutionary. There was a frame-shift of one nucleotide in the draft rat genomic sequence, which disrupted the ORF and was expected to be due to a sequencing error.

```
>ref|NW_042664.1|Rn10_210 Rattus norvegicus chromosome 10 WGS supercontig
          Length = 1962622

 Score = 2769 bits (1440), Expect = 0.0
 Identities = 1613/1697 (95%), Gaps = 11/1697 (0%)
 Strand = Plus / Minus


Query: 73      ggctttgatggaatatcagatactgaaaatgtcttcctgcctgttcatccttctgtttct 132
                |||||||||||||||||||||| ||||||||||||||||||||||||||||||||||||
Sbjct: 1490171 ggctttgatggaatatcagatattgaaaatgtcttcctgcctgttcatccttctgtttct 1490112

Query: 133     cacgcctggcatcttatgcatttgtcctctccagtgtacatgcacagagaggcacaggca 192
                |||||||||||| |||||||||||||||||||| |||| ||||||||||||||||||||
Sbjct: 1490111 cacgcctggcattttatgcatttgtcctctccaatgtatatgcacagagaggcacaggca 1490052

Query: 193     tgtggactgttcaggcagaaacttgactacattaccacctggactgcaggagaacattat 252
                |||||||||||||||||||| |||||||||||||||||||||||| |||||| ||||
Sbjct: 1490051 tgtggactgttcaggcagaaacctgactacattaccacctggactgcaagagaac-ttat 1489993

Query: 253     acatttaaacctgtcttataaccactttactgatctgcataaccagttaaccccatatac 312
                |||||||||||||||||||||||||||||||||||||||||||||||||||| |||||
Sbjct: 1489992 acatttaaacctgtcttataaccactttactgatctgcataaccagttaacccttatac 1489933

Query: 313     caatctgagaaccctggatatttcaaacaacaggcttgaaagtctgcctgctcagttacc 372
                ||||||||| ||||||||||||||||||||||||||||||||||||| ||||||||
Sbjct: 1489932 caatctgaggaccctggatatttcaaacaacaggcttgaaagtctgcctgcccagttacc 1489873

Query: 373     tcggtctctctggaacatgtctgctgctaacaacaatattaaacttcttgacaaatctga 432
                |||||||||||||||||||||||||||||||||| |||||||| ||||||||||||||
Sbjct: 1489872 tcggtctctctggaacatgtctgctgctaacaacaacattaaactacttgacaaatctga 1489813

Query: 433     tactgcttatcagtggaaccttaaatacctggatgtttctaagaatatgctggaaaaggt 492
                |||||||||||||||||||||||||||||||||||||||||||||||||| ||||||||||
Sbjct: 1489812 tactgcttatcagtggaaccttaaatacctggatgtttctaagaatatgttggaaaaggt 1489753

Query: 493     tgttctcattaaaaataccctaagaagtctcgaggttcttaacctcagcagtaacaagct 552
                |||||||||||||||||| |||||||||| |||||||||||||||||||||||| || ||
Sbjct: 1489752 tgttctcattaaaaataccttaagaagtcttgaggttcttaacctcagcagtaataaact 1489693

Query: 553     ttggacagttccaaccaacatgccttccaaactgcatatcgtgg-acctgtctaataact 611
                |||||||||||||||||||||||||||||||| ||||| |||| ||||||||||||||
Sbjct: 1489692 ttggacagttccaaccaacatgccttccaaactacatattgtggnacctgtctaataact 1489633

Query: 612     cactgac-acaaatccttccagggacattaataaacctgacaaatctcacacatctttac 670
                ||||||  ||||||||||||||||||||||||||||||||||||||||||||||||||||
Sbjct: 1489632 cactgancacaaatccttccagggacattaataaacctgacaaatctcacacatctttac 1489573

Query: 671     ctgcacaacaataaattcacattcattccagaacagtcttttgaccaacttttgcagttg 730
                |||||||||||||||||||||||||||||| |||||||||||||||| |||||||||
Sbjct: 1489572 ctgcacaacaataaattcacattcattccagatcagtcttttgaccaactcttgcagttg 1489513

Query: 731     caagagataactcttcataataacaggtggtcatgtgaccataaacaaaacattacttac 790
                |||||||||||||||||||||||||||||||||||||||||||| ||||||||||||||||
Sbjct: 1489512 caagagataactcttcataataacaggtggtcatgtgaccatacacaaaacattacttac 1489453

Query: 791     ttattgaagtgggtgatggaaacgaaagcccatgtgatagggactccttgttctaagcaa 850
                | | |||||||| |||||||||| |||||||||||||||||| ||||||||||||||||
Sbjct: 1489452 tcactgaagtggatgatggaaacaaaagcccatgtgatagggattccttgttctaagcaa 1489393

Query: 851     gtatcctctctaaaggaacagagcatgtaccccacacctcctgggtttacctcaagctta 910
                |||||||||| |||||||||||||||||||||| ||||| || ||||| |||||||||
Sbjct: 1489392 gtatcctctctgaaggaacagagcatgtaccccacgcctcccggatttacttcaagctta 1489333

Query: 911     tttactatgagtgagatgcagacagtggacaccattaactctttgagtatggtaactcaa 970
                |||||||||||||||||||||||||||||||||||||||||| ||||||||||||||||
Sbjct: 1489332 tttactatgagtgagatgcagacagtggacaccattaactctctgagtatggtaactcaa 1489273

Query: 971     cccaaagtgaccaaaacacccaaacaatatcgaggaaaggaaaccacatttggtgtcact 1030
                || |||||||||| | |||||||||||||||||||| || ||||||||||||||||
Sbjct: 1489272 cctaaagtgaccaatatacccaaacaatatcgaggaaaagacaccacatttggtgtcacc 1489213
```

```
Query: 1031    ctaagcaaagataccacttttagtagcactgatagggctgtggtggcctacccagaagac 1090
               |||||||||| |||||||||||||||||||||||||| ||| | ||||||||||||||
Sbjct: 1489212 ctaagcaaagacaccacttttagtagcactgatagggctctggagccctacccagaagac 1489153

Query: 1091    acacccacagaaatgaccaattcccatgaagcagcagctgcaactctaactattcacctc 1150
               |||||||||||||||||| ||| | ||||||||||||||||||||||||||||||||
Sbjct: 1489152 acacccacagaaatgaccagttcacgtgaagcagcagctgcaactctaactattcacctc 1489093

Query: 1151    caggatggaatgagttcaaatgcaagcctcaccagtgcaacaaagtcac-ccccaagccc 1209
               |||||||||||||||||||||||||||||||||||||||| |||| || | ||||| || |
Sbjct: 1489092 caggatggaatgagttcaaatgcaagcctcaccagtgcagcaaaatc-ctcccca-gcac 1489035

Query: 1210    c-gtgaccctcagcatagctcgtggcatgccaaataacttctctgaaatgcctcgacaaa 1268
               | |||||||||||||| || |||||||||||||||| |||||||||||||||| ||| |
Sbjct: 1489034 ctgtgaccctcagcataactagtggcatgccaaataatttctctgaaatgcctcaacaga 1488975

Query: 1269    gcacaaccctcaacttacggagggaagaaaccactgcaaatggaaacactcggccacctt 1328
               |||||||||| |||||||||||||||||||| |||||||||| ||| |||| ||||||||
Sbjct: 1488974 gcacaacccttaacttacggagggaagaaacaactgcaaatgtaaagactcagccacctt 1488915

Query: 1329    c-tgcggctagtgcttggaaagtaaatgcctcgctccttttaatgctcaatgctgtggtc 1387
               | | |||||||||||||||||||||||||||| |||||||||||||||||||||||||||
Sbjct: 1488914 cct-cggctagtgcttggaaagtaaatgcctcactccttttaatgctcaatgctgtggtc 1488856

Query: 1388    atgctggcaggctgagggtctgcagtttctgaaacgaaggagaaccttcctccatgatgt 1447
               |||||||||||||||||||||||||||||||||| |||||||||||||||| ||||||
Sbjct: 1488855 atgctggcaggctgagggtctgcagtttctgaaatgaaggagaaccttcctccctgatgt 1488796

Query: 1448    acagttgggaaaac-gtgcccctatctaaccagtgattcaagctatattatgtattcaag 1506
               |||||||||||||  | |||| |||||||||||||||||||||||| ||||||||||||
Sbjct: 1488795 acagttgggaaaatag-gcccttatctaaccagtgattcaagctatactatgtattcaag 1488737

Query: 1507    aaagccagtcttatatttctgactttgatgtaaatgaagtaatttgtcttaattaaaaga 1566
               ||||||||| || |||||||||||||||||||||||||| ||||||||||||||||
Sbjct: 1488736 aaagccagtattgtatttctgactttgatgtaaatgaagtaacttgtcttaattaaaaga 1488677

Query: 1567    agtgcacaatgtcttggtacttgctgctattttcctgtcttaagtaaaactaatgacttt 1626
               ||||||||||||||||||||||||||||||||||||||||||||||||||||||||||||
Sbjct: 1488676 agtgcacaatgtcttggtacttgctgctattttcctgtcttaagtaaaactaatgacttt 1488617

Query: 1627    ttttttttaatgaaatgttttctttttaaggcttcaacttattgcacaaactataaagagc 1686
               |||||| |||||||||||| |||||||||||||||||| |||||||| ||||||||||
Sbjct: 1488616 ttttttaaatgaaatgtttccttttttaaggcttcaacttactgcacaaagtataaagagc 1488557

Query: 1687    atctaaactttaatatgtattttatgtatgtttacactgtcaaatgtctgggacaaaata 1746
               |||||||||||||||||||||||||||||||||||| |||||||||||||||||||||||
Sbjct: 1488556 atctaaactttaatatgtattttatgtatgtttacattgtcaaatgtctgggacaaaata 1488497

Query: 1747    aaaggcctatgctcctg 1763
               |||||||||||||||||
Sbjct: 1488496 aaaggcctatgctcctg 1488480
```

Figure 6.2.

The cloned rat *omgp* CDS. The start and stop codons of the 1323bp rat *omgp* CDS are shown in bold type (ATG and TGA, respectively). The sequence selected as an *in situ* hybridisation target for a ^{35}S-labelled 45-mer antisense DNA oligonucleotide is highlighted in yellow.

Rat *omgp* CDS (Genbank Accession No. AY316298)

```
   1 ATGGAATATC AGATATTGAA AATGTCTTCC TGCCTGTTCA TCCTTCTGTT TCTCACGCCT
  61 GGCATTTTAT GCATTTGTCC TCTCCAATGT ATATGCACAG AGAGGCACAG GCATGTGGAC
 121 TGTTCAGGCA GAAACCTGAC TACATTACCA CCTGGACTGC AAGAGAACAT TATACATTTA
 181 AACCTGTCTT ATAACCACTT TACTGATCTG CATAACCAGT TAACCCCTTA TACCAATCTG
 241 AGGACCCTGG ATATTTCAAA CAACAGGCTT GAAAGTCTGC CTGCCCAGTT ACCTCGGTCT
 301 CTCTGGAACA TGTCTGCTGC TAACAACAAC ATTAAACTAC TTGACAAATC TGATACTGCT
 361 TATCAGTGGA ACCTTAAATA CCTGGATGTT TCTAAGAATA TGTTGGAAAA GGTTGTTCTC
 421 ATTAAAAATA CCTTAAGAAG TCTTGAGGTT CTTAACCTCA GCAGTAATAA ACTTTGGACA
 481 GTTCCAACCA ACATGCCTTC CAAACTACAT ATTGTGGACC TGTCTAATAA CTCACTGACA
 541 CAAATCCTTC CAGGGACATT AATAAACCTG ACAAATCTCA CACATCTTTA CCTGCACAAC
 601 AATAAATTCA CATTCATTCC AGATCAGTCT TTTGACCAAC TCTTGCAGTT GCAAGAGATA
 661 ACTCTTCATA ATAACAGGTG GTCATGTGAC CATACACAAA ACATTACTTA CTTACTGAAG
 721 TGGATGATGG AAACAAAAGC CCATGTGATA GGGATTCCTT GTTCTAAGCA AGTATCCTCT
 781 CTGAAGGAAC AGAGCATGTA CCCCACGCCT CCCGGATTTA CTTCAAGCTT ATTTACTATG
 841 AGTGAGATGC AGACAGTGGA CACCATTAAC TCTCTGAGTA TGGTAACTCA ACCTAAAGTG
 901 ACCAATATAC CCAAACAATA TCGAGGAAAA GACACCACAT TTGGTGTCAC CCTAAGCAAA
 961 GACACCACTT TTAGTAGCAC TGATAGGGCT CTGGAGCCCT ACCCAGAAGA CACACCCACA
1021 GAAATGACCA GTTCACGTGA AGCAGCAGCT GCAACTCTAA CTATTCACCT CCAGGATGGA
1081 ATGAGTTCAA ATGCAAGCCT CACCAGTGCA GCAAAATCCT CCCCAGCACC TGTGACCCTC
1141 AGCATAACTA GTGGCATGCC AAATAATTTC TCTGAAATGC CTCAACAGAG CACAACCCTT
1201 AACTTACGGA GGGAAGAAAC AACTGCAAAT GTAAAGACTC AGCCACCTTC CTCGGCTAGT
1261 GCTTGGAAAG TAAATGCCTC ACTCCTTTTA ATGCTCAATG CTGTGGTCAT GCTGGCAGGC
1321 TGA
```

Figure 6.3.

Alignment of the cloned rat *omgp* CDS against the draft rat genome. The frame-shift sequencing error in the *omgp* CDS of the draft rat genomic contig, NW_042664, is highlighted in yellow (corresponding to position 169 of the cloned rat *omgp* CDS), as are two other obvious sequencing errors. Only one unpredictable mismatch, highlighted in red (corresponding to position 713 of the cloned CDS), was ultimately found between the cloned and draft genomic sequences. Potentially, this could have been due to either a sequencing error in the draft rat genome, or a PCR generated point mutation in the cloned sequence.

```
>ref|NW_042664.1|Rn10_210 Rattus norvegicus chromosome 10 WGS supercontig
          Length = 1962622

 Score = 2496 bits (1298), Expect = 0.0
 Identities = 1321/1325 (99%), Gaps = 3/1325 (0%)
 Strand = Plus / Plus


Query: 1       atggaatatcagatattgaaaatgtcttcctgcctgttcatccttctgtttctcacgcct 60
                ||||||||||||||||||||||||||||||||||||||||||||||||||||||||||||
Sbjct: 1490164 atggaatatcagatattgaaaatgtcttcctgcctgttcatccttctgtttctcacgcct 1490105

Query: 61      ggcattttatgcatttgtcctctccaatgtatatgcacagagaggcacaggcatgtggac 120
                ||||||||||||||||||||||||||||||||||||||||||||||||||||||||||||
Sbjct: 1490104 ggcattttatgcatttgtcctctccaatgtatatgcacagagaggcacaggcatgtggac 1490045

Query: 121     tgttcaggcagaaacctgactacattaccacctggactgcaagagaacattatacattta 180
                |||||||||||||||||||||||||||||||||||||||||||| ||||||||||||
Sbjct: 1490044 tgttcaggcagaaacctgactacattaccacctggactgcaagagaac-ttatacattta 1489986

Query: 181     aacctgtcttataaccactttactgatctgcataaccagttaacccctataccaatctg 240
                ||||||||||||||||||||||||||||||||||||||||||||||||||||||||||||
Sbjct: 1489985 aacctgtcttataaccactttactgatctgcataaccagttaacccctataccaatctg 1489926

Query: 241     aggaccctggatatttcaaacaacaggcttgaaagtctgcctgcccagttacctcggtct 300
                ||||||||||||||||||||||||||||||||||||||||||||||||||||||||||||
Sbjct: 1489925 aggaccctggatatttcaaacaacaggcttgaaagtctgcctgcccagttacctcggtct 1489866

Query: 301     ctctggaacatgtctgctgctaacaacaacattaaactacttgacaaatctgatactgct 360
                ||||||||||||||||||||||||||||||||||||||||||||||||||||||||||||
Sbjct: 1489865 ctctggaacatgtctgctgctaacaacaacattaaactacttgacaaatctgatactgct 1489806

Query: 361     tatcagtggaaccttaaatacctggatgtttctaagaatatgttggaaaaggttgttctc 420
                ||||||||||||||||||||||||||||||||||||||||||||||||||||||||||||
Sbjct: 1489805 tatcagtggaaccttaaatacctggatgtttctaagaatatgttggaaaaggttgttctc 1489746

Query: 421     attaaaaataccttaagaagtcttgaggttcttaacctcagcagtaataaactttggaca 480
                ||||||||||||||||||||||||||||||||||||||||||||||||||||||||||||
Sbjct: 1489745 attaaaaataccttaagaagtcttgaggttcttaacctcagcagtaataaactttggaca 1489686

Query: 481     gttccaaccaacatgccttccaaactacatattgtgg-acctgtctaataactcactga- 538
                |||||||||||||||||||||||||||||||||| ||||||||||||||||||||| |
Sbjct: 1489685 gttccaaccaacatgccttccaaactacatattgtggnacctgtctaataactcactgan 1489626

Query: 539     cacaaatccttccagggacattaataaacctgacaaatctcacacatctttacctgcaca 598
                ||||||||||||||||||||||||||||||||||||||||||||||||||||||||||||
Sbjct: 1489625 cacaaatccttccagggacattaataaacctgacaaatctcacacatctttacctgcaca 1489566

Query: 599     acaataaattcacattcattccagatcagtcttttgaccaactcttgcagttgcaagaga 658
                ||||||||||||||||||||||||||||||||||||||||||||||||||||||||||||
Sbjct: 1489585 acaataaattcacattcattccagatcagtcttttgaccaactcttgcagttgcaagaga 1489506

Query: 659     taactcttcataataacaggtggtcatgtgaccatacacaaaacattacttacttactga 718
                |||||||||||||||||||||||||||||||||||||||||||||||||| ||||| |
Sbjct: 1489525 taactcttcataataacaggtggtcatgtgaccatacacaaaacattacttact-actga 1489446

Query: 719     agtggatgatggaaacaaaagcccatgtgatagggattccttgttctaagcaagtatcct 778
                ||||||||||||||||||||||||||||||||||||||||||||||||||||||||||||
Sbjct: 1489465 agtggatgatggaaacaaaagcccatgtgatagggattccttgttctaagcaagtatcct 1489386

Query: 779     ctctgaaggaacagagcatgtaccccacgcctcccggatttacttcaagcttatttacta 838
                ||||||||||||||||||||||||||||||||||||||||||||||||||||||||||||
Sbjct: 1489385 ctctgaaggaacagagcatgtaccccacgcctcccggatttacttcaagcttatttacta 1489326

Query: 839     tgagtgagatgcagacagtggacaccattaactctctgagtatggtaactcaacctaaag 898
                ||||||||||||||||||||||||||||||||||||||||||||||||||||||||||||
Sbjct: 1489325 tgagtgagatgcagacagtggacaccattaactctctgagtatggtaactcaacctaaag 1489266

Query: 899     tgaccaatatacccaaacaatatcgaggaaaagacaccacatttggtgtcaccctaagca 958
                ||||||||||||||||||||||||||||||||||||||||||||||||||||||||||||
Sbjct: 1489265 tgaccaatatacccaaacaatatcgaggaaaagacaccacatttggtgtcaccctaagca 1489206
```

```
Query: 959     aagacaccacttttagtagcactgatagggctctggagccctacccagaagacacaccca 1018
               ||||||||||||||||||||||||||||||||||||||||||||||||||||||||||||
Sbjct: 1489205 aagacaccacttttagtagcactgatagggctctggagccctacccagaagacacaccca 1489146

Query: 1019    cagaaatgaccagttcacgtgaagcagcagctgcaactctaactattcacctccaggatg 1078
               ||||||||||||||||||||||||||||||||||||||||||||||||||||||||||||
Sbjct: 1489145 cagaaatgaccagttcacgtgaagcagcagctgcaactctaactattcacctccaggatg 1489086

Query: 1079    gaatgagttcaaatgcaagcctcaccagtgcagcaaaatcctccccagcacctgtgaccc 1138
               ||||||||||||||||||||||||||||||||||||||||||||||||||||||||||||
Sbjct: 1489085 gaatgagttcaaatgcaagcctcaccagtgcagcaaaatcctccccagcacctgtgaccc 1489026

Query: 1139    tcagcataactagtggcatgccaaataatttctctgaaatgcctcaacagagcacaaccc 1198
               ||||||||||||||||||||||||||||||||||||||||||||||||||||||||||||
Sbjct: 1489025 tcagcataactagtggcatgccaaataatttctctgaaatgcctcaacagagcacaaccc 1488966

Query: 1199    ttaacttacggagggaagaaacaactgcaaatgtaaagactcagccaccttcctcggcta 1258
               ||||||||||||||||||||||||||||||||||||||||||||||||||||||||||||
Sbjct: 1488965 ttaacttacggagggaagaaacaactgcaaatgtaaagactcagccaccttcctcggcta 1488906

Query: 1259    gtgcttggaaagtaaatgcctcactccttttaatgctcaatgctgtggtcatgctggcag 1318
               ||||||||||||||||||||||||||||||||||||||||||||||||||||||||||||
Sbjct: 1488605 gtgcttggaaagtaaatgcctcactccttttaatgctcaatgctgtggtcatgctggcag 1488846

Query: 1319    gctga 1323
               |||||
Sbjct: 1488545 gctga 1488841
```

Figure 6.4.

Alignment of the cloned rat *omgp* CDS against the latest build of the rat genome. The cloned *omgp* CDS is identical to that contained on contig NW_047336, which was released as part of the latest build of the rat genome. This confirms that the mismatch observed between position 713 (T) of the cloned CDS and the corresponding nucleotide (C) in the draft rat genomic contig, NW_042664, was the result of a genomic sequencing error.

```
>ref|NW_047336.1|Rn10_1856 Rattus norvegicus chromosome 10 WGS supercontig
          Length = 24143058

 Score = 2544 bits (1323), Expect = 0.0
 Identities = 1323/1323 (100%)
 Strand = Plus / Minus


Query: 1       atggaatatcagatattgaaaatgtcttcctgcctgttcatccttctgtttctcacgcct 60
                ||||||||||||||||||||||||||||||||||||||||||||||||||||||||||||
Sbjct: 6689639 atggaatatcagatattgaaaatgtcttcctgcctgttcatccttctgtttctcacgcct 6689580

Query: 61      ggcattttatgcatttgtcctctccaatgtatatgcacagagaggcacaggcatgtggac 120
                ||||||||||||||||||||||||||||||||||||||||||||||||||||||||||||
Sbjct: 6689579 ggcattttatgcatttgtcctctccaatgtatatgcacagagaggcacaggcatgtggac 6689520

Query: 121     tgttcaggcagaaacctgactacattaccacctggactgcaagagaacattatacattta 180
                ||||||||||||||||||||||||||||||||||||||||||||||||||||||||||||
Sbjct: 6689519 tgttcaggcagaaacctgactacattaccacctggactgcaagagaacattatacattta 6689460

Query: 181     aacctgtcttataaccactttactgatctgcataaccagttaacccctataccaatctg 240
                ||||||||||||||||||||||||||||||||||||||||||||||||||||||||||||
Sbjct: 6689459 aacctgtcttataaccactttactgatctgcataaccagttaacccctataccaatctg 6689400

Query: 241     aggaccctggatatttcaaacaacaggcttgaaagtctgcctgcccagttacctcggtct 300
                ||||||||||||||||||||||||||||||||||||||||||||||||||||||||||||
Sbjct: 6689399 aggaccctggatatttcaaacaacaggcttgaaagtctgcctgcccagttacctcggtct 6689340

Query: 301     ctctggaacatgtctgctgctaacaacaacattaaactacttgacaaatctgatactgct 360
                ||||||||||||||||||||||||||||||||||||||||||||||||||||||||||||
Sbjct: 6689339 ctctggaacatgtctgctgctaacaacaacattaaactacttgacaaatctgatactgct 6689280

Query: 361     tatcagtggaaccttaaatacctggatgtttctaagaatatgttggaaaaggttgttctc 420
                ||||||||||||||||||||||||||||||||||||||||||||||||||||||||||||
Sbjct: 6689279 tatcagtggaaccttaaatacctggatgtttctaagaatatgttggaaaaggttgttctc 6689220

Query: 421     attaaaaataccttaagaagtcttgaggttcttaacctcagcagtaataaactttggaca 480
                ||||||||||||||||||||||||||||||||||||||||||||||||||||||||||||
Sbjct: 6689219 attaaaaataccttaagaagtcttgaggttcttaacctcagcagtaataaactttggaca 6689160

Query: 481     gttccaaccaacatgccttccaaactacatattgtggacctgtctaataactcactgaca 540
                ||||||||||||||||||||||||||||||||||||||||||||||||||||||||||||
Sbjct: 6689159 gttccaaccaacatgccttccaaactacatattgtggacctgtctaataactcactgaca 6689100

Query: 541     caaatccttccagggacattaataaacctgacaaatctcacacatctttacctgcacaac 600
                ||||||||||||||||||||||||||||||||||||||||||||||||||||||||||||
Sbjct: 6689099 caaatccttccagggacattaataaacctgacaaatctcacacatctttacctgcacaac 6689040

Query: 601     aataaattcacattcattccagatcagtcttttgaccaactcttgcagttgcaagagata 660
                ||||||||||||||||||||||||||||||||||||||||||||||||||||||||||||
Sbjct: 6689039 aataaattcacattcattccagatcagtcttttgaccaactcttgcagttgcaagagata 6688980

Query: 661     actcttcataataacaggtggtcatgtgaccatacacaaaacattacttacttactgaag 720
                ||||||||||||||||||||||||||||||||||||||||||||||||||||||||||||
Sbjct: 6688979 actcttcataataacaggtggtcatgtgaccatacacaaaacattacttacttactgaag 6688920

Query: 721     tggatgatggaaacaaaagcccatgtgatagggattccttgttctaagcaagtatcctct 780
                ||||||||||||||||||||||||||||||||||||||||||||||||||||||||||||
Sbjct: 6688919 tggatgatggaaacaaaagcccatgtgatagggattccttgttctaagcaagtatcctct 6688860

Query: 781     ctgaaggaacagagcatgtaccccacgcctcccggatttacttcaagcttatttactatg 840
                ||||||||||||||||||||||||||||||||||||||||||||||||||||||||||||
Sbjct: 6688859 ctgaaggaacagagcatgtaccccacgcctcccggatttacttcaagcttatttactatg 6688800

Query: 841     agtgagatgcagacagtggacaccattaactctctgagtatggtaactcaacctaaagtg 900
                ||||||||||||||||||||||||||||||||||||||||||||||||||||||||||||
Sbjct: 6688799 agtgagatgcagacagtggacaccattaactctctgagtatggtaactcaacctaaagtg 6688740

Query: 901     accaatatacccaaacaatatcgaggaaaagacaccacatttggtgtcaccctaagcaaa 960
                ||||||||||||||||||||||||||||||||||||||||||||||||||||||||||||
Sbjct: 6688739 accaatatacccaaacaatatcgaggaaaagacaccacatttggtgtcaccctaagcaaa 6688680
```

```
Query: 961     gacaccacttttagtagcactgatagggctctggagccctacccagaagacacacccaca 1020
               ||||||||||||||||||||||||||||||||||||||||||||||||||||||||||||
Sbjct: 6688679 gacaccacttttagtagcactgatagggctctggagccctacccagaagacacacccaca 6688620

Query: 1021    gaaatgaccagttcacgtgaagcagcagctgcaactctaactattcacctccaggatgga 1080
               ||||||||||||||||||||||||||||||||||||||||||||||||||||||||||||
Sbjct: 6688619 gaaatgaccagttcacgtgaagcagcagctgcaactctaactattcacctccaggatgga 6688560

Query: 1081    atgagttcaaatgcaagcctcaccagtgcagcaaaatcctccccagcacctgtgaccctc 1140
               ||||||||||||||||||||||||||||||||||||||||||||||||||||||||||||
Sbjct: 6688559 atgagttcaaatgcaagcctcaccagtgcagcaaaatcctccccagcacctgtgaccctc 6688500

Query: 1141    agcataactagtggcatgccaaataatttctctgaaatgcctcaacagagcacaacccctt 1200
               ||||||||||||||||||||||||||||||||||||||||||||||||||||||||||||
Sbjct: 6688499 agcataactagtggcatgccaaataatttctctgaaatgcctcaacagagcacaacccctt 6688440

Query: 1201    aacttacggagggaagaaacaactgcaaatgtaaagactcagccaccttcctcggctagt 1260
               ||||||||||||||||||||||||||||||||||||||||||||||||||||||||||||
Sbjct: 6688439 aacttacggagggaagaaacaactgcaaatgtaaagactcagccaccttcctcggctagt 6688380

Query: 1261    gcttggaaagtaaatgcctcactccttttaatgctcaatgctgtggtcatgctggcaggc 1320
               ||||||||||||||||||||||||||||||||||||||||||||||||||||||||||||
Sbjct: 6688379 gcttggaaagtaaatgcctcactccttttaatgctcaatgctgtggtcatgctggcaggc 6688320

Query: 1321    tga 1323
               |||
Sbjct: 6688319 tga 6688317
```

Figure 6.5.

Alignment of the predicted rat, mouse and human OMgp amino acid sequences. The predicted rat sequence is 95% identical to that of mouse, and 90% identical to that of human.

```
Rat  : 1   MEYQILKMSSCLFILLFLTPGILCICPLQCICTERHRHVDCSGRNLTTLPPGLQENIIHL 60
Mouse: 1   MEYQILKMSSCLFILLFLTPGILCICPLQCTCTERHRHVDCSGRNLTTLPPGLQENIIHL 60
Human: 1   MEYQILKMSLCLFILLFLTPXILCICPLQCICTERHRHVDCSGRNLSTLPSGLQENIIHL 60

Rat  : 61  NLSYNHFTDLHNQLTPYTNLRTLDISNNRLESLPAQLPRSLWNMSAANNNIKLLDKSDTA 120
Mouse: 61  NLSYNHFTDLHNQLTPYTNLRTLDISNNRLESLPAQLPRSLWNMSAANNNIKLLDKSDTA 120
Human: 61  NLSYNHFTDLHNQLTQYTNLRTLDISNNRLESLPAHLPRSLWNMSAANNNIKLLDKSDTA 120

Rat  : 121 YQWNLKYLDVSKNMLEKVVLIKNTLRSLEVLNLSSNKLWTVPTNMPSKLHIVDLSNNSLT 180
Mouse: 121 YQWNLKYLDVSKNMLEKVVLIKNTLRSLEVLNLSSNKLWTVPTNMPSKLHIVDLSNNSLT 180
Human: 121 YQWNLKYLDVSKNMLEKVVLIKNTLRSLEVLNLSSNKLWTVPTNMPSKLHIVDLSNNSLT 180

Rat  : 181 QILPGTLINLTNLTHLYLHNNKFTFIPDQSFDQLLQLQEITLHNNRWSCDHTQNITYLLK 240
Mouse: 181 QILPGTLINLTNLTHLYLHNNKFTFIPEQSFDQLLQLQEITLHNNRWSCDHKQNITYLLK 240
Human: 181 QILPGTLINLTNLTHLYLHNNKFTFIPDQSFDQLFQLQEITLYNNRWSCDHKQNITYLLK 240

Rat  : 241 WMMETKAHVIGIPCSKQVSSLKEQSMYPTPPGFTSSLFTMSEMQTVDTINSLSMVTQPKV 300
Mouse: 241 WVMETKAHVIGTPCSKQVSSLKEQSMYPTPPGFTSSLFTMSEMQTVDTINSLSMVTQPKV 300
Human: 241 WMMETKAHVIGTPCSTQISSLKEHNMYPTPSGFTSSLFTVSGMQTVDTINSLSVVTQPKV 300

Rat  : 301 TNIPKQYRGKDTTFGVTLSKDTTFSSTDRALEPYPEDTPTEMTSSREAAAATLTIHLQDG 360
Mouse: 301 TKTPKQYRGKETTFGVTLSKDTTFSSTDRAVVAYPEDTPTEMTNSHEAAAATLTIHLQDG 360
Human: 301 TKIPKQYRTKETTFGATLSKDTTFTSTDKAFVPYPEDTSTETINSHEAAAATLTIHLQDG 360

Rat  : 361 MSSNASLTSAAKSSPAPVTLSITSGMPNNFSEMPQQSTTLNLRREETTANVKTQPPSSAS 420
Mouse: 361 MSSNASLTSATKSPPSPVTLSIARGMPNNFSEMPRQSTTLNLRREETTANGNTRPPSAAS 420
Human: 361 MVTNTSLTSSTKSSPTPMTLSITSGMPNNFSEMPQQSTTLNLWREETTTNVKTPLPSVAN 420

Rat  : 421 AWK 423
Mouse: 421 AWK 423
Human: 421 AWK 423
```

Figure 6.6.

Radioactive *in situ* hybridisation for *omgp* in the uninjured adult rodent nervous system. A-F show negative images of the film exposed to slides hybridized with ^{35}S-labelled 45-mer DNA oligonucleotide antisense probe. The top row shows sections reacted only with the radiolabelled antisense probe, and the bottom row shows the respective competitive control sections which were reacted with a mixture of radiolabelled antisense probe and excess unlabelled antisense probe. The lack of signal in the competitive control sections demonstrates the binding specificity of the antisense probe. A, strong signal was observed in the neocortex and pyriform cortex of the rostral forebrain. B and C, *omgp* was strongly expressed in the neocortex and hippocampal formation, and moderately in the habenular nucleus in B. D, moderate signal was detectable in the cerebellar cortex, and strong signal could be observed in discrete nuclei within the brainstem. E, strong expression of *omgp* was found in the grey matter of the spinal cord. F, DRGs expressed *omgp* mRNA at moderate/high levels.

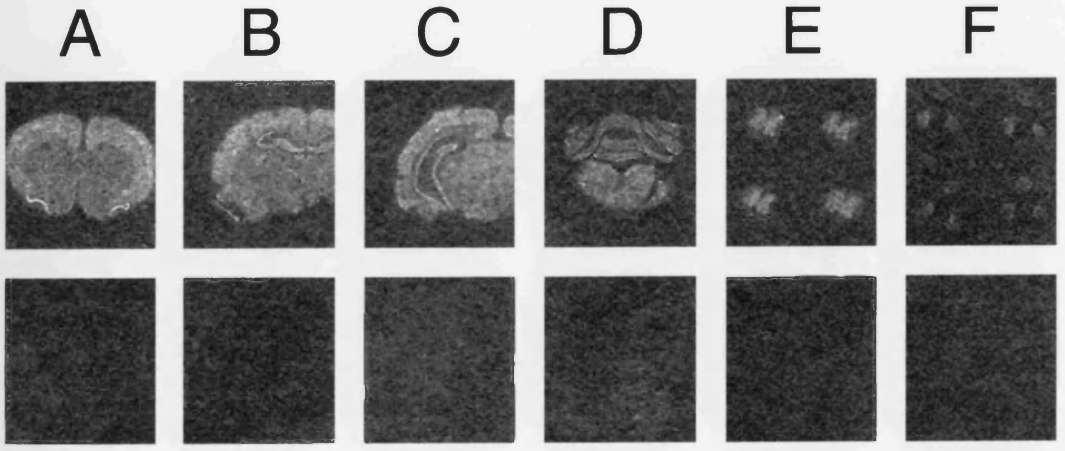
A
B
C
D
E
F

Figure 6.7.

Expression of mRNAs for myelin-associated inhibitors of neurite outgrowth, and *ngr*, in neocortex of adult rat. *omgp* is expressed by neurons in layers II-VI, but the large pyramidal neurons do not exhibit strong signal. Expression of *nogo-a* includes many large cells presumed to be neurons, and smaller cells which may include oligodendrocytes. Large, presumptive pyramidal projection neurons are particularly prominent. *nogo-66* expression is similar to that of *nogo-a*, except that expression by glia is more difficult to identify (since neuronal signal is much stronger). *ngr*, is expressed by neurons (i.e. cortical neurons express both *ngr* and its ligands) but not by glia. M = molecular layer; W = white matter. Scale bar = 500μm.

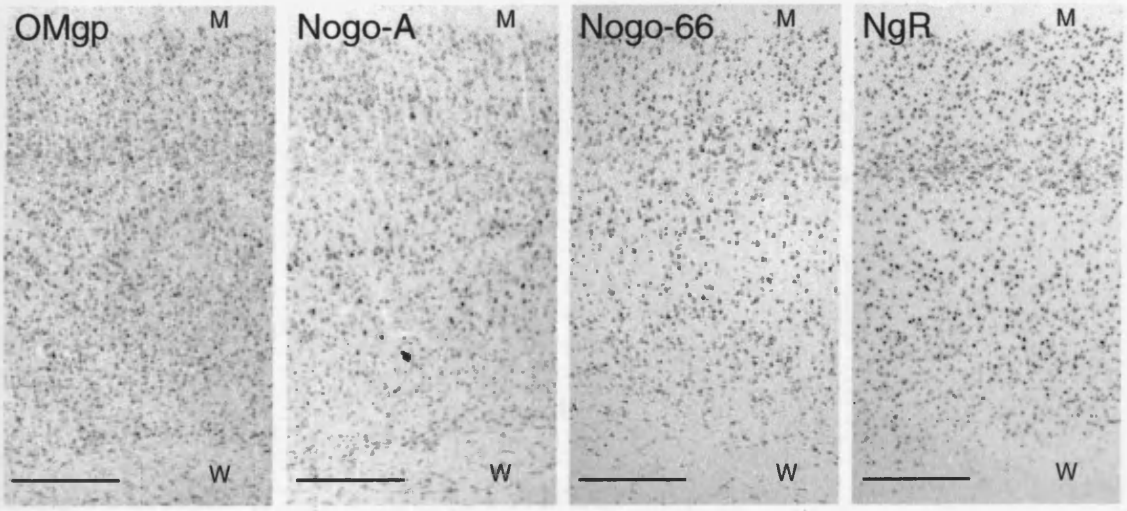
OMgp
M
W
Nogo-A
M
W
Nogo-66
M
W
NgR
M
W

Figure 6.8.

Non-radioactive *in situ* hybridisation of the uninjured adult rodent nervous system. Sections were reacted with a DIG-labelled antisense riboprobe.

A. Moderate to strong signal for *omgp* was detectable in the dentate gyrus, and CA4 cells of the hippocampal formation. Neurons of the dentate hilus also strongly expressed the transcript. Scale bar = 200μm.

B. In the cerebellum, weak expression of *omgp* was found in the granule cell layer (G), and strong expression in the Purkinje cells (arrows). Moderate to strong signal for *omgp* was also present in neurons of the vestibular nuclei (V). Stronger expression was detectable in some larger neurons within the brainstem. Scale bar = 400μm.

C. Higher power image of cerebellar cortex showing strong expression of *omgp* by Purkinje cells (arrows), and moderate expression by cerebellar granule neurons (G). Scale bar = 100μm.

D. In the spinal cord, *omgp* was strongly expressed by neurons throughout the grey matter, but especially by the larger motor neurons of the ventral horn. Scale bar = 400μm.

E. Moderate to strong *omgp* expression was observed in DRG neurons. Scale bar = 100μm.

F. Similarly, SCG neurons were found to exhibit variable levels of *omgp* expression, from moderate to strong. Scale bar = 200μm.

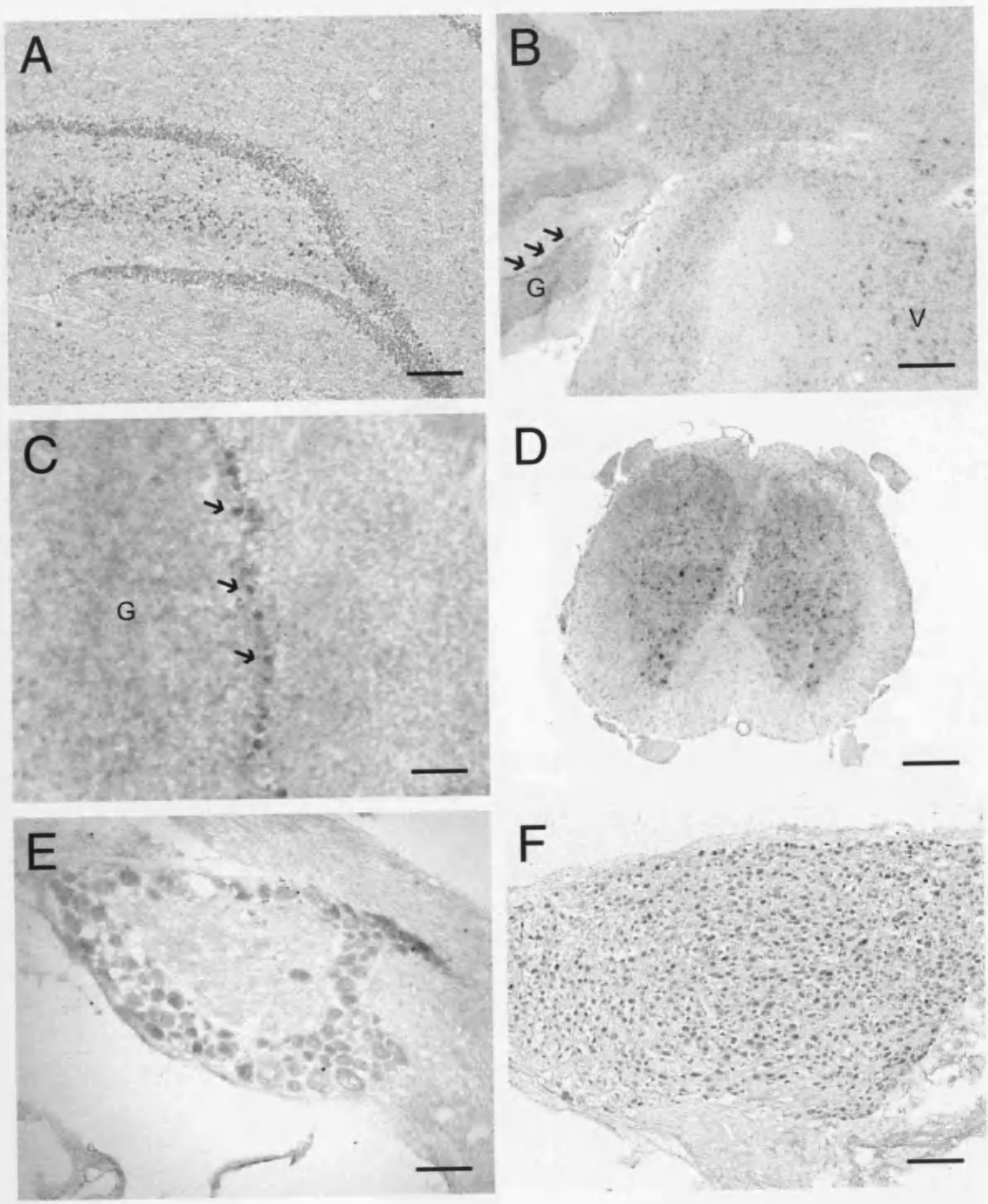
A
B
G
V
C
G
D
E
F

Figure 6.9.

In situ hybridisation for *omgp* in a section of thalamus, 16 days after grafting of a segment of autologous tibial nerve. The only sign of *omgp* regulation was found in the ventral blade of the dentate gyrus (arrowheads), ipsilateral to the graft (g), in which the expression of *omgp* appeared to have ceased. This was only observed in one of three animals. c = cortex. Scale bar = 500μm.

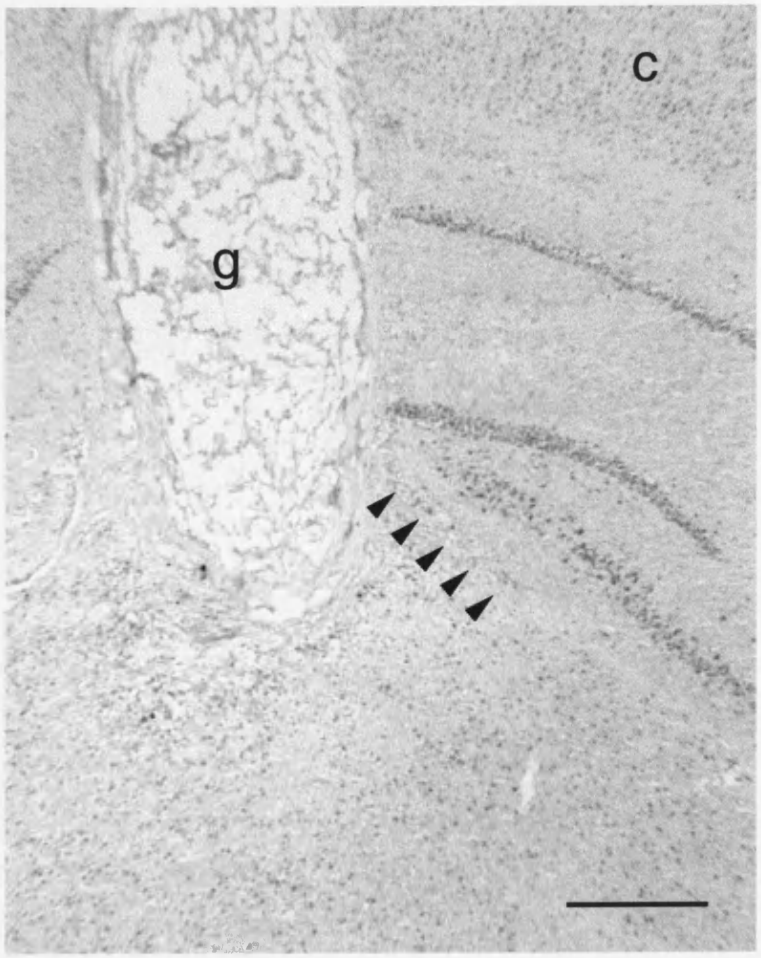
c
g

CHAPTER 7

Construction of Replication-Incompetent HSV-1 for the Expression of the NgR Antagonist Peptide, NEP1-40

INTRODUCTION

Nogo extracellular peptide 1-40 (NEP1-40) is an antagonist peptide to the Nogo-66 receptor (NgR) and comprises the first forty amino acids of the NgR ligand, Nogo-66 (Grandpre et al., 2002). It was originally described following the process of identifying residues within Nogo-66 responsible for the binding and activation of NgR (Fournier et al., 2001). Initially, Fournier et al. constructed five different overlapping 25-residue alkaline-phosphatase fusion proteins of Nogo-66 in order to identify the region active in inducing growth cone collapse and inhibiting neurite outgrowth through NgR. Interestingly, only the Nogo-66(31-55) fusion protein exhibited any inhibitory effect, and this was three-fold lower than that observed for the entire Nogo-66 fusion protein. Binding assays showed that residues 31-33 (SEEL) are particularly important for high-affinity binding: Nogo-66(1-30) does not bind NgR; Nogo-66(1-31) possesses a dissociation constant (Kd) of 24 +/- 11nM; and Nogo-66(1-33), or longer fusion proteins, possess an improved Kd of 11-14+/-3nM. Similarly, the first ten amino terminal residues of Nogo-66 (RIYKGVIQAI) were also shown to be important for binding to NgR; Nogo-66(6-40) was shown to bind with significantly reduced affinity, and Nogo-66(11-40) did not bind at all. Thus, it was established that Nogo-66(1-40), i.e. NEP1-40, possessed the highest binding affinity for NgR of these various truncated forms of Nogo-66. Assessment of the activity of NEP1-40 *in vitro* seemed to show that it did not cause growth cone collapse of E12 chick DRG neurons at a dose of 20nM; however, it should be borne in mind that sample sizes were not reported and if this experiment were repeated on a larger scale there may be a statistically significant, but slight, increase in growth cone collapse in the presence of NEP1-40.

The addition of 1μM NEP1-40 partially blocks the inhibitory activity of a substrate of CNS myelin on E12 chick DRG neurite outgrowth (Grandpre et al., 2002). This is in keeping with the finding that NEP1-40 is an antagonist of Nogo-66 induced neurite-outgrowth inhibition, but exhibits no antagonist activity against MAG, OMgp (Barton et al., 2003), or Nogo-A specific peptide (Grandpre et al., 2002). Nogo-A is a major inhibitory constituent of CNS myelin and the Nogo-A specific peptide is thought to act through an as yet unidentified receptor (or receptor complex). There are, of course, numerous inhibitory molecules which may be present within extracts of CNS, such as chondroitin sulphate proteoglycans and semaphorins, whose effects would not be expected to be neutralized by NEP1-40.

In vivo studies demonstrated that the intrathecal infusion of NEP1-40 (75μg per kg body weight per day) by osmotic minipump after midthoracic dorsal hemisection, over a period of four weeks, resulted in significantly enhanced growth of injured CST axons (Grandpre et al., 2002). Rostral to the lesion site, numerous ectopic CST fibres were identified, particularly in grey matter. Furthermore, there was a more than 10-fold increase in sprouting from the injured dorsal CST into adjacent tracts in NEP1-40 treated animals, compared to the PBS treated control animals. In the NEP1-40 treated rats, many sinuous fibres were found to by-pass the lesion within the intact ventral half of the spinal cord. Many of these ectopic fibres were found in both grey and white matter up to a distance of 11-15mm caudal to the lesion site (20-30 axons per section per animal at this distance). There is some suggestion that these regenerating fibres may have been derived from the sprouting of intact collaterals or spared ventral CST fibres, induced by NEP1-40. However, the authors did not note any abnormal CST fibre sprouting in uninjured NEP1-40 treated rats, suggesting that the molecule's activity is confined to injured axons. NEP1-40 has interesting effects on serotonergic fibres within the injured spinal cord. In PBS-treated control animals, the ventral horn caudal to the lesion exhibited a 40% reduction in 5-hydroxytryptamine (serotonin) density compared to that rostral to the lesion. However, in NEP1-40 treated animals, the density was similar caudally and rostrally. This is in agreement with the preliminary findings that sprouting of serotonergic fibres of the raphespinal tract is enhanced following spinal injury in the *ngr*

null mutant mouse (Kim et al., 2003a). In terms of functional recovery, locomotor activity – as measured using the BBB scale – was found to be significantly improved in the NEP1-40 treated animals compared to the PBS control treated animals after 28 days (~15 vs. ~11).

NEP1-40 has yielded promising results both *in vitro* and *in vivo*. The administration of NEP1-40 to primary cultures of E12 chick DRG neurons grown on a substrate of (i) Nogo-66, or (ii) CNS myelin, greatly enhances neurite outgrowth (Grandpre et al., 2002). Also, after midthoracic dorsal hemisection in rats, intrathecal infusion of NEP1-40 (75μg per kg body weight per day) by mini-osmotic pump has been claimed to elicit significant regeneration of lesioned CST axons (Grandpre et al., 2002). Even subcutaneous administration of the antagonist peptide (11.6mg per kg body weight per day) commencing 1 week after midthoracic dorsal hemisection of the spinal cord for a duration of 14 days has been reported to elicit significant regeneration of injured CST axons, sprouting of serotonergic fibres, synapse reformation and ultimately enhanced locomotor recovery (Li and Strittmatter, 2003). That intrathecal infusion or delayed systemic administration of the peptide have produced such results prompted the question of whether targeted viral delivery of a secreted form of the antagonist peptide would achieve a comparable, if not better, regenerative response.

SUMMARY OF METHODS

Expression and Purification of Nogo-66-$(His)_6$

Nogo-66 was amplified from adult rat brain cDNA. The forward primer, CCC ATA TGA GGA TAT ATA AGG GCG TGA TC, encoded an internal *Nde*I restriction site and in-frame start codon whilst the reverse primer, CTC CTC GAG TCA GTG GTG GTG GTG GTG GTG CTT CAT GGA ATC AAC TAA ATC, encoded an internal inframe $(His)_6$-tag and stop codon followed by *Xho*I restriction endonuclease site. The PCR was undertaken with the proof-reading DNA polymerase, *Pfu* (Promega), with the first five annealing cycles at 42°C and the remaining 25 annealing cycles a 55°C.

The PCR product was ligated into pET23a(+) (Novagen) between the *Nde*I and *Xho*I restriction sites, respectively. Chemically competent BL21 λDE3 lysogen cells (Novagen) were transformed as described in Chapter 2. Bacterial expression of Nogo-66 was induced by incubating the transformed bacteria, under standard bacterial growth conditions, with 100mM IPTG for three hours.

Total cell protein samples were obtained from induced and uninduced transformed bacteria for analysis by SDS-PAGE. Fractionation of induced transformed bacteria was performed using the protocol provided in the pET system manual (Novagen). Media, periplasmic, soluble cytoplasmic and insoluble cytoplasmic fractions were isolated. Protein samples were resolved by SDS-PAGE against Rainbow molecular weight marker (Amersham), on a 20% polyacrylamide gel, and visualized with Coomassie stain.

For purification of Nogo-66-$(His)_6$, the insoluble cytoplasmic fraction was solubilized in 6M urea and passed through a nickel-primed HiTrap™ column (Amersham) using FPLC apparatus (Amersham), as per the manufacturer's instructions. Protein was eluted from the column with 6M urea containing a rising concentration of imidazole (0→500mM) over the course of 10 minutes. Ten 1 minute fractions of eluent were captured, and placed at -20°C for longterm storage.

Samples of induced and uninduced transformed bacteria, as well as elution fractions 2-8 were resolved by SDS-PAGE with MES buffer, on a pre-made 12% Bis-Tris NuPAGE® gel (Invitrogen), against a broadrange pre-stained SDS-PAGE molecular weight standard (Bio-rad). Bands of protein were visualized with Colloidal Coomassie® Stain (Invitrogen).

Construction of HSV-1 Expressing Secreted-Tagged NEP1-40

NEP1-40 was cloned by PCR from adult rat brain cDNA. The forward primer, ACT GAA GCT TGA GGA TAT ATA AGG GCG TGA TCC A, contained an internal *Hin*dIII restriction and the reverse primer, ATC GCT CGA GAG AAT TAC TGT ATT TCT GAA CCA ATT CC, contained an internal *Xho*I restriction site. The PCR product

was ligated inframe into pSecTagA (Invitrogen) between the *Hin*dIII and *Xho*I restriction sites, respectively. A further round of PCR was performed using a forward primer against the T7 promoter, with an internal *Eco*R1 restriction site to facilitate clonal screening, and a reverse primer against pcDNA3.1 BGH reverse priming site. The primer sequences were ACT GGA ATT CTA ATA CGA CTC ACT ATA GGG and ACT GAT GCA TTA GAA GGC ACA GTC GAG G, respectively. This PCR product was ligated into the blunted *Hin*dIII restriction sites of the pR19 hrGFP WPRE shuttle vector backbone, thus replacing hrGFP. Screening for the correct orientation of the insert was performed by plasmid digestion with the *Eco*RI restriction endonuclease.

The *Sca*I-linearized shuttle vector, pR19 mNEP1-40 WPRE, was used in a co-transfection of 27/12/M:4 cells with 1764/4-/27in/RL1+ viral DNA for the generation of recombinant HSV-1. *Eco*RI-digested viral DNA, from nine different purified plaques, was analysed by southern blotting. *Eco*RI-digested pR19 mNEP1-40 WPRE was used as a positive control, and *Eco*RI-digested 1764/4-/27in/RL1+/pR19 hrGFP WPRE as a negative control. Hybridisation was performed with ^{32}P-radiolabelled PCR product of mNEP1-40.

Western Blot of Virally Transduced BHKs

BHKs were cultured in 24-well plates, and transduced with 1764/4-/27in/RL1+/pR19 mNEP1-40 WPRE at an MOI of 1 when 80% confluent. 1764/4-/27in/RL1+/pR19 hrGFP WPRE (MOI=1) and mock transduction served as negative controls. After 48 hours, growth media was removed and filtered using Microcon® columns (Millipore Corporation), with a 3KDa cut-off., as per the manufacturer's instructions. The protein samples were resuspended in 1xPBS containing a cocktail of protease inhibitors (Sigma). The transduced cells were harvested in boiling lysis buffer (1% w/v SDS, 0.1% Triton-X 100, 10mM DTT in PBS). A lysate of stable cells expressing a myc-tagged protein of ~60KDa served as a positive control (kindly provided by Emma Willoughby, Department of Immunology and Molecular Pathology, UCL). Protein concentrations were determined by spectrophotometry using RcDc reagent (Bio-Rad). Samples were resolved by SDS-PAGE on a 20% polyacrylamide gel, against Rainbow molecular weight marker

(Amersham). Western blotting was performed as described in Chapter 2. The membrane was probed with a mouse monoclonal anti-myc antibody (Invitrogen) at a concentration of 1:500. HRP-conjugated goat anti-mouse antibody was applied at a concentration of 1:2000. The membrane was reacted with ECL reagent (Amersham), as per the manufacturer's instructions, and exposed to X-OMAT radiographic film (Kodak).

Immunocytochemistry of Virally Transduced BHKs

BHK cells were cultured on uncoated 13mm glass coverslips, transduced with 1764/4-/27in/RL1+/pR19 mNEP1-40 WPRE (MOIs of 1, 5 and 20) when 80% confluent, and fixed with 4% PFA after 48 hours. Transduction with 1764/4-/27in/RL1+/pR19 hrGFP WPRE (MOI=1), and mock transduction, served as negative controls. Immunocytochemistry was performed as described in Chapter 2, with a mouse monoclonal anti-myc primary antibody (Invitrogen) at a dilution of 1:500.

Injection of Cervical Spinal Cord with Replication-Incompetent HSV-1

Six uninjured adult Sprague-Dawley rats were injected with 2 x 10^6 pfu of virus at the level of the cervical spinal cord (as described in Chapter 2). Three rats received 1764/4-/27in/RL1+/pR19 mNEP1-40 WPRE, and the three control rats received 1764/4-/27in/RL1+/pR19 hrGFP WPRE. Animals were culled at 8 days post operation (dpo), and the tissue processed for mNEP1-40 expression by immunohistochemistry with anti-*myc* antibody (Invitrogen), or for hrGFP expression by fluorescence microscopy.

RESULTS

In order to construct a HSV-1 vector for targeted delivery of NEP1-40, it would first be necessary to modify the peptide such that it would be secreted, and detectable by immunohistochemistry. These modifications could potentially alter the activity of NEP1-40, so it was decided that an *in vitro* system should be established to determine whether a modified form of NEP1-40 is antagonistic to the effects of Nogo-66.

Recombinant Nogo-66

Purified bacterially-expressed recombinant Nogo-66 has previously been reported to be active in inducing growth cone collapse, and neurite outgrowth inhibition (Fournier et al., 2001). It was decided that a similar bacterial expression system should be used to produce Nogo-66 with a carboxy terminal $(His)_6$-tag, for subsequent Nickel-based solid phase purification of the peptide. This was achieved by PCR amplification of Nogo-66 from rat single-stranded DNA using a forward primer containing an in-frame start codon, and a reverse primer containing an in-frame $(His)_6$-tag coding sequence and stop codon. This fragment was ligated into the bacterial inducible expression vector, pET23a(+) (Fig.7.1.A), and sequenced prior to the transformation of BL21 λDE3 lysogen *E.coli*. Expression of the peptide was induced with 100mM IPTG, and fractionation was performed to identify the compartmentalisation of the peptide by SDS-PAGE (Fig. 7.1.C).

The majority of the 73 residue protein (Fig. 7.1.B), was detectable as a ~10KDa band in the insoluble cytoplasmic fraction (Fig. 7.1.C). This is indicative of inclusion body formation, which occurs commonly with highly expressed recombinant proteins in bacteria. For the purification of the recombinant protein, the insoluble cytoplasmic fraction was solubilized in 6M urea and passed through Nickel-primed HiTrap™ columns. The protein was eluted from the columns using a rising concentration of imidazole (0→500mM) over a 10 minute period on an automated FPLC machine (Figs 7.2.A and 7.2.B). Fractions of eluent were collected at 1 minute intervals. These were resolved by SDS-PAGE, and visualized with Colloidal Coomassie® stain (Fig. 7.2.C).

The absorbance data (280nm) obtained by spectrophotometry during FPLC revealed at least two overlapping peaks, suggesting some impurity of the eluted Nogo-66-$(His)_6$, which formed the last of the peaks (Figs. 7.2.A and 7.2.B). A comparison of the pattern of protein expression in the induced and uninduced transformed bacteria indicated that at least four proteins were induced by the addition of IPTG (Fig 7.2.C, denoted by asterisks). By far the strongest of these bands was formed by a ~10KDa protein, consistent with being Nogo-66-$(His)_6$, which eluted primarily in fractions 6 and 7;

however, fraction 6 was contaminated with the three other unknown induced proteins (~7KDa, ~45KDa, and ~100KDa) as well as trace amounts of other proteins. Since fraction 7 contained a significant amount of the recombinant protein and appeared to be relatively pure, it was decided that this fraction should be renatured and used in the *in vitro* assay of growth cone collapse and neurite outgrowth inhibition.

Replication-Incompetent HSV-1 Expression of mNEP1-40

The modification of the peptide such that it would be secreted, and detectable by immunohistochemistry, was achieved by cloning the NEP1-40 coding sequence into pSecTagA (Invitrogen) (Figs 7.3.A and 7.3.B). In doing so, the peptide coding sequence acquired an in-frame amino terminal Ig κ leader sequence, and carboxy terminal MycHis tag, for secretion and epitope detection, respectively. The coding sequence of the modified peptide (mNEP1-40), which was amplified by PCR (Fig. 7.3.C) and predicted to give rise to a 100 amino acid peptide (Fig. 7.3.D), was subcloned into a pR19 shuttle vector, between a CMV promoter and woodchuck postranscriptional regulatory element (WPRE) (Figs. 7.4.A and 7.4.B). The latter has been widely reported to enhance exogenous gene expression (Zufferey et al., 1999; Loeb et al., 1999), apparently by stabilising the mRNA. The correct DNA sequence was confirmed by automated fluorescent dye sequencing, before the pR19 shuttle vector – which also contains flanking regions for homologous recombination into the latency associated transcript (LAT) region of the herpes virus genome - was used in a co-transfection of genetically modified complementing BHK cells (27/12/M:4) with mutant HSV-1 viral DNA to generate recombinant replication-incompetent HSV-1. This viral backbone is termed 1764/4-/27in/RL1+; it possesses a mutant form of the viral transactivator, VP16, and is deleted for ICP4, thus rendering it incapable of replication without complementation for the wildtype forms of these genes. A southern blot was performed on the viral DNA obtained after plaque purification to confirm the presence of mNEP1-40 (Fig. 7.4.C).

***In Vitro* Assessment of mNEP1-40 Antagonist Activity**

Since PC12 cells have been reported to express NgR (Fournier et al., 2003), and can be readily induced to sprout axons using the βNGF subunit (Greene and Tischler, 1976), it

was thought that these would make an ideal *in vitro* model to examine the growth cone collapsing activity of Nogo-66-$(His)_6$, and the antagonist effect of mNEP1-40. However, it was first necessary to establish a protocol for the measurement of growth cone collapse. There were two potential ways of achieving this: (i) monitor growth cone collapse and neurite retraction in real-time, or (ii) counting collapsed growth cones after exposure.

Without having renatured the Nogo-66-$(His)_6$, a feasibility study was performed for the first of these methods using ice-cold HBSS as a substitute. The growth media was replaced with ice-cold HBSS, and the effect on the growth cones monitored continuously by microscopy for 30 minutes, with images being captured at one minute intervals to form a time-lapse reel (Fig. 7.5). Although crude, the experiment clearly showed that growth cone collapse and neurite retraction was widespread and could be monitored in such a fashion.

As a feasibility study for the second of the two methods, the differentiated PC12 cells were removed to a tissue culture hood where 10µl PBS was added per 500µl of growth media. The cells were immediately returned to the incubator, and pre-warmed 20% PFA was added to the growth media to give a final concentration of 4% PFA 15 minutes later. After a further 10 minutes, images were captured by microscopy to determine whether the growth cones had been successfully fixed, or whether they had collapsed in the processing. The result was that growth cones could be readily fixed and clearly visualized (Fig. 7.6).

On balance, the second of the two methods seemed most appropriate, given the ease with which growth cones could be fixed and visualized. In contrast, the first of the two methods requires specialized apparatus for incubating the cells whilst under microscopic observation, and would also have largely restricted assessment to a single microscopic field.

Expression of mNEP1-40 from Virally Transduced BHKs

In order to (i) demonstrate that HSV-1 expressed mNEP1-40 is secreted and myc-tagged, and (ii) purify the peptide for assessment of antagonistic activity in an *in vitro* assay of growth cone collapse, it was necessary to transduce cultured cells with the virus and harvest the growth media. To this end, BHKs were transduced with 1764/4-/27in/RL1+/pR19 mNEP1-40 WPRE at a multiplicity of infection (MOI) of 1. Mock transduced BHKs, and those transduced with the equivalent virus expressing hrGFP (MOI=1), were employed as negative controls. After 48 hours the supernatant was harvested and concentrated using Microcon® columns, with a 3KDa cut-off. The protein samples were resuspended in PBS with a cocktail of protease inhibitors, and analysed by western blot. The only detectable band was that of the positive control myc-tagged protein at ~60KDa (not shown). A western blot of the cell lysates produced similar results (Fig. 7.7); only the ~60KDa positive control myc-tagged protein was detectable.

Expression of mNEP1-40 by virally transduced BHKs was subsequently assessed by immunocytochemistry. After 48 hours, no expression was detectable in cells transduced at an MOI of 1. However, sporadic expression (by <1% of cells) was evident at an MOI of 5 (Fig. 7.8.C). The number of cells expressing mNEP1-40 increased with increasing MOI, but even at an MOI of 20 the percentage of cells expressing the peptide remained low (Figs. 7.8.A and 7.8.B). This result was unexpected and remains to be explained.

Injection of HSV-1 Expressing mNEP1-40 into Adult Rat Cervical Spinal Cord

Three adult Sprague-Dawley rats received 5µl injections of 1764/4-/27in/RL1+/pR19 mNEP1-40 WPRE (at a stock concentration of $4x10^8$ pfu/ml) into their cervical spinal cords. A further three rats were treated identically with 1764/4-/27in/RL1+/pR19 eGFP WPRE. The animals were culled at 8dpo, and the tissue processed for mNEP1-40 and eGFP expression, respectively.

Expression of mNEP1-40 could be detected in cells bordering the injection site, and sporadically by neurons and their processes up to several millimetres rostral and caudal from the injection site (Figs. 7.8.D-F). However, the extent of neuronal expression of

mNEP1-40 was considerably lower than that observed for the eGFP-expressing virus (Fig. 7.8.G).

DISCUSSION

The original aims of the work reported herein were (i) to construct a tagged-secreted form of NEP1-40 which could be expressed by HSV-1, (ii) to develop an *in vitro* assay to determine whether such a modified form of NEP1-40 exhibited antagonistic activity to Nogo-66, and (iii) to establish whether targeted-delivery of such a peptide to the injured nervous system with a replication-incompetent HSV-1 vector was conducive to axonal regeneration.

Expression of Modified NEP1-40 from HSV-1

Unfortunately, although the construction of a HSV-1 vector for the expression of a modified form of NEP1-40 (termed mNEP1-40) was successful, the level of expression was unexpectedly low both *in vitro* and *in vivo*. Indeed, in BHK cells, an MOI of 5 was necessary for the peptide to be detectable by immunocytochemistry; and, even then, fewer than 1% of total cell population were immunopositive. In theory, and usually in practice, an MOI of 1 should be sufficient to achieve near 100% cell expression of a transgene (e.g. eGFP) in these cells. This is indicative of a problem with transcription and translation of the transgene, rather than viral transduction of the cell line – since the HSV-1 vector backbone was not altered in the process of construction. One possible explanation for the poor expression of NEP1-40 is its relatively short coding sequence (303bp); there is at least some circumstantial evidence that small transgenes are not well expressed by HSV-1, although this usually relates to sequences considerably shorter than 300bp (Dr. R.S. Coffin, personal communication).

Analysing the growth media of virally transduced BHKs for the expression of mNEP1-40 was of two-fold importance: (i) to demonstrate that mNEP1-40 is secreted by virally transduced cells, and (ii) to concentrate the peptide in order to assess its antagonistic activity in an *in vitro* assay of Nogo-66 induced growth cone collapse. The failure to

detect the peptide in the growth media of BHKs transduced at an MOI of 1 is probably a reflection of the high MOI required (minimum of 5) for detection of mNEP1-40 in the cytoplasm of BHKs by immunocytochemistry.

Bacterial Expression of Recombinant Nogo-66-$(His)_6$

A carboxy terminal $(His)_6$-tagged form of Nogo-66 was successfully purified by FPLC from a bacterial expression system, and a suitable protocol for analysing growth cone collapse in differentiated PC12 cells was devised. However, due to the failure to detect and concentrate mNEP1-40 from the growth media of virally transduced BHKs, as well as the overall time constraints, the peptide was not renatured and its activity in inducing growth cone collapse or inhibiting neurite outgrowth was not assessed.

Summary

Ultimately, further work is required. If the time were available, it would first be necessary to renature the bacterial Nogo-66-$(His)_6$ and demonstrate its activity in inducing growth cone collapse or inhibiting neurite outgrowth. This could be achieved using differentiated PC12 cells, as previously suggested, or with primary cultures of embryonic neocortical neurons, for example. Assuming that the Nogo-66-$(His)_6$ is active, then it would be desirable to express and purify mNEP1-40 – ideally from a the growth media of a stable cell line – in order to assess its antagonist activity against Nogo-66. This would also demonstrate that the peptide is secreted. Then, numerous approaches could be taken to optimise the level of HSV-1 mediated expression of NEP1-40. If these were successful, studies in spinal injury models would be warranted.

To date, all of the published *in vivo* data on NEP1-40 has been produced by Strittmatter's laboratory (Grandpre et al., 2002; Li and Strittmatter, 2003). It is somewhat surprising that no independent reports of its activity in spinal injury models have yet emerged, given that more than two years has elapsed since the potent *in vivo* effects of NEP1-40 on axonal regeneration were first described. Nonetheless, it is reasonable to assume that these promising findings are the result of blocking Nogo-66 signalling through NgR, but not that of MAG or OMgp (Barton et al., 2003). Whether targeted viral delivery of a

secreted form of NEP1-40 to a lesion site will achieve similar results to those obtained with continuous intrathecal or subcutaneous infusion of the peptide remains to be seen.

CONCLUSION

Owing to numerous technical difficulties and time constraints, it was not possible to see this project to completion. However, there is still potential for this virus; but, the demonstration of mNEP1-40 antagonism of Nogo-66 and the optimisation of viral transgene expression are inevitably necessary before any meaningful *in vivo* studies can be undertaken.

Figure 7.1.

Bacterial Expression of Nogo-66-$(His)_6$.

A, Schematic representation of the pET23a(+)-Nogo-66-$(His)_6$ vector. B, The Nogo-66-$(His)_6$ open reading frame and its translation to the Nogo-66-$(His)_6$ peptide sequence. C, SDS-PAGE of total cell protein from uninduced (Un) and induced (In) pET23a(+)-Nogo-66-$(His)_6$ transformed BL21 λDE3 lysogen *E.coli*. Adjacent lanes show the medium (M), periplasmic (P), soluble cytoplasmic (SC) and insoluble cytoplasmic (IC) fractions of IPTG-induced transformed bacteria. Protein samples were resolved on a 20% polyacrylamide gel against high molecular weight Rainbow marker (Amersham). Nogo-66-$(His)_6$ is evident as an inducible ~10KDa band. It localizes primarily to the insoluble cytoplasmic fraction, presumably as inclusion bodies. Mw = molecular weight marker.

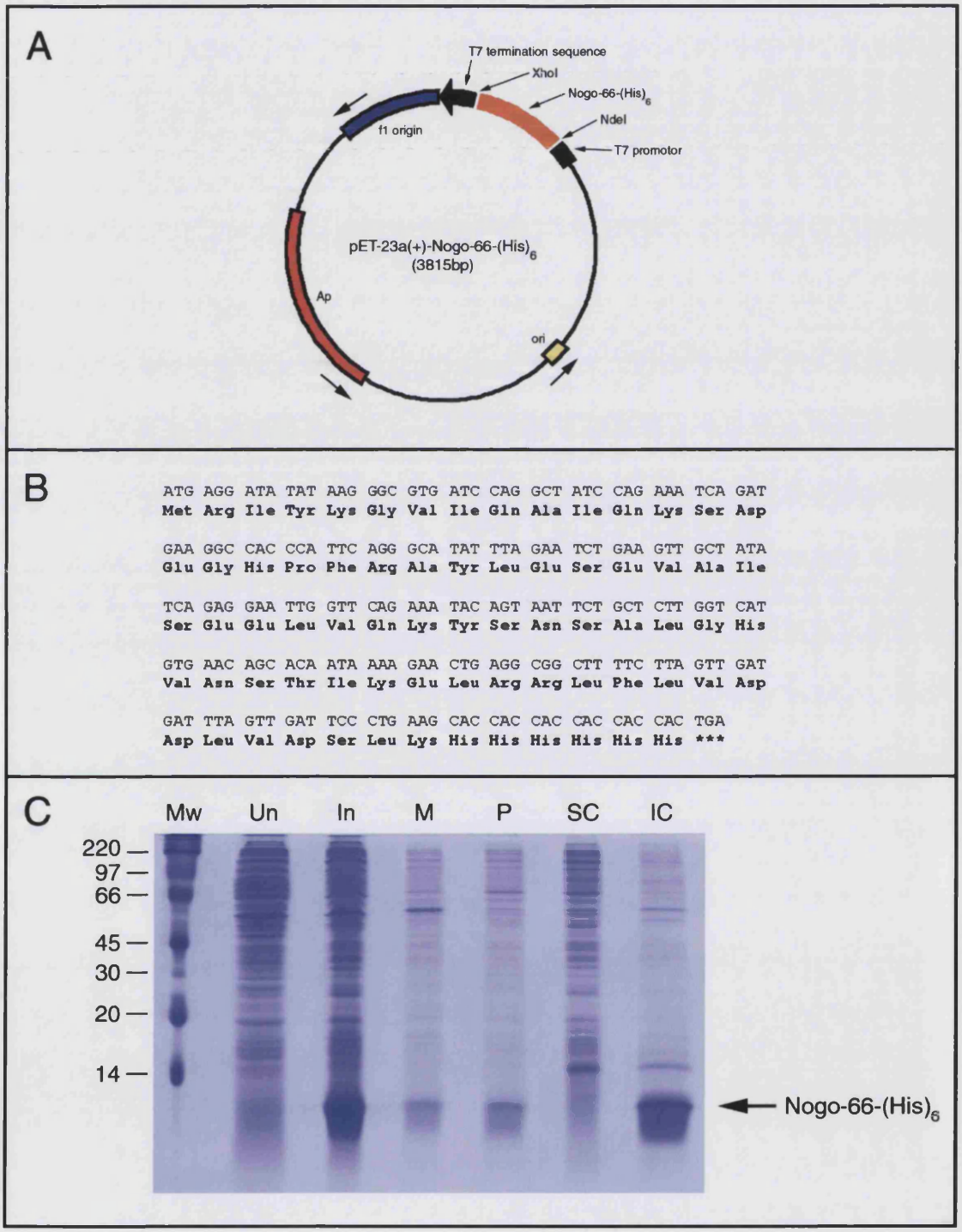
A
T7 termination sequence
XhoI
Nogo-66-(His)6
NdeI
T7 promotor
f1 origin
pET-23a(+)-Nogo-66-(His)6
(3815bp)
Ap
ori
B
ATG AGG ATA TAT AAG GGC GTG ATC CAG GCT ATC CAG AAA TCA GAT
Met Arg Ile Tyr Lys Gly Val Ile Gln Ala Ile Gln Lys Ser Asp
GAA GGC CAC CCA TTC AGG GCA TAT TTA GAA TCT GAA GTT GCT ATA
Glu Gly His Pro Phe Arg Ala Tyr Leu Glu Ser Glu Val Ala Ile
TCA GAG GAA TTG GTT CAG AAA TAC AGT AAT TCT GCT CTT GGT CAT
Ser Glu Glu Leu Val Gln Lys Tyr Ser Asn Ser Ala Leu Gly His
GTG AAC AGC ACA ATA AAA GAA CTG AGG CGG CTT TTC TTA GTT GAT
Val Asn Ser Thr Ile Lys Glu Leu Arg Arg Leu Phe Leu Val Asp
GAT TTA GTT GAT TCC CTG AAG CAC CAC CAC CAC CAC CAC TGA
Asp Leu Val Asp Ser Leu Lys His His His His His His ***
C
Mw
Un
In
M
P
SC
IC
220
97
66
45
30
20
14
Nogo-66-(His)6

Figure 7.2.

Purification of bacterial Nogo-66-$(His)_6$. A, Spectrophotometric absorbance measurements of FPLC eluent, at a wavelength of 280nm (A280), with respect to time. B, A280 measurements of eluent with respect to the rising concentration of imidazole (0% = 0mM, 100% = 500mM). C, SDS-PAGE of total cell protein from IPTG-induced (In), and uninduced (Un), pET23a(+)-Nogo-66-$(His)_6$ transformed BL21 λDE3 lysogen *E.coli*. FPLC elution fractions 2-8 were analysed in the adjacent lanes. Protein samples were resolved on a 12% Bis-Tris NuPAGE® gel (Invitrogen) against a broadrange pre-stained molecular weight marker (Amersham). Bands of protein were visualized with Colloidal Coomassie® Stain (Invitrogen). Asterisks denote the major differences in protein expression between IPTG-induced and uninduced pET23a(+)-Nogo-66-$(His)_6$ transformed bacteria. Nogo-66-$(His)_6$ was found to elute predominantly in fractions 6 and 7, and is represented by a ~10KDa band.

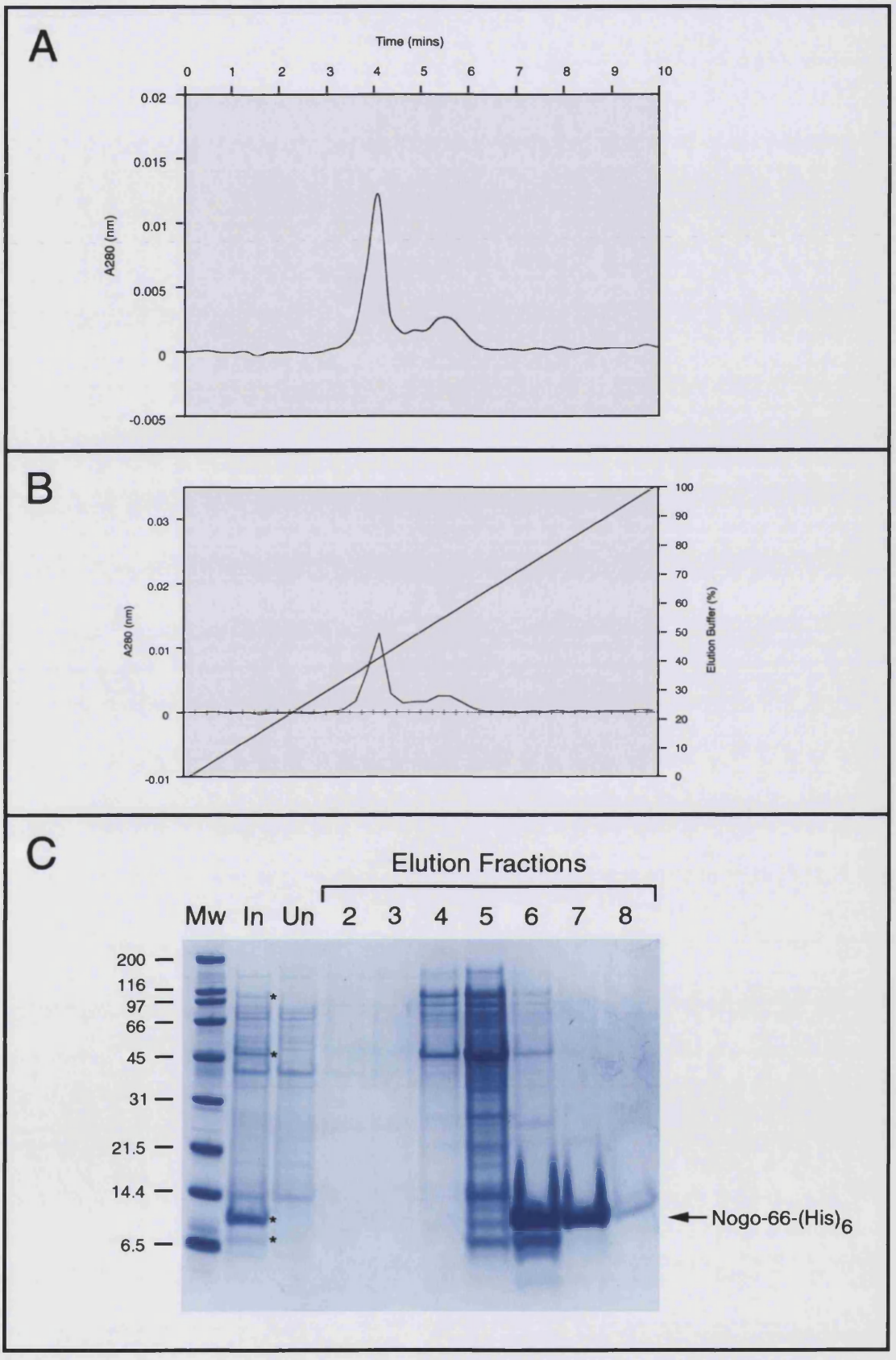
A
Time (mins)
0 1 2 3 4 5 6 7 8 9 10
0.02
0.015
0.01
0.005
0
-0.005
A280 (nm)
B
0.03
0.02
0.01
0
-0.01
A280 (nm)
100 90 80 70 60 50 40 30 20 10 0
Elution Buffer (%)
C
Elution Fractions
Mw In Un 2 3 4 5 6 7 8
200
116
97
66
45
31
21.5
14.4
6.5
Nogo-66-(His)6

Figure 7.3.

Construction of modified form of NEP1-40 antagonist peptide (mNEP1-40). A, schematic representation of the multiple cloning site of pSecTagA (Invitrogen). B, schematic representation of pSecTagA NEP1-40. C, schematic representation of mNEP1-40 PCR product for subcloning into the pR19 shuttle vector. D, coding sequence of mNEP1-40, and translated peptide sequence.

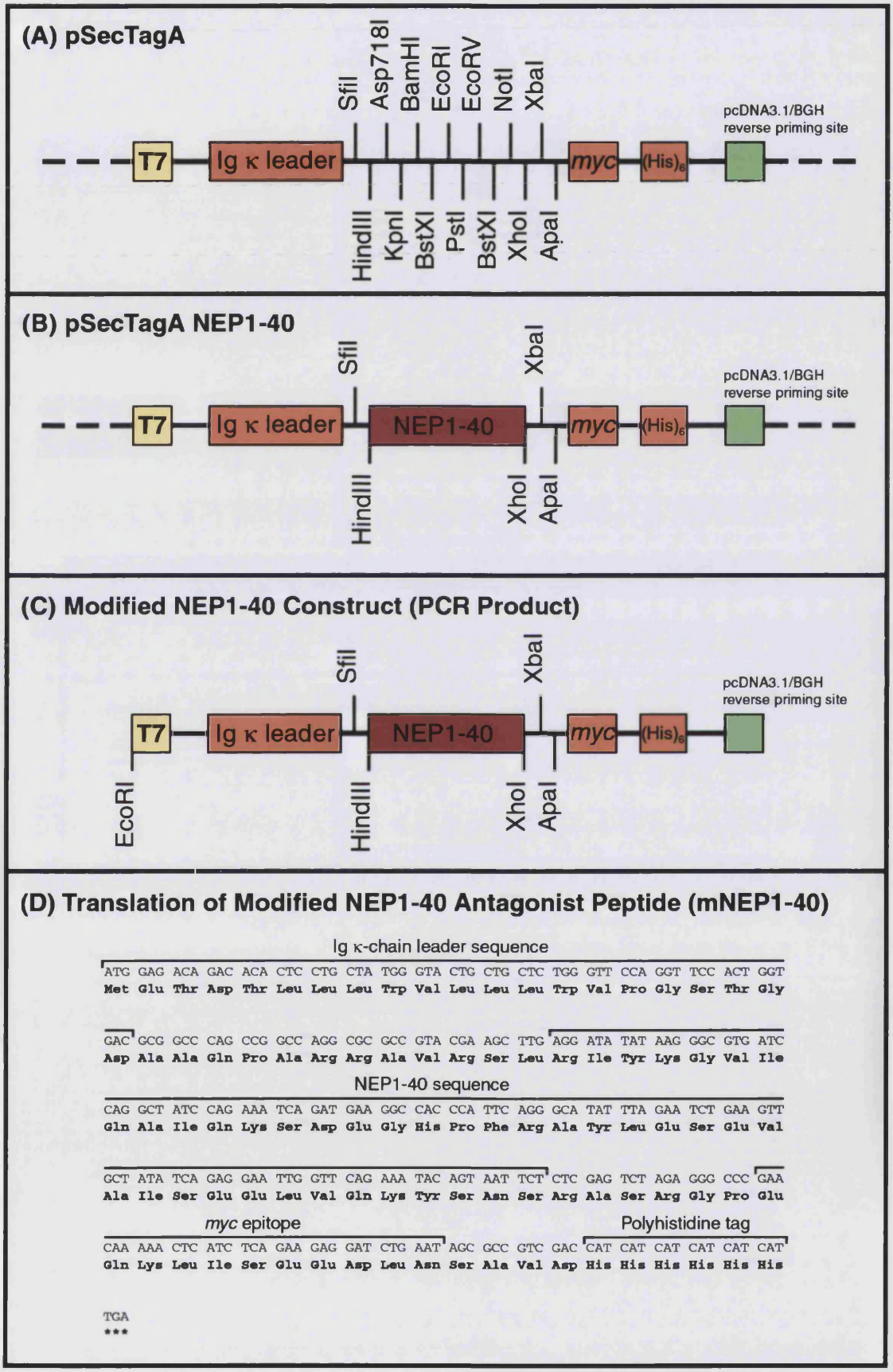
(A) pSecTagA
SfiI
Asp718I
BamHI
EcoRI
EcoRV
NotI
XbaI
pcDNA3.1/BGH
reverse priming site
T7
Ig κ leader
myc
(His)6
HindIII
KpnI
BstXI
PstI
BstXI
XhoI
ApaI
(B) pSecTagA NEP1-40
SfiI
XbaI
pcDNA3.1/BGH
reverse priming site
T7
Ig κ leader
NEP1-40
myc
(His)6
HindIII
XhoI
ApaI
(C) Modified NEP1-40 Construct (PCR Product)
SfiI
XbaI
pcDNA3.1/BGH
reverse priming site
T7
Ig κ leader
NEP1-40
myc
(His)6
EcoRI
HindIII
XhoI
ApaI
(D) Translation of Modified NEP1-40 Antagonist Peptide (mNEP1-40)
Ig κ-chain leader sequence
ATG GAG ACA GAC ACA CTC CTG CTA TGG GTA CTG CTG CTC TGG GTT CCA GGT TCC ACT GGT
Met Glu Thr Asp Thr Leu Leu Leu Trp Val Leu Leu Leu Trp Val Pro Gly Ser Thr Gly
GAC GCG GCC CAG CCG GCC AGG CGC GCC GTA CGA AGC TTG AGG ATA TAT AAG GGC GTG ATC
Asp Ala Ala Gln Pro Ala Arg Arg Ala Val Arg Ser Leu Arg Ile Tyr Lys Gly Val Ile
NEP1-40 sequence
CAG GCT ATC CAG AAA TCA GAT GAA GGC CAC CCA TTC AGG GCA TAT TTA GAA TCT GAA GTT
Gln Ala Ile Gln Lys Ser Asp Glu Gly His Pro Phe Arg Ala Tyr Leu Glu Ser Glu Val
GCT ATA TCA GAG GAA TTG GTT CAG AAA TAC AGT AAT TCT CTC GAG TCT AGA GGG CCC GAA
Ala Ile Ser Glu Glu Leu Val Gln Lys Tyr Ser Asn Ser Arg Ala Ser Arg Gly Pro Glu
myc epitope
Polyhistidine tag
CAA AAA CTC ATC TCA GAA GAG GAT CTG AAT AGC GCC GTC GAC CAT CAT CAT CAT CAT CAT
Gln Lys Leu Ile Ser Glu Glu Asp Leu Asn Ser Ala Val Asp His His His His His His
TGA
***

Figure 7.4.

Construction of replication-incompetent HSV-1 for the expression of mNEP1-40. A, schematic representation of pR19 hrGFP WPRE shuttle vector (Biovex Ltd.). B, schematic representation of pR19 mNEP1-40 WPRE shuttle vector. C, Southern blot for recombination of the pR19 mNEP1-40 WPRE cassette into 1764/4-/27in/RL1+ HSV-1 vector backbone.

(A) pR19 hrGFP WPRE

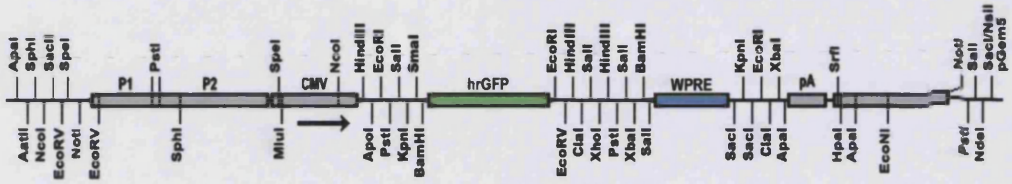

(B) pR19 mNEP1-40 WPRE

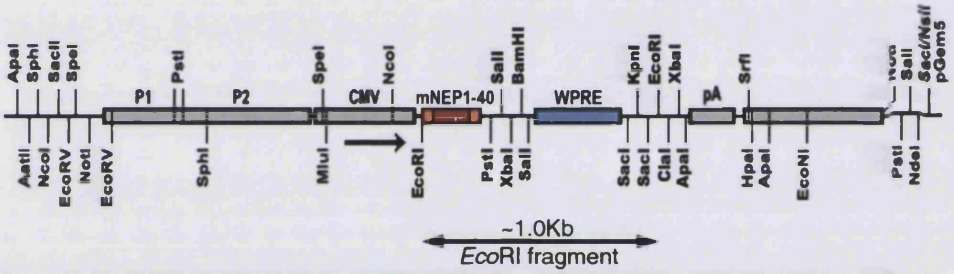

(C) Southern Blot for Recombinant Viral Plaques (1764/4-/27in/RL1+/pR19 mNEP1-40 WPRE)

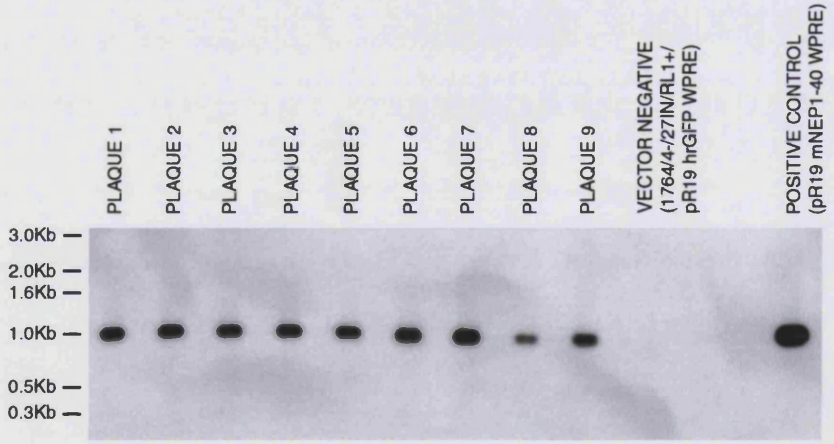

All DNA samples were digested with *Eco*RI. The blot was probed with radiolabeled mNEP1-40 PCR product.

Figure 7.5.

Microscopic capture of growth cone collapse and neurite retraction in cold-shocked differentiated PC12 cells. The growth media was replaced with ice-cold 1x HBSS, after induction of differentiation and neurite outgrowth by incubation with 100ng βNGF/ml media for 48 hours. Images of a single field were captured at one minute intervals, for a duration of 30 minutes. A time course is presented, illustrating widespread neurite retraction from 1 to 30 minutes post cold-shock. Scale bar = 50μm.

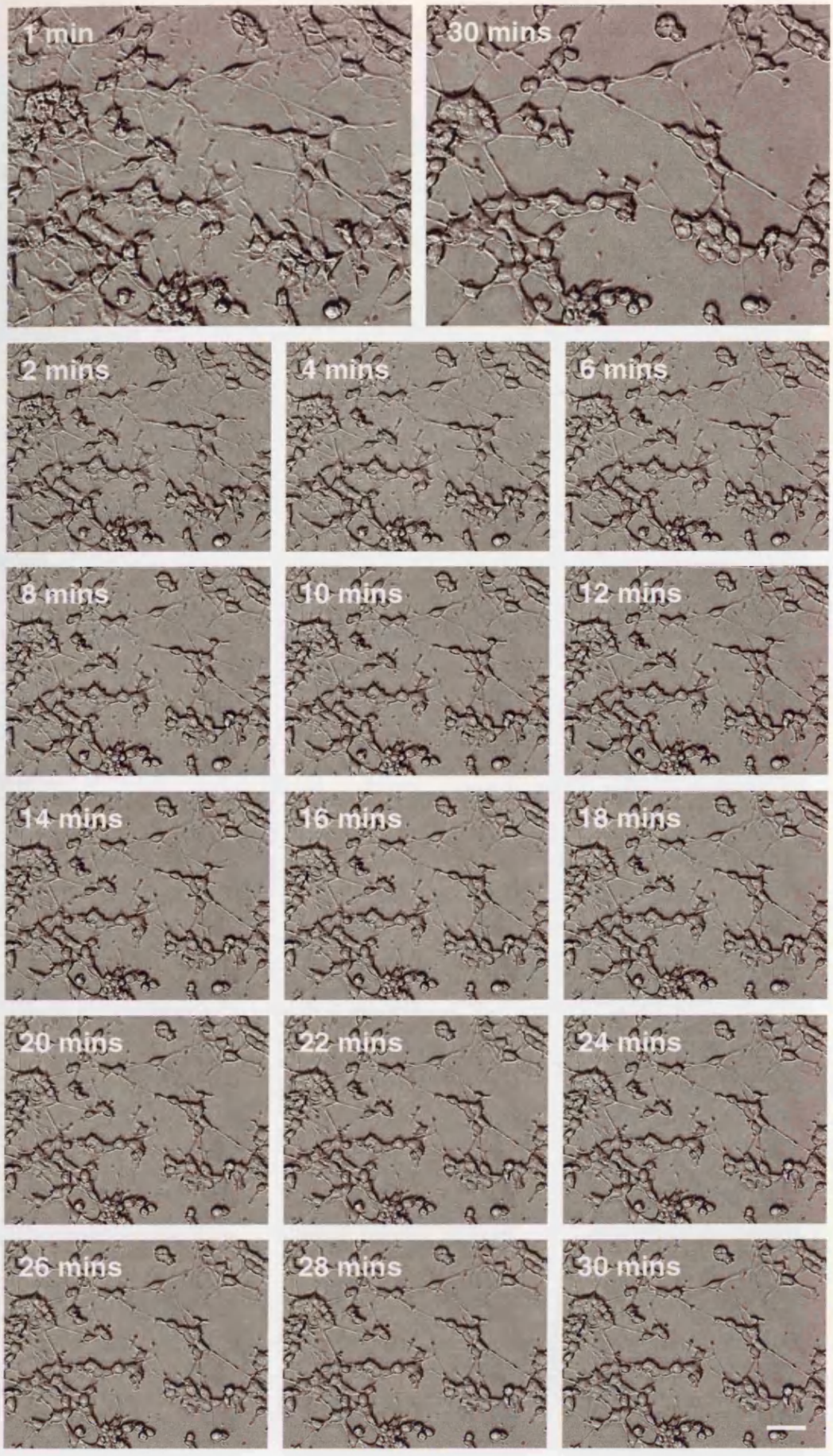
1 min
30 mins
2 mins
4 mins
6 mins
8 mins
10 mins
12 mins
14 mins
16 mins
18 mins
20 mins
22 mins
24 mins
26 mins
28 mins
30 mins

Figure 7.6.

Fixation of differentiated PC12 cells. Growth cones are indicated by arrows.

Scale bar = 50μm.

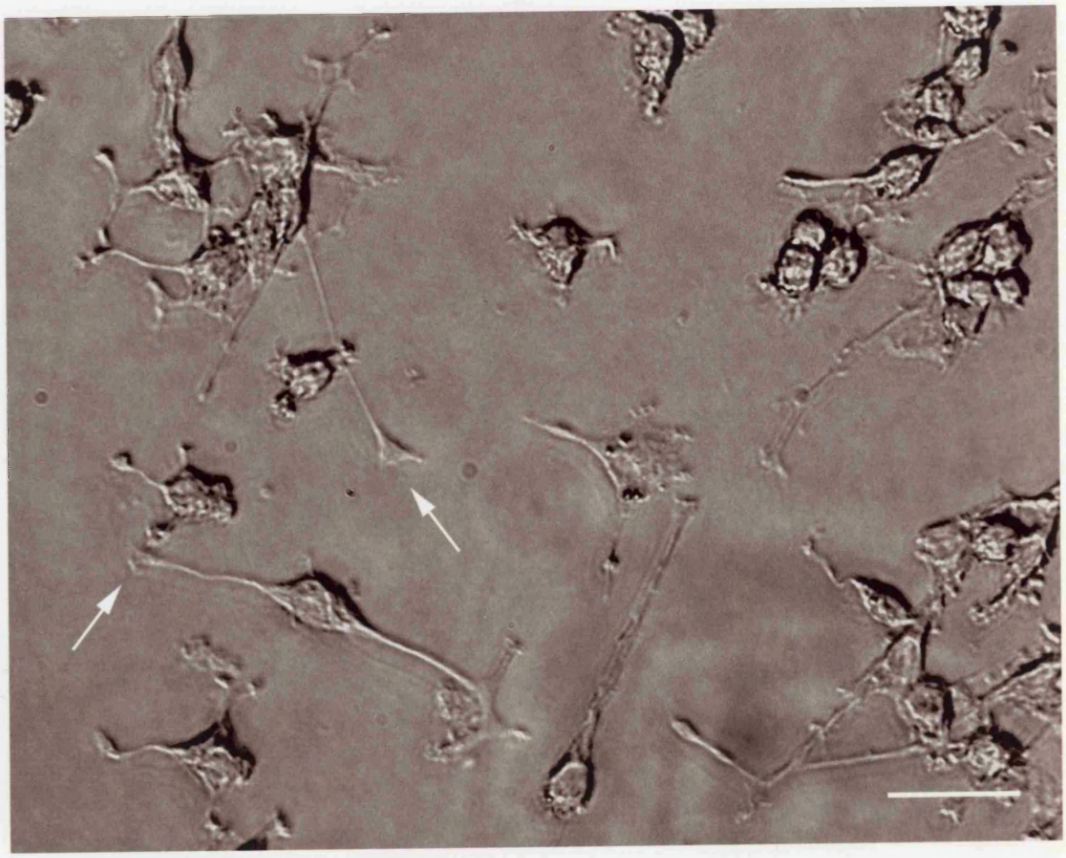

Figure 7.7.

Western blot for myc-tagged protein in the cell lysate of virally transduced BHKs. Cultured cells were transduced at an MOI of 1, and harvested at 48 hours post transduction. 20μg of protein were loaded per well, and resolved on a 20% polyacrylamide gel against high-molecular weight Rainbow marker (Amersham). The membrane was probed with anti-myc antibody (Invitrogen) at a dilution of 1:500, followed by HRP-conjugated goat anti-mouse antibody (Dako) at a dilution of 1:2000. The membrane was reacted with ECL reagent (Amersham), and exposed to film for 1 minute. The only detectable band was that of the positive control protein at ~60KDa. mNEP1-40 should have been detectable as a ~10KDa band. No additional bands were visible on longer exposure.

220
97
66
45
30
20.1
14.3
PLAQUE 1
PLAQUE 2
PLAQUE 3
PLAQUE 4
PLAQUE 5
PLAQUE 6
PLAQUE 7
PLAQUE 8
PLAQUE 9
1764/4-/27in/RL1+/pR19 mNEP1-40 WPRE
BHKs
VECTOR NEGATIVE CONTROL
(1764/4-/27in/RL1+/pR19 hrGFP WPRE)
POSITIVE CONTROL
(~60KDa myc-tagged protein)
mNEP1-40

Figure 7.8.

HSV-1 mediated transgene expression *in vitro* and *in vivo*.

A, HSV-1 mediated expression of mNEP1-40 (red) by BHKs after 48 hours, following transduction at an MOI of 20. B, the same field as in A visualized with the nuclear stain, bisbenzimide (blue). C, HSV-1 mediated expression of mNEP1-40 (red) by BHKs after 48 hours, following transduction at an MOI of 5. Perinuclear localization of mNEP1-40 is visible. D, Horizontal section of adult Sprague-Dawley rat cervical spinal cord, caudal to the injection site, 8 days post injection of $2x10^6$ pfu of 1764/4-/27in/RL1+/pR19 mNEP1-40 WPRE. Numerous mNEP1-40 expressing cells, some of which exhibit a neuronal morphology, can be seen spread diffusely throughout the field. The spinal canal is denoted by an asterisk. E and F, mNEP1-40 expressing cells were also present rostral to the injection site. Some of these also exhibited a neuronal morphology. G, Horizontal section through the ventral horn, 8 days post injection of $2x10^6$ pfu of 1764/4-/27in/RL1+/pR19 eGFP WPRE. A considerably higher level of transgene expression (green) is evident, compared to that obtained with 1764/4-/27in/RL1+/pR19 mNEP1-40 WPRE. eGFP, a non-secreted protein, clearly undergoes extensive axonal transport. (Scale bars A = 100μm, B = 100μm, C = 50μm, D = 100μm, E = 100μm, F = 50μm, G = 50μm).

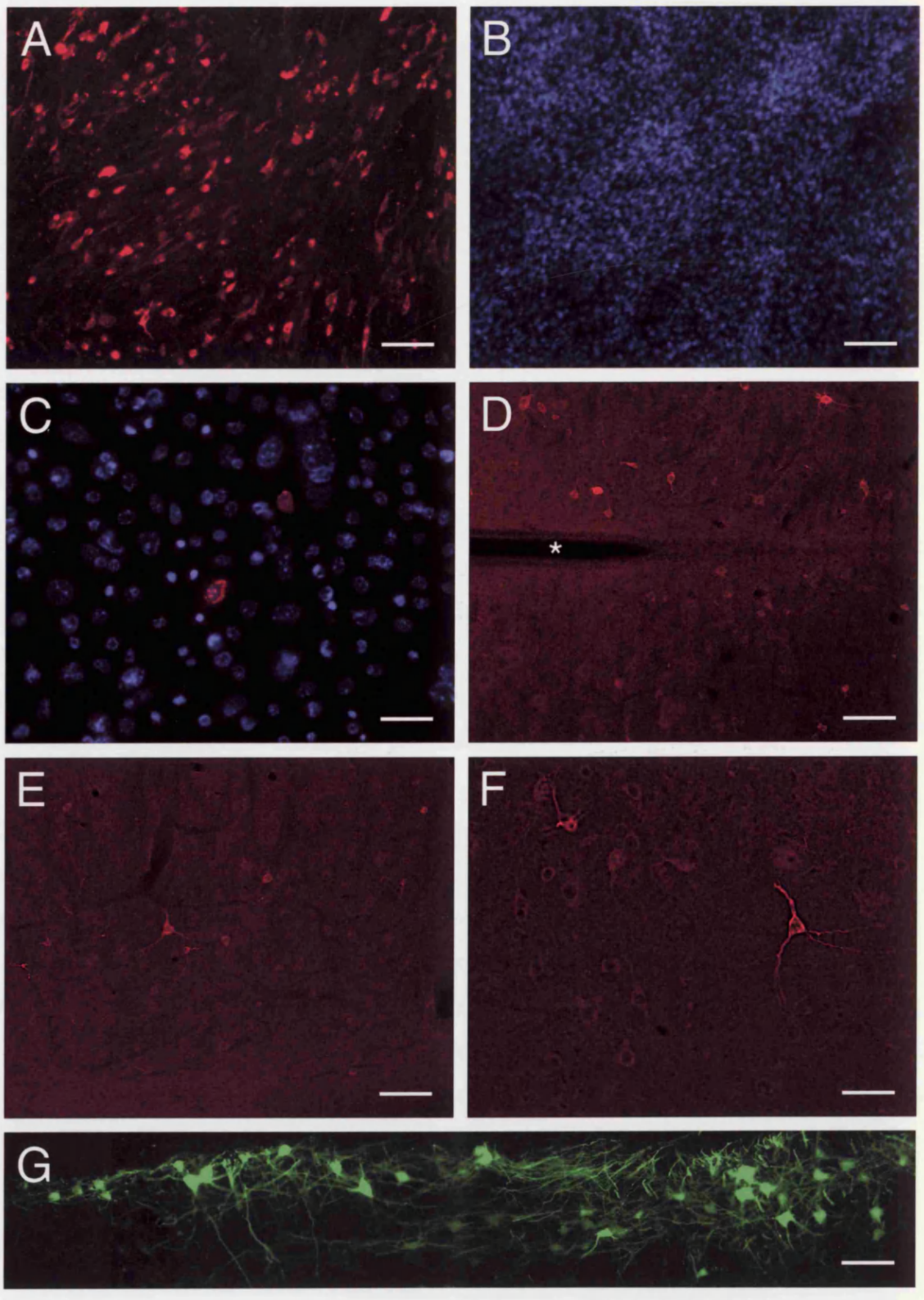
A
B
C
D
*
E
F
G

CHAPTER 8

Development of an HSV-1 Platform for the Mediation of RNA interference

INTRODUCTION

The discovery of short interfering RNAs (siRNAs), and the characterisation of their mechanism of action, has resulted in their widespread use in functional genomics over recent years. They suppress endogenous gene expression postranscriptionally by targeting short, and perfectly complementary, contiguous sequences of mRNA to those encoded in the antisense arm of the siRNA. This is achieved through the formation of a specialized complex of proteins, termed the RNA induced silencing complex (RISC) (Martinez et al., 2002). The controlled degradation of target mRNA is mediated by an as yet unidentified nuclease. If the target sequence is carefully selected, a single species of mRNA can be effectively targeted with greater than 90% downregulation of its normal level of protein expression (Elbashir et al., 2001c).

Traditionally, siRNAs were chemically synthesized and consisted of separate annealed sense and antisense strands of between 19-21 nucleotides, each with a 3' di-uridine overhang. These were typically used for *in vitro* functional genomic studies (reviewed by Bargmann, 2001), for example in the transfection of morphologically distinct *D.melangaster* cell lines to rapidly screen for genes underlying the cellular appearance (Kiger et al., 2003). Relatively recently, it was discovered that RNA-polymerase type III dependent promoters, such as U6 and H1, could be harnessed to transcribe short hairpin forms of siRNA from DNA vectors (Yu et al., 2002a; Sui et al., 2002a; Paul et al., 2002b; Paddison et al., 2002b; Miyagishi and Taira, 2002b). The activity of short hairpin RNA (shRNA) was found to be almost comparable to that of siRNA.

In the past, gene therapy has been limited to the supplementation of host cell gene expression. However, the developments in shRNA technology have, in turn, lead to the construction of effective virus-based gene therapy systems for the suppression of host cell gene expression. Reports have now emerged of successful delivery of functionally active shRNAs, driven by RNA polymerase III dependent promoters, using lentivirus (Rubinson et al., 2003), retrovirus (Brummelkamp et al., 2002b) and adenovirus (Shen et al., 2003). Invariably, in the fullness of time, viral systems will permit many new lines of experimental enquiry, especially into (i) gene function *in vivo*, and (ii) the molecular treatment of diseases (such as cancers, heritable genetic disorders in which mutant proteins are expressed, as well as viral diseases). Of course, gene silencing systems that can be effectively applied *in vivo* to neurons, which are post-mitotic, will also have enormous value in the study of CNS injury.

Many different proteins are expressed in CNS injury states that have been shown to be inhibitory to axonal regeneration *in vivo*, or neurite outgrowth *in vitro*. In the past, attempts to neutralise the activity of such molecules have included the administration of function-blocking antibodies (Schnell and Schwab, 1990; Schnell and Schwab, 1993), peptide antagonists (Grandpre et al., 2002), dominant negative proteins (Fischer et al., 2004) or chemical inhibitors of downstream signalling pathways (Dergham et al., 2002; Fournier et al., 2003). With any one of these methods, it is difficult to say with great certainty that the observed effects are the sole result of impeding the activity of the protein of interest. However, with the advent of RNAi technology, it should become increasingly less difficult to achieve transient, specific and effective knockdown of a given target protein – and this should yield more accurate results.

The aim of the work reported herein was to determine whether a platform for the expression of functional shRNA could be established in HSV-1, which is neurotropic and is inherently suited to gene therapy applications within the CNS. As a proof of principle, eGFP was targeted. However, a vector expressing shRNA against *ngr*, which would be of particular interest in the study of spinal injury, was also constructed.

Activation of the double-stranded RNA dependent protein kinase (PKR) in eukaryotic cells brings about absolute cellular shut-down of translation (Clemens and Elia, 1997), which is an obvious impediment to DNA-vector based attempts to specifically downregulate a target gene using a long-hairpin RNA approach. However, HSV-1 has evolved to overcome this host-cell activity through the function of ICP34.5 – the neurovirulence factor – which has been shown to prevent the PKR response to double-stranded RNA (He et al., 1997; Randazzo et al., 1997; Leib et al., 2000). For this reason, HSV-1 is theoretically well-suited to both short- and long-hairpin approaches to post-transcriptional gene silencing (PTGS). Since it is already known that RNA polymerase II dependent promoters work well when flanked by the LAT promoters, whereas no data are yet available on the function of RNA polymerase III dependent promoters in this context, it was decided that a direct comparison of the two approaches should be made against eGFP in an *in vitro* assay.

SUMMARY OF METHODS

Construction of HSV-1 for the Expression of Short-Hairpin RNA (against eGFP or NgR)

First, the pBluescript II SK+ plasmid (Stratagene; Fig 1A) was digested with *Apa*I, blunted with T4 DNA polymerase and re-ligated. This vector was termed pBS (*Apa*I minus) (Fig 1B). The human U6 snRNA promoter sequence (-265 to +1) was amplified by nested PCR from HT1080 cell line genomic DNA (extracted with DNAzol (Gibco), according to the manufacturer's instructions), using the primer pairs: (i) CAA AAC GCA CCA CGT GAC and CAG GGG CCA TGC TAA TCT T, followed by (ii) AGT CAC TAG TCA AGG TCG GGC AGG AAG A and ACT GAA GCT TCA GTC TGG GCC CGG TGT TTC GTC CTT TCC AAG. The PCR product was digested with *Spe*I and *Xho*I, resolved on a 1% agarose gel, excised, purified with GFX columns (Amersham) and ligated between the *Spe*I and *Xho*I sites of pBS (*Apa*I minus). This vector was termed pBS (*Apa*I minus) U6 (Fig 1C). The promoter sequence was verified by automated fluorescent dye sequencing. Preparation of the vector backbone for ligation of the short-hairpin encoding oligonucleotide entailed digestion with *Apa*I and *Xho*I, and

subsequent gel-purification of the backbone fragment. The custom-made, FPLC-purified, 5′-phosphorylated sense and antisense deoxyribonucleotides were mixed in equimolar ratio, heated to 65°C for 10mins in annealing buffer (10nm Tris-HCl, 100mM NaCl, 1mM EDTA in DEPC water), and left to cool to room temperature overnight. These hybridized adaptor sequences were subsequently ligated into the *Apa*I and *Xho*I digested backbone. GT116 cells (Invivogen), which have been genetically modified specifically for the propagation of DNA hairpin structures, were used in the transformation. These *E.coli* lack the *sbcC* and *sbcD* proteins that are involved in recognition and cleavage of such structures (Connelly et al., 1998).

Originally, it was intended that a previously reported anti-eGFP shRNA sequence (Yu et al., 2002b) should be used in the construction of the HSV-1 U6 anti-eGFP shRNA vector. However, this was hindered by the fact that mutation/recombination of the custom-made adaptor sequence always arose during plasmid propagation. Ultimately, a new unverified target sequence within eGFP was selected, which did not produce any of these complications. Each shRNA encoding adaptor sequence consisted of annealed sense and antisense PAGE purified oligonucleotides. For the construction of HSV-1 anti-eGFP shRNA the sense and antisense oligonucleotides were **AAGCTGACCCTGAAGTTCA**-TTCAAGAGA-**TGAACTTCAGGGTCAGCTT**-TTTTTT*AGATCT*C and TCGAG*AGATCT*AAAAAA-**AAGCTGACCCTGAAGTTCA**-TCTCTTGAA-**TGAACTTCAGGGTCAGCTT**-GGCC,
respectively. The target sequence, AAGCTGACCCTGAAGTTCA, corresponds to bases 124 to 142 of the eGFP coding sequence of peGFP-N1 (Clontech) (Genbank Accession No. U55762). For the construction of HSV-1 anti-NgR shRNA the sense and antisense oligonucleotides were **AATGAGCCCAAGGTCACAA**-TTCAAGAGA-**TTGTGACCTTGGGCTCATT**-TTTTTT*AGATCT*C and TCGAG*AGATCT*AAAAAA-**AATGAGCCCAAGGTCACAA**-TCTCTTGAA-**TTGTGACCTTGGGCTCATT**-GGCC,
respectively. The target sequence, AATGAGCCCAAGGTCACAA, corresponds to bases 103 to 121 of the rat *ngr* reference sequence (Genbank Accession No. NM_053613). In both constructs, a previously reported loop sequence, TTCAAGAGA, was used (Brummelkamp et al., 2002a). Also, in each case, a *Bgl*II restriction site (*AGATCT*) was incorporated after the poly-thymidine transcription termination signal, so

that a gain of sensitivity to the *Bgl*II restriction endonuclease could be employed as screening method for positive clones. The shRNA encoding sequence in the pBS (*Apa*I minus) U6 shRNA vector was verified by automated fluorescent dye sequencing, prior to the subcloning of the U6 shRNA cassette into the shuttle vector.

The pR19 shuttle vector into which the human U6 promoter, complete with hairpin sequence, were to be cloned had to be modified. pR19 IRES eGFP (Fig. 8.3.A) was digested with *Eco*RV to remove a small fragment (~200bp) from the upstream LAT flanking region, creating the vector pR19 (*Spe*I minus) IRES eGFP. This eliminated a superfluous *Spe*I site, which would have otherwise prevented the excision of the CMV promoter and IRES eGFP sequence using the *Spe*I and *Xho*I restriction sites. These sites were required for the insertion of the human U6 shRNA cassette, which was excised from the relevant pBS (*Apa*I minus) U6 shRNA vector with the *Spe*I and *Xho*I restriction endonucleases. This final shuttle vector, termed pR19 (*Spe*I minus) U6 shRNA, was linearized with *Sca*I for co-transfection with 1764/4-/27in/RL1+ viral DNA to generate recombinant HSV-1.

Construction of HSV-1 for the Expression of Long-Hairpin RNA against eGFP

For the purpose of generating long hairpin RNAs, the RNA polymerase II dependent CMV promoter is suitable, meaning that the unmodified pR19 backbone vector was identified as an appropriate shuttle vector in which to construct the long hairpin sequence against eGFP. The first strand of the hairpin (antisense) was amplified by PCR using the primers GTC AAA GCT TAA GTC GTG CTG CTT CAT GTG and GTC ACT CGA GGT CAA TCG ATA CGT AAA CGG CCA CAA GTT C. This strand corresponds to bases 65-251 of the eGFP coding sequence within the template vector peGFP-N1 (Genbank accession No. U55762), and was ligated into the pR19 backbone between the *Hind*III and *Xho*I restriction sites. The primers were designed such that the forward primer contained an internal *Hind*III site and the reverse primer, both *Xho*I and *Cla*I *sites*. The second strand of the hairpin (sense) was amplified by PCR using the primers GTC AAA GCT TGT CAA TCG ATA CGT AAA CGG CCA CAA GTT C and GTC ACT CGA GAA GTC GTG CTG CTT CAT GTG. The forward primer contained internal

*Hind*III and *Cla*I restriction sites and the reverse primer a *Xho*I site. The intermediate 'pR19 AS eGFP strand' vector was linearized with *Cla*I and *Xho*I and the second strand (sense) was ligated between these sites. Purpose-engineered GT116 *E.coli* (Invivogen), which have a ΔsbcCD genotype (Connelly et al., 1998), were transformed (as described in Chapter 2) for the propagation of the hairpin-containing plasmid. The shuttle vector was used to co-transfect 27/12/M:4 cells with 1764/4-/27in/RL1+/pR19 hrGFP WPRE viral DNA in order to generate recombinant HSV-1.

Lentivirus (LV)

All lentiviruses used in this study were kindly provided by Sam Wilson (Department of Immunology and Molecular Pathology, UCL). The viruses were replication-incompetent second generation HIV-1, pseudotyped with the vesicular stomatitis virus coat protein G (VSV-G) for enhanced transduction of non-dividing cells. A modified form of a previously reported vector genome, pHR-SIN-CSGW (Demaison et al., 2002), in which the U6-shRNA cassette had been incorporated and the eGFP gene replaced with PAC, was used in a three-plasmid transient transfection with pCMVR8.91 (the packaging plasmid) and pMD-G (the VSV-G expressing plasmid). The growth medium, which contained recombinant HIV-1, was collected and stored at -80°C.

The lentivirus cassette for the expression of shRNA contained the human U6 promoter (-315 to +1), followed by *Sal*I and *Xba*I sites. The shRNA encoding adaptor sequence was ligated between the *Sal*I site, which had first been blunted with mung bean nuclease, and the *Xba*I site. The shRNA had been designed such that sense strand of 23 nucleotides was transcribed first, followed by TTCG loop sequence, and then the 23 nucleotide antisense strand. A poly-thymidine transcription termination signal was incorporated immediately after the antisense strand sequence. The sense and antisense oligonucleotides used in the construction of the anti-eGFP shRNA encoding adaptor sequence for lentivirus were **TTCATCTGCACCACCGGCAAGC**-TTCG-**GCTTGCCGGTGGTGCAGATGAAC**-TTTTT and CTAG-AAAAA-**GTTCATCTGCACCACCGGCAAGC**-CGAA-**GCTTGCCGGTGGTGCAGATGAA**, respectively. The target sequence, GTTCATCTGCACCACCGGCAAGC, corresponds to residues 138-160

of the eGFP coding sequence of peGFP-N1 (Clontech) (Genbank Accession No. U55762). The sense and antisense oligonucleotides used in the construction of anti-LacZ shRNA encoding adaptor sequence were **CTGTGATTGCGTCTGGGTTTGC**-TTCG-**GCAAGCCCGGGCGTAATCATAGC**-TTTTT and CTAG-AAAAA-**GCTATGATTACGCCCGGGCTTGC**-CGAA-**GCAAACCCAGACGCAATCACAG**, respectively. The target sequence, CTATGATTACGCCCGGGCTTGC, corresponds to bases 5-26 of the β-galactosidase coding sequence (Genbank Accession No. M34519).

Construction of eGFP-Expressing Stable Cell Line

BHK cells were transfected with *Apa*LI-linearized peGFP-N1 (Clontech), and an eGFP-expressing stable cell line was generated as described in Chapter 2. Based on cellular fluorescence and morphology, clone 2B1 was selected for use in the experiments reported here. Analysis by flow cytometry revealed that the green fluorescence measurements (FL1-H) of the 2B1 clone was 10^3 fold higher than that of normal BHKs.

Viral Transduction of the 2B1 Cell Line

2B1 cells were transduced with 1764/4-/27in/RL1+/pR19 anti-eGFP shRNA, 1764/4-/27in/RL1+/pR19 anti-NgR shRNA, or 1764/4-/27in/RL1+/pR19 anti-eGFP lhRNA at an MOI of 5, or the cells were mock transduced. Alternatively, 2B1 cells were transduced with LV anti-eGFP shRNA or LV anti-LacZ shRNA, or the cells were mock transduced. Four days post infection, cellular fluorescence was analysed by flow cytometry, as described in Chapter 2.

Double Transduction of BHKs with HSV-1

BHKs were transduced with 1764/4-/27in/RL1+/pR19 anti-eGFP shRNA, 1764/4-/27in/RL1+/pR19 anti-NgR shRNA, or 1764/4-/27in/RL1+/pR19 anti-eGFP lhRNA at an MOI of 5, or the cells were mock transduced. 24 hours later, the cells were superinfected with 1764/4-/27in/RL1+/pR19 eGFP WPRE at an MOI of 1. After a further 48 hours, cellular fluorescence was analysed by flow cytometry.

Transduction of Dissociated Cultures of Rat P8 Cerebellar Granule Neurons

Dissociated cultures of rat P8 cerebellar granule neurons were prepared as described in Chapter 2. After 2 days in culture, the cells were transduced with 1764/4-/27in/RL1+/pR19 anti-NgR shRNA, 1764/4-/27in/RL1+/pR19 anti-eGFP shRNA, or 1764/4-/27in/RL1+/pR19 eGFP WPRE at an MOI of 1, or the cells were mock transduced. After a further 2 days in culture, total RNA was extracted using Trizol reagent (Gibco). These samples were treated with DNaseI (DNA-free; Ambion) to eliminate any contaminating genomic DNA, as per the manufacturer's instructions. cDNA was subsequently produced, as described in Chapter 2, for analysis by quantitative PCR.

Taqman® Quantitative PCR

Quantitative PCR was performed as described in Chapter 2. The forward (CGT GGC TTG CAC AGT CTT GA) and reverse (AGG TCC CGG AAG GCA TGT) rat *ngr* primers corresponded to bases 595-614 and 657-674 of NM_053613, respectively. The Probe (CGT CTC CTC TTG CAC CAG AAC CAT GTG) corresponded to bases 616-642, and possessed a 5′ 6-FAM Fluor label. The concentration of primers and probe were optimized (Fig. 2.1), as recommended by the manufacturer, prior to use in sample analysis. The ribosomal 18S subunit was used as an endogenous control, i.e. for normalisation of sample values (Eukaryotic ribosomal 18S subunit; Pre-Developed Taqman® Assay Reagents; Applied Biosystems, UK.). The PCR of *ngr* and 18S was performed on an ABI7000 as singleplex reactions. The standard curves and 'no template control' reactions were included on the same plate as the respective samples. Each reaction was performed in triplicate.

RESULTS

Construction of HSV-1 for the Expression of Short-Hairpin RNA

The human U6 promoter (-265 to +1) was ligated into the *Spe*I and *Xho*I sites of an *Apa*I minus version of pBluescript II SK+ (Figs. 8.1.A-C). The shRNA encoding adaptor sequence was ligated between the *Apa*I site, within the U6 promoter fragment, and the

vector *Xho*I site (Fig. 8.1.D). The shRNA encoding adaptor sequence for both the anti-eGFP and anti-NgR constructs followed a generic design (Fig. 8.1.E), in which the sense and antisense strands of the hairpin were each 19 nucleotides long, and separated by a standard nine-nucleotide loop sequence, with the sense strand being transcribed first (Brummelkamp et al., 2002a). A poly-thymidine transcription termination signal followed the antisense strand. This, in turn, was followed by a *Bgl*II restriction site, so that a gain of restriction endonuclease sensitivity could be used to identify positive clones. The adaptor sequence was designed such that it had an upstream *Apa*I overhang, and downstream *Xho*I overhang, for ligation into the pBS (*Apa*I minus) U6 vector (Fig. 8.1.C). The generic shRNA derived from this U6 shRNA cassette would be expected to be processed by Dicer to form conventional siRNA (Fig. 8.2).

The U6 shRNA cassette was subcloned into the *Spe*I and *Xho*I sites of a modified form of the pR19 IRES eGFP shuttle vector, which lacked a superfluous *Spe*I site in the upstream LAT flanking region (Figs. 8.3.A-C). The shuttle vector was used in a co-transfection with 1764/4-/27in/RL1+ viral DNA in order to generate recombinant HSV-1, expressing shRNA from the LAT regions (Figs. 8.4.D and E). Southern blots were performed to detect recombinant viral plaques of HSV-1 anti-eGFP shRNA and HSV-1 anti-NgR shRNA (Figs. 8.4.A and B).

Construction of HSV-1 for the Expression of Long-Hairpin RNA against eGFP

The antisense strand of the long-hairpin encoding sequence, corresponding to bases 65-251 of the eGFP coding sequence, was ligated into the *Hind*III and *Xho*I sites of the pR19 IRES eGFP shuttle vector, thus replacing the IRES eGFP transgene (Figs. 8.5.A and B). The sense strand, corresponding to exactly the same region of the eGFP coding sequence, was subcloned between the *Cla*I and *Xho*I sites (Fig. 8.5.C). This shuttle vector was termed pR19 anti-eGFP lhRNA and was used in a co-transfection with 1764/4-/27in/RL1+ viral DNA in order to generate recombinant HSV-1. A southern blot was performed to detect recombinant viral plaques (Fig. 8.5.D).

Stable eGFP-Expressing BHK cells (clone 2B1)

A stable eGFP-expressing BHK cell line, termed clone 2B1, was generated for use in *in vitro* assays of anti-eGFP shRNA activity. These cells are fibroblasts, and are readily transducible with HSV-1. Fluorescence and bright field microscopy, as well as flow cytometry, were used to gauge the intensity and uniformity of eGFP expression (Fig. 8.6.A-C). By microscopy, most of the cells appeared to express eGFP at similar intensity (Fig. 8.6.A). However, when compared to BHKs by flow cytometry, it was apparent that 7.6% of the 2B1 population was non-fluorescent according to FL1-H measurements. In contrast, 88.6% of 2B1 cells were highly fluorescent, and 3.8% weakly fluorescent (Fig. 8.6.C).

eGFP Expression by 2B1 Cells Transduced with HSV-1 anti-eGFP shRNA

2B1 cells were transduced with HSV-1 anti-eGFP shRNA, HSV-1 anti-NgR shRNA, or HSV-1 anti-eGFP lhRNA at an MOI of 5, or the cells were mock transduced. Four days post transduction, cellular fluorescence was assessed by microscopy and flow cytometry (Fig. 8.7.A and B). No difference in the level of fluorescence was discernible between mock transduced, HSV-1 anti-NgR shRNA or HSV-1 anti-eGFP lhRNA transduced cells by fluorescence microscopy. However, the HSV-1 anti-eGFP shRNA transduced cells appeared slightly less fluorescent (Fig. 8.7.A). By flow cytometry, 32.9% and 30.8% reduction in median fluorescence were detected in the HSV-1 anti-NgR shRNA and HSV-1 anti-eGFP lhRNA treated cells, compared to mock transduced cells. HSV-1 anti-eGFP shRNA transduction resulted in a 59.7% reduction in median fluorescence (Fig. 8.7.B and C).

eGFP Expression by 2B1 Cells Transduced with LV anti-eGFP shRNA

Another postgraduate research student, Sam Wilson, in the Department of Immunology and Molecular Pathology at UCL had also been constructing viruses expressing shRNA. However, he had made lentiviruses (VSV-G pseudotyped second generation replication-incompetent HIV-1) for the expression of shRNA against various targets, including eGFP. In the preliminary experiments, it had been shown that the LV anti-eGFP shRNA virus reduced eGFP expression by stable eGFP-expressing Hela cells by ~90%. Having

discussed the similarity of the two projects, it was decided that his LV anti-eGFP shRNA virus be assayed in the *in vitro* system reported here to (i) confirm the previous finding and, thus, validate the assay system, and (ii) make a crude comparison with the equivalent HSV-1 vector.

First, it was necessary to establish whether the BHK cells can be transduced with lentivirus. Using a lentivirus expressing eGFP, it appeared that these cells were readily amenable to transduction, with apparently all cells expressing eGFP after two days (Fig. 8.8.A). The lentivirus U6-shRNA cassette was slightly different to that used in HSV-1 (Fig. 8.8.B). The shRNA encoding sequence had been blunt ligated into the transcription start site, consisted of longer 23-nucleotide sense and antisense hairpin strands, and contained a shorter four-nucleotide loop sequence than was used in HSV-1. Other differences are described in the summary of methods. LV anti-eGFP shRNA, or LV anti-LacZ shRNA, were used to transduce 2B1 cells. After four days, the fluorescence of virally-transduced and mock transduced cells was compared by microscopy and flow cytometry (Fig. 8.8.C-D). No difference between the cellular fluorescence of mock or LV anti-LacZ transduced 2B1 cells was obvious by microscopy. In comparison, LV anti-eGFP shRNA transduced cells were barely visible by fluorescence microscopy (Fig. 8.8.C). By flow cytometry, median fluorescence readings were reduced by 85.4% and 4.4% in LV anti-eGFP shRNA and LV anti-LacZ shRNA samples, respectively, compared to mock transduced 2B1 cells (Figs. 8.8.D and E).

Effect of HSV-1 anti-eGFP shRNA on the Onset of eGFP Expression

BHKs were first transduced with HSV-1 anti-eGFP shRNA, HSV-1 anti-NgR shRNA, or HSV-1 anti-eGFP lhRNA at an MOI of 5, or the cells were mock transduced. 24 hours later, the cells were transduced with HSV-1 eGFP WPRE at an MOI of 1. Fluorescence microscopy and flow cytometry were performed to determine cellular fluorescence (Figs. 8.9.A-C). By microscopy, the level of fluorescence was similar in the HSV-1 eGFP-only and HSV-1 anti-eGFP shRNA samples, whereas it was considerably higher in the HSV-1 anti-NgR shRNA and HSV-1 anti-eGFP lhRNA samples (Fig. 8.9.A). This was confirmed by flow cytometry (Figs. 8.9.B and C). The median fluorescence values were

normalized against those of the HSV-1 eGFP-only sample. The median fluorescence of the HSV-1 anti-eGFP shRNA, HSV-1 anti-NgR shRNA, and HSV-1 anti-eGFP lhRNA samples were 81.8%, 214.7% and 255.0% relative to that of the control HSV-1 eGFP-only sample, respectively (Fig. 8.9.D).

Expression of *ngr* by HSV-1 Transduced Rat P8 Cerebellar Granule Cells

Dissociated cultures of rat P8 cerebellar granule cells were transduced, after two days in culture, with HSV-1 anti-NgR shRNA, HSV-1 anti-eGFP shRNA, or HSV-1 eGFP WPRE at an MOI of 1, or the cells were mock transduced. After a further 2 days in culture, *ngr* transcript expression was analysed by quantitative PCR. Relative to the level of *ngr* mRNA detectable in mock transduced P8 CGCs, the HSV-1 anti-NgR shRNA sample contained 20.8% less of the transcript. This compared to a 9.3% and 6.9% reduction in transcript levels in the HSV-1 anti-eGFP shRNA and HSV-1 eGFP WPRE samples, respectively (Fig. 8.10).

DISCUSSION

The aim of the work reported here was to demonstrate, as a proof of principle, that HSV-1 can be successfully manipulated for the delivery of functional shRNA. To this end, recombinant HSV-1 was generated to drive transcription of shRNA against eGFP or NgR from the human U6 promoter. In addition, recombinant virus was constructed for the expression of long hairpin RNA. The rationale for this being that the viral protein ICP34.5 should block with the mammalian host cell PKR response, which otherwise occurs in the presence of long double stranded RNA and results in the absolute shut-down of cellular translation. It was thought that, if successful, this approach would obviate the need to limit the RNA hairpin length to less than 30bp, and that it could potentially be more efficacious than shRNA owing to the longer target sequence.

HSV-1 Mediated Delivery of anti-eGFP shRNA and lhRNA

Of the two anti-eGFP viruses, only that expressing the shRNA against eGFP had any effect on the expression of eGFP by the 2B1 stable cell line. Flow cytometric analysis

revealed a 59.7% reduction in fluorescence, which was also apparent by fluorescence microscopy, compared to mock transduced 2B1 cells. In contrast, the anti-eGFP lhRNA virus exhibited no more effect in reducing the fluorescence profile of the stable cells than did the anti-NgR shRNA virus. Therefore, this must be considered a non-specific effect resulting from the process of viral transduction.

Even in the experiment in which BHKS were first infected with viruses expressing hairpins, and then superinfected 24 hours later with a virus expressing eGFP, it appeared that the virally-expressed anti-eGFP hairpins had an effect on the resultant eGFP expression. Although, in absolute terms, there was only a marginal reduction in fluorescence compared to the eGFP only control sample, this must be considered in the context of viral gene dosage and the role of viral proteins, such as ICP0, which are known to effect a generalized upregulation in gene expression soon after transduction (Samaniego et al., 1997; Jordan and Schaffer, 1997; Kawaguchi et al., 1997a). For example, the anti-NgR shRNA and anti-eGFP lhRNA samples, like the anti-eGFP shRNA sample, were transduced on two occasions: first with the virus of interest at an MOI of 5, and 24 hours later with an eGFP-expressing virus at an MOI of 1. Whereas the eGFP only sample was first mock transduced, and 24 hours later transduced with an eGFP-expressing virus at an MOI of 1. In other words, the control sample contained only one sixth the number of copies of viral genome as the samples of interest. That the level of fluorescence observed in the anti-NgR shRNA and anti-eGFP lhRNA samples was greater than two-fold higher than the level of fluorescence observed in the eGFP only control sample is of considerable significance. It implies that the level of fluorescence of the anti-eGFP shRNA sample would have been equally as high if it did not have any effect on eGFP expression. The fact that the level of fluorescence in the anti-eGFP shRNA sample was only marginally lower than that of the eGFP only sample is somewhat irrelevant in this experimental model, since it has to be compared directly to the anti-NgR shRNA sample to account for the effect of viral gene dosage. In this light, it would appear that HSV-1 mediated delivery of anti-eGFP shRNA has a significant effect on eGFP gene expression, whereas HSV-1 mediated delivery of anti-eGFP lhRNA has none.

The HSV-1 viral genome has a considerable propensity to rearrange itself by homologous recombination, and the complete lack of activity of the anti-eGFP lhRNA obviously raises the question of whether the lhRNA sequence might have been lost during the rounds of viral replication needed to produce a high-titre stock. If that were the case, there would be no conceivable future for HSV-1-mediated lhRNA delivery. The absence of anti-eGFP activity could potentially be explained by the selection of ineffectual target sequence. However, in this study, bases 65-251 of the eGFP coding sequence were targeted which, of course, includes sequences that were effectively targeted by the HSV-1 and LV anti-eGFP shRNA vectors (bases 124-142, and 138-160, respectively). It is unlikely the difference in strand order (antisense-loop-sense in the long-hairpin construct vs. sense-loop-antisense in the short-hairpin constructs) would have had any bearing on the difference in effect, since the long double-stranded RNA should be endogenously processed to multiple different siRNAs of 21-23 nucleotides in length (Elbashir et al., 2001b). Structurally, these siRNAs should have 180° of rotational symmetry – thus, the initial strand order would be irrelevant. In any event, it is clear that there was no PKR response (which can elicit complete translational shut-down). Nonetheless, further work will be necessary before any definitive conclusions can be made about the value of this system in HSV-1, particularly in view of the recent description of additional measures that can be taken to enhance the silencing activity of long-hairpin systems (Shinagawa and Ishii, 2003); these entail the removal of both the 5′ mRNA cap and 3′ polyadenylate tail, such that the transcribed long-hairpin RNA is retained within the nucleus.

HSV-1 vs. Lentivirus

The median fluorescence of 2B1 cells was reduced by 85.4% or 4.4%, following transduction with lentivirus expressing anti-eGFP shRNA or anti-LacZ shRNA, respectively. The latter is a non-specific effect relating to the process of viral transduction. There are several potential explanations for the difference in effect between lentivirus and HSV-1 mediated delivery of anti-eGFP shRNA.

First, and probably most important, is the difference in eGFP target sequence. It is well documented that the selection of an appropriate target sequence within the transcript of

interest is critical to the success of RNAi (Elbashir et al., 2001c). This is, in part, believed to be due to the fact that only one siRNA stand is assembled into the RNA induced silencing complex (RISC) (Martinez et al., 2002), and that this association is influenced by strand nucleotide composition (Schwarz et al., 2003; Khvorova et al., 2003). Should the sense siRNA strand have the greater affinity for RISC than the antisense strand, then optimal silencing of the target will not be observed. Although algorithms have been devised for the selection of appropriate target sequence, this has not totally eliminated the trial-and-error element of the process. Ideally, numerous siRNAs should be synthesized and their effect on the target molecule characterized *in vitro*, in order to select the target sequence that produces optimal knock-down. Unfortunately, in this instance, there was insufficient time to undertake this screening process prior to the construction of recombinant HSV-1. Originally, a verified target sequence within eGFP was selected (Yu et al., 2002b) but, inexplicably, this was always found to mutate during plasmid amplification. Ultimately, a new target sequence within the eGFP coding sequence (bases 124-142) was selected using an algorithm (Elbashir et al., 2001c). This was unverified experimentally, but did not mutate during plasmid amplification. The target sequence used in the lentivirus construct, which was very effective in silencing eGFP expression, corresponded to bases 138–160 of the eGFP coding sequence.

It should also be noted that there are two commonly used lengths of human U6 promoter, -265 to +1 (Lee et al., 2002; Paddison et al., 2002a) and -315 to +1 (Sui et al., 2002b); the shorter form was used in HSV-1, and the longer form in the lentivirus. This is unlikely to account for much difference in effect between the two viruses, since both forms of the promoter have been used successfully in DNA vectors to dramatically reduce target gene expression (Lee et al., 2002; Paddison et al., 2002a; Sui et al., 2002b).

It is also possible, but unlikely, that some of the difference in effect could be attributed to alternative shRNA cloning strategies. In HSV-1, the shRNA coding sequence is cloned into an *Apa*I overhang, the first base of which corresponds to the transcription start site. This would result in a 5′ pentanucleotide overhang which, theoretically, should be degraded (Fig. 8.2). In lentivirus, the shRNA coding sequence was ligated blunt to the

transcription start site, meaning that no 5′ overhanging sequence would be present in the hairpin structure. Also, the sense and antisense strands of the hairpin were designed to be 23 nucleotides in length, with a 4-nucleotide loop sequence. This compares with strand lengths of 19 nucleotides, and a loop sequence of 9 nucleotides, in the HSV-1 construct. It would be surprising if these differences had any major impact on the functional activity of the respective shRNA, but relatively little has so far been reported on such aspects of shRNA design.

HSV-1 Mediated Delivery of anti-NgR shRNA

Quantitative PCR of P8 rat cerebellar granule neurons revealed a 30% reduction in *ngr* mRNA levels, after transduction with the anti-NgR shRNA virus. However, this compared to 9.3% and 6.9% reduction in *ngr* mRNA levels following transduction with HSV-1 anti-eGFP shRNA or HSV-1 eGFP WPRE, respectively. Such a non-specific effect on mRNA expression is not uncommon following viral transduction (Malmgaard, 2004). By immunocytochemistry, no obvious difference in NgR expression could be observed between samples.

Summary

A convincing reduction in eGFP expression was achieved in two different experimental models using HSV-1 mediated delivery of anti-eGFP shRNA. However, no effect was apparent using HSV-1 for the expression of anti-eGFP lhRNA. Whether this virus is actually expressing lhRNA is not yet known, and requires further investigation. The HSV-1 mediated delivery of anti-NgR shRNA resulted in a slight reduction in *ngr* mRNA levels in primary cultures of postnatal rat cerebellar granule neurons, but this effect was considerably less convincing than the results obtained for the anti-eGFP shRNA HSV-1 virus and can probably can accounted for by the selection of poor target sequence within the *ngr* mRNA. The extent of silencing activity achieved with the anti-NgR shRNA HSV-1 vector was not sufficient to warrant any specific *in vitro* or *in vivo* studies of *ngr* gene function

That lentivirus was so much better in reducing eGFP expression by a stable cell line, than was HSV-1, is probably indicative of a finer level of optimisation of the target sequence rather than inherent differences in the level of U6 promoter activity in a viral context. An ideal way to confirm this would be to construct an HSV-1 vector using the same U6-anti-eGFP shRNA cassette as that employed in the construction of the lentivirus. This would enable a direct comparison of HSV-1 and lentivirus, which was not permitted here due to numerous differences in U6-shRNA construct specification, and would yield important data regarding the inherent suitability of HSV-1 for the expression of functional shRNA.

CONCLUSION

As a proof of principle, it has been demonstrated that HSV-1 is capable of delivering functionally active shRNA *in vitro*. The degree of silencing activity was not as great as that which has been achieved using other types of virus, but there appears to be plenty of scope for optimisation – not least, in the selection of target sequences and the verification of their susceptibility to the activity of shRNA.

Figure 8.1.

Construction of the U6-shRNA cassette. A, Schematic representation of the multiple cloning site (MCS) of pBluescript II SK+. B, Schematic representation of the MCS after the vector was linearized with *Apa*I, blunted with T4 DNA polymerase, and religated to generate the vector pBluescript (*Apa*I minus). C, The human U6 promoter was ligated into pBluescript (*Apa*I minus) between *Spe*I and *Xho*I, to generate the vector termed pBS U6. D, The appropriate short-hairpin RNA coding sequence was ligated between the *Apa*I sites and *Xho*I sites of pBS U6. E, Schematic illustration of the generic U6-shRNA cassette. The design of the hairpins is such that the antisense strand is transcribed first, followed by a loop sequence, and then the sense strand. A polythymine tract serves as the transcription stop signal. The *Bgl*II site was incorporated for screening purposes.

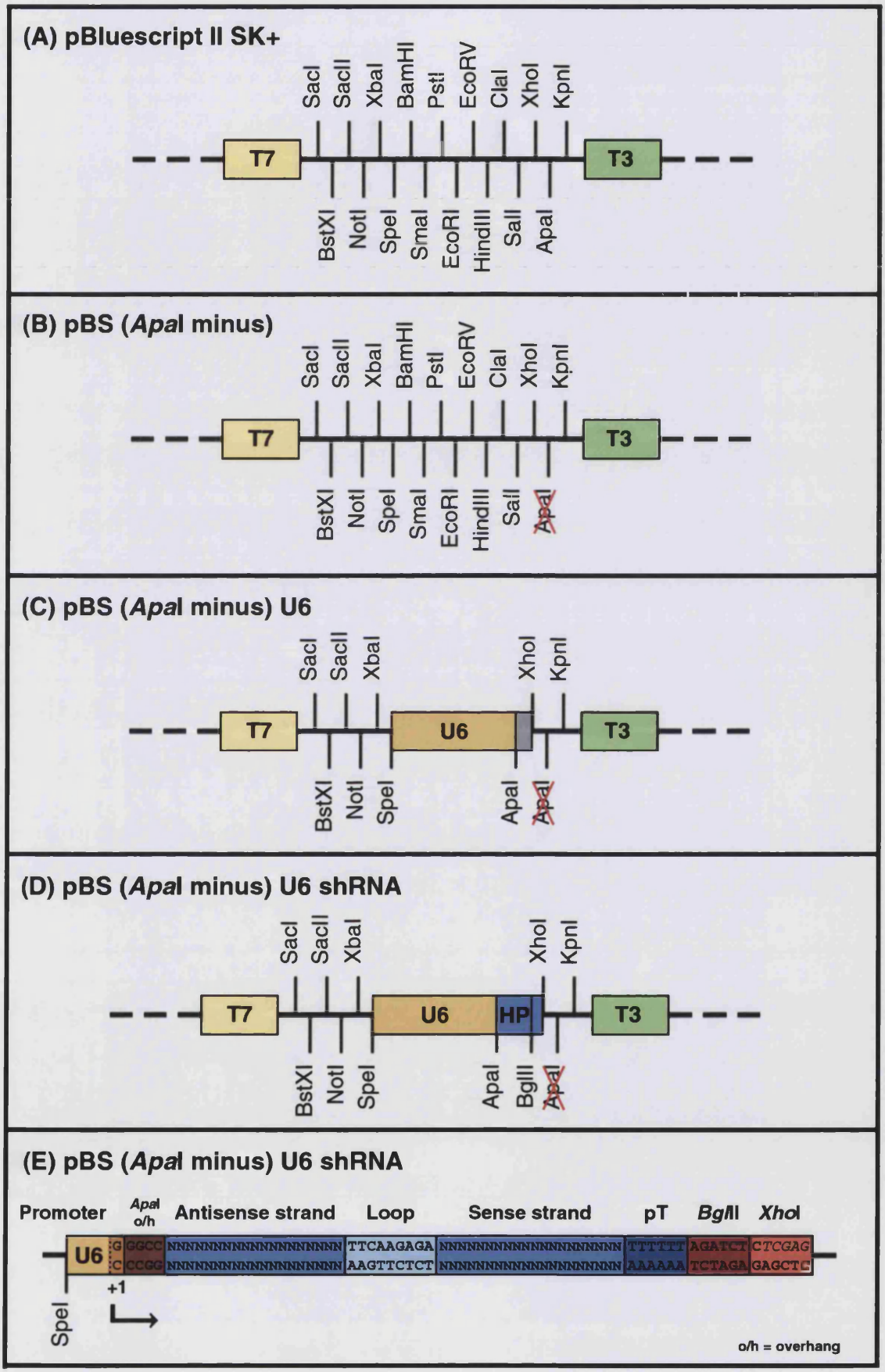
(A) pBluescript II SK+
SacI
SacII
XbaI
BamHI
PstI
EcoRV
ClaI
XhoI
KpnI
T7
T3
BstXI
NotI
SpeI
SmaI
EcoRI
HindIII
SalI
ApaI
(B) pBS (ApaI minus)
SacI
SacII
XbaI
BamHI
PstI
EcoRV
ClaI
XhoI
KpnI
T7
T3
BstXI
NotI
SpeI
SmaI
EcoRI
HindIII
SalI
ApaI
(C) pBS (ApaI minus) U6
SacI
SacII
XbaI
XhoI
KpnI
T7
U6
T3
BstXI
NotI
SpeI
ApaI
ApaI
(D) pBS (ApaI minus) U6 shRNA
SacI
SacII
XbaI
XhoI
KpnI
T7
U6
HP
T3
BstXI
NotI
SpeI
ApaI
BglII
ApaI
(E) pBS (ApaI minus) U6 shRNA
Promoter
ApaI o/h
Antisense strand
Loop
Sense strand
pT
BglII
XhoI
U6
GGCC
CCGG
NNNNNNNNNNNNNNNNNNN
TTCAAGAGA
AAGTTCTCT
NNNNNNNNNNNNNNNNNNN
TTTTTT
AAAAAA
AGATCT
TCTAGA
CTCGAG
GAGCTC
+1
SpeI
o/h = overhang

Figure 8.2.

Illustration of the theoretical structure of generic pR19 U6 derived shRNA. Dicer-mediated processing of this shRNA should result in the formation of conventional siRNA.

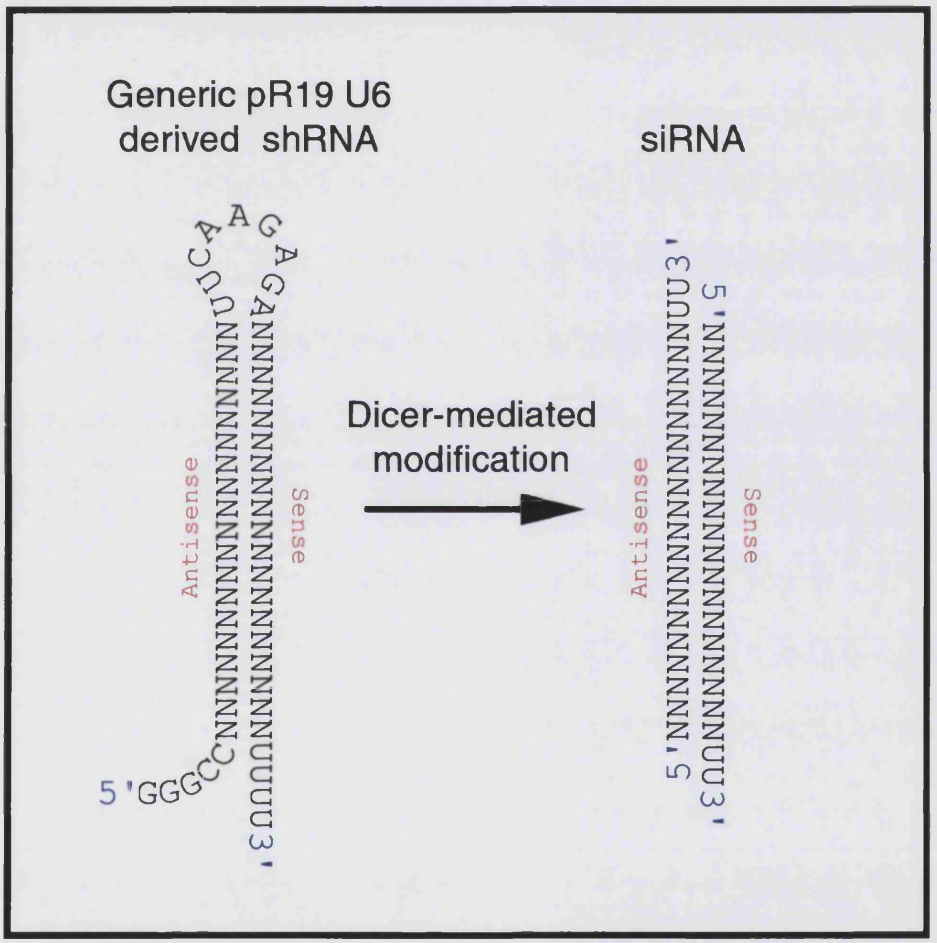

Figure 8.3.

Construction of HSV-1 for the expression of shRNA. A, Schematic representation of the pR19 IRES eGFP shuttle vector. B, Schematic representation of pR19 (*Spe*I minus) IRES eGFP. The vector was digested with *Eco*RV, and the backbone purified and religated to remove the superfluous *Spe*I site. C, The appropriate U6-shRNA cassette was excised from pBS U6 shRNA vector using *Spe*I and *Xho*I, and ligated into the corresponding sites within pR19 (*Spe*I minus), to replace the IRES eGFP. The final shuttle vector was termed pR19 (*Spe*I minus) U6 shRNA. D, Schematic representation of 1764/4-/27in/RL1+ HSV-1 genomic DNA. ICP4 and virion host shut-off (vhs) genes have been deleted. A 12bp function-blocking mutation is present in the transactivating domain of VMW65 (also known as VP16). E, Schematic representation of homologous recombination of the pR19 U6 shRNA cassette into the LAT regions of 1764/4-/27in/RL1+ HSV-1 DNA.

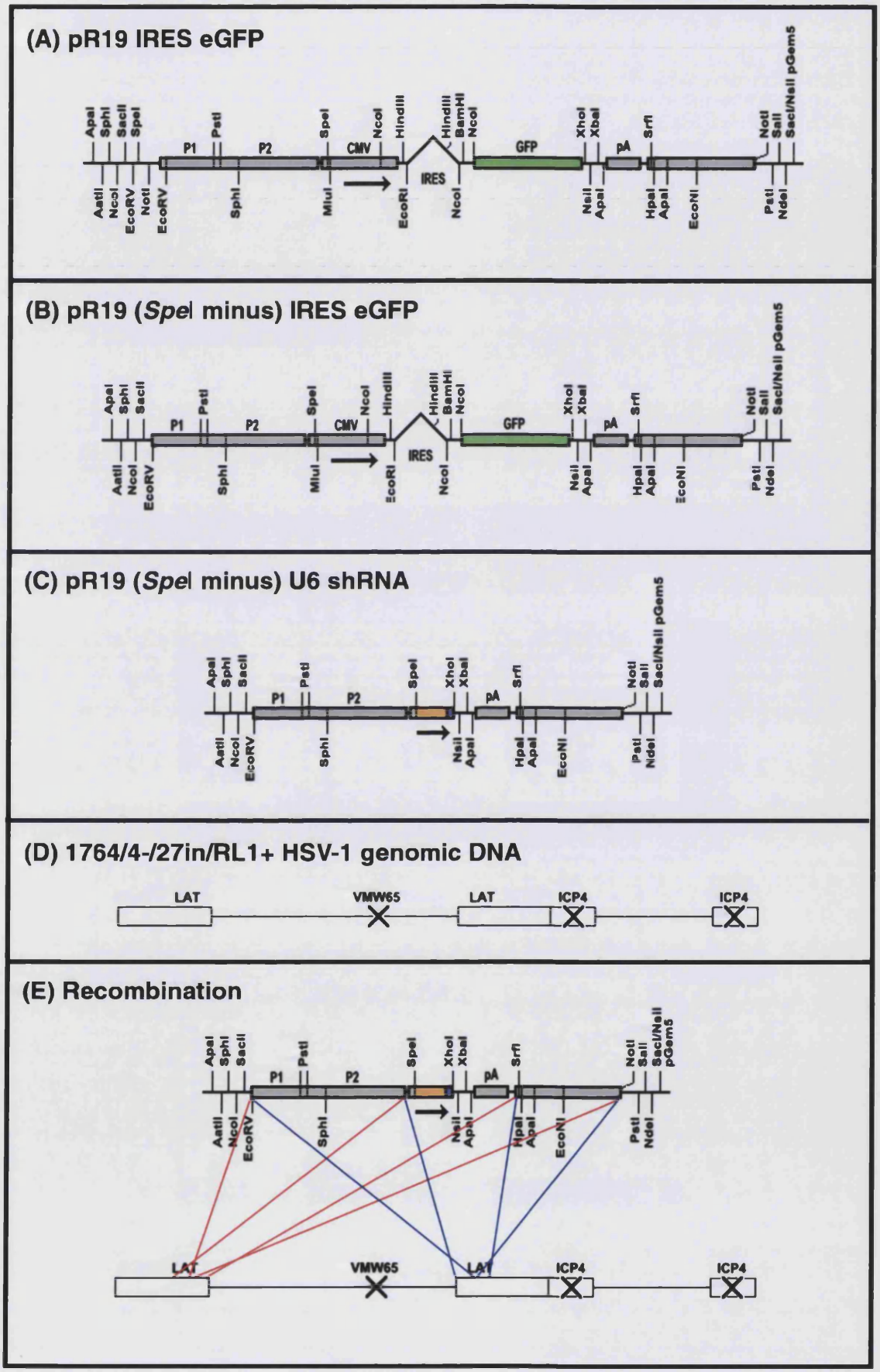
(A) pR19 IRES eGFP
ApaI SphI SacII SpeI PstI SpeI NcoI HindIII HindIII BamHI NcoI XhoI XbaI SrfI NotI SalI SacI/NsiI pGem5
P1 P2 CMV IRES GFP pA
AatII NcoI EcoRV NotI EcoRV SphI MluI EcoRI NcoI NsiI ApaI HpaI ApaI EcoNI PstI NdeI
(B) pR19 (SpeI minus) IRES eGFP
ApaI SphI SacII PstI SpeI NcoI HindIII HindIII BamHI NcoI XhoI XbaI SrfI NotI SalI SacI/NsiI pGem5
P1 P2 CMV IRES GFP pA
AatII NcoI EcoRV SphI MluI EcoRI NcoI NsiI ApaI HpaI ApaI EcoNI PstI NdeI
(C) pR19 (SpeI minus) U6 shRNA
ApaI SphI SacII PstI SpeI XhoI XbaI SrfI NotI SalI SacI/NsiI pGem5
P1 P2 pA
AatII NcoI EcoRV SphI NsiI ApaI HpaI ApaI EcoNI PstI NdeI
(D) 1764/4-/27in/RL1+ HSV-1 genomic DNA
LAT VMW65 LAT ICP4 ICP4
(E) Recombination
ApaI SphI SacII PstI SpeI XhoI XbaI SrfI NotI SalI SacI/NsiI pGem5
P1 P2 pA
AatII NcoI EcoRV SphI NsiI ApaI HpaI ApaI EcoNI PstI NdeI
LAT VMW65 LAT ICP4 ICP4

Figure 8.4.

Southern blots for the identification of recombinant HSV-1. A, Blot for 1764/4-/27in/RL1+/pR19 anti-eGFP shRNA viral DNA. B, Blot for 1764/4-/27in/RL1+/pR19 anti-NgR shRNA viral DNA. In both cases, 1764/4-/27in/RL1+/pR19 eGFP WPRE viral DNA served as the negative control. All samples were digested with *Spe*I and *Xho*I. The membranes were probed with ^{32}P-labelled U6 PCR product, and exposed to film overnight.

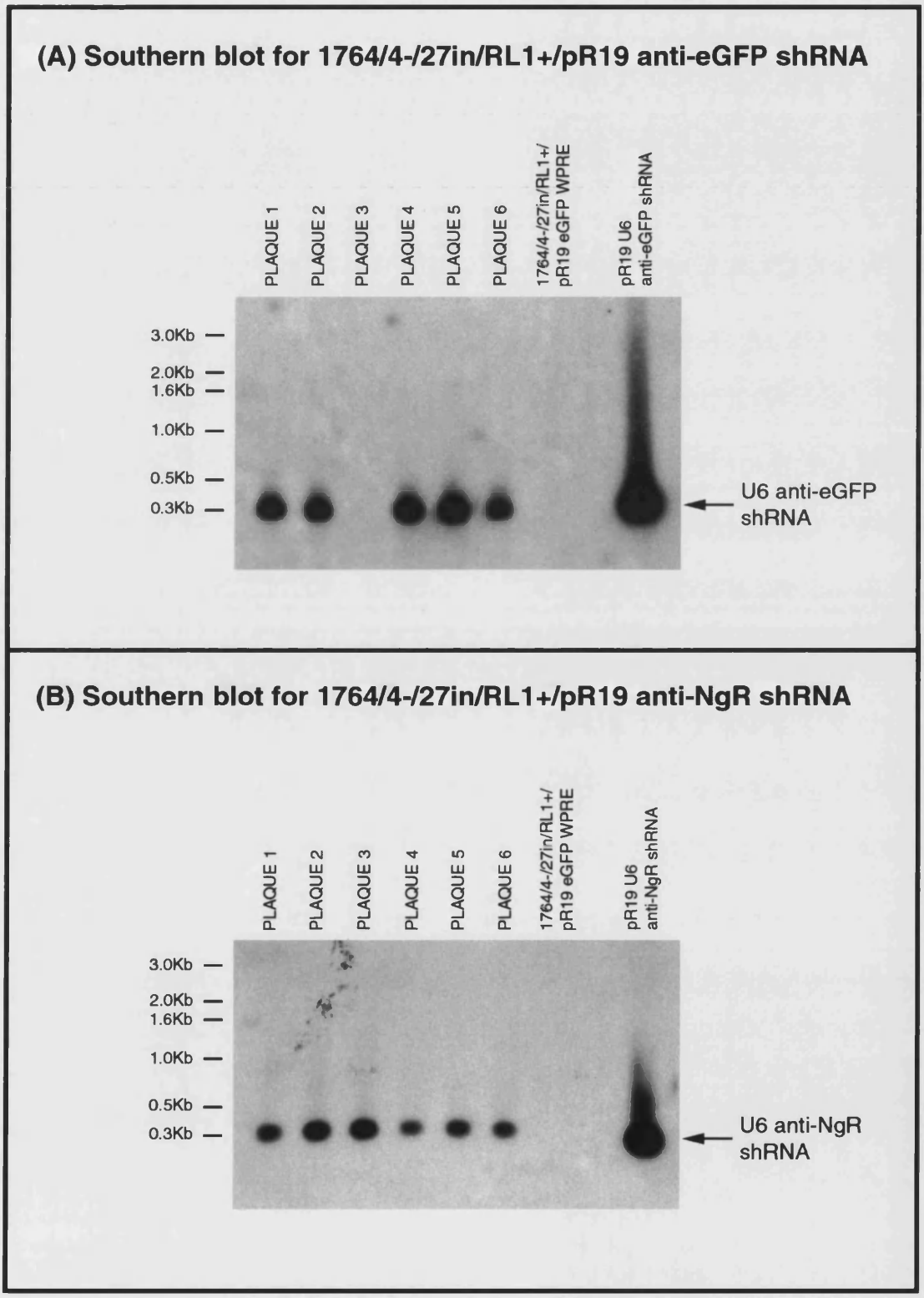
(A) Southern blot for 1764/4-/27in/RL1+/pR19 anti-eGFP shRNA
PLAQUE 1
PLAQUE 2
PLAQUE 3
PLAQUE 4
PLAQUE 5
PLAQUE 6
1764/4-/27in/RL1+/ pR19 eGFP WPRE
pR19 U6 anti-eGFP shRNA
3.0Kb
2.0Kb
1.6Kb
1.0Kb
0.5Kb
0.3Kb
U6 anti-eGFP shRNA
(B) Southern blot for 1764/4-/27in/RL1+/pR19 anti-NgR shRNA
PLAQUE 1
PLAQUE 2
PLAQUE 3
PLAQUE 4
PLAQUE 5
PLAQUE 6
1764/4-/27in/RL1+/ pR19 eGFP WPRE
pR19 U6 anti-NgR shRNA
3.0Kb
2.0Kb
1.6Kb
1.0Kb
0.5Kb
0.3Kb
U6 anti-NgR shRNA

Figure 8.5.

Construction of HSV-1 for the expression of anti-eGFP long-hairpin RNA. A, Schematic representation of the pR19 IRES eGFP shuttle vector. B, The antisense strand against eGFP, containing a 3′ *Cla*I site, was ligated between the *Hind*III and *Xho*I sites. C, The sense eGFP strand was subsequently ligated between the *Cla*I and *Xho*I sites. D, Southern blot for the identification of recombinant 1764/4-/27in/RL1+/pR19 anti-eGFP lhRNA. All samples were digested with *Hind*III and *Xho*I. The gel-purified *Cla*I-*Xho*I fragment of pR19 anti-eGFP lhRNA, which had been radiolabelled with ^{32}P, was used in probing the membrane. The hybridized blot was exposed to film overnight. In recombinant samples, a single band was present at ~0.3Kb. The negative control sample, 1764/4-/27in/RL1+/pR19 eGFP WPRE, exhibited a single strong band at ~4.5Kb due to the presence of the full-length eGFP coding sequence within a larger fragment of *Hind*III and *Xho*I digested viral DNA. Plaques 2 was selected for the generation high titre viral stocks.

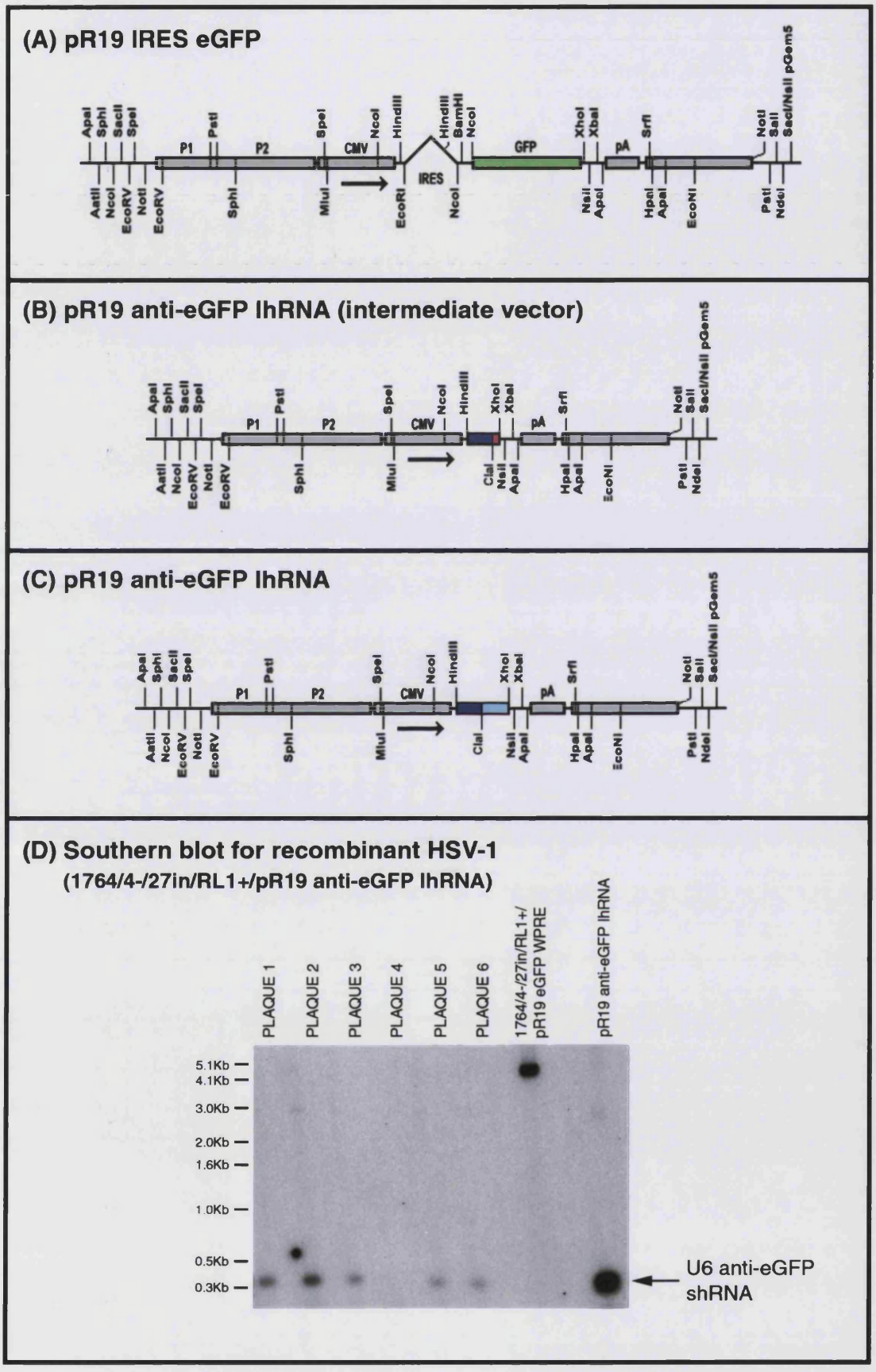
(A) pR19 IRES eGFP
ApaI SphI SacII SpeI
PstI
SpeI
NcoI
HindIII
HindIII BamHI
NcoI
XhoI XbaI
SrfI
NotI SalI SacI/NaeI pQem5
P1
P2
CMV
IRES
GFP
pA
AatII NcoI EcoRV NotI
EcoRV
SphI
MluI
EcoRI
NcoI
NaeI ApaI
HpaI ApaI
EcoNI
PstI NdeI
(B) pR19 anti-eGFP lhRNA (intermediate vector)
ApaI SphI SacII SpeI
PstI
SpeI
NcoI
HindIII
XhoI XbaI
SrfI
NotI SalI SacI/NaeI pQem5
P1
P2
CMV
pA
AatII NcoI EcoRV NotI
EcoRV
SphI
MluI
ClaI NaeI ApaI
HpaI ApaI
EcoNI
PstI NdeI
(C) pR19 anti-eGFP lhRNA
ApaI SphI SacII SpeI
PstI
SpeI
NcoI
HindIII
XhoI XbaI
SrfI
NotI SalI SacI/NaeI pQem5
P1
P2
CMV
pA
AatII NcoI EcoRV NotI
EcoRV
SphI
MluI
ClaI
NaeI ApaI
HpaI ApaI
EcoNI
PstI NdeI
(D) Southern blot for recombinant HSV-1
(1764/4-/27in/RL1+/pR19 anti-eGFP lhRNA)
PLAQUE 1
PLAQUE 2
PLAQUE 3
PLAQUE 4
PLAQUE 5
PLAQUE 6
1764/4-/27in/RL1+/ pR19 eGFP WPRE
pR19 anti-eGFP lhRNA
5.1Kb
4.1Kb
3.0Kb
2.0Kb
1.6Kb
1.0Kb
0.5Kb
0.3Kb
U6 anti-eGFP shRNA

Figure 8.6.

Stable eGFP-expressing BHK cells (clone 2B1). A, 2B1 cells viewed by fluorescence microscopy. B, Same microscopic field as in A, viewed under bright field illumination. Scale bars in A and B = 100μm. C, Histogram, obtained by flow cytometry, indicating the difference in fluorescence (FL1-H) between 2B1 cells (green outline) and standard BHK cells (black outline). The median fluorescence exhibited by the 2B1 clone is 10^3 times greater than that of standard BHK cells. However, although 88.6% of 2B1 cells were found to be highly fluorescent, 7.6% were in the same FL1-H range as standard BHK cells and were considered non-fluorescent. The remaining 3.8% of 2B1 cells were classed as lowly fluorescent.

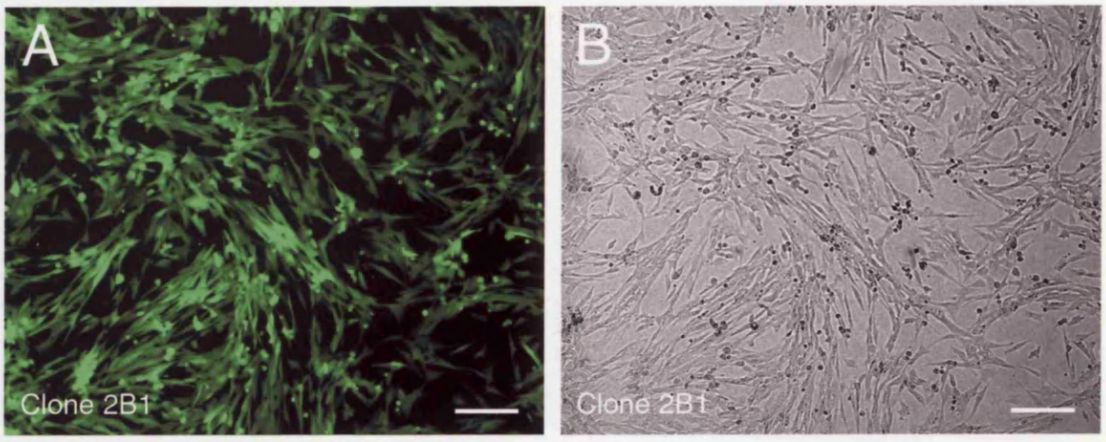
A
Clone 2B1
B
Clone 2B1

C

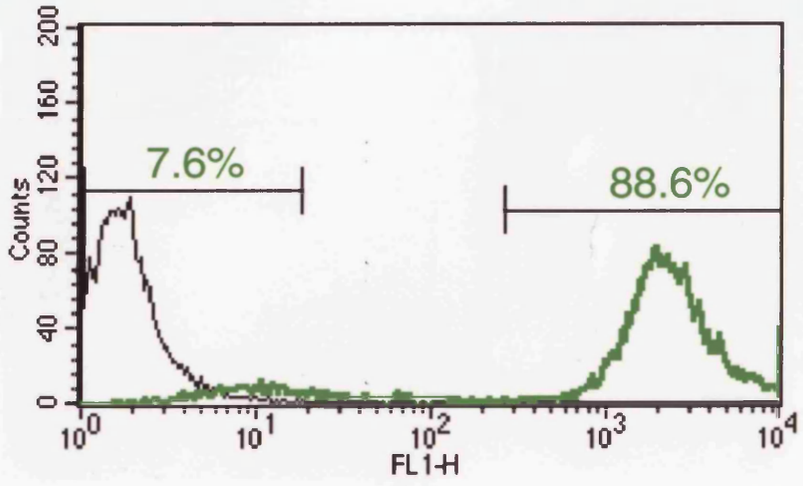
7.6%
88.6%
Counts
0
40
80
120
160
200
10^0
10^1
10^2
10^3
10^4
FL1-H

Figure 8.7.

Transduction of 2B1 cells by HSV-1 vectors expressing hairpin constructs. A, fluorescence and bright field microscopy of mock, HSV-1 anti-eGFP shRNA, HSV-1 anti-NgR shRNA and HSV-1 anti-eGFP lhRNA transduced 2B1 cells, 96 hours post transduction. B, Histogram, obtained by flow cytometry, showing the fluorescence profile of mock (pink outline), HSV-1 anti-eGFP shRNA (green outline), HSV-1 anti-NgR shRNA (blue outline), and HSV-1 anti-eGFP lhRNA (brown outline) transduced 2B1 cells. C, Graph showing the median fluorescence, and standard error, of each sample relative to that of mock transduced cells. A one-tailed Student's t-test was performed on the virus-transduced samples vs. the mock transduced sample. *** = $p<0.005$.

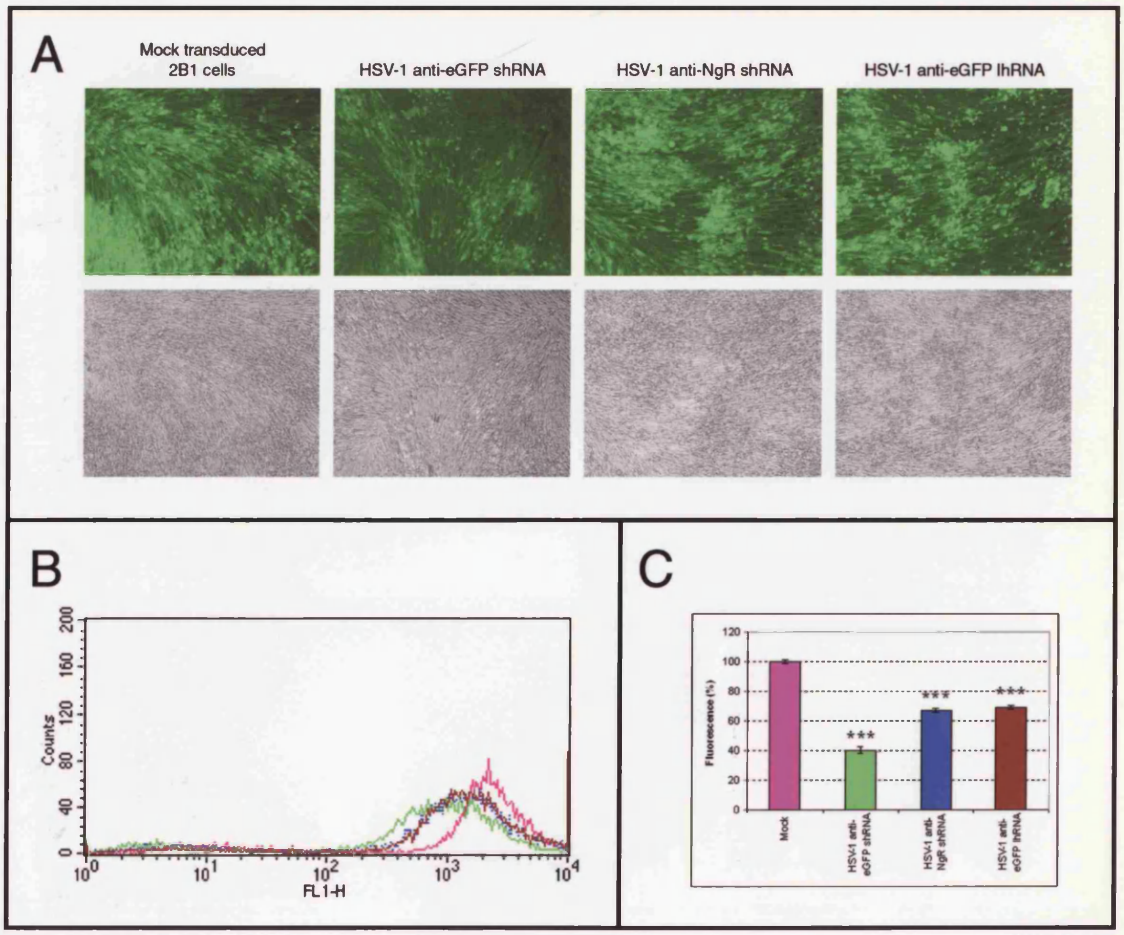
A
Mock transduced 2B1 cells
HSV-1 anti-eGFP shRNA
HSV-1 anti-NgR shRNA
HSV-1 anti-eGFP lhRNA
B
Counts
FL1-H
C
Fluorescence (%)
Mock
HSV-1 anti-eGFP shRNA
HSV-1 anti-NgR shRNA
HSV-1 anti-eGFP lhRNA
***

Figure 8.8.

Transduction of 2B1 cells by lentivirus expressing hairpin constructs. A, Fluorescence and bright field microscopy of standard BHK cells, 48 hours after transduction with lentivirus expressing eGFP. This was performed to ensure that this type of lentivirus is able to transduce the BHK cell type at high efficiency. B, Schematic representation of the U6-shRNA cassette present in both the anti-eGFP shRNA and anti-lacZ shRNA lentiviruses. C, Fluorescence and bright field microscopy of mock, LV anti-eGFP shRNA and LV anti-LacZ shRNA transduced 2B1 cells. Almost no fluorescent signal is detectable in LV anti-eGFP shRNA treated cells. D, Histogram, obtained by flow cytometry, of the fluorescence profile of mock (pink outline), LV anti-eGFP shRNA (green outline), and LV anti-LacZ shRNA (blue outline) transduced 2B1 cells. E, Graph showing the median fluorescence, and standard error, of each sample relative to that of mock transduced cells. A one-tailed Student's t-test was performed on the virus-transduced samples vs. the mock transduced sample. ** = $p<0.01$.

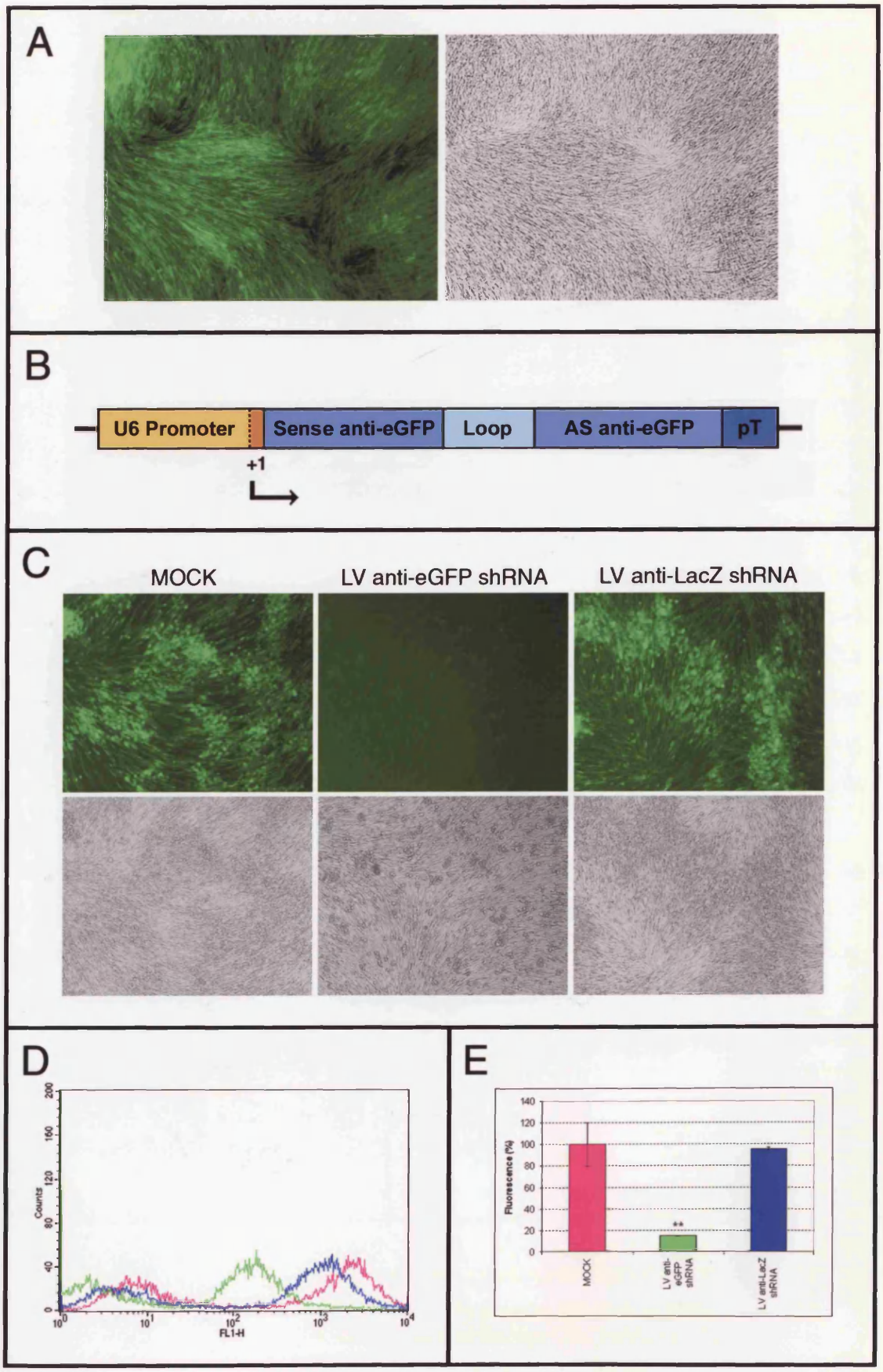
A
B
U6 Promoter
Sense anti-eGFP
Loop
AS anti-eGFP
pT
+1
C
MOCK
LV anti-eGFP shRNA
LV anti-LacZ shRNA
D
Counts
FL1-H
E
Fluorescence (%)
MOCK
LV anti-eGFP shRNA
LV anti-LacZ shRNA

Figure 8.9.

Double transduction of BHK cells with HSV-1 to assess the effect of hairpin constructs on the onset of eGFP expression. On day 1, BHK cells were transduced with HSV-1 anti-eGFP shRNA, HSV-1 anti-NgR shRNA or HSV-1 anti-lhRNA, or cells were mock transduced. On day 2, all samples, except one previously mock transduced sample, were transduced with HSV-1 eGFP WPRE. After 48 hours, samples were viewed by fluorescence and bright field microscopy (A), and were analysed by flow cytometry for their fluorescence profile (B). A composite of the histograms (C), obtained by flow cytometry, illustrates the difference in fluorescence profile the samples. The HSV-1 anti-eGFP shRNA (green outline) and the HSV-1 eGFP only (black outline) samples have similar fluorescence profiles, whereas those of both the HSV-1 anti-NgR shRNA (blue outline) and the HSV-1 anti-eGFP lhRNA (pink outline) samples appear to have more fluorescent profiles. This was confirmed by analysis of the median fluorescence values of each sample, relative to that of the HSV-1 eGFP only sample. The standard error is indicated. Whilst a slight reduction in fluorescence was observed in the HSV-1 anti-eGFP shRNA sample compared to the HSV-1 eGFP sample, there was greater than two-fold increase in median fluorescence values in the HSV-1 anti-NgR shRNA and HSV-1 anti-lhRNA samples compared to the same sample. The median fluorescence values obtained from mock transduced cells were 23% that of the HSV-1 eGFP only treated cells. This shows that the level of fluorescence in the control HSV-1 eGFP only sample was considerably lower than that of the clone 2B1 stable eGFP-expressing BHK cell line, where the magnitude of difference between fluorescence profiles of standard BHK cells and 2B1 cells was of the order of 10^3. A two-tailed Student's t-test was performed on the double virus-transduced, and mock transduced sample, vs. the HSV-1 eGFP only transduced sample. * = $p<0.05$. *** = $p<0.005$.

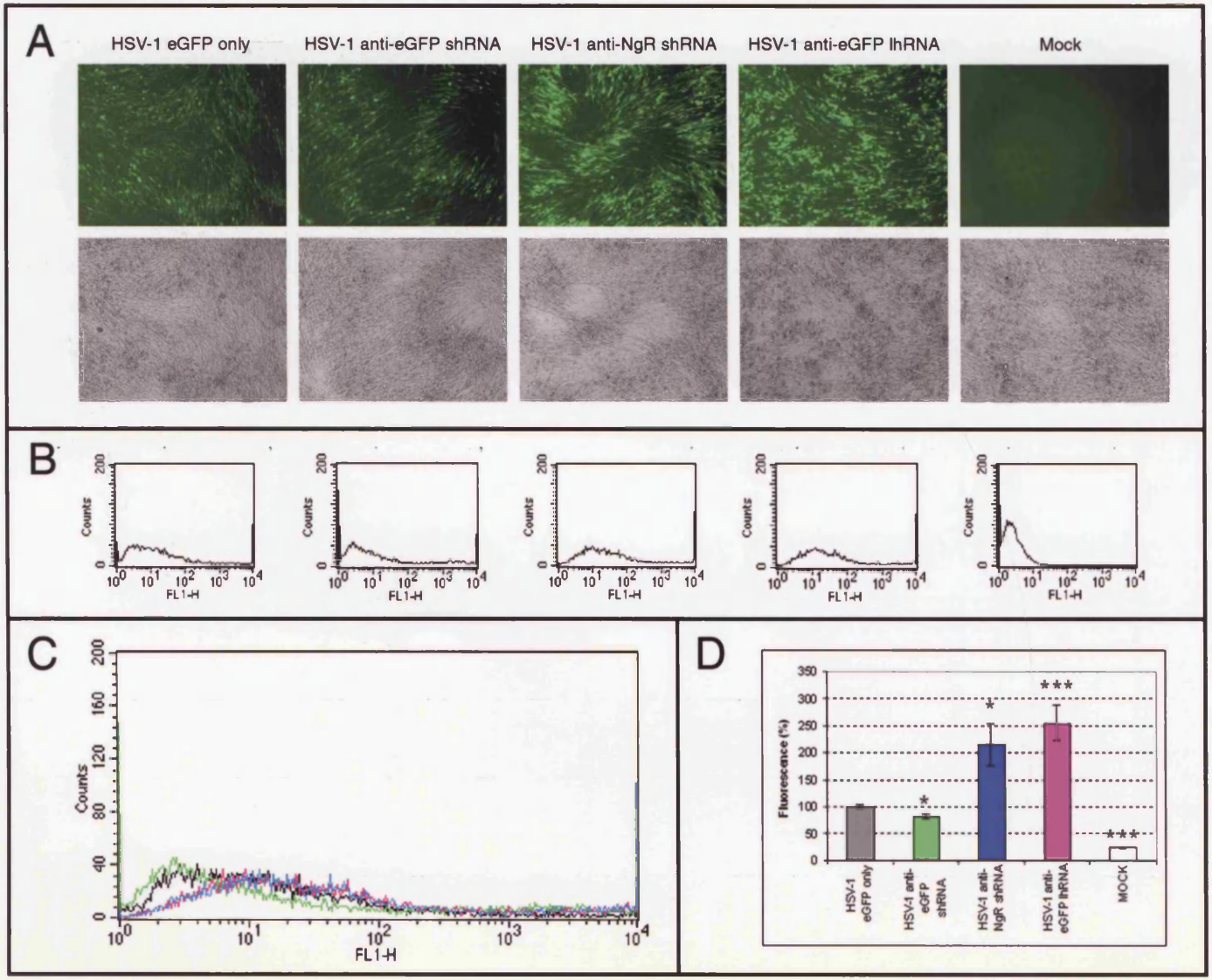
A
HSV-1 eGFP only
HSV-1 anti-eGFP shRNA
HSV-1 anti-NgR shRNA
HSV-1 anti-eGFP lhRNA
Mock
B
Counts
FL1-H
C
Counts
FL1-H
D
Fluorescence (%)
HSV-1 eGFP only
HSV-1 anti-eGFP shRNA
HSV-1 anti-NgR shRNA
HSV-1 anti-eGFP lhRNA
MOCK

Figure 8.10.

Quantitative PCR for *ngr* in HSV-1 transduced rat P8 CGCs. The level of *ngr* in HSV-1 anti-NgR shRNA, HSV-1 anti-eGFP shRNA and HSV-1 eGFP WPRE transduced samples is shown relative to that of mock transduced rat P8 CGCs. For each sample, the standard error of the mean is indicated. The largest reduction in *ngr* transcript levels was achieved with HSV-1 anti-NgR shRNA (20.8%), whereas HSV-1 anti-eGFP shRNA (9.3%) and HSV-1 eGFP WPRE (6.9%) each brought about a smaller non-specific reduction. A one-tailed Student's t-test was performed on the virus-transduced samples vs. the untransduced sample. * = $p<0.05$.

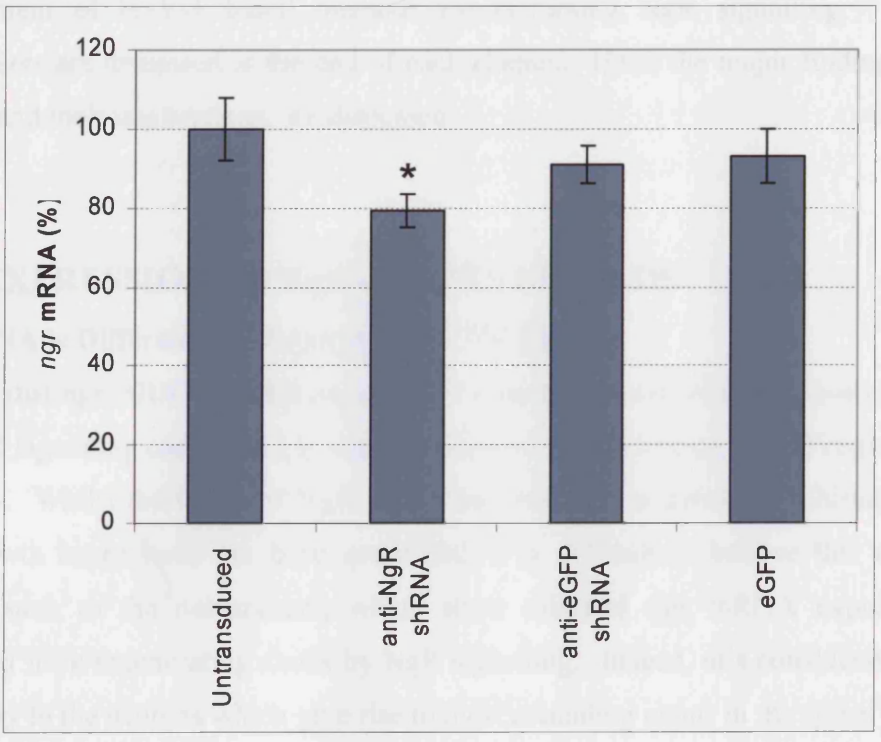
120
100
80
60
40
20
0
ngr mRNA (%)
*
Untransduced
anti-NgR shRNA
anti-eGFP shRNA
eGFP

CHAPTER 9

General Discussion

The work reported in this thesis was principally focussed on the expression patterns of NgR and some of its ligands in the healthy and injured nervous system, and the development of HSV-1 based methods for disrupting NgR signalling. Individual experiments are discussed at the end of each chapter. Here, the major findings of these studies, and their implications, are discussed.

THE EXPRESSION OF NgR AND ITS LIGANDS

ngr mRNA is Differentially Expressed by CNS Neurons

The fact that *ngr* mRNA is difficult to detect in many types of neuron appears to suggest that NgR signalling cannot be a general mechanism for preventing axonal regeneration in the CNS. Whilst the levels of NgR expression required to transduce inhibitory signals into growth cones have not been quantified, it is difficult to believe that neurons in regions such as the neostriatum, which show minimal *ngr* mRNA expression, are prevented from regenerating axons by NgR signalling. Indeed, this consideration would also apply to the neurons which give rise to most ascending axons in the spinal cord. The receptors which allow postnatal DRG neurons *in vitro* to show growth cone collapse in response to CNS myelin, MAG and Nogo are unknown, but *in vivo* DRG neurons do not behave as if they are affected by NgR ligands: their axons do not respond to treatment with the IN-1 antibody (Oudega et al., 2000), and when DRG neurons are transplanted into the dorsal columns of the spinal cord their axons regenerate rapidly in the white matter (Davies et al., 1997; Davies et al., 1999). It is not known whether the DRG neurons that survive isolation and transplantation and successfully regenerate axons express NgR, but *ngr* transcript expression has not been found to be subject to regulation in response to mechanical CNS injury (Chapter 3; Hunt et al., 2002b). Nonetheless,

chemical injury, achieved through the administration of kainic acid, has been reported to induce changes in *ngr* expression in the hippocampus (Josephson et al., 2002; Mingorance et al., 2004).

ngr mRNA Expression Does Not Correlate with Lack of Regenerative Ability

In experiments in which peripheral nerve grafts were placed in the thalamus or cerebellum to stimulate regeneration of axons from intrinsic CNS neurons, it was found that regenerating cells did not alter their expression of *ngr* mRNA (Chapter 3; Hunt et al., 2002b). The neurons that regenerated axons into grafts in the thalamus, those in the thalamic reticular nucleus, did not express *ngr* mRNA, but the neurons that regenerated axons into grafts in the cerebellum, those of the deep cerebellar nuclei, remained strongly *ngr* mRNA positive in the grafted animals.

That *ngr* expression does not correlate with an inability to regenerate axons into peripheral nerve grafts is perhaps not surprising since NgR, alone, is insufficient to transduce intracellular signals. This finding needs to be considered in the context of $p75^{NTR}$ and LINGO-1 expression, which are both believed to be necessary for successful axon-inhibitory signalling (Fig. 9.1.A). Neurons that regenerate axons into peripheral nerve grafts to thalamus or cerebellum are known to upregulate $p75^{NTR}$ (Vaudano et al., 1998). The expression of LINGO-1 by TRN or DCN is yet to be reported following peripheral nerve graft to thalamus and cerebellum, respectively; however, from the observations of *ngr* expression in this experimental model, one would assume that it may be absent in the regenerating DCN neurons.

Expression of Nogo by Neurons is Correlated with High Regenerative Capacity

Nogo mRNA is strongly expressed by many, but not all, neurons as well as by oligodendrocytes. Curiously, *nogo-66* and/or *nogo-a* mRNA expression seems to be particularly strong in neurons with a pronounced capacity for axonal regeneration, e.g. motor neurons, DRG neurons (Chapter 3; Huber et al., 2002; Hunt et al., 2002b), and intrinsic CNS neurons such as those in the thalamic reticular nucleus (Chapter 3; Hunt et al., 2002b) and deep cerebellar nuclei (Huber et al., 2002; Hunt et al., 2002b), which

have greater than normal ability to regenerate axons into nerve grafts in the brain (Morrow et al., 1993; Chaisuksunt et al., 2000b; reviewed by Anderson et al., 1998; Anderson and Lieberman, 1999). This correlation is not absolute, since neocortical projection neurons express *nogo* mRNA (Chapters 3 and 4; Hunt et al., 2002b; Hunt et al., 2003), but do not regenerate axons into nerve grafts in the spinal cord (Richardson et al., 1984) although they have shown greater ability than any other neurons to regenerate within the CNS in experiments using antibodies to Nogo (see Chapter 1).

Nogo-A has been consistently detected by immunohistochemistry in the perikarya and/or axons of various classes of neuron during development, as well as in adulthood. For example, it is expressed in the developing axons of embryonic rat sciatic nerve (Chapter 4; Wang et al., 2002c) and some developing CNS fibre tracts (Chapter 4; Tozaki et al., 2002), and also in the axons of mature DRG and spinal motor neurons (Chapter 4). Intriguingly, Nogo-A continues to be expressed in axons undergoing regeneration in the injured sciatic nerve. Similarly, Nogo-A immunoreactive fibres, consistent with being sprouting neurites, are detectable in dorsal column lesion sites following a concomitant conditioning lesion to the sciatic nerve. It is difficult to explain why a putatively axon-inhibitory molecule should be present in developing and regenerating axons, but at least one other member of the reticulon family of proteins exhibits a similar developmental expression pattern (Kumamaru et al., 2004). One theory is that Nogo-A may act by contact suppression of interstitial axonal sprouting, thereby driving axonal growth in longitudinal arrays (Raisman, 2004).

In dissociated cultures of adult rat DRG neurons, and embryonic mouse and rat neocortical neurons, Nogo-A localizes to the central domain of the growth cone, axonal varicosities and branch points. Its appearance is strikingly similar to that of SCG10, a growth-associated protein which is involved in controlling microtubule dynamics (Lutjens et al., 2000). These findings indicate that neuronal Nogo-A may play a role in axonal growth or guidance in the developing or regenerating nervous system. Unfortunately, however, it is still not known whether Nogo-A is found at the surface of neurons.

nogo mRNA Expression in Peripheral Nerve

Whether *nogo* mRNA is present in peripheral nerve trunks is of particular relevance to axonal regeneration. In the original papers describing Nogo there was a difference of opinion: Nogo-B mRNA was detected by Chen et al. (2000) in sciatic nerve, but no form of Nogo was found by GrandPre et al.(2000). In a further study the Northern blot showing Nogo-B in peripheral nerve was published again (Huber et al., 2002), and Nogo-A protein was apparently detectable in nerve (i.e. in DRG axons) by immunohistochemistry but not in Western Blots. In one of the studies presented here, no evidence for *nogo* mRNA in intact sciatic nerve was found using a *nogo-66* probe, but strong expression in scattered cells within the distal stumps of nerves 3 days after injury was detected (Chapter 3; Hunt et al., 2002b). Since motor neurons and some sensory and sympathetic neurons express NgR, although not strongly, and DRG neurons are sensitive to Nogo *in vitro*, it would obviously be of interest to know what form of Nogo is expressed in damaged nerves, by which cells it is expressed, whether the upregulation is transient or prolonged, and whether the protein is reaching the cell surface.

Neuronal Expression of *omgp* mRNA

Like Nogo, OMgp was first identified as a myelin protein but has subsequently been found to be expressed by neurons (Chapter 6; Habib et al., 1998c). There is also evidence to suggest that OMgp may be acting as receptor in its own right – although, a co-receptor is yet to be identified. Both findings are frequently overlooked (Wang et al., 2002b; Filbin, 2003), and yet are of great significance since they infer a role for OMgp in the function of neurons by which it is expressed. Curiously, there is not yet any credible evidence that OMgp is in fact inhibitory to axonal regeneration *in vivo*.

Neuronal Co-Expression of Nogo-A, OMgp and NgR

The fact that Nogo and OMgp are co-expressed with NgR in adult neurons is intriguing. Of the major Nogo isoforms, there is convincing evidence (Josephson et al., 2001; Huber et al., 2002; Tozaki et al., 2002; Hunt et al., 2003) that Nogo-A is expressed in neocortical neurons, cerebellar deep nucleus neurons, Purkinje cells, DRG neurons, spinal motor neurons and others. Neocortical neurons and Purkinje cells have been

shown to be responsive to the monoclonal antibody IN-1 (Zagrebelsky et al., 1998), which raises the possibility that reverse signalling is occurring through Nogo-A acting as a receptor. In addition, the expression of Nogo-A in growing axons of developing neurons (Chapter 4; Tozaki et al., 2002) raises some interesting issues. Many or most fibre tracts in the developing CNS, including the corticospinal tracts, take the form of bundles of neurites with little intervening space or glial cytoplasm (Guillery and Walsh, 1987; Gorgels et al., 1989; Joosten et al., 1989; Williams et al., 1991). It has been presumed that the axons are not mutually inhibited because they do not express NgR or other Nogo receptors at that stage of development (Wang et al., 2002c). A comprehensive study of the onset of NgR expression in different neurons would be important for interpreting the role of NgR ligands in axonal growth. However, the most convincing study suggests that NgR is more widely expressed in the nervous system during development than it is in the adult (Josephson et al., 2002). Nogo-A might mediate inhibitory interactions between different fibre tracts, assuming that the onset of expression of NgR or other receptors varies (Fig. 9.1.B). It has long been known that neurite outgrowth can be inhibited by contact with other neurites (Kapfhammer and Raper, 1987), particularly their growth cones (Ivins and Pittman, 1989). Further studies of the expression of NgR, Nogo-A and OMgp in developing neurons are clearly required. However, no pathfinding errors or other developmental abnormalities of the corticospinal tract have been reported in the *ngr* null mutant mouse.

Neurons which Respond to IN-1 mAb *In Vivo* Express *nogo* and *omgp* mRNA

A curious observation relating to the ability of IN-1 to enhance axonal regeneration, sprouting and growth-related gene expression is that the neurons which respond best- cerebral cortical neurons, cerebellar Purkinje cells and retinal ganglion cells - strongly express mRNAs for *nogo-66* and *omgp*. In the cerebellum, Purkinje cells express both *nogo-66* and *omgp* much more strongly than granule cells, whereas *ngr* is more strongly expressed by granule cells. Thus, in CNS neurons *nogo-66* and *omgp* expression correlates even better with their ability to respond to IN-1 than does *ngr* expression, although NgR is a major receptor for oligodendrocyte Nogo. The possibility exists that IN-1 acts *in vivo* by binding to neuronal Nogo and directly stimulating neurons, rather

than by dis-inhibiting them. The best *in vitro* evidence for such a mechanism comes from the work by Mingorance et al. (2004), who showed that neurite outgrowth from mouse P4 cerebellar granule neurons, cultured on poly-L-ornithine coated glass coverslips, was significantly enhanced by treatment with the IN-1 antibody. However, in opposition to this, Huber et al. (2002) cite unpublished experiments showing that IN-1 does not enhance neurite outgrowth from DRG neurons grown on laminin, and immunohistochemical evidence that IN-1 binds mainly to white matter (Huber et al., 2002). In any event, the environment, surrounding neurons *in vivo* is complex and could influence the effects of IN-1 binding to neuronal surfaces. For example, it has been shown that NGF downregulates RhoA in growth cones attached to laminin but not in growth cones attached to L1 (Liu et al., 2002c). IN-1 was originally reported to bind both the large and small myelin inhibitory proteins, suggesting that it recognises a site common to at least two forms of Nogo (although the possibility that NI-35 is a degradation product of the larger protein has not been ruled out), and would be expected to bind neuronal Nogo. Furthermore, Fournier et al. (2002) claim that IN-1 recognises other myelin proteins. If this is the case, it would be interesting to see if IN-1 binds OMgp, which is also expressed by cortical neurons.

POTENTIAL FOR HSV-1 MEDIATED DISRUPTION OF NgR-LIGAND INTERACTIONS

Genetically modified HSV-1 has been shown to permit widespread and effective gene delivery to the central nervous system (Lilley et al., 2001). Whilst a high level of HSV-1 transgene expression can be readily achieved in many classes of neuron *in vivo*, there are some classes of neuron, e.g. neocortical neurons, in which the expression of the transgene has been found to be dependent on the strain of HSV-1, as well as its transgene promoter type (Dr. R.S. Coffin, personal communication). However, neocortical neurons in particular appear to be much more amenable to expression from less disabled stains of HSV-1, such as the 1764/4-/27in/RL1+ strain of virus that was used in the studies reported here.

The successful establishment of a platform for the expression of functional shRNA in HSV-1 (Chapter 8), albeit in need of optimisation, should permit new lines of experimental enquiry in the injured nervous system. Admittedly, the activity of such viruses has not yet been demonstrated *in vivo* but, on the assumption that their effect *in vivo* would be comparable to that *in vitro*, these HSV-1 vectors could potentially be of considerable value in the study of the NgR-ligand interactions in the injured nervous system. In terms of NgR silencing, the obvious targets for viral transduction would be either the neocortical projection neurons which give rise to the corticospinal tract, or the retinal ganglion cells which give rise to the optic nerve. Both classes of neuron strongly express *ngr* transcripts *in vivo*, and there is already some evidence that disruption of NgR-ligand interactions enhances axonal regeneration in both systems (Grandpre et al., 2002; Fischer et al., 2004).

There are, of course, means of disrupting the NgR-ligand interaction without having to silence expression of the respective proteins. These include the use of dominant negative NgR (Fischer et al., 2004) or antagonist peptides such as NEP1-40 (Grandpre et al., 2002); both of which can be modified, where necessary, to be expressed from a viral vector such as HSV-1. It is unfortunate that in the study presented in this thesis (Chapter 7), the expression of a tagged-secreted form of NEP1-40 from HSV-1 was relatively poor, both *in vitro* and *in vivo*. Almost certainly this anomaly was specific to the NEP1-40 transgene cassette, which may not have been compatible with HSV-1, owing to the relatively short transgene sequence. Nonetheless, the premise for the study, that targeted viral delivery of a secreted form of NEP1-40 to a corticospinal tract lesion site should elicit comparable if not more extensive axonal regeneration than was previously reported (Grandpre et al., 2002), still stands.

CONCLUDING REMARKS

Because NgR is a common receptor for at least three inhibitory ligands present in the CNS it is tempting to believe that it plays a significant role in blocking CNS regeneration.

Nonetheless, numerous factors suggest caution in interpreting the importance of NgR signalling as an explanation for the overwhelming failure of regeneration in the CNS of adult mammals: the differential expression of NgR; its apparent dependence on both $p75^{NTR}$ and LINGO-1 for the formation of a functional receptor complex; the existence of other receptors for NgR ligands (Niederost et al., 2002); the absence of myelin, MAG and Nogo from lesion sites which are, nonetheless, demonstrably inhibitory; the ability of transplanted and otherwise suitably stimulated neurons to grow axons in white matter; and, of course, the absence of enhanced CNS axonal regeneration in the *ngr* null mutant mouse (Kim et al., 2003a).

Ultimately, however, there is still sufficient evidence to suggest that NgR signalling plays an important part in preventing the sprouting and regeneration of the axons of some classes of neuron, including neocortical neurons and retinal ganglion cells, and it remains a valid target for the study of CNS axonal regeneration in those systems.

Figure 9.1.

A. Diagram illustrating the known distribution, theoretical interactions and signalling pathways of molecules involved in NgR-mediated growth cone collapse/neurite outgrowth inhibition in response to contact with oligodendrocyte membranes. The $p75^{NTR}$ low-affinity neurotrophin receptor acts as a co-receptor mediating signalling from NgR (Yamashita et al., 2002; Wang et al., 2002a), as does LINGO-1 (Mi et al., 2004). Note that the schematic representation of the MAG interaction with NgR is not true to the physical interaction, since experiments using a mutant form of the MAG protein, consisting only of a solubilized form of the first three immunoglobulin domains, show that it fails to bind to NgR (Domeniconi et al., 2002). There may be a separate receptor to the Nogo-A specific N-terminal domain, which in some models of Nogo conformation is exposed at the surface of oligodendrocytes. Other receptors (not shown) for NgR ligands may be expressed by the many neurons that lack NgR. Activation of the Rho A GTPase is believed to be downstream of NgR and Nogo-A signalling. We have speculated that the LIM kinase may be downstream of Rho A, as it is known to alter the cytoskeleton in response to Sema 3A signalling via Rho A (Aizawa et al., 2001). Neuronal Nogo and OMgp could have functions unrelated to growth cone collapse (e.g. OMgp expression by fibroblasts suppresses mitogenesis; (Habib et al., 1998a)). That Nogo and OMgp act as receptors remains a possibility. PKA = protein kinase A.

B. Diagram illustrating the possible interactions between NgR and its ligands on the surfaces of adjacent neurons. Although OMgp and Nogo were originally identified as myelin proteins they are strongly expressed by neurons. NgR may also bind to NgR in apposing membranes or within the same membrane (in *cis*) (Liu et al., 2002; Fournier et al., 2002). The roles of neuronal Nogo and OMgp are obscure but they are presumably capable of acting as inhibitory ligands for NgR on other neurons. These interactions may take place between growing or regenerating axons. Nogo-A is present in growing axons (Huber et al., 2002; Tozaki et al., 2002) and *ngr* mRNA is widely expressed during development (Josephson et al., 2002). Inhibitory interactions between adjacent axonal sprouts following injury may limit regeneration. Another physiological function in the adult may be to suppress sprouting at synapses.

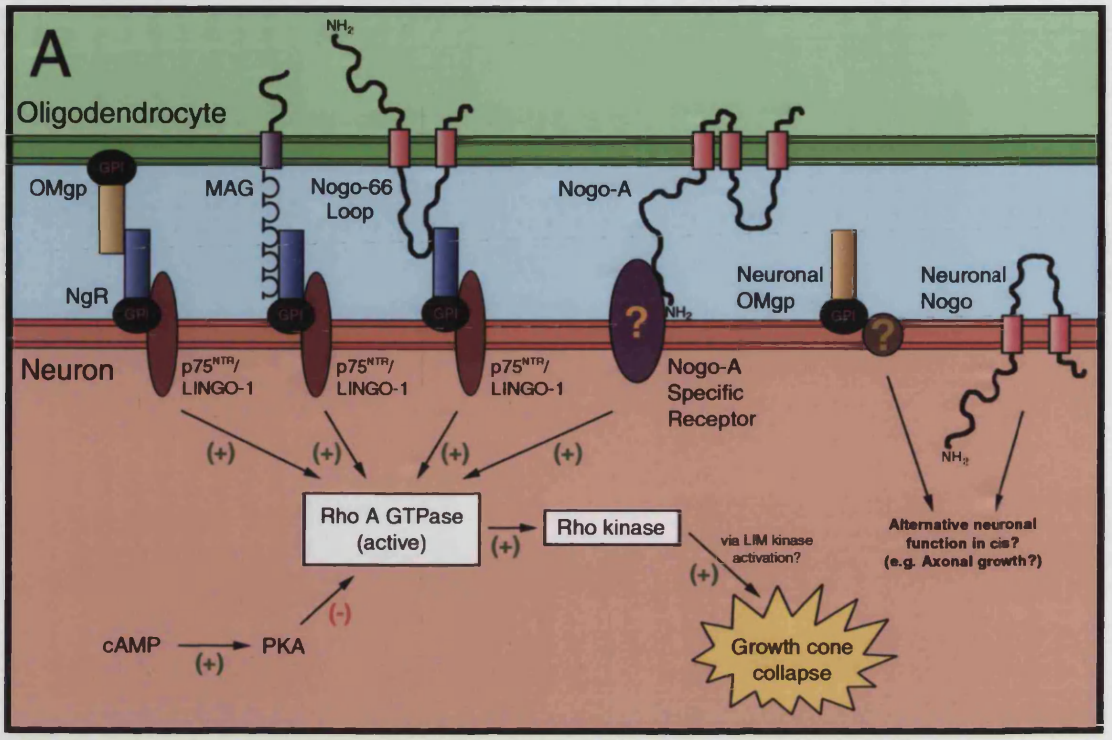
A
Oligodendrocyte
NH2
OMgp
GPI
MAG
Nogo-66
Loop
Nogo-A
NgR
Neuronal
OMgp
Neuronal
Nogo
Neuron
p75NTR/
LINGO-1
p75NTR/
LINGO-1
p75NTR/
LINGO-1
Nogo-A
Specific
Receptor
(+)
(+)
(+)
(+)
Rho A GTPase
(active)
(+)
Rho kinase
via LIM kinase
activation?
(+)
Alternative neuronal
function in cis?
(e.g. Axonal growth?)
(-)
cAMP
(+)
PKA
Growth cone
collapse

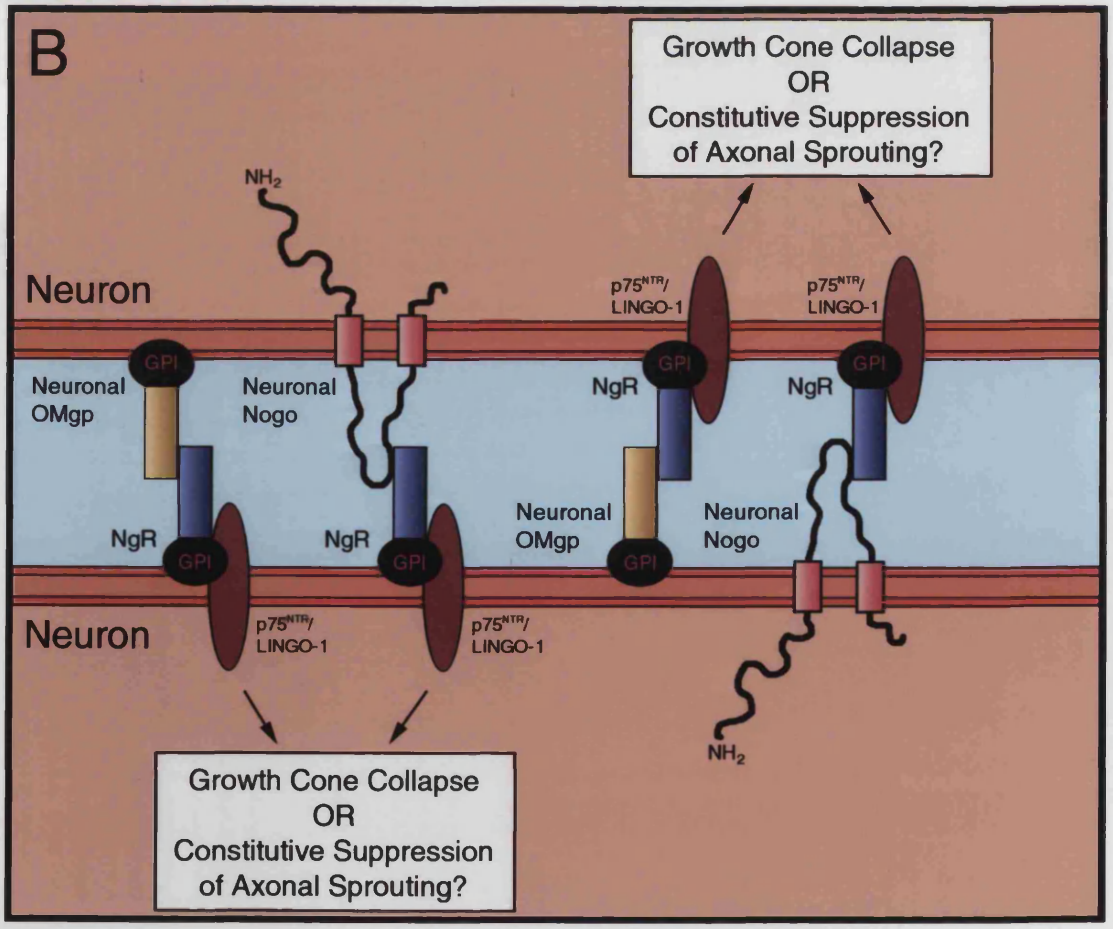
B
Growth Cone Collapse
OR
Constitutive Suppression
of Axonal Sprouting?
NH2
Neuron
p75NTR/
LINGO-1
p75NTR/
LINGO-1
GPI
Neuronal
OMgp
Neuronal
Nogo
NgR
NgR
NgR
NgR
Neuronal
OMgp
Neuronal
Nogo
Neuron
p75NTR/
LINGO-1
p75NTR/
LINGO-1
NH2
Growth Cone Collapse
OR
Constitutive Suppression
of Axonal Sprouting?

REFERENCES

Abbas-Terki, T, Blanco-Bose, W, Deglon, N, Pralong, W, and Aebischer, P (2002) Lentiviral-mediated RNA interference. Hum.Gene Ther. 13: 2197-2201.

Ace, CI, McKee, TA, Ryan, JM, Cameron, JM, and Preston, CM (1989) Construction and characterization of a herpes simplex virus type 1 mutant unable to transinduce immediate-early gene expression. J.Virol. 63: 2260-2269.

Acevedo, L, Yu, J, Erdjument-Bromage, H, Miao, RQ, Kim, JE, Fulton, D, Tempst, P, Strittmatter, SM, and Sessa, WC (2004) A new role for Nogo as a regulator of vascular remodeling. Nat.Med. 10: 382-388.

Acheson, A, Conover, JC, Fandl, JP, DeChiara, TM, Russell, M, Thadani, A, Squinto, SP, Yancopoulos, GD, and Lindsay, RM (1995) A BDNF autocrine loop in adult sensory neurons prevents cell death. Nature 374: 450-453.

Aigner, L, Arber, S, Kapfhammer, JP, Laux, T, Schneider, C, Botteri, F, Brenner, HR, and Caroni, P (1995) Overexpression of the neural growth-associated protein GAP-43 induces nerve sprouting in the adult nervous system of transgenic mice. Cell 83: 269-278.

Aigner, L and Caroni, P (1993) Depletion of 43-kD growth-associated protein in primary sensory neurons leads to diminished formation and spreading of growth cones. J.Cell Biol. 123: 417-429.

Aigner, L and Caroni, P (1995) Absence of persistent spreading, branching, and adhesion in GAP-43-depleted growth cones. J.Cell Biol. 128: 647-660.

Aizawa, H, Wakatsuki, S, Ishii, A, Moriyama, K, Sasaki, Y, Ohashi, K, Sekine-Aizawa, Y, Sehara-Fujisawa, A, Mizuno, K, Goshima, Y, and Yahara, I (2001) Phosphorylation of

cofilin by LIM-kinase is necessary for semaphorin 3A-induced growth cone collapse. Nat.Neurosci. 4: 367-373.

An, DS, Xie, Y, Mao, SH, Morizono, K, Kung, SK, and Chen, IS (2003) Efficient lentiviral vectors for short hairpin RNA delivery into human cells. Hum.Gene Ther. 14: 1207-1212.

Anderson, PN, Campbell, G, Zhang, Y, and Lieberman, AR (1998) Cellular and molecular correlates of the regeneration of adult mammalian CNS axons into peripheral nerve grafts. Prog.Brain Res. 117: 211-232.

Anderson, PN and Lieberman, AR (1999) Intrinsic determinants of differential axonal regeneration by adult mammalian CNS neurons. In *Degeneration and Regeneration in the Nervous System* (Saunders, NR and Dziegielewska, KM, eds.), pp. 53-75. Harwood Academic Press, Reading, UK.

Anderson, PN, Mitchell, J, and Mayor, D (1978) The role of calcium ions in the synthesis and transport of noradrenaline carrier vesicles in guinea-pig sympathetic neurons in vitro. J.Neurocytol. 7: 623-636.

Bacchetti, S, Evelegh, MJ, Muirhead, B, Sartori, CS, and Huszar, D (1984) Immunological characterization of herpes simplex virus type 1 and 2 polypeptide(s) involved in viral ribonucleotide reductase activity. J.Virol. 49: 591-593.

Baehr, M and Bunge, RP (1990) Growth of adult rat retinal ganglion cell neurites on astrocytes. Glia 3: 293-300.

Baetge, EE and Hammang, JP (1991) Neurite outgrowth in PC12 cells deficient in GAP-43. Neuron 6: 21-30.

Bandtlow, CE, Schmidt, MF, Hassinger, TD, Schwab, ME, and Kater, SB (1993) Role of intracellular calcium in NI-35-evoked collapse of neuronal growth cones. Science 259: 80-83.

Banks, P, Mangnall, D, and Mayor, D (1969) The re-distribution of cytochrome oxidase, noradrenaline and adenosine triphosphate in adrenergic nerves constricted at two points. J.Physiol 200: 745-762.

Barde, YA, Edgar, D, and Thoenen, H (1982) Purification of a new neurotrophic factor from mammalian brain. EMBO J. 1: 549-553.

Bareyre, FM, Haudenschild, B, and Schwab, ME (2002) Long-lasting sprouting and gene expression changes induced by the monoclonal antibody IN-1 in the adult spinal cord. J.Neurosci. 22: 7097-7110.

Bargmann, CI (2001) High-throughput reverse genetics: RNAi screens in Caenorhabditis elegans. Genome Biol. 2: REVIEWS1005

Barker, PA (2004) p75NTR is positively promiscuous: novel partners and new insights. Neuron 42: 529-533.

Barton, WA, Liu, BP, Tzvetkova, D, Jeffrey, PD, Fournier, AE, Sah, D, Cate, R, Strittmatter, SM, and Nikolov, DB (2003) Structure and axon outgrowth inhibitor binding of the Nogo-66 receptor and related proteins. EMBO J. 22: 3291-3302.

Bartsch, U, Bandtlow, CE, Schnell, L, Bartsch, S, Spillmann, AA, Rubin, BP, Hillenbrand, R, Montag, D, Schwab, ME, and Schachner, M (1995) Lack of evidence that myelin-associated glycoprotein is a major inhibitor of axonal regeneration in the CNS. Neuron 15: 1375-1381.

Batterson, W and Roizman, B (1983) Characterization of the herpes simplex virion-associated factor responsible for the induction of alpha genes. J.Virol. 46: 371-377.

Beattie, MS, Bresnahan, JC, Komon, J, Tovar, CA, Van Meter, M, Anderson, DK, Faden, AI, Hsu, CY, Noble, LJ, Salzman, S, and Young, W (1997) Endogenous repair after spinal cord contusion injuries in the rat. Exp.Neurol. 148: 453-463.

Beattie, MS, Farooqui, AA, and Bresnahan, JC (2000) Review of current evidence for apoptosis after spinal cord injury. J.Neurotrauma 17: 915-925.

Beattie, MS, Harrington, AW, Lee, R, Kim, JY, Boyce, SL, Longo, FM, Bresnahan, JC, Hempstead, BL, and Yoon, SO (2002) ProNGF induces p75-mediated death of oligodendrocytes following spinal cord injury. Neuron 36: 375-386.

Becker, T, Anliker, B, Becker, CG, Taylor, J, Schachner, M, Meyer, RL, and Bartsch, U (2000) Tenascin-R inhibits regrowth of optic fibers in vitro and persists in the optic nerve of mice after injury. Glia 29: 330-346.

Benfey, M and Aguayo, AJ (1982) Extensive elongation of axons from rat brain into peripheral nerve grafts. Nature 296: 150-152.

Benfey, M, Bunger, UR, Vidal-Sanz, M, Bray, GM, and Aguayo, AJ (1985) Axonal regeneration from GABAergic neurons in the adult rat thalamus. J.Neurocytol. 14: 279-296.

Benowitz, LI and Routtenberg, A (1997) GAP-43: an intrinsic determinant of neuronal development and plasticity. Trends Neurosci. 20: 84-91.

Berkelaar, M, Clarke, DB, Wang, YC, Bray, GM, and Aguayo, AJ (1994) Axotomy results in delayed death and apoptosis of retinal ganglion cells in adult rats. J.Neurosci. 14: 4368-4374.

Berry, M (1982) Post-injury myelin-breakdown products inhibit axonal growth: an hypothesis to explain the failure of axonal regeneration in the mammalian central nervous system. Bibl.Anat. 1-11.

Berry, M, Carlile, J, and Hunter, A (1996) Peripheral nerve explants grafted into the vitreous body of the eye promote the regeneration of retinal ganglion cell axons severed in the optic nerve. J.Neurocytol. 25: 147-170.

Berry, M, Carlile, J, Hunter, A, Tsang, W, Rosustrel, P, and Sievers, J (1999) Optic nerve regeneration after intravitreal peripheral nerve implants: trajectories of axons regrowing through the optic chiasm into the optic tracts. J.Neurocytol. 28: 721-741.

Berry, M, Rees, L, Hall, S, Yiu, P, and Sievers, J (1988) Optic axons regenerate into sciatic nerve isografts only in the presence of Schwann cells. Brain Res.Bull. 20: 223-231.

Berry, M, Rees, L, and Sievers, J (1986) Regeneration of axons in the mammalian visual system. Exp.Brain Res.Suppl. 113: 18-33.

Bibel, M, Hoppe, E, and Barde, YA (1999) Biochemical and functional interactions between the neurotrophin receptors trk and p75NTR. EMBO J. 18: 616-622.

Birnboim, HC and Doly, J (1979) A rapid alkaline extraction procedure for screening recombinant plasmid DNA. Nucleic Acids Res. 7: 1513-1523.

Blits, B, Dijkhuizen, PA, Boer, GJ, and Verhaagen, J (2000) Intercostal nerve implants transduced with an adenoviral vector encoding neurotrophin-3 promote regrowth of injured rat corticospinal tract fibers and improve hindlimb function. Exp.Neurol. 164: 25-37.

Boyd, JG and Gordon, T (2001) The neurotrophin receptors, trkB and p75, differentially regulate motor axonal regeneration. J.Neurobiol. 49: 314-325.

Bradbury, EJ, Khemani, S, Von, R, King, Priestley, JV, and McMahon, SB (1999) NT-3 promotes growth of lesioned adult rat sensory axons ascending in the dorsal columns of the spinal cord. Eur.J.Neurosci. 11: 3873-3883.

Bradbury, EJ, Moon, LD, Popat, RJ, King, VR, Bennett, GS, Patel, PN, Fawcett, JW, and McMahon, SB (2002) Chondroitinase ABC promotes functional recovery after spinal cord injury. Nature 416: 636-640.

Bregman, BS, Kunkel-Bagden, E, Schnell, L, Dai, HN, Gao, D, and Schwab, ME (1995) Recovery from spinal cord injury mediated by antibodies to neurite growth inhibitors. Nature 378: 498-501.

Brochu, G, Maler, L, and Hawkes, R (1990) Zebrin II: a polypeptide antigen expressed selectively by Purkinje cells reveals compartments in rat and fish cerebellum. J.Comp Neurol. 291: 538-552.

Brummelkamp, TR, Bernards, R, and Agami, R (2002a) A system for stable expression of short interfering RNAs in mammalian cells. Science 296: 550-553.

Brummelkamp, TR, Bernards, R, and Agami, R (2002b) Stable suppression of tumorigenicity by virus-mediated RNA interference. Cancer Cell 2: 243-247.

Bruni, R and Roizman, B (1998) Herpes simplex virus 1 regulatory protein ICP22 interacts with a new cell cycle-regulated factor and accumulates in a cell cycle-dependent fashion in infected cells. J.Virol. 72: 8525-8531.

Bryant, HE, Wadd, SE, Lamond, AI, Silverstein, SJ, and Clements, JB (2001) Herpes simplex virus IE63 (ICP27) protein interacts with spliceosome-associated protein 145 and inhibits splicing prior to the first catalytic step. J.Virol. 75: 4376-4385.

Buffo, A, Holtmaat, AJ, Savio, T, Verbeek, JS, Oberdick, J, Oestreicher, AB, Gispen, WH, Verhaagen, J, Rossi, F, and Strata, P (1997) Targeted overexpression of the neurite growth-associated protein B-50/GAP-43 in cerebellar Purkinje cells induces sprouting after axotomy but not axon regeneration into growth-permissive transplants. J.Neurosci. 17: 8778-8791.

Buffo, A, Zagrebelsky, M, Huber, AB, Skerra, A, Schwab, ME, Strata, P, and Rossi, F (2000) Application of neutralizing antibodies against NI-35/250 myelin-associated neurite growth inhibitory proteins to the adult rat cerebellum induces sprouting of uninjured purkinje cell axons. J.Neurosci. 20: 2275-2286.

Cadelli, D and Schwab, ME (1991) Regeneration of Lesioned Septohippocampal Acetylcholinesterase-positive Axons is Improved by Antibodies Against the Myelin-associated Neurite Growth Inhibitors NI-35/250. Eur.J.Neurosci. 3: 825-832.

Cai, D, Deng, K, Mellado, W, Lee, J, Ratan, RR, and Filbin, MT (2002) Arginase I and polyamines act downstream from cyclic AMP in overcoming inhibition of axonal growth MAG and myelin in vitro. Neuron 35: 711-719.

Cai, D, Qiu, J, Cao, Z, McAtee, M, Bregman, BS, and Filbin, MT (2001) Neuronal cyclic AMP controls the developmental loss in ability of axons to regenerate. J.Neurosci. 21: 4731-4739.

Cai, D, Shen, Y, De Bellard, M, Tang, S, and Filbin, MT (1999) Prior exposure to neurotrophins blocks inhibition of axonal regeneration by MAG and myelin via a cAMP-dependent mechanism. Neuron 22: 89-101.

Campadelli-Fiume, G, Cocchi, F, Menotti, L, and Lopez, M (2000) The novel receptors that mediate the entry of herpes simplex viruses and animal alphaherpesviruses into cells. Rev.Med.Virol. 10: 305-319.

Campbell, G, Holt, JK, Shotton, HR, Anderson, PN, Bavetta, S, and Lieberman, AR (1999) Spontaneous axonal regeneration after optic nerve injury in adult rat. Neuroreport 10: 3955-3960.

Canning, DR, Hoke, A, Malemud, CJ, and Silver, J (1996) A potent inhibitor of neurite outgrowth that predominates in the extracellular matrix of reactive astrocytes. Int.J.Dev.Neurosci. 14: 153-175.

Carenini, S, Montag, D, Cremer, H, Schachner, M, and Martini, R (1997) Absence of the myelin-associated glycoprotein (MAG) and the neural cell adhesion molecule (N-CAM) interferes with the maintenance, but not with the formation of peripheral myelin. Cell Tissue Res. 287: 3-9.

Carim-Todd, L, Escarceller, M, Estivill, X, and Sumoy, L (2003) LRRN6A/LERN1 (leucine-rich repeat neuronal protein 1), a novel gene with enriched expression in limbic system and neocortex. Eur.J.Neurosci. 18: 3167-3182.

Carlstedt, T (1985) Regenerating axons form nerve terminals at astrocytes. Brain Res. 347: 188-191.

Carlstedt, T (1988) Reinnervation of the mammalian spinal cord after neonatal dorsal root crush. J.Neurocytol. 17: 335-350.

Caroni, P (1997) Intrinsic neuronal determinants that promote axonal sprouting and elongation. Bioessays 19: 767-775.

Caroni, P, Savio, T, and Schwab, ME (1988) Central nervous system regeneration: oligodendrocytes and myelin as non-permissive substrates for neurite growth. Prog.Brain Res. 78: 363-370.

Caroni, P and Schwab, ME (1988a) Antibody against myelin-associated inhibitor of neurite growth neutralizes nonpermissive substrate properties of CNS white matter. Neuron 1: 85-96.

Caroni, P and Schwab, ME (1988b) Two membrane protein fractions from rat central myelin with inhibitory properties for neurite growth and fibroblast spreading. J.Cell Biol. 106: 1281-1288.

Carter, BD, Kaltschmidt, C, Kaltschmidt, B, Offenhauser, N, Bohm-Matthaei, R, Baeuerle, PA, and Barde, YA (1996) Selective activation of NF-kappa B by nerve growth factor through the neurotrophin receptor p75. Science 272: 542-545.

Carulli, D, Buffo, A, Botta, C, Altruda, F, and Strata, P (2002) Regenerative and survival capabilities of Purkinje cells overexpressing c-Jun. Eur.J.Neurosci. 16: 105-118.

Cedar, H (1988) DNA methylation and gene activity. Cell 53: 3-4.

Chaisuksunt, V, Campbell, G, Zhang, Y, Schachner, M, Lieberman, AR, and Anderson, PN (2003) Expression of regeneration-related molecules in injured and regenerating striatal and nigral neurons. J.Neurocytol. 32: 161-183.

Chaisuksunt, V, Zhang, Y, Anderson, PN, Campbell, G, Vaudano, E, Schachner, M, and Lieberman, AR (2000a) Axonal regeneration from CNS neurons in the cerebellum and brainstem of adult rats: correlation with the patterns of expression and distribution of messenger RNAs for L1, CHL1, c-jun and growth-associated protein-43. Neuroscience 100: 87-108.

Chaisuksunt, V, Zhang, Y, Anderson, PN, Campbell, G, Vaudano, E, Schachner, M, and Lieberman, AR (2000b) Axonal regeneration from CNS neurons in the cerebellum and brainstem of adult rats: correlation with the patterns of expression and distribution of messenger RNAs for L1, CHL1, c-jun and growth-associated protein-43. Neuroscience 100: 87-108.

Chen, MS, Huber, AB, van der Haar, ME, Frank, M, Schnell, L, Spillmann, AA, Christ, F, and Schwab, ME (2000) Nogo-A is a myelin-associated neurite outgrowth inhibitor and an antigen for monoclonal antibody IN-1. Nature 403: 434-439.

Chen, ZJ, Negra, M, Levine, A, Ughrin, Y, and Levine, JM (2002) Oligodendrocyte precursor cells: reactive cells that inhibit axon growth and regeneration. J.Neurocytol. 31: 481-495.

Cheng, HL, Randolph, A, Yee, D, Delafontaine, P, Tennekoon, G, and Feldman, EL (1996) Characterization of insulin-like growth factor-I and its receptor and binding proteins in transected nerves and cultured Schwann cells. J.Neurochem. 66: 525-536.

Chong, MS, Reynolds, ML, Irwin, N, Coggeshall, RE, Emson, PC, Benowitz, LI, and Woolf, CJ (1994) GAP-43 expression in primary sensory neurons following central axotomy. J.Neurosci. 14: 4375-4384.

Chong, MS, Woolf, CJ, Haque, NS, and Anderson, PN (1999) Axonal regeneration from injured dorsal roots into the spinal cord of adult rats. J.Comp Neurol. 410: 42-54.

Chong, MS, Woolf, CJ, Turmaine, M, Emson, PC, and Anderson, PN (1996) Intrinsic versus extrinsic factors in determining the regeneration of the central processes of rat dorsal root ganglion neurons: the influence of a peripheral nerve graft. J.Comp Neurol. 370: 97-104.

Clemens, MJ and Elia, A (1997) The double-stranded RNA-dependent protein kinase PKR: structure and function. J.Interferon Cytokine Res. 17: 503-524.

Cogoni, C and Macino, G (2000) Post-transcriptional gene silencing across kingdoms. Curr.Opin.Genet.Dev. 10: 638-643.

Cohen, S (1960) Purification and metabolic effects of the nerve growth-promoting protein from mouse salivary gland and its neuro-cytotoxic antiserum. Proc.Natl.Acad.Sci.U.S.A 46: 302-311.

Connelly, JC, Kirkham, LA, and Leach, DR (1998) The SbcCD nuclease of Escherichia coli is a structural maintenance of chromosomes (SMC) family protein that cleaves hairpin DNA. Proc.Natl.Acad.Sci.U.S.A 95: 7969-7974.

Conover, JC, Erickson, JT, Katz, DM, Bianchi, LM, Poueymirou, WT, McClain, J, Pan, L, Helgren, M, Ip, NY, Boland, P, and . (1995) Neuronal deficits, not involving motor neurons, in mice lacking BDNF and/or NT4. Nature 375: 235-238.

Cordon-Cardo, C, Tapley, P, Jing, SQ, Nanduri, V, O'Rourke, E, Lamballe, F, Kovary, K, Klein, R, Jones, KR, Reichardt, LF, and . (1991) The trk tyrosine protein kinase mediates the mitogenic properties of nerve growth factor and neurotrophin-3. Cell 66: 173-183.

Cosgaya, JM, Chan, JR, and Shooter, EM (2002) The neurotrophin receptor p75NTR as a positive modulator of myelination. Science 298: 1245-1248.

Costigan, M, Befort, K, Karchewski, L, Griffin, RS, D'Urso, D, Allchorne, A, Sitarski, J, Mannion, JW, Pratt, RE, and Woolf, CJ (2002) Replicate high-density rat genome oligonucleotide microarrays reveal hundreds of regulated genes in the dorsal root ganglion after peripheral nerve injury. BMC.Neurosci. 3: 16

Curtis, R, Scherer, SS, Somogyi, R, Adryan, KM, Ip, NY, Zhu, Y, Lindsay, RM, and DiStefano, PS (1994) Retrograde axonal transport of LIF is increased by peripheral nerve injury: correlation with increased LIF expression in distal nerve. Neuron 12: 191-204.

Curtis, R, Stewart, HJ, Hall, SM, Wilkin, GP, Mirsky, R, and Jessen, KR (1992) GAP-43 is expressed by nonmyelin-forming Schwann cells of the peripheral nervous system. J.Cell Biol. 116: 1455-1464.

David, S (1988) Neurite outgrowth from mammalian CNS neurons on astrocytes in vitro may not be mediated primarily by laminin. J.Neurocytol. 17: 131-144.

Davies, SJ, Fitch, MT, Memberg, SP, Hall, AK, Raisman, G, and Silver, J (1997) Regeneration of adult axons in white matter tracts of the central nervous system. Nature 390: 680-683.

Davies, SJ, Goucher, DR, Doller, C, and Silver, J (1999) Robust regeneration of adult sensory axons in degenerating white matter of the adult rat spinal cord. J.Neurosci. 19: 5810-5822.

de Leon, M, Nahin, RL, Molina, CA, De Leon, DD, and Ruda, MA (1995) Comparison of c-jun, junB, and junD mRNA expression and protein in the rat dorsal root ganglia following sciatic nerve transection. J.Neurosci.Res. 42: 391-401.

De Winter, F, Oudega, M, Lankhorst, AJ, Hamers, FP, Blits, B, Ruitenberg, MJ, Pasterkamp, RJ, Gispen, WH, and Verhaagen, J (2002) Injury-induced class 3 semaphorin expression in the rat spinal cord. Exp.Neurol. 175: 61-75.

Dechant, G and Barde, YA (2002) The neurotrophin receptor p75(NTR): novel functions and implications for diseases of the nervous system. Nat.Neurosci. 5: 1131-1136.

Della-Bianca, V, Rossi, F, Armato, U, Dal Pra, I, Costantini, C, Perini, G, Politi, V, and Della, VG (2001) Neurotrophin p75 receptor is involved in neuronal damage by prion peptide-(106-126). J.Biol.Chem. 276: 38929-38933.

Deller, T, Haas, CA, Naumann, T, Joester, A, Faissner, A, and Frotscher, M (1997) Up-regulation of astrocyte-derived tenascin-C correlates with neurite outgrowth in the rat dentate gyrus after unilateral entorhinal cortex lesion. Neuroscience 81: 829-846.

DeLuca, NA, McCarthy, AM, and Schaffer, PA (1985) Isolation and characterization of deletion mutants of herpes simplex virus type 1 in the gene encoding immediate-early regulatory protein ICP4. J.Virol. 56: 558-570.

Demaison, C, Parsley, K, Brouns, G, Scherr, M, Battmer, K, Kinnon, C, Grez, M, and Thrasher, AJ (2002) High-level transduction and gene expression in hematopoietic repopulating cells using a human immunodeficiency [correction of imunodeficiency] virus type 1-based lentiviral vector containing an internal spleen focus forming virus promoter. Hum.Gene Ther. 13: 803-813.

Dergham, P, Ellezam, B, Essagian, C, Avedissian, H, Lubell, WD, and McKerracher, L (2002) Rho signaling pathway targeted to promote spinal cord repair. J.Neurosci. 22: 6570-6577.

Deshmane, SL and Fraser, NW (1989) During latency, herpes simplex virus type 1 DNA is associated with nucleosomes in a chromatin structure. J.Virol. 63: 943-947.

Di Paolo, G, Lutjens, R, Pellier, V, Stimpson, SA, Beuchat, MH, Catsicas, S, and Grenningloh, G (1997) Targeting of SCG10 to the area of the Golgi complex is mediated by its NH2-terminal region. J.Biol.Chem. 272: 5175-5182.

Ding, J, Hu, B, Tang, LS, and Yip, HK (2001) Study of the role of the low-affinity neurotrophin receptor p75 in naturally occurring cell death during development of the rat retina. Dev.Neurosci. 23: 390-398.

Dirac, AM and Bernards, R (2003) Reversal of senescence in mouse fibroblasts through lentiviral suppression of p53. J.Biol.Chem. 278: 11731-11734.

DiStefano, PS and Curtis, R (1994) Receptor mediated retrograde axonal transport of neurotrophic factors is increased after peripheral nerve injury. Prog.Brain Res. 103: 35-42.

Dobson, AT, Sederati, F, Devi-Rao, G, Flanagan, WM, Farrell, MJ, Stevens, JG, Wagner, EK, and Feldman, LT (1989) Identification of the latency-associated transcript promoter by expression of rabbit beta-globin mRNA in mouse sensory nerve ganglia latently infected with a recombinant herpes simplex virus. J.Virol. 63: 3844-3851.

Domeniconi, M, Cao, Z, Spencer, T, Sivasankaran, R, Wang, K, Nikulina, E, Kimura, N, Cai, H, Deng, K, Gao, Y, He, Z, and Filbin, M (2002) Myelin-associated glycoprotein interacts with the Nogo66 receptor to inhibit neurite outgrowth. Neuron 35: 283-290.

Donovan, MJ, Hahn, R, Tessarollo, L, and Hempstead, BL (1996) Identification of an essential nonneuronal function of neurotrophin 3 in mammalian cardiac development. Nat.Genet. 14: 210-213.

Doster, SK, Lozano, AM, Aguayo, AJ, and Willard, MB (1991) Expression of the growth-associated protein GAP-43 in adult rat retinal ganglion cells following axon injury. Neuron 6: 635-647.

Dou, CL and Levine, JM (1994) Inhibition of neurite growth by the NG2 chondroitin sulfate proteoglycan. J.Neurosci. 14: 7616-7628.

Doyu, M, Sobue, G, Ken, E, Kimata, K, Shinomura, T, Yamada, Y, Mitsuma, T, and Takahashi, A (1993) Laminin A, B1, and B2 chain gene expression in transected and regenerating nerves: regulation by axonal signals. J.Neurochem. 60: 543-551.

Dupuis, L, Gonzalez de Aguilar, JL, di Scala, F, Rene, F, de Tapia, M, Pradat, PF, Lacomblez, L, Seihlan, D, Prinjha, R, Walsh, FS, Meininger, V, and Loeffler, JP (2002) Nogo provides a molecular marker for diagnosis of amyotrophic lateral sclerosis. Neurobiol.Dis. 10: 358-365.

Eather, TF, Pollock, M, and Myers, DB (1986) Proximal and distal changes in collagen content of peripheral nerve that follow transection and crush lesions. Exp.Neurol. 92: 299-310.

Elbashir, SM, Harborth, J, Lendeckel, W, Yalcin, A, Weber, K, and Tuschl, T (2001a) Duplexes of 21-nucleotide RNAs mediate RNA interference in cultured mammalian cells. Nature 411: 494-498.

Elbashir, SM, Lendeckel, W, and Tuschl, T (2001b) RNA interference is mediated by 21- and 22-nucleotide RNAs. Genes Dev. 15: 188-200.

Elbashir, SM, Martinez, J, Patkaniowska, A, Lendeckel, W, and Tuschl, T (2001c) Functional anatomy of siRNAs for mediating efficient RNAi in Drosophila melanogaster embryo lysate. EMBO J. 20: 6877-6888.

Erickson, JT, Conover, JC, Borday, V, Champagnat, J, Barbacid, M, Yancopoulos, G, and Katz, DM (1996) Mice lacking brain-derived neurotrophic factor exhibit visceral sensory neuron losses distinct from mice lacking NT4 and display a severe developmental deficit in control of breathing. J.Neurosci. 16: 5361-5371.

Ernfors, P, Lee, KF, Kucera, J, and Jaenisch, R (1994) Lack of neurotrophin-3 leads to deficiencies in the peripheral nervous system and loss of limb proprioceptive afferents. Cell 77: 503-512.

Ernfors, P, Wetmore, C, Olson, L, and Persson, H (1990) Identification of cells in rat brain and peripheral tissues expressing mRNA for members of the nerve growth factor family. Neuron 5: 511-526.

Farooque, M, Badonic, T, Olsson, Y, and Holtz, A (1995) Astrocytic reaction after graded spinal cord compression in rats: immunohistochemical studies on glial fibrillary acidic protein and vimentin. J.Neurotrauma 12: 41-52.

Fawcett, JW and Asher, RA (1999) The glial scar and central nervous system repair. Brain Res.Bull. 49: 377-391.

Fawcett, JW, Housden, E, Smith-Thomas, L, and Meyer, RL (1989) The growth of axons in three-dimensional astrocyte cultures. Dev.Biol. 135: 449-458.

Federoff, HJ, Grabczyk, E, and Fishman, MC (1988) Dual regulation of GAP-43 gene expression by nerve growth factor and glucocorticoids. J.Biol.Chem. 263: 19290-19295.

Feinberg, AP and Vogelstein, B (1983) A technique for radiolabelling DNA restriction endonuclease fragments to high specific activity. Anal.Biochem. 132: 6-13.

Fernandes, KJ, Fan, DP, Tsui, BJ, Cassar, SL, and Tetzlaff, W (1999) Influence of the axotomy to cell body distance in rat rubrospinal and spinal motoneurons: differential regulation of GAP-43, tubulins, and neurofilament-M. J.Comp Neurol. 414: 495-510.

Ferretti, P, Zhang, F, and O'Neill, P (2003) Changes in spinal cord regenerative ability through phylogenesis and development: lessons to be learnt. Dev.Dyn. 226: 245-256.

Fidler, PS, Schuette, K, Asher, RA, Dobbertin, A, Thornton, SR, Calle-Patino, Y, Muir, E, Levine, JM, Geller, HM, Rogers, JH, Faissner, A, and Fawcett, JW (1999) Comparing astrocytic cell lines that are inhibitory or permissive for axon growth: the major axon-inhibitory proteoglycan is NG2. J.Neurosci. 19: 8778-8788.

Filbin, MT (2003) Myelin-associated inhibitors of axonal regeneration in the adult mammalian CNS. Nat.Rev.Neurosci. 4: 703-713.

Fire, A, Xu, S, Montgomery, MK, Kostas, SA, Driver, SE, and Mello, CC (1998) Potent and specific genetic interference by double-stranded RNA in Caenorhabditis elegans. Nature 391: 806-811.

Fischer, D, He, Z, and Benowitz, LI (2004) Counteracting the Nogo receptor enhances optic nerve regeneration if retinal ganglion cells are in an active growth state. J.Neurosci. 24: 1646-1651.

Fitch, MT, Doller, C, Combs, CK, Landreth, GE, and Silver, J (1999) Cellular and molecular mechanisms of glial scarring and progressive cavitation: in vivo and in vitro analysis of inflammation-induced secondary injury after CNS trauma. J.Neurosci. 19: 8182-8198.

Fok-Seang, J, DiProspero, NA, Meiners, S, Muir, E, and Fawcett, JW (1998) Cytokine-induced changes in the ability of astrocytes to support migration of oligodendrocyte precursors and axon growth. Eur.J.Neurosci. 10: 2400-2415.

Fournier, AE, Gould, GC, Liu, BP, and Strittmatter, SM (2002) Truncated soluble Nogo receptor binds Nogo-66 and blocks inhibition of axon growth by myelin. J.Neurosci. 22: 8876-8883.

Fournier, AE, Grandpre, T, and Strittmatter, SM (2001) Identification of a receptor mediating Nogo-66 inhibition of axonal regeneration. Nature 409: 341-346.

Fournier, AE, Takizawa, BT, and Strittmatter, SM (2003) Rho kinase inhibition enhances axonal regeneration in the injured CNS. J.Neurosci. 23: 1416-1423.

Fruh, K, Ahn, K, Djaballah, H, Sempe, P, van Endert, PM, Tampe, R, Peterson, PA, and Yang, Y (1995) A viral inhibitor of peptide transporters for antigen presentation. Nature 375: 415-418.

Fruttiger, M, Montag, D, Schachner, M, and Martini, R (1995) Crucial role for the myelin-associated glycoprotein in the maintenance of axon-myelin integrity. Eur.J.Neurosci. 7: 511-515.

Fujita, N, Kemper, A, Dupree, J, Nakayasu, H, Bartsch, U, Schachner, M, Maeda, N, Suzuki, K, and Popko, B (1998) The cytoplasmic domain of the large myelin-associated glycoprotein isoform is needed for proper CNS but not peripheral nervous system myelination. J.Neurosci. 18: 1970-1978.

Funakoshi, H, Frisen, J, Barbany, G, Timmusk, T, Zachrisson, O, Verge, VM, and Persson, H (1993) Differential expression of mRNAs for neurotrophins and their receptors after axotomy of the sciatic nerve. J.Cell Biol. 123: 455-465.

Garcia-Valenzuela, E, Gorczyca, W, Darzynkiewicz, Z, and Sharma, SC (1994) Apoptosis in adult retinal ganglion cells after axotomy. J.Neurobiol. 25: 431-438.

Gard, AL, Maughon, RH, and Schachner, M (1996) In vitro oligodendrogliotrophic properties of cell adhesion molecules in the immunoglobulin superfamily: myelin-associated glycoprotein and N-CAM. J.Neurosci.Res. 46: 415-426.

Giehl, KM (2001) Trophic dependencies of rodent corticospinal neurons. Rev.Neurosci. 12: 79-94.

Ginham, R, Harrison, DC, Facci, L, Skaper, S, and Philpott, KL (2001) Upregulation of death pathway molecules in rat cerebellar granule neurons undergoing apoptosis. Neurosci.Lett. 302: 113-116.

Goldman, S (2003) Glia as neural progenitor cells. Trends Neurosci. 26: 590-596.

Goldstein, DJ and Weller, SK (1988) Factor(s) present in herpes simplex virus type 1-infected cells can compensate for the loss of the large subunit of the viral ribonucleotide reductase: characterization of an ICP6 deletion mutant. Virology 166: 41-51.

Gomez, VM, Averill, S, King, V, Yang, Q, Perez, ED, Chacon, SC, Ward, R, Nieto-Sampedro, M, Priestley, J, and Taylor, J (2003) Transplantation of olfactory ensheathing cells fails to promote significant axonal regeneration from dorsal roots into the rat cervical cord. J.Neurocytol. 32: 53-70.

Gorgels, TG, De Kort, EJ, Van Aanholt, HT, and Nieuwenhuys, R (1989) A quantitative analysis of the development of the pyramidal tract in the cervical spinal cord in the rat. Anat.Embryol.(Berl) 179: 377-385.

Gotz, B, Scholze, A, Clement, A, Joester, A, Schutte, K, Wigger, F, Frank, R, Spiess, E, Ekblom, P, and Faissner, A (1996) Tenascin-C contains distinct adhesive, anti-adhesive, and neurite outgrowth promoting sites for neurons. J.Cell Biol. 132: 681-699.

Gotz, R, Koster, R, Winkler, C, Raulf, F, Lottspeich, F, Schartl, M, and Thoenen, H (1994) Neurotrophin-6 is a new member of the nerve growth factor family. Nature 372: 266-269.

Grandpre, T, Li, S, and Strittmatter, SM (2002) Nogo-66 receptor antagonist peptide promotes axonal regeneration. Nature 417: 547-551.

Grandpre, T, Nakamura, F, Vartanian, T, and Strittmatter, SM (2000) Identification of the Nogo inhibitor of axon regeneration as a Reticulon protein. Nature 403: 439-444.

Gravel, C and Hawkes, R (1990) Parasagittal organization of the rat cerebellar cortex: direct comparison of Purkinje cell compartments and the organization of the spinocerebellar projection. J.Comp Neurol. 291: 79-102.

Greene, LA and Tischler, AS (1976) Establishment of a noradrenergic clonal line of rat adrenal pheochromocytoma cells which respond to nerve growth factor. Proc.Natl.Acad.Sci.U.S.A 73: 2424-2428.

Greenwood, K and Butt, AM (2003) Evidence that perinatal and adult NG2-glia are not conventional oligodendrocyte progenitors and do not depend on axons for their survival. Mol.Cell Neurosci. 23: 544-558.

Grill, R, Murai, K, Blesch, A, Gage, FH, and Tuszynski, MH (1997) Cellular delivery of neurotrophin-3 promotes corticospinal axonal growth and partial functional recovery after spinal cord injury. J.Neurosci. 17: 5560-5572.

Grishok, A, Pasquinelli, AE, Conte, D, Li, N, Parrish, S, Ha, I, Baillie, DL, Fire, A, Ruvkun, G, and Mello, CC (2001) Genes and mechanisms related to RNA interference regulate expression of the small temporal RNAs that control C. elegans developmental timing. Cell 106: 23-34.

Grumet, M, Flaccus, A, and Margolis, RU (1993) Functional characterization of chondroitin sulfate proteoglycans of brain: interactions with neurons and neural cell adhesion molecules. J.Cell Biol. 120: 815-824.

Gschwendtner, A, Liu, Z, Hucho, T, Bohatschek, M, Kalla, R, Dechant, G, and Raivich, G (2003) Regulation, cellular localization, and function of the p75 neurotrophin receptor (p75NTR) during the regeneration of facial motoneurons. Mol.Cell Neurosci. 24: 307-322.

Guillery, RW and Walsh, C (1987) Changing glial organization relates to changing fiber order in the developing optic nerve of ferrets. J.Comp Neurol. 265: 203-217.

Guillin, O, Diaz, J, Carroll, P, Griffon, N, Schwartz, JC, and Sokoloff, P (2001) BDNF controls dopamine D3 receptor expression and triggers behavioural sensitization. Nature 411: 86-89.

Gupta, SK, Poduslo, JF, Dunn, R, Roder, J, and Mezei, C (1990) Myelin-associated glycoprotein gene expression in the presence and absence of Schwann cell-axonal contact. Dev.Neurosci. 12: 22-33.

Habib, AA, Gulcher, JR, Hognason, T, Zheng, L, and Stefansson, K (1998a) The OMgp gene, a second growth suppressor within the NF1 gene. Oncogene 16: 1525-1531.

Habib, AA, Marton, LS, Allwardt, B, Gulcher, JR, Mikol, DD, Hognason, T, Chattopadhyay, N, and Stefansson, K (1998b) Expression of the oligodendrocyte-myelin glycoprotein by neurons in the mouse central nervous system. J.Neurochem. 70: 1704-1711.

Habib, AA, Marton, LS, Allwardt, B, Gulcher, JR, Mikol, DD, Hognason, T, Chattopadhyay, N, and Stefansson, K (1998c) Expression of the oligodendrocyte-myelin glycoprotein by neurons in the mouse central nervous system. J.Neurochem. 70: 1704-1711.

Hai, T and Curran, T (1991) Cross-family dimerization of transcription factors Fos/Jun and ATF/CREB alters DNA binding specificity. Proc.Natl.Acad.Sci.U.S.A 88: 3720-3724.

Hai, T and Hartman, MG (2001) The molecular biology and nomenclature of the activating transcription factor/cAMP responsive element binding family of transcription factors: activating transcription factor proteins and homeostasis. Gene 273: 1-11.

Hai, T, Wolfgang, CD, Marsee, DK, Allen, AE, and Sivaprasad, U (1999) ATF3 and stress responses. Gene Expr. 7: 321-335.

Hall, S and Berry, M (1989) Electron microscopic study of the interaction of axons and glia at the site of anastomosis between the optic nerve and cellular or acellular sciatic nerve grafts. J.Neurocytol. 18: 171-184.

Hall, SM, Kent, AP, Curtis, R, and Robertson, D (1992) Electron microscopic immunocytochemistry of GAP-43 within proximal and chronically denervated distal stumps of transected peripheral nerve. J.Neurocytol. 21: 820-831.

Hallbook, F, Ibanez, CF, and Persson, H (1991) Evolutionary studies of the nerve growth factor family reveal a novel member abundantly expressed in Xenopus ovary. Neuron 6: 845-858.

Ham, J, Babij, C, Whitfield, J, Pfarr, CM, Lallemand, D, Yaniv, M, and Rubin, LL (1995) A c-Jun dominant negative mutant protects sympathetic neurons against programmed cell death. Neuron 14: 927-939.

Hamilton, AJ and Baulcombe, DC (1999) A species of small antisense RNA in posttranscriptional gene silencing in plants. Science 286: 950-952.

Hammond, SM, Caudy, AA, and Hannon, GJ (2001) Post-transcriptional gene silencing by double-stranded RNA. Nat.Rev.Genet. 2: 110-119.

Harding, DI, Greensmith, L, Mason, M, Anderson, PN, and Vrbova, G (1999) Overexpression of GAP-43 induces prolonged sprouting and causes death of adult motoneurons. Eur.J.Neurosci. 11: 2237-2242.

Harrington, AW, Leiner, B, Blechschmitt, C, Arevalo, JC, Lee, R, Morl, K, Meyer, M, Hempstead, BL, Yoon, SO, and Giehl, KM (2004) Secreted proNGF is a pathophysiological death-inducing ligand after adult CNS injury. Proc.Natl.Acad.Sci.U.S.A 101: 6226-6230.

Harvey, AR and Tan, MM (1992) Spontaneous regeneration of adult rat retinal ganglion cell axons in vivo. Neuroreport 3: 239-242.

Hawkes, R and Leclerc, N (1989) Purkinje cell axon collateral distributions reflect the chemical compartmentation of the rat cerebellar cortex. Brain Res. 476: 279-290.

He, B, Gross, M, and Roizman, B (1997) The gamma(1)34.5 protein of herpes simplex virus 1 complexes with protein phosphatase 1alpha to dephosphorylate the alpha subunit of the eukaryotic translation initiation factor 2 and preclude the shutoff of protein synthesis by double-stranded RNA-activated protein kinase. Proc.Natl.Acad.Sci.U.S.A 94: 843-848.

Hempstead, BL, Martin-Zanca, D, Kaplan, DR, Parada, LF, and Chao, MV (1991) High-affinity NGF binding requires coexpression of the trk proto-oncogene and the low-affinity NGF receptor. Nature 350: 678-683.

Herdegen, T, Kovary, K, Buhl, A, Bravo, R, Zimmermann, M, and Gass, P (1995) Basal expression of the inducible transcription factors c-Jun, JunB, JunD, c-Fos, FosB, and Krox-24 in the adult rat brain. J.Comp Neurol. 354: 39-56.

Herdegen, T, Leah, JD, Manisali, A, Bravo, R, and Zimmermann, M (1991) c-JUN-like immunoreactivity in the CNS of the adult rat: basal and transynaptically induced expression of an immediate-early gene. Neuroscience 41: 643-654.

Hermanns, S, Reiprich, P, and Muller, HW (2001) A reliable method to reduce collagen scar formation in the lesioned rat spinal cord. J.Neurosci.Methods 110: 141-146.

Heumann, R, Korsching, S, Bandtlow, C, and Thoenen, H (1987) Changes of nerve growth factor synthesis in nonneuronal cells in response to sciatic nerve transection. J.Cell Biol. 104: 1623-1631.

Hill, A, Jugovic, P, York, I, Russ, G, Bennink, J, Yewdell, J, Ploegh, H, and Johnson, D (1995) Herpes simplex virus turns off the TAP to evade host immunity. Nature 375: 411-415.

Hillenbrand, R, Molthagen, M, Montag, D, and Schachner, M (1999) The close homologue of the neural adhesion molecule L1 (CHL1): patterns of expression and promotion of neurite outgrowth by heterophilic interactions. Eur.J.Neurosci. 11: 813-826.

Hirsch, S and Bahr, M (1999) Immunocytochemical characterization of reactive optic nerve astrocytes and meningeal cells. Glia 26: 36-46.

Hirsch, S, Labes, M, and Bahr, M (2000) Changes in BDNF and neurotrophin receptor expression in degenerating and regenerating rat retinal ganglion cells. Restor.Neurol.Neurosci. 17: 125-134.

Holliday, R (1987) DNA methylation and epigenetic defects in carcinogenesis. Mutat.Res. 181: 215-217.

Hu, H (2001) Cell-surface heparan sulfate is involved in the repulsive guidance activities of Slit2 protein. Nat.Neurosci. 4: 695-701.

Hu, WH, Hausmann, ON, Yan, MS, Walters, WM, Wong, PK, and Bethea, JR (2002) Identification and characterization of a novel Nogo-interacting mitochondrial protein (NIMP). J.Neurochem. 81: 36-45.

Huang, ZJ, Kirkwood, A, Pizzorusso, T, Porciatti, V, Morales, B, Bear, MF, Maffei, L, and Tonegawa, S (1999) BDNF regulates the maturation of inhibition and the critical period of plasticity in mouse visual cortex. Cell 98: 739-755.

Huber, AB, Weinmann, O, Brosamle, C, Oertle, T, and Schwab, ME (2002) Patterns of Nogo mRNA and protein expression in the developing and adult rat and after CNS lesions. J.Neurosci. 22: 3553-3567.

Hunt, D, Coffin, RS, and Anderson, PN (2002a) The Nogo receptor, its ligands and axonal regeneration in the spinal cord; a review. J.Neurocytol. 31: 93-120.

Hunt, D, Coffin, RS, Prinjha, RK, Campbell, G, and Anderson, PN (2003) Nogo-A expression in the intact and injured nervous system. Mol.Cell Neurosci. 24: 1083-1102.

Hunt, D, Hossain-Ibrahim, K, Mason, MR, Coffin, RS, Lieberman, AR, Winterbottom, J, and Anderson, PN (2004) ATF3 upregulation in glia during Wallerian degeneration: differential expression in peripheral nerves and CNS white matter. BMC.Neurosci. 5: 9

Hunt, D, Mason, MR, Campbell, G, Coffin, R, and Anderson, PN (2002b) Nogo receptor mRNA expression in intact and regenerating CNS neurons. Mol.Cell Neurosci. 20: 537-552.

Hutvagner, G, McLachlan, J, Pasquinelli, AE, Balint, E, Tuschl, T, and Zamore, PD (2001) A cellular function for the RNA-interference enzyme Dicer in the maturation of the let-7 small temporal RNA. Science 293: 834-838.

Indo, Y, Tsuruta, M, Hayashida, Y, Karim, MA, Ohta, K, Kawano, T, Mitsubuchi, H, Tonoki, H, Awaya, Y, and Matsuda, I (1996) Mutations in the TRKA/NGF receptor gene in patients with congenital insensitivity to pain with anhidrosis. Nat.Genet. 13: 485-488.

Inman, DM and Steward, O (2003) Physical size does not determine the unique histopathological response seen in the injured mouse spinal cord. J.Neurotrauma 20: 33-42.

Ip, NY, Ibanez, CF, Nye, SH, McClain, J, Jones, PF, Gies, DR, Belluscio, L, Le Beau, MM, Espinosa, R, III, Squinto, SP, and . (1992) Mammalian neurotrophin-4: structure, chromosomal localization, tissue distribution, and receptor specificity. Proc.Natl.Acad.Sci.U.S.A 89: 3060-3064.

Ivins, JK and Pittman, RN (1989) Growth cone-growth cone interactions in cultures of rat sympathetic neurons. Dev.Biol. 135: 147-157.

Jacob, RJ, Morse, LS, and Roizman, B (1979) Anatomy of herpes simplex virus DNA. XII. Accumulation of head-to-tail concatemers in nuclei of infected cells and their role in the generation of the four isomeric arrangements of viral DNA. J.Virol. 29: 448-457.

Jap Tjoen, SE, Schmidt-Michels, M, Oestreicher, AB, Gispen, WH, and Schotman, P (1992) Inhibition of nerve growth factor-induced B-50/GAP-43 expression by antisense oligomers interferes with neurite outgrowth of PC12 cells. Biochem.Biophys.Res.Commun. 187: 839-846.

Jenkins, R and Hunt, SP (1991) Long-term increase in the levels of c-jun mRNA and jun protein-like immunoreactivity in motor and sensory neurons following axon damage. Neurosci.Lett. 129: 107-110.

Jin, WL, Liu, YY, Liu, HL, Yang, H, Wang, Y, Jiao, XY, and Ju, G (2003) Intraneuronal localization of Nogo-A in the rat. J.Comp Neurol. 458: 1-10.

Joester, A and Faissner, A (2001) The structure and function of tenascins in the nervous system. Matrix Biol. 20: 13-22.

Johnson, D, Lanahan, A, Buck, CR, Sehgal, A, Morgan, C, Mercer, E, Bothwell, M, and Chao, M (1986) Expression and structure of the human NGF receptor. Cell 47: 545-554.

Johnson, EM, Jr., Osborne, PA, Rydel, RE, Schmidt, RE, and Pearson, J (1983) Characterization of the effects of autoimmune nerve growth factor deprivation in the developing guinea-pig. Neuroscience 8: 631-642.

Johnson, PA, Wang, MJ, and Friedmann, T (1994) Improved cell survival by the reduction of immediate-early gene expression in replication-defective mutants of herpes simplex virus type 1 but not by mutation of the virion host shutoff function. J.Virol. 68: 6347-6362.

Johnson, RS, van Lingen, B, Papaioannou, VE, and Spiegelman, BM (1993) A null mutation at the c-jun locus causes embryonic lethality and retarded cell growth in culture. Genes Dev. 7: 1309-1317.

Jones, KR and Reichardt, LF (1990) Molecular cloning of a human gene that is a member of the nerve growth factor family. Proc.Natl.Acad.Sci.U.S.A 87: 8060-8064.

Jones, L, Hamilton, AJ, Voinnet, O, Thomas, CL, Maule, AJ, and Baulcombe, DC (1999) RNA-DNA interactions and DNA methylation in post-transcriptional gene silencing. Plant Cell 11: 2291-2301.

Jones, LL, Oudega, M, Bunge, MB, and Tuszynski, MH (2001) Neurotrophic factors, cellular bridges and gene therapy for spinal cord injury. J.Physiol 533: 83-89.

Jones, LL, Sajed, D, and Tuszynski, MH (2003) Axonal regeneration through regions of chondroitin sulfate proteoglycan deposition after spinal cord injury: a balance of permissiveness and inhibition. J.Neurosci. 23: 9276-9288.

Joosten, EA, Gribnau, AA, and Dederen, PJ (1989) Postnatal development of the corticospinal tract in the rat. An ultrastructural anterograde HRP study. Anat.Embryol.(Berl) 179: 449-456.

Jordan, R and Schaffer, PA (1997) Activation of gene expression by herpes simplex virus type 1 ICP0 occurs at the level of mRNA synthesis. J.Virol. 71: 6850-6862.

Jorgensen, RA, Cluster, PD, English, J, Que, Q, and Napoli, CA (1996) Chalcone synthase cosuppression phenotypes in petunia flowers: comparison of sense vs. antisense constructs and single-copy vs. complex T-DNA sequences. Plant Mol.Biol. 31: 957-973.

Josephson, A, Trifunovski, A, Widmer, HR, Widenfalk, J, Olson, L, and Spenger, C (2002) Nogo-receptor gene activity: cellular localization and developmental regulation of mRNA in mice and humans. J.Comp Neurol. 453: 292-304.

Josephson, A, Widenfalk, J, Widmer, HW, Olson, L, and Spenger, C (2001) NOGO mRNA expression in adult and foetal human and rat nervous tissue and in weight drop injury. Exp.Neurol. 169: 319-328.

Kalcheim, C, Carmeli, C, and Rosenthal, A (1992) Neurotrophin 3 is a mitogen for cultured neural crest cells. Proc.Natl.Acad.Sci.U.S.A 89: 1661-1665.

Kalderon, N and Fuks, Z (1996) Structural recovery in lesioned adult mammalian spinal cord by x-irradiation of the lesion site. Proc.Natl.Acad.Sci.U.S.A 93: 11179-11184.

Kapfhammer, JP and Raper, JA (1987) Collapse of growth cone structure on contact with specific neurites in culture. J.Neurosci. 7: 201-212.

Kaplan, DR, Hempstead, BL, Martin-Zanca, D, Chao, MV, and Parada, LF (1991) The trk proto-oncogene product: a signal transducing receptor for nerve growth factor. Science 252: 554-558.

Kappler, J, Junghans, U, Koops, A, Stichel, CC, Hausser, HJ, Kresse, H, and Muller, HW (1997) Chondroitin/dermatan sulphate promotes the survival of neurons from rat embryonic neocortex. Eur.J.Neurosci. 9: 306-318.

Karns, LR, Ng, SC, Freeman, JA, and Fishman, MC (1987) Cloning of complementary DNA for GAP-43, a neuronal growth-related protein. Science 236: 597-600.

Kawaguchi, Y, Bruni, R, and Roizman, B (1997a) Interaction of herpes simplex virus 1 alpha regulatory protein ICP0 with elongation factor 1delta: ICP0 affects translational machinery. J.Virol. 71: 1019-1024.

Kawaguchi, Y, Van Sant, C, and Roizman, B (1997b) Herpes simplex virus 1 alpha regulatory protein ICP0 interacts with and stabilizes the cell cycle regulator cyclin D3. J.Virol. 71: 7328-7336.

Kawasaki, H and Taira, K (2004) Induction of DNA methylation and gene silencing by short interfering RNAs in human cells. Nature

Kay, BK, Williamson, MP, and Sudol, M (2000) The importance of being proline: the interaction of proline-rich motifs in signaling proteins with their cognate domains. FASEB J. 14: 231-241.

Kenney, AM and Kocsis, JD (1998) Peripheral axotomy induces long-term c-Jun amino-terminal kinase-1 activation and activator protein-1 binding activity by c-Jun and junD in adult rat dorsal root ganglia In vivo. J.Neurosci. 18: 1318-1328.

Ketting, RF, Fischer, SE, Bernstein, E, Sijen, T, Hannon, GJ, and Plasterk, RH (2001) Dicer functions in RNA interference and in synthesis of small RNA involved in developmental timing in C. elegans. Genes Dev. 15: 2654-2659.

Khvorova, A, Reynolds, A, and Jayasena, SD (2003) Functional siRNAs and miRNAs exhibit strand bias. Cell 115: 209-216.

Kiger, A, Baum, B, Jones, S, Jones, M, Coulson, A, Echeverri, C, and Perrimon, N (2003) A functional genomic analysis of cell morphology using RNA interference. J.Biol. 2: 27

Kim, JE, Liu, BP, Yang, X, and Strittmatter, SM (2003a) Recovery from spinal injury in mice lacking the Nogo-66 Receptor (Program No. 415.11).

Kim, JE, Bonilla, IE, Qiu, D, and Strittmatter, SM (2003b) Nogo-C is sufficient to delay nerve regeneration. Mol.Cell Neurosci. 23: 451-459.

Kim, JE, Li, S, Grandpre, T, Qiu, D, and Strittmatter, SM (2003c) Axon regeneration in young adult mice lacking Nogo-A/B. Neuron 38: 187-199.

Klein, R, Jing, SQ, Nanduri, V, O'Rourke, E, and Barbacid, M (1991a) The trk proto-oncogene encodes a receptor for nerve growth factor. Cell 65: 189-197.

Klein, R, Nanduri, V, Jing, SA, Lamballe, F, Tapley, P, Bryant, S, Cordon-Cardo, C, Jones, KR, Reichardt, LF, and Barbacid, M (1991b) The trkB tyrosine protein kinase is a receptor for brain-derived neurotrophic factor and neurotrophin-3. Cell 66: 395-403.

Korsching, S and Thoenen, H (1985) Nerve growth factor supply for sensory neurons: site of origin and competition with the sympathetic nervous system. Neurosci.Lett. 54: 201-205.

Kottis, V, Thibault, P, Mikol, D, Xiao, ZC, Zhang, R, Dergham, P, and Braun, PE (2002) Oligodendrocyte-myelin glycoprotein (OMgp) is an inhibitor of neurite outgrowth. J.Neurochem. 82: 1566-1569.

Kovalchuk, Y, Hanse, E, Kafitz, KW, and Konnerth, A (2002) Postsynaptic Induction of BDNF-Mediated Long-Term Potentiation. Science 295: 1729-1734.

Krautstrunk, M, Scholtes, F, Martin, D, Schoenen, J, Schmitt, AB, Plate, D, Nacimiento, W, Noth, J, and Brook, GA (2002) Increased expression of the putative axon growth-repulsive extracellular matrix molecule, keratan sulphate proteoglycan, following traumatic injury of the adult rat spinal cord. Acta Neuropathol.(Berl) 104: 592-600.

Kromer, LF and Cornbrooks, CJ (1985) Transplants of Schwann cell cultures promote axonal regeneration in the adult mammalian brain. Proc.Natl.Acad.Sci.U.S.A 82: 6330-6334.

Kubo, T, Yamashita, T, Yamaguchi, A, Hosokawa, K, and Tohyama, M (2002) Analysis of genes induced in peripheral nerve after axotomy using cDNA microarrays. J.Neurochem. 82: 1129-1136.

Kumamaru, E, Kuo, CH, Fujimoto, T, Kohama, K, Zeng, LH, Taira, E, Tanaka, H, Toyoda, T, and Miki, N (2004) Reticulon3 expression in rat optic and olfactory systems. Neurosci.Lett. 356: 17-20.

LaBoissiere, S and O'Hare, P (2000) Analysis of HCF, the cellular cofactor of VP16, in herpes simplex virus-infected cells. J.Virol. 74: 99-109.

Lai, KO, Fu, WY, Ip, FC, and Ip, NY (1998) Cloning and expression of a novel neurotrophin, NT-7, from carp. Mol.Cell Neurosci. 11: 64-76.

Lamballe, F, Klein, R, and Barbacid, M (1991) trkC, a new member of the trk family of tyrosine protein kinases, is a receptor for neurotrophin-3. Cell 66: 967-979.

Langenberg, AG, Corey, L, Ashley, RL, Leong, WP, and Straus, SE (1999) A prospective study of new infections with herpes simplex virus type 1 and type 2. Chiron HSV Vaccine Study Group. N.Engl.J.Med. 341: 1432-1438.

Large, TH, Bodary, SC, Clegg, DO, Weskamp, G, Otten, U, and Reichardt, LF (1986) Nerve growth factor gene expression in the developing rat brain. Science 234: 352-355.

Latchman, DS (1990) Current status review: molecular biology of herpes simplex virus latency. J.Exp.Pathol.(Oxford) 71: 133-141.

Lauren, J, Airaksinen, MS, Saarma, M, and Timmusk, T (2003) Two novel mammalian Nogo receptor homologs differentially expressed in the central and peripheral nervous systems. Mol.Cell Neurosci. 24: 581-594.

Laux, T, Fukami, K, Thelen, M, Golub, T, Frey, D, and Caroni, P (2000) GAP43, MARCKS, and CAP23 modulate PI(4,5)P(2) at plasmalemmal rafts, and regulate cell cortex actin dynamics through a common mechanism. J.Cell Biol. 149: 1455-1472.

Le Roux, PD and Reh, TA (1995) Independent regulation of primary dendritic and axonal growth by maturing astrocytes in vitro. Neurosci.Lett. 198: 5-8.

Lee, JK, Kim, JE, Sivula, M, and Strittmatter, SM (2004) Nogo receptor antagonism promotes stroke recovery by enhancing axonal plasticity. J.Neurosci. 24: 6209-6217.

Lee, KF, Bachman, K, Landis, S, and Jaenisch, R (1994) Dependence on p75 for innervation of some sympathetic targets. Science 263: 1447-1449.

Lee, KF, Li, E, Huber, LJ, Landis, SC, Sharpe, AH, Chao, MV, and Jaenisch, R (1992) Targeted mutation of the gene encoding the low affinity NGF receptor p75 leads to deficits in the peripheral sensory nervous system. Cell 69: 737-749.

Lee, NS, Dohjima, T, Bauer, G, Li, H, Li, MJ, Ehsani, A, Salvaterra, P, and Rossi, J (2002) Expression of small interfering RNAs targeted against HIV-1 rev transcripts in human cells. Nat.Biotechnol. 20: 500-505.

Lee, RC and Ambros, V (2001) An extensive class of small RNAs in Caenorhabditis elegans. Science 294: 862-864.

Lee, W, Mitchell, P, and Tjian, R (1987) Purified transcription factor AP-1 interacts with TPA-inducible enhancer elements. Cell 49: 741-752.

Lehmann, M, Fournier, A, Selles-Navarro, I, Dergham, P, Sebok, A, Leclerc, N, Tigyi, G, and McKerracher, L (1999) Inactivation of Rho signaling pathway promotes CNS axon regeneration. J.Neurosci. 19: 7537-7547.

Leib, DA, Machalek, MA, Williams, BR, Silverman, RH, and Virgin, HW (2000) Specific phenotypic restoration of an attenuated virus by knockout of a host resistance gene. Proc.Natl.Acad.Sci.U.S.A 97: 6097-6101.

Leibrock, J, Lottspeich, F, Hohn, A, Hofer, M, Hengerer, B, Masiakowski, P, Thoenen, H, and Barde, YA (1989) Molecular cloning and expression of brain-derived neurotrophic factor. Nature 341: 149-152.

Lengyel, P, Samanta, H, Pichon, J, Dougherty, J, Slattery, E, and Farrell, P (1980) Double-stranded RNA and the enzymology of interferon action. Ann.N.Y.Acad.Sci. 350: 441-447.

Leopardi, R, Ward, PL, Ogle, WO, and Roizman, B (1997) Association of herpes simplex virus regulatory protein ICP22 with transcriptional complexes containing EAP, ICP4, RNA polymerase II, and viral DNA requires posttranslational modification by the U(L)13 proteinkinase. J.Virol. 71: 1133-1139.

Levi-Montalcini, R and Hamburger, V (1951) Selective growth stimulating effects of mouse sarcoma on the sensory and sympathetic nervous system of the chick embryo. J.Exp.Zool. 116: 321-361.

Li, M, Shibata, A, Li, C, Braun, PE, McKerracher, L, Roder, J, Kater, SB, and David, S (1996) Myelin-associated glycoprotein inhibits neurite/axon growth and causes growth cone collapse. J.Neurosci.Res. 46: 404-414.

Li, Q, Qi, B, Oka, K, Shimakage, M, Yoshioka, N, Inoue, H, Hakura, A, Kodama, K, Stanbridge, EJ, and Yutsudo, M (2001) Link of a new type of apoptosis-inducing gene ASY/Nogo-B to human cancer. Oncogene 20: 3929-3936.

Li, S and Strittmatter, SM (2003) Delayed systemic Nogo-66 receptor antagonist promotes recovery from spinal cord injury. J.Neurosci. 23: 4219-4227.

Li, Y, Sauve, Y, Li, D, Lund, RD, and Raisman, G (2003) Transplanted olfactory ensheathing cells promote regeneration of cut adult rat optic nerve axons. J.Neurosci. 23: 7783-7788.

Lilley, CE, Groutsi, F, Han, Z, Palmer, JA, Anderson, PN, Latchman, DS, and Coffin, RS (2001) Multiple immediate-early gene-deficient herpes simplex virus vectors allowing efficient gene delivery to neurons in culture and widespread gene delivery to the central nervous system in vivo. J.Virol. 75: 4343-4356.

Lindsay, RM (1988) Nerve growth factors (NGF, BDNF) enhance axonal regeneration but are not required for survival of adult sensory neurons. J.Neurosci. 8: 2394-2405.

Lipardi, C, Wei, Q, and Paterson, BM (2001) RNAi as random degradative PCR: siRNA primers convert mRNA into dsRNAs that are degraded to generate new siRNAs. Cell 107: 297-307.

Liu, BP, Fournier, A, Grandpre, T, and Strittmatter, SM (2002) Myelin-Associated Glycoprotein as a Functional Ligand for the Nogo-66 Receptor. Science 297: 1190-3.

Liu, L, Persson, JK, Svensson, M, and Aldskogius, H (1998) Glial cell responses, complement, and clusterin in the central nervous system following dorsal root transection. Glia 23: 221-238.

Liuzzi, FJ and Lasek, RJ (1987) Astrocytes block axonal regeneration in mammals by activating the physiological stop pathway. Science 237: 642-645.

Loeb, JE, Cordier, WS, Harris, ME, Weitzman, MD, and Hope, TJ (1999) Enhanced expression of transgenes from adeno-associated virus vectors with the woodchuck hepatitis virus posttranscriptional regulatory element: implications for gene therapy. Hum.Gene Ther. 10: 2295-2305.

Low, K, Orberger, G, Schmitz, B, Martini, R, and Schachner, M (1994) The L2/HNK-1 carbohydrate is carried by the myelin associated glycoprotein and sulphated glucuronyl glycolipids in muscle but not cutaneous nerves of adult mice. Eur.J.Neurosci. 6: 1773-1781.

Lutjens, R, Igarashi, M, Pellier, V, Blasey, H, Di Paolo, G, Ruchti, E, Pfulg, C, Staple, JK, Catsicas, S, and Grenningloh, G (2000) Localization and targeting of SCG10 to the trans-Golgi apparatus and growth cone vesicles. Eur.J.Neurosci. 12: 2224-2234.

Lyons, WE, Mamounas, LA, Ricaurte, GA, Coppola, V, Reid, SW, Bora, SH, Wihler, C, Koliatsos, VE, and Tessarollo, L (1999) Brain-derived neurotrophic factor-deficient mice develop aggressiveness and hyperphagia in conjunction with brain serotonergic abnormalities. Proc.Natl.Acad.Sci.U.S.A 96: 15239-15244.

Magnusson, C, Libelius, R, and Tagerud, S (2003) Nogo (Reticulon 4) expression in innervated and denervated mouse skeletal muscle. Mol.Cell Neurosci. 22: 298-307.

Maisonpierre, PC, Belluscio, L, Squinto, S, Ip, NY, Furth, ME, Lindsay, RM, and Yancopoulos, GD (1990) Neurotrophin-3: a neurotrophic factor related to NGF and BDNF. Science 247: 1446-1451.

Malmgaard, L (2004) Induction and Regulation of IFNs During Viral Infections. J.Interferon Cytokine Res. 24: 439-454.

Marcus, J, Dupree, JL, and Popko, B (2002) Myelin-associated glycoprotein and myelin galactolipids stabilize developing axo-glial interactions. J.Cell Biol. 156: 567-577.

Mardy, S, Miura, Y, Endo, F, Matsuda, I, Sztriha, L, Frossard, P, Moosa, A, Ismail, EA, Macaya, A, Andria, G, Toscano, E, Gibson, W, Graham, GE, and Indo, Y (1999) Congenital insensitivity to pain with anhidrosis: novel mutations in the TRKA (NTRK1) gene encoding a high-affinity receptor for nerve growth factor. Am.J.Hum.Genet. 64: 1570-1579.

Margolis, RU and Margolis, RK (1994) Aggrecan-versican-neurocan family proteoglycans. Methods Enzymol. 245: 105-126.

Martin, D, Robe, P, Franzen, R, Delree, P, Schoenen, J, Stevenaert, A, and Moonen, G (1996) Effects of Schwann cell transplantation in a contusion model of rat spinal cord injury. J.Neurosci.Res. 45: 588-597.

Martinez, J, Patkaniowska, A, Urlaub, H, Luhrmann, R, and Tuschl, T (2002) Single-stranded antisense siRNAs guide target RNA cleavage in RNAi. Cell 110: 563-574.

Martini, R (1994) Expression and functional roles of neural cell surface molecules and extracellular matrix components during development and regeneration of peripheral nerves. J.Neurocytol. 23: 1-28.

Martini, R, Schachner, M, and Brushart, TM (1994) The L2/HNK-1 carbohydrate is preferentially expressed by previously motor axon-associated Schwann cells in reinnervated peripheral nerves. J.Neurosci. 14: 7180-7191.

Martini, R, Schachner, M, and Faissner, A (1990) Enhanced expression of the extracellular matrix molecule J1/tenascin in the regenerating adult mouse sciatic nerve. J.Neurocytol. 19: 601-616.

Martini, R, Xin, Y, Schmitz, B, and Schachner, M (1992) The L2/HNK-1 Carbohydrate Epitope is Involved in the Preferential Outgrowth of Motor Neurons on Ventral Roots and Motor Nerves. Eur.J.Neurosci. 4: 628-639.

Mason, MR, Campbell, G, Caroni, P, Anderson, PN, and Lieberman, AR (2000) Overexpression of GAP-43 in thalamic projection neurons of transgenic mice does not enable them to regenerate axons through peripheral nerve grafts. Exp.Neurol. 165: 143-152.

Mason, MR, Lieberman, AR, and Anderson, PN (2003) Corticospinal neurons up-regulate a range of growth-associated genes following intracortical, but not spinal, axotomy. Eur.J.Neurosci. 18: 789-802.

McAdams, BD and McLoon, SC (1995) Expression of chondroitin sulfate and keratan sulfate proteoglycans in the path of growing retinal axons in the developing chick. J.Comp Neurol. 352: 594-606.

McCaffery, CA, Raju, TR, and Bennett, MR (1984) Effects of cultured astroglia on the survival of neonatal rat retinal ganglion cells in vitro. Dev.Biol. 104: 441-448.

McKeon, RJ, Schreiber, RC, Rudge, JS, and Silver, J (1991) Reduction of neurite outgrowth in a model of glial scarring following CNS injury is correlated with the expression of inhibitory molecules on reactive astrocytes. J.Neurosci. 11: 3398-3411.

McKerracher, L (2002) Ganglioside rafts as MAG receptors that mediate blockade of axon growth. Proc.Natl.Acad.Sci.U.S.A 99: 7811-7813.

McKerracher, L, David, S, Jackson, DL, Kottis, V, Dunn, RJ, and Braun, PE (1994) Identification of myelin-associated glycoprotein as a major myelin-derived inhibitor of neurite growth. Neuron 13: 805-811.

Meier, S, Brauer, AU, Heimrich, B, Schwab, ME, Nitsch, R, and Savaskan, NE (2003) Molecular analysis of Nogo expression in the hippocampus during development and following lesion and seizure. FASEB J. 17: 1153-1155.

Meiners, S and Geller, HM (1997) Long and short splice variants of human tenascin differentially regulate neurite outgrowth. Mol.Cell Neurosci. 10: 100-116.

Meiners, S, Powell, EM, and Geller, HM (1995) A distinct subset of tenascin/CS-6-PG-rich astrocytes restricts neuronal growth in vitro. J.Neurosci. 15: 8096-8108.

Mellerick, DM and Fraser, NW (1987) Physical state of the latent herpes simplex virus genome in a mouse model system: evidence suggesting an episomal state. Virology 158: 265-275.

Merkler, D, Metz, GA, Raineteau, O, Dietz, V, Schwab, ME, and Fouad, K (2001) Locomotor recovery in spinal cord-injured rats treated with an antibody neutralizing the myelin-associated neurite growth inhibitor Nogo-A. J.Neurosci. 21: 3665-3673.

Metzler, DW and Wilcox, KW (1985) Isolation of herpes simplex virus regulatory protein ICP4 as a homodimeric complex. J.Virol. 55: 329-337.

Mey, J and Thanos, S (1993) Intravitreal injections of neurotrophic factors support the survival of axotomized retinal ganglion cells in adult rats in vivo. Brain Res. 602: 304-317.

Meyer, M, Matsuoka, I, Wetmore, C, Olson, L, and Thoenen, H (1992) Enhanced synthesis of brain-derived neurotrophic factor in the lesioned peripheral nerve: different mechanisms are responsible for the regulation of BDNF and NGF mRNA. J.Cell Biol. 119: 45-54.

Mi, S, Lee, X, Shao, Z, Thill, G, Ji, B, Relton, J, Levesque, M, Allaire, N, Perrin, S, Sands, B, Crowell, T, Cate, RL, McCoy, JM, and Pepinsky, RB (2004) LINGO-1 is a component of the Nogo-66 receptor/p75 signaling complex. Nat.Neurosci. 7: 221-228.

Mikol, DD, Alexakos, MJ, Bayley, CA, Lemons, RS, Le Beau, MM, and Stefansson, K (1990a) Structure and chromosomal localization of the gene for the oligodendrocyte-myelin glycoprotein. J.Cell Biol. 111: 2673-2679.

Mikol, DD, Gulcher, JR, and Stefansson, K (1990b) The oligodendrocyte-myelin glycoprotein belongs to a distinct family of proteins and contains the HNK-1 carbohydrate. J.Cell Biol. 110: 471-479.

Mikol, DD, Rongnoparut, P, Allwardt, BA, Marton, LS, and Stefansson, K (1993) The oligodendrocyte-myelin glycoprotein of mouse: primary structure and gene structure. Genomics 17: 604-610.

Mikol, DD and Stefansson, K (1988) A phosphatidylinositol-linked peanut agglutinin-binding glycoprotein in central nervous system myelin and on oligodendrocytes. J.Cell Biol. 106: 1273-1279.

Millhouse, S and Wigdahl, B (2000) Molecular circuitry regulating herpes simplex virus type 1 latency in neurons. J.Neurovirol. 6: 6-24.

Ming, GL, Wong, ST, Henley, J, Yuan, XB, Song, HJ, Spitzer, NC, and Poo, MM (2002) Adaptation in the chemotactic guidance of nerve growth cones. Nature 417: 411-418.

Mingorance, A, Fontana, X, Sole, M, Burgaya, F, Urena, JM, Teng, FY, Tang, BL, Hunt, D, Anderson, PN, Bethea, JR, Schwab, ME, Soriano, E, and Del Rio, JA (2004) Regulation of Nogo and Nogo receptor during the development of the entorhino-hippocampal pathway and after adult hippocampal lesions. Mol.Cell Neurosci. 26: 34-49.

Minichiello, L, Korte, M, Wolfer, D, Kuhn, R, Unsicker, K, Cestari, V, Rossi-Arnaud, C, Lipp, HP, Bonhoeffer, T, and Klein, R (1999) Essential role for TrkB receptors in hippocampus-mediated learning. Neuron 24: 401-414.

Miyagishi, M and Taira, K (2002a) U6 promoter-driven siRNAs with four uridine 3' overhangs efficiently suppress targeted gene expression in mammalian cells. Nat.Biotechnol. 20: 497-500.

Miyagishi, M and Taira, K (2002b) U6 promoter-driven siRNAs with four uridine 3' overhangs efficiently suppress targeted gene expression in mammalian cells. Nat.Biotechnol. 20: 497-500.

Monnier, PP, Sierra, A, Schwab, JM, Henke-Fahle, S, and Mueller, BK (2003) The Rho/ROCK pathway mediates neurite growth-inhibitory activity associated with the chondroitin sulfate proteoglycans of the CNS glial scar. Mol.Cell Neurosci. 22: 319-330.

Montero-Menei, CN, Pouplard-Barthelaix, A, Gumpel, M, and Baron-Van Evercooren, A (1992) Pure Schwann cell suspension grafts promote regeneration of the lesioned septo-hippocampal cholinergic pathway. Brain Res. 570: 198-208.

Moon, LD, Asher, RA, Rhodes, KE, and Fawcett, JW (2001) Regeneration of CNS axons back to their target following treatment of adult rat brain with chondroitinase ABC. Nat.Neurosci. 4: 465-466.

Morgan, C, Rose, HM, and Mednis, B (1968) Electron microscopy of herpes simplex virus. I. Entry. J.Virol. 2: 507-516.

Morgenstern, DA, Asher, RA, and Fawcett, JW (2002) Chondroitin sulphate proteoglycans in the CNS injury response. Prog.Brain Res. 137: 313-332.

Morgenstern, DA, Asher, RA, Naidu, M, Carlstedt, T, Levine, JM, and Fawcett, JW (2003) Expression and glycanation of the NG2 proteoglycan in developing, adult, and damaged peripheral nerve. Mol.Cell Neurosci. 24: 787-802.

Morris, KV, Chan, SW, Jacobsen, SE, and Looney, DJ (2004) Small interfering RNA-induced transcriptional gene silencing in human cells. Science 305: 1289-1292.

Morrow, DR, Campbell, G, Lieberman, AR, and Anderson, PN (1993) Differential regenerative growth of CNS axons into tibial and peroneal nerve grafts in the thalamus of adult rats. Exp.Neurol. 120: 60-69.

Mukhopadhyay, G, Doherty, P, Walsh, FS, Crocker, PR, and Filbin, MT (1994) A novel role for myelin-associated glycoprotein as an inhibitor of axonal regeneration. Neuron 13: 757-767.

Mullen, MA, Gerstberger, S, Ciufo, DM, Mosca, JD, and Hayward, GS (1995) Evaluation of colocalization interactions between the IE110, IE175, and IE63 transactivator proteins of herpes simplex virus within subcellular punctate structures. J.Virol. 69: 476-491.

Nagarajan, R, Le, N, Mahoney, H, Araki, T, and Milbrandt, J (2002) Deciphering peripheral nerve myelination by using Schwann cell expression profiling. Proc.Natl.Acad.Sci.U.S.A 99: 8998-9003.

Nakagomi, S, Suzuki, Y, Namikawa, K, Kiryu-Seo, S, and Kiyama, H (2003) Expression of the activating transcription factor 3 prevents c-Jun N-terminal kinase-induced neuronal death by promoting heat shock protein 27 expression and Akt activation. J.Neurosci. 23: 5187-5196.

Niclou, SP, Franssen, EH, Ehlert, EM, Taniguchi, M, and Verhaagen, J (2003) Meningeal cell-derived semaphorin 3A inhibits neurite outgrowth. Mol.Cell Neurosci. 24: 902-912.

Nie, DY, Zhou, ZH, Ang, BT, Teng, FY, Xu, G, Xiang, T, Wang, CY, Zeng, L, Takeda, Y, Xu, TL, Ng, YK, Faivre-Sarrailh, C, Popko, B, Ling, EA, Schachner, M, Watanabe, K, Pallen, CJ, Tang, BL, and Xiao, ZC (2003) Nogo-A at CNS paranodes is a ligand of Caspr: possible regulation of K(+) channel localization. EMBO J. 22: 5666-5678.

Niederost, B, Oertle, T, Fritsche, J, McKinney, RA, and Bandtlow, CE (2002) Nogo-A and myelin-associated glycoprotein mediate neurite growth inhibition by antagonistic regulation of RhoA and Rac1. J.Neurosci. 22: 10368-10376.

Nieke, J and Schachner, M (1985) Expression of the neural cell adhesion molecules L1 and N-CAM and their common carbohydrate epitope L2/HNK-1 during development and after transection of the mouse sciatic nerve. Differentiation 30: 141-151.

Nilsson, AS, Fainzilber, M, Falck, P, and Ibanez, CF (1998) Neurotrophin-7: a novel member of the neurotrophin family from the zebrafish. FEBS Lett. 424: 285-290.

Nilsson, M, Ford, J, Bohm, S, and Toftgard, R (1997) Characterization of a nuclear factor that binds juxtaposed with ATF3/Jun on a composite response element specifically mediating induced transcription in response to an epidermal growth factor/Ras/Raf signaling pathway. Cell Growth Differ. 8: 913-920.

Nykanen, A, Haley, B, and Zamore, PD (2001) ATP requirements and small interfering RNA structure in the RNA interference pathway. Cell 107: 309-321.

Nykjaer, A, Lee, R, Teng, KK, Jansen, P, Madsen, P, Nielsen, MS, Jacobsen, C, Kliemannel, M, Schwarz, E, Willnow, TE, Hempstead, BL, and Petersen, CM (2004) Sortilin is essential for proNGF-induced neuronal cell death. Nature 427: 843-848.

Oertle, T, Huber, C, van der, PH, and Schwab, ME (2003a) Genomic Structure and Functional Characterisation of the Promoters of Human and Mouse nogo/rtn4. J.Mol.Biol. 325: 299-323.

Oertle, T, van der Haar, ME, Bandtlow, CE, Robeva, A, Burfeind, P, Buss, A, Huber, AB, Simonen, M, Schnell, L, Brosamle, C, Kaupmann, K, Vallon, R, and Schwab, ME (2003b) Nogo-A inhibits neurite outgrowth and cell spreading with three discrete regions. J.Neurosci. 23: 5393-5406.

Oliver, L, Wald, A, Kim, M, Zeh, J, Selke, S, Ashley, R, and Corey, L (1995) Seroprevalence of herpes simplex virus infections in a family medicine clinic. Arch.Fam.Med. 4: 228-232.

Osborne, SL, Corcoran, SL, Prinjha, RK, and Moore, SE (2004) Nogo A expression in the adult enteric nervous system. Neurogastroenterol.Motil. 16: 465-474.

Oudega, M and Hagg, T (1996) Nerve growth factor promotes regeneration of sensory axons into adult rat spinal cord. Exp.Neurol. 140: 218-229.

Oudega, M and Hagg, T (1999) Neurotrophins promote regeneration of sensory axons in the adult rat spinal cord. Brain Res. 818: 431-438.

Oudega, M, Rosano, C, Sadi, D, Wood, PM, Schwab, ME, and Hagg, T (2000) Neutralizing antibodies against neurite growth inhibitor NI-35/250 do not promote regeneration of sensory axons in the adult rat spinal cord. Neuroscience 100: 873-883.

Paddison, PJ, Caudy, AA, Bernstein, E, Hannon, GJ, and Conklin, DS (2002b) Short hairpin RNAs (shRNAs) induce sequence-specific silencing in mammalian cells. Genes Dev. 16: 948-958.

Paddison, PJ, Caudy, AA, Bernstein, E, Hannon, GJ, and Conklin, DS (2002a) Short hairpin RNAs (shRNAs) induce sequence-specific silencing in mammalian cells. Genes Dev. 16: 948-958.

Paino, CL and Bunge, MB (1991) Induction of axon growth into Schwann cell implants grafted into lesioned adult rat spinal cord. Exp.Neurol. 114: 254-257.

Panagiotidis, CA, Lium, EK, and Silverstein, SJ (1997) Physical and functional interactions between herpes simplex virus immediate-early proteins ICP4 and ICP27. J.Virol. 71: 1547-1557.

Parkinson, DB, Dong, Z, Bunting, H, Whitfield, J, Meier, C, Marie, H, Mirsky, R, and Jessen, KR (2001) Transforming growth factor beta (TGFbeta) mediates Schwann cell death in vitro and in vivo: examination of c-Jun activation, interactions with survival signals, and the relationship of TGFbeta-mediated death to Schwann cell differentiation. J.Neurosci. 21: 8572-8585.

Pasterkamp, RJ, Anderson, PN, and Verhaagen, J (2001) Peripheral nerve injury fails to induce growth of lesioned ascending dorsal column axons into spinal cord scar tissue expressing the axon repellent Semaphorin3A. Eur.J.Neurosci. 13: 457-471.

Pasterkamp, RJ, Giger, RJ, Ruitenberg, MJ, Holtmaat, AJ, De Wit, J, De Winter, F, and Verhaagen, J (1999) Expression of the gene encoding the chemorepellent semaphorin III is induced in the fibroblast component of neural scar tissue formed following injuries of adult but not neonatal CNS. Mol.Cell Neurosci. 13: 143-166.

Paul, CE, Vereker, E, Dickson, KM, and Barker, PA (2004) A pro-apoptotic fragment of the p75 neurotrophin receptor is expressed in p75NTRExonIV null mice. J.Neurosci. 24: 1917-1923.

Paul, CP, Good, PD, Winer, I, and Engelke, DR (2002a) Effective expression of small interfering RNA in human cells. Nat.Biotechnol. 20: 505-508.

Paul, CP, Good, PD, Winer, I, and Engelke, DR (2002b) Effective expression of small interfering RNA in human cells. Nat.Biotechnol. 20: 505-508.

Paxinos, G and Watson, C (1986) *The Rat Brain in Stereotaxic Coordinates*. Academic Press, Sydney.

Pearlman, AL and Sheppard, AM (1996) Extracellular matrix in early cortical development. Prog.Brain Res. 108: 117-134.

Pearson, AG, Gray, CW, Pearson, JF, Greenwood, JM, During, MJ, and Dragunow, M (2003) ATF3 enhances c-Jun-mediated neurite sprouting. Brain Res.Mol.Brain Res. 120: 38-45.

Pedraza, L, Frey, AB, Hempstead, BL, Colman, DR, and Salzer, JL (1991) Differential expression of MAG isoforms during development. J.Neurosci.Res. 29: 141-148.

Phillips, HS, Hains, JM, Laramee, GR, Rosenthal, A, and Winslow, JW (1990) Widespread expression of BDNF but not NT3 by target areas of basal forebrain cholinergic neurons. Science 250: 290-294.

Pignot, V, Hein, AE, Barske, C, Wiessner, C, Walmsley, AR, Kaupmann, K, Mayeur, H, Sommer, B, Mir, AK, and Frentzel, S (2003) Characterization of two novel proteins, NgRH1 and NgRH2, structurally and biochemically homologous to the Nogo-66 receptor. J.Neurochem. 85: 717-728.

Poduslo, JF (1984) Regulation of myelination: biosynthesis of the major myelin glycoprotein by Schwann cells in the presence and absence of myelin assembly. J.Neurochem. 42: 493-503.

Poffenberger, KL, Idowu, AD, Fraser-Smith, EB, Raichlen, PE, and Herman, RC (1994) A herpes simplex virus type 1 ICP22 deletion mutant is altered for virulence and latency in vivo. Arch.Virol. 139: 111-119.

Poffenberger, KL, Raichlen, PE, and Herman, RC (1993) In vitro characterization of a herpes simplex virus type 1 ICP22 deletion mutant. Virus Genes 7: 171-186.

Pot, C, Simonen, M, Weinmann, O, Schnell, L, Christ, F, Stoeckle, S, Berger, P, Rulicke, T, Suter, U, and Schwab, ME (2002) Nogo-A expressed in Schwann cells impairs axonal regeneration after peripheral nerve injury. J.Cell Biol. 159: 29-35.

Powell, EM, Fawcett, JW, and Geller, HM (1997) Proteoglycans provide neurite guidance at an astrocyte boundary. Mol.Cell Neurosci. 10: 27-42.

Powell, EM and Geller, HM (1999) Dissection of astrocyte-mediated cues in neuronal guidance and process extension. Glia 26: 73-83.

Preston, CM (2000) Repression of viral transcription during herpes simplex virus latency. J.Gen.Virol. 81: 1-19.

Preston, VG, Palfreyman, JW, and Dutia, BM (1984) Identification of a herpes simplex virus type 1 polypeptide which is a component of the virus-induced ribonucleotide reductase. J.Gen.Virol. 65 (Pt 9): 1457-1466.

Prinjha, RK, Hill, C, Irving, E, Roberts, J, Campbell, C, Parsons, A, Davis, R, Morrow, R, Woodhams, PL, Philpott, KL, Pangalos, M, and Walsh, FS (2002) Mapping the functional inhibitory sites of Nogo-A. Discovery of regulated expression following neuronal injury. Society for Neuroscience Abstract Viewer 2002 333.12

Prinjha, R, Moore, SE, Vinson, M, Blake, S, Morrow, R, Christie, G, Michalovich, D, Simmons, DL, and Walsh, FS (2000) Inhibitor of neurite outgrowth in humans. Nature 403: 383-384.

Pyykonen, I and Koistinaho, J (1991) c-fos protein like immunoreactivity in non-neuronal cells of rat peripheral nerve after transection. Acta Neuropathol.(Berl) 82: 66-71.

Qi, B, Qi, Y, Watari, A, Yoshioka, N, Inoue, H, Minemoto, Y, Yamashita, K, Sasagawa, T, and Yutsudo, M (2003) Pro-apoptotic ASY/Nogo-B protein associates with ASYIP. J.Cell Physiol 196: 312-318.

Raineteau, O, Z'Graggen, WJ, Thallmair, M, and Schwab, ME (1999) Sprouting and regeneration after pyramidotomy and blockade of the myelin-associated neurite growth inhibitors NI 35/250 in adult rats. Eur.J.Neurosci. 11: 1486-1490.

Raisman, G (2001) Olfactory ensheathing cells - another miracle cure for spinal cord injury? Nat.Rev.Neurosci. 2: 369-375.

Raisman, G (2004) Myelin inhibitors: does NO mean GO? Nat.Rev.Neurosci. 5: 157-161.

Raivich, G, Bohatschek, M, Da Costa, C, Iwata, O, Galiano, M, Hristova, M, Nateri, AS, Makwana, M, Riera-Sans, L, Wolfer, DP, Lipp, HP, Aguzzi, A, Wagner, EF, and Behrens, A (2004) The AP-1 transcription factor c-Jun is required for efficient axonal regeneration. Neuron 43: 57-67.

Ramer, LM, Au, E, Richter, MW, Liu, J, Tetzlaff, W, and Roskams, AJ (2004) Peripheral olfactory ensheathing cells reduce scar and cavity formation and promote regeneration after spinal cord injury. J.Comp Neurol. 473: 1-15.

Ramer, MS, Priestley, JV, and McMahon, SB (2000) Functional regeneration of sensory axons into the adult spinal cord. Nature 403: 312-316.

Ramon Y Cajal, S (1928) *Degeneration and Regeneration of the Nervous System* (translated by May, RM). Hafner Publishing Company, New York (reprint of 1928 edition).

Ramon-Cueto, A and Nieto-Sampedro, M (1994) Regeneration into the spinal cord of transected dorsal root axons is promoted by ensheathing glia transplants. Exp.Neurol. 127: 232-244.

Randazzo, BP, Tal-Singer, R, Zabolotny, JM, Kesari, S, and Fraser, NW (1997) Herpes simplex virus 1716, an ICP 34.5 null mutant, is unable to replicate in CV-1 cells due to a translational block that can be overcome by coinfection with SV40. J.Gen.Virol. 78 (Pt 12): 3333-3339.

Rasheed, S, Nelson-Rees, WA, Toth, EM, Arnstein, P, and Gardner, MB (1974) Characterization of a newly derived human sarcoma cell line (HT-1080). Cancer 33: 1027-1033.

Razin, A (1998) CpG methylation, chromatin structure and gene silencing-a three-way connection. EMBO J. 17: 4905-4908.

Razin, A and Riggs, AD (1980) DNA methylation and gene function. Science 210: 604-610.

Reichert, F, Saada, A, and Rotshenker, S (1994) Peripheral nerve injury induces Schwann cells to express two macrophage phenotypes: phagocytosis and the galactose-specific lectin MAC-2. J.Neurosci. 14: 3231-3245.

Reier, PJ and Houle, JD (1988) The glial scar: its bearing on axonal elongation and transplantation approaches to CNS repair. Adv.Neurol. 47: 87-138.

Reier, PJ, Stensaas, LJ, and Guth, L (1983) The astrocytic scar as an impediment to regeneration in the central nervous system. In *Spinal Cord Reconstruction* (Kao, CC, Bunge, RP and Reier, PJ, eds.), pp. 163-195. Raven Press, New York.

Rezajooi, K, Pavlides, M, Winterbottom, J, Stallcup, WB, Hamlyn, PJ, Lieberman, AR, and Anderson, PN (2004) NG2 proteoglycan expression in the peripheral nervous system: upregulation following injury and comparison with CNS lesions. Mol.Cell Neurosci. 25: 572-584.

Rice, SA, Long, MC, Lam, V, Schaffer, PA, and Spencer, CA (1995) Herpes simplex virus immediate-early protein ICP22 is required for viral modification of host RNA polymerase II and establishment of the normal viral transcription program. J.Virol. 69: 5550-5559.

Richardson, PM, Issa, VM, and Aguayo, AJ (1984) Regeneration of long spinal axons in the rat. J.Neurocytol. 13: 165-182.

Richardson, PM, McGuinness, UM, and Aguayo, AJ (1980) Axons from CNS neurons regenerate into PNS grafts. Nature 284: 264-265.

Richardson, PM, McGuinness, UM, and Aguayo, AJ (1982) Peripheral nerve autografts to the rat spinal cord: studies with axonal tracing methods. Brain Res. 237: 147-162.

Richardson, PM and Verge, VM (1986) The induction of a regenerative propensity in sensory neurons following peripheral axonal injury. J.Neurocytol. 15: 585-594.

Rico, B, Xu, B, and Reichardt, LF (2002) TrkB receptor signaling is required for establishment of GABAergic synapses in the cerebellum. Nat.Neurosci. 5: 225-233.

Riddell, JS, Enriquez-Denton, M, Toft, A, Fairless, R, and Barnett, SC (2004) Olfactory ensheathing cell grafts have minimal influence on regeneration at the dorsal root entry zone following rhizotomy. Glia 47: 150-167.

Ridet, JL, Pencalet, P, Belcram, M, Giraudeau, B, Chastang, C, Philippon, J, Mallet, J, Privat, A, and Schwartz, L (2000) Effects of spinal cord X-irradiation on the recovery of paraplegic rats. Exp.Neurol. 161: 1-14.

Riederer, BM, Pellier, V, Antonsson, B, Di Paolo, G, Stimpson, SA, Lutjens, R, Catsicas, S, and Grenningloh, G (1997) Regulation of microtubule dynamics by the neuronal growth-associated protein SCG10. Proc.Natl.Acad.Sci.U.S.A 94: 741-745.

Rodriguez-Tebar, A, Jeffrey, PL, Thoenen, H, and Barde, YA (1989) The survival of chick retinal ganglion cells in response to brain-derived neurotrophic factor depends on their embryonic age. Dev.Biol. 136: 296-303.

Roizman, B and Sears, AE (1996) Herpes simplex viruses and their replication. In *Field's Virology* (Third Edition) (Fields, BN, Knipe DM, Howley, PM, Chanock, RM, Melnick, JL, Monath, TP, Roizman, B and Straus, SE, eds.). Lippincott-Raven, Philadelphia.

Romero, MI, Rangappa, N, Garry, MG, and Smith, GM (2001) Functional regeneration of chronically injured sensory afferents into adult spinal cord after neurotrophin gene therapy. J.Neurosci. 21: 8408-8416.

Rosenthal, SL, Stanberry, LR, Biro, FM, Slaoui, M, Francotte, M, Koutsoukos, M, Hayes, M, and Bernstein, DI (1997) Seroprevalence of herpes simplex virus types 1 and 2 and cytomegalovirus in adolescents. Clin.Infect.Dis. 24: 135-139.

Rotshenker, S, Aamar, S, and Barak, V (1992) Interleukin-1 activity in lesioned peripheral nerve. J.Neuroimmunol. 39: 75-80.

Routtenberg, A and Lovinger, DM (1985) Selective increase in phosphorylation of a 47-kDa protein (F1) directly related to long-term potentiation. Behav.Neural Biol. 43: 3-11.

Rubinson, DA, Dillon, CP, Kwiatkowski, AV, Sievers, C, Yang, L, Kopinja, J, Rooney, DL, Ihrig, MM, McManus, MT, Gertler, FB, Scott, ML, and Van Parijs, L (2003) A lentivirus-based system to functionally silence genes in primary mammalian cells, stem cells and transgenic mice by RNA interference. Nat.Genet. 33: 401-406.

Rudge, JS and Silver, J (1990) Inhibition of neurite outgrowth on astroglial scars in vitro. J.Neurosci. 10: 3594-3603.

Rutka, JT, Giblin, J, Dougherty, DV, McCulloch, JR, DeArmond, SJ, and Rosenblum, ML (1986) An ultrastructural and immunocytochemical analysis of leptomeningeal and meningioma cultures. J.Neuropathol.Exp.Neurol. 45: 285-303.

Sacks, WR and Schaffer, PA (1987) Deletion mutants in the gene encoding the herpes simplex virus type 1 immediate-early protein ICP0 exhibit impaired growth in cell culture. J.Virol. 61: 829-839.

Salonen, V, Peltonen, J, Roytta, M, and Virtanen, I (1987) Laminin in traumatized peripheral nerve: basement membrane changes during degeneration and regeneration. J.Neurocytol. 16: 713-720.

Salzer, JL, Holmes, WP, and Colman, DR (1987) The amino acid sequences of the myelin-associated glycoproteins: homology to the immunoglobulin gene superfamily. J.Cell Biol. 104: 957-965.

Samaniego, LA, Wu, N, and DeLuca, NA (1997) The herpes simplex virus immediate-early protein ICP0 affects transcription from the viral genome and infected-cell survival in the absence of ICP4 and ICP27. J.Virol. 71: 4614-4625.

Sambrook, J and Russell, DW (2001) *Molecular Cloning: A Laboratory Manual.* (Third Edition). Cold Spring Harbor Laboratory Press, New York.

Sandrock, AW, Jr. and Matthew, WD (1987) Substrate-bound nerve growth factor promotes neurite growth in peripheral nerve. Brain Res. 425: 360-363.

Satoh, JI and Kuroda, Y (2002) Cytokines and neurotrophic factors fail to affect Nogo-A mRNA expression in differentiated human neurones: implications for inflammation-related axonal regeneration in the central nervous system. Neuropathol.Appl.Neurobiol. 28: 95-106.

Scarlato, M, Ara, J, Bannerman, P, Scherer, S, and Pleasure, D (2003) Induction of neuropilins-1 and -2 and their ligands, Sema3A, Sema3F, and VEGF, during Wallerian degeneration in the peripheral nervous system. Exp.Neurol. 183: 489-498.

Schafer, M, Fruttiger, M, Montag, D, Schachner, M, and Martini, R (1996) Disruption of the gene for the myelin-associated glycoprotein improves axonal regrowth along myelin in C57BL/Wlds mice. Neuron 16: 1107-1113.

Scherr, M, Battmer, K, Ganser, A, and Eder, M (2003) Modulation of gene expression by lentiviral-mediated delivery of small interfering RNA. Cell Cycle 2: 251-257.

Schnell, L, Schneider, R, Kolbeck, R, Barde, YA, and Schwab, ME (1994) Neurotrophin-3 enhances sprouting of corticospinal tract during development and after adult spinal cord lesion. Nature 367: 170-173.

Schnell, L and Schwab, ME (1990) Axonal regeneration in the rat spinal cord produced by an antibody against myelin-associated neurite growth inhibitors. Nature 343: 269-272.

Schnell, L and Schwab, ME (1993) Sprouting and regeneration of lesioned corticospinal tract fibres in the adult rat spinal cord. Eur.J.Neurosci. 5: 1156-1171.

Schwab, ME (1996) Molecules inhibiting neurite growth: a minireview. Neurochem.Res. 21: 755-761.

Schwab, ME and Caroni, P (1988) Oligodendrocytes and CNS myelin are nonpermissive substrates for neurite growth and fibroblast spreading in vitro. J.Neurosci. 8: 2381-2393.

Schwab, ME and Schnell, L (1991) Channeling of developing rat corticospinal tract axons by myelin-associated neurite growth inhibitors. J.Neurosci. 11: 709-721.

Schwarz, DS, Hutvagner, G, Du, T, Xu, Z, Aronin, N, and Zamore, PD (2003) Asymmetry in the assembly of the RNAi enzyme complex. Cell 115: 199-208.

Sekulovich, RE, Leary, K, and Sandri-Goldin, RM (1988) The herpes simplex virus type 1 alpha protein ICP27 can act as a trans-repressor or a trans-activator in combination with ICP4 and ICP0. J.Virol. 62: 4510-4522.

Shea, TB, Perrone-Bizzozero, NI, Beermann, ML, and Benowitz, LI (1991) Phospholipid-mediated delivery of anti-GAP-43 antibodies into neuroblastoma cells prevents neuritogenesis. J.Neurosci. 11: 1685-1690.

Sheedlo, HJ, Srinivasan, B, Brun-Zinkernagel, AM, Roque, CH, Lambert, W, Wordinger, RJ, and Roque, RS (2002) Expression of p75(NTR) in photoreceptor cells of dystrophic rat retinas. Brain Res.Mol.Brain Res. 103: 71-79.

Shen, C, Buck, AK, Liu, X, Winkler, M, and Reske, SN (2003) Gene silencing by adenovirus-delivered siRNA. FEBS Lett. 539: 111-114.

Shen, Y, Mani, S, Donovan, SL, Schwob, JE, and Meiri, KF (2002) Growth-associated protein-43 is required for commissural axon guidance in the developing vertebrate nervous system. J.Neurosci. 22: 239-247.

Shieh, MT and Spear, PG (1991) Fibroblast growth factor receptor: does it have a role in the binding of herpes simplex virus? Science 253: 208-210.

Shimizu-Okabe, C, Matsuda, Y, Koito, H, and Yoshida, S (2001) L-isoform but not S-isoform of myelin associated glycoprotein promotes neurite outgrowth of mouse cerebellar neurons. Neurosci.Lett. 311: 203-205.

Shinagawa, T and Ishii, S (2003) Generation of Ski-knockdown mice by expressing a long double-strand RNA from an RNA polymerase II promoter. Genes Dev. 17: 1340-1345..

Shy, ME, Shi, Y, Wrabetz, L, Kamholz, J, and Scherer, SS (1996) Axon-Schwann cell interactions regulate the expression of c-jun in Schwann cells. J.Neurosci.Res. 43: 511-525.

Sievers, J, Pehlemann, FW, Gude, S, and Berry, M (1994) Meningeal cells organize the superficial glia limitans of the cerebellum and produce components of both the interstitial matrix and the basement membrane. J.Neurocytol. 23: 135-149.

Siironen, J, Sandberg, M, Vuorinen, V, and Roytta, M (1992) Expression of type I and III collagens and fibronectin after transection of rat sciatic nerve. Reinnervation compared with denervation. Lab Invest 67: 80-87.

Simonen, M, Pedersen, V, Weinmann, O, Schnell, L, Buss, A, Ledermann, B, Christ, F, Sansig, G, van der, PH, and Schwab, ME (2003) Systemic deletion of the myelin-associated outgrowth inhibitor Nogo-A improves regenerative and plastic responses after spinal cord injury. Neuron 38: 201-211.

Sivasankaran, R, Pei, J, Wang, KC, Zhang, YP, Shields, CB, Xu, XM, and He, Z (2004) PKC mediates inhibitory effects of myelin and chondroitin sulfate proteoglycans on axonal regeneration. Nat.Neurosci. 7: 261-268.

Skene, JH and Willard, M (1981) Axonally transported proteins associated with axon growth in rabbit central and peripheral nervous systems. J.Cell Biol. 89: 96-103.

Smeyne, RJ, Klein, R, Schnapp, A, Long, LK, Bryant, S, Lewin, A, Lira, SA, and Barbacid, M (1994) Severe sensory and sympathetic neuropathies in mice carrying a disrupted Trk/NGF receptor gene. Nature 368: 246-249.

Smith, CA, Bates, P, Rivera-Gonzalez, R, Gu, B, and DeLuca, NA (1993) ICP4, the major transcriptional regulatory protein of herpes simplex virus type 1, forms a tripartite complex with TATA-binding protein and TFIIB. J.Virol. 67: 4676-4687.

Snow, DM, Lemmon, V, Carrino, DA, Caplan, AI, and Silver, J (1990) Sulfated proteoglycans in astroglial barriers inhibit neurite outgrowth in vitro. Exp.Neurol. 109: 111-130.

Snow, DM, Watanabe, M, Letourneau, PC, and Silver, J (1991) A chondroitin sulfate proteoglycan may influence the direction of retinal ganglion cell outgrowth. Development 113: 1473-1485.

Soares, HD, Chen, SC, and Morgan, JI (2001) Differential and prolonged expression of Fos-lacZ and Jun-lacZ in neurons, glia, and muscle following sciatic nerve damage. Exp.Neurol. 167: 1-14.

Sobreviela, T, Clary, DO, Reichardt, LF, Brandabur, MM, Kordower, JH, and Mufson, EJ (1994) TrkA-immunoreactive profiles in the central nervous system: colocalization with neurons containing p75 nerve growth factor receptor, choline acetyltransferase, and serotonin. J.Comp Neurol. 350: 587-611.

Song, XY, Zhong, JH, Wang, X, and Zhou, XF (2004) Suppression of p75NTR does not promote regeneration of injured spinal cord in mice. J.Neurosci. 24: 542-546.

Spillmann, AA, Bandtlow, CE, Lottspeich, F, Keller, F, and Schwab, ME (1998) Identification and characterization of a bovine neurite growth inhibitor (bNI-220). J.Biol.Chem. 273: 19283-19293.

Squinto, SP, Stitt, TN, Aldrich, TH, Davis, S, Bianco, SM, Radziejewski, C, Glass, DJ, Masiakowski, P, Furth, ME, Valenzuela, DM, and . (1991) trkB encodes a functional receptor for brain-derived neurotrophic factor and neurotrophin-3 but not nerve growth factor. Cell 65: 885-893.

Stalberg, E, Hilton-Brown, P, and Rydin, E (1986) Capacity of the motor neurone to alter its peripheral field. In *Recent Achievements in Restorative Neurology 2. Progressive*

Neuromuscular Diseases (Dimitrijevic, MR, Kakulas, BA and Vrbova G, eds.), pp.237-253. Karger Press, New York.

Stewart, HJ (1995) Expression of c-Jun, Jun B, Jun D and cAMP response element binding protein by Schwann cells and their precursors in vivo and in vitro. Eur.J.Neurosci. 7: 1366-1375.

Stewart, SA, Dykxhoorn, DM, Palliser, D, Mizuno, H, Yu, EY, An, DS, Sabatini, DM, Chen, IS, Hahn, WC, Sharp, PA, Weinberg, RA, and Novina, CD (2003) Lentivirus-delivered stable gene silencing by RNAi in primary cells. RNA. 9: 493-501.

Stichel, CC, Hermanns, S, Luhmann, HJ, Lausberg, F, Niermann, H, D'Urso, D, Servos, G, Hartwig, HG, and Muller, HW (1999) Inhibition of collagen IV deposition promotes regeneration of injured CNS axons. Eur.J.Neurosci. 11: 632-646.

Stow, ND and Stow, EC (1986) Isolation and characterization of a herpes simplex virus type 1 mutant containing a deletion within the gene encoding the immediate early polypeptide Vmw110. J.Gen.Virol. 67 (Pt 12): 2571-2585.

Stow, ND and Wilkie, NM (1976) An improved technique for obtaining enhanced infectivity with herpes simplex virus type 1 DNA. J.Gen.Virol. 33: 447-458.

Strittmatter, SM, Fankhauser, C, Huang, PL, Mashimo, H, and Fishman, MC (1995) Neuronal pathfinding is abnormal in mice lacking the neuronal growth cone protein GAP-43. Cell 80: 445-452.

Subang, MC and Richardson, PM (2001) Synthesis of leukemia inhibitory factor in injured peripheral nerves and their cells. Brain Res. 900: 329-331.

Sui, G, Soohoo, C, Affar, eB, Gay, F, Shi, Y, Forrester, WC, and Shi, Y (2002a) A DNA vector-based RNAi technology to suppress gene expression in mammalian cells. Proc.Natl.Acad.Sci.U.S.A 99: 5515-5520.

Sui, G, Soohoo, C, Affar, eB, Gay, F, Shi, Y, Forrester, WC, and Shi, Y (2002b) A DNA vector-based RNAi technology to suppress gene expression in mammalian cells. Proc.Natl.Acad.Sci.U.S.A 99: 5515-5520.

Tabara, H, Grishok, A, and Mello, CC (1998) RNAi in C. elegans: soaking in the genome sequence. Science 282: 430-431.

Tacke, R and Martini, R (1990) Changes in expression of mRNA specific for cell adhesion molecules (L1 and NCAM) in the transected peripheral nerve of the adult rat. Neurosci.Lett. 120: 227-230.

Takami, T, Oudega, M, Bates, ML, Wood, PM, Kleitman, N, and Bunge, MB (2002) Schwann cell but not olfactory ensheathing glia transplants improve hindlimb locomotor performance in the moderately contused adult rat thoracic spinal cord. J.Neurosci. 22: 6670-6681.

Takeda, M, Kato, H, Takamiya, A, Yoshida, A, and Kiyama, H (2000) Injury-specific expression of activating transcription factor-3 in retinal ganglion cells and its colocalized expression with phosphorylated c-Jun. Invest Ophthalmol.Vis.Sci. 41: 2412-2421.

Tang, S, Qiu, J, Nikulina, E, and Filbin, MT (2001) Soluble myelin-associated glycoprotein released from damaged white matter inhibits axonal regeneration. Mol.Cell Neurosci. 18: 259-269.

Taniuchi, M, Clark, HB, and Johnson, EM, Jr. (1986) Induction of nerve growth factor receptor in Schwann cells after axotomy. Proc.Natl.Acad.Sci.U.S.A 83: 4094-4098.

Tatagiba, M, Rosahl, S, Gharabaghi, A, Blomer, U, Brandis, A, Skerra, A, Samii, M, and Schwab, ME (2002) Regeneration of auditory nerve following complete sectioning and intrathecal application of the IN-1 antibody. Acta Neurochir.(Wien.) 144: 181-187.

Tessarollo, L, Vogel, KS, Palko, ME, Reid, SW, and Parada, LF (1994) Targeted mutation in the neurotrophin-3 gene results in loss of muscle sensory neurons. Proc.Natl.Acad.Sci.U.S.A 91: 11844-11848.

Tew, EM, Anderson, PN, Saffrey, MJ, and Burnstock, G (1998) Intrastriatal grafts of rat colonic smooth muscle lacking myenteric ganglia stimulate axonal sprouting and regeneration. J.Anat. 192 (Pt 1): 25-35.

Thoenen, H, Bandtlow, C, Heumann, R, Lindholm, D, Meyer, M, and Rohrer, H (1988) Nerve growth factor: cellular localization and regulation of synthesis. Cell Mol.Neurobiol. 8: 35-40.

Timmons, L, Court DL, and Fire, A (2001) Ingestion of bacterially expressed dsRNAs can produce specific and potent genetic interference in Caenorhabditis elegans. Gene 263: 103-112.

Timmusk, T, Belluardo, N, Metsis, M, and Persson, H (1993) Widespread and developmentally regulated expression of neurotrophin-4 mRNA in rat brain and peripheral tissues. Eur.J.Neurosci. 5: 605-613.

Towbin, H, Staehelin, T, and Gordon, J (1992) Electrophoretic transfer of proteins from polyacrylamide gels to nitrocellulose sheets: procedure and some applications. 1979. Biotechnology 24: 145-149.

Tozaki, H, Kawasaki, T, Takagi, Y, and Hirata, T (2002) Expression of Nogo protein by growing axons in the developing nervous system. Brain Res.Mol.Brain Res. 104: 111-119.

Tsujino, H, Kondo, E, Fukuoka, T, Dai, Y, Tokunaga, A, Miki, K, Yonenobu, K, Ochi, T, and Noguchi, K (2000) Activating transcription factor 3 (ATF3) induction by axotomy in sensory and motoneurons: A novel neuronal marker of nerve injury. Mol.Cell Neurosci. 15: 170-182.

Tuffereau, C, Benejean, J, Blondel, D, Kieffer, B, and Flamand, A (1998) Low-affinity nerve-growth factor receptor (P75NTR) can serve as a receptor for rabies virus. EMBO J. 17: 7250-7259.

Turk, SR, Kik, NA, Birch, GM, Chiego, DJ, Jr., and Shipman, C, Jr. (1989) Herpes simplex virus type 1 ribonucleotide reductase null mutants induce lesions in guinea pigs. Virology 173: 733-735.

Turnley, AM and Bartlett, PF (1998) MAG and MOG enhance neurite outgrowth of embryonic mouse spinal cord neurons. Neuroreport 9: 1987-1990.

Tuszynski, MH, Gabriel, K, Gage, FH, Suhr, S, Meyer, S, and Rosetti, A (1996) Nerve growth factor delivery by gene transfer induces differential outgrowth of sensory, motor, and noradrenergic neurites after adult spinal cord injury. Exp.Neurol. 137: 157-173.

Tuszynski, MH, Murai, K, Blesch, A, Grill, R, and Miller, I (1997) Functional characterization of NGF-secreting cell grafts to the acutely injured spinal cord. Cell Transplant. 6: 361-368.

Vaudano, E, Campbell, G, Anderson, PN, Davies, AP, Woolhead, C, Schreyer, DJ, and Lieberman, AR (1995) The effects of a lesion or a peripheral nerve graft on GAP-43 upregulation in the adult rat brain: an in situ hybridization and immunocytochemical study. J.Neurosci. 15: 3594-3611.

Vaudano, E, Campbell, G, Hunt, SP, and Lieberman, AR (1998) Axonal injury and peripheral nerve grafting in the thalamus and cerebellum of the adult rat: upregulation of c-jun and correlation with regenerative potential. Eur.J.Neurosci. 10: 2644-2656.

Vaudano, E, Woolhead, C, Anderson, PN, Lieberman, AR, and Hunt, SP (1993) Molecular changes in Purkinje cells (PC) and deep cerebellar nuclei (DCN) neurons after lesion or insertion of a peripheral nerve graft into the adult rat cerebellum. Soc. Neurosci. Abstr. 19: 1510.

Venkatesh, K, Lee-Osbourne, J, Oberheim, NA, Wychowski, T, Ali, Z, Kornack, DR, Welch, D, Kantor, D, Therianos, S, Kolodkin, AL, and Giger, RJ (2003) Structure-function analysis of the nogo receptor gene family: implications for regeneration. Program No. 142.12. Society for Neuroscience, Washington D.C.

Verge, VM, Tetzlaff, W, Richardson, PM, and Bisby, MA (1990) Correlation between GAP43 and nerve growth factor receptors in rat sensory neurons. J.Neurosci. 10: 926-934.

Villegas-Perez, MP, Vidal-Sanz, M, Rasminsky, M, Bray, GM, and Aguayo, AJ (1993) Rapid and protracted phases of retinal ganglion cell loss follow axotomy in the optic nerve of adult rats. J.Neurobiol. 24: 23-36.

Vinson, M, Strijbos, PJ, Rowles, A, Facci, L, Moore, SE, Simmons, DL, and Walsh, FS (2001) Myelin-associated glycoprotein interacts with ganglioside GT1b. A mechanism for neurite outgrowth inhibition. J.Biol.Chem. 276: 20280-20285.

Viskochil, D, Cawthon, R, O'Connell, P, Xu, GF, Stevens, J, Culver, M, Carey, J, and White, R (1991) The gene encoding the oligodendrocyte-myelin glycoprotein is embedded within the neurofibromatosis type 1 gene. Mol.Cell Biol. 11: 906-912.

von Bartheld, CS, Byers, MR, Williams, R, and Bothwell, M (1996) Anterograde transport of neurotrophins and axodendritic transfer in the developing visual system. Nature 379: 830-833.

von Schack, D, Casademunt, E, Schweigreiter, R, Meyer, M, Bibel, M, and Dechant, G (2001) Complete ablation of the neurotrophin receptor p75NTR causes defects both in the nervous and the vascular system. Nat.Neurosci. 4: 977-978.

Vourc'h, P, Dessay, S, Mbarek, O, Marouillat, VS, Muh, JP, and Andres, C (2003a) The oligodendrocyte-myelin glycoprotein gene is highly expressed during the late stages of myelination in the rat central nervous system. Brain Res.Dev.Brain Res. 144: 159-168.

Vourc'h, P, Martin, I, Marouillat, S, Adrien, JL, Barthelemy, C, Moraine, C, Muh, JP, and Andres, C (2003b) Molecular analysis of the oligodendrocyte myelin glycoprotein gene in autistic disorder. Neurosci.Lett. 338: 115-118.

Vyas, AA, Patel, HV, Fromholt, SE, Heffer-Lauc, M, Vyas, KA, Dang, J, Schachner, M, and Schnaar, RL (2002) Gangliosides are functional nerve cell ligands for myelin-associated glycoprotein (MAG), an inhibitor of nerve regeneration. Proc.Natl.Acad.Sci.U.S.A 99: 8412-8417.

Wagner, EK and Bloom, DC (1997) Experimental investigation of herpes simplex virus latency. Clin.Microbiol.Rev. 10: 419-443.

Wagner, EK, Flanagan, WM, Devi-Rao, G, Zhang, YF, Hill, JM, Anderson, KP, and Stevens, JG (1988) The herpes simplex virus latency-associated transcript is spliced during the latent phase of infection. J.Virol. 62: 4577-4585.

Wallace, MC, Tator, CH, and Lewis, AJ (1987) Chronic regenerative changes in the spinal cord after cord compression injury in rats. Surg.Neurol. 27: 209-219.

Waller, AV (1850) Experiments on the section of the glossopharyngeal and hypoglossal nerves of the frog, and observations on the alterations produced thereby in the structure of their primitive fibres. Philosophical Transactions of the Royal Society of London 140: 423-429.

Walmsley, AR, McCombie, G, Neumann, U, Marcellin, D, Hillenbrand, R, Mir, AK, and Frentzel, S (2004) Zinc metalloproteinase-mediated cleavage of the human Nogo-66 receptor. J.Cell Sci. 117: 4591-4602.

Walsh, FS, Meiri, K, and Doherty, P (1997) Cell signalling and CAM-mediated neurite outgrowth. Soc.Gen.Physiol Ser. 52: 221-226.

Walsh, GS, Krol, KM, Crutcher, KA, and Kawaja, MD (1999) Enhanced neurotrophin-induced axon growth in myelinated portions of the CNS in mice lacking the p75 neurotrophin receptor. J.Neurosci. 19: 4155-4168.

Wang, KC, Kim, JA, Sivasankaran, R, Segal, R, and He, Z (2002a) P75 interacts with the Nogo receptor as a co-receptor for Nogo, MAG and OMgp. Nature 420: 74-78.

Wang, KC, Koprivica, V, Kim, JA, Sivasankaran, R, Guo, Y, Neve, RL, and He, Z (2002b) Oligodendrocyte-myelin glycoprotein is a Nogo receptor ligand that inhibits neurite outgrowth. Nature 417: 941-944.

Wang, X, Chun, SJ, Treloar, H, Vartanian, T, Greer, CA, and Strittmatter, SM (2002c) Localization of Nogo-A and Nogo-66 receptor proteins at sites of axon-myelin and synaptic contact. J.Neurosci. 22: 5505-5515.

Weber, JR and Skene, JH (1998) The activity of a highly promiscuous AP-1 element can be confined to neurons by a tissue-selective repressive element. J.Neurosci. 18: 5264-5274.

Weibel, D, Cadelli, D, and Schwab, ME (1994) Regeneration of lesioned rat optic nerve fibers is improved after neutralization of myelin-associated neurite growth inhibitors. Brain Res. 642: 259-266.

Weidner, N, Grill, RJ, and Tuszynski, MH (1999) Elimination of basal lamina and the collagen "scar" after spinal cord injury fails to augment corticospinal tract regeneration. Exp.Neurol. 160: 40-50.

Wetmore, C, Ernfors, P, Persson, H, and Olson, L (1990) Localization of brain-derived neurotrophic factor mRNA to neurons in the brain by in situ hybridization. Exp.Neurol. 109: 141-152.

Widenfalk, J, Lundstromer, K, Jubran, M, Brene, S, and Olson, L (2001) Neurotrophic factors and receptors in the immature and adult spinal cord after mechanical injury or kainic acid. J.Neurosci. 21: 3457-3475.

Williams, RW, Borodkin, M, and Rakic, P (1991) Growth cone distribution patterns in the optic nerve of foetal monkeys: implications for mechanisms of axon guidance. J.Neurosci. 11: 1081-1094.

Wilson, N, Esfandiary, E, and Bedi, KS (2000) Cryosections of pre-irradiated adult rat spinal cord tissue support axonal regeneration in vitro. Int.J.Dev.Neurosci. 18: 735-741.

Wiznerowicz, M and Trono, D (2003) Conditional suppression of cellular genes: lentivirus vector-mediated drug-inducible RNA interference. J.Virol. 77: 8957-8961.

Wong, ST, Henley, JR, Kanning, KC, Huang, KH, Bothwell, M, and Poo, MM (2002) A p75(NTR) and Nogo receptor complex mediates repulsive signaling by myelin-associated glycoprotein. Nat.Neurosci. 5: 1302-1308.

Woolhead, CL, Zhang, Y, Lieberman, AR, Schachner, M, Emson, PC, and Anderson, PN (1998) Differential effects of autologous peripheral nerve grafts to the corpus striatum of adult rats on the regeneration of axons of striatal and nigral neurons and on the expression of GAP-43 and the cell adhesion molecules N-CAM and L1. J.Comp Neurol. 391: 259-273.

WuDunn, D and Spear, PG (1989) Initial interaction of herpes simplex virus with cells is binding to heparan sulfate. J.Virol. 63: 52-58.

Xu, F, Schillinger, JA, Sternberg, MR, Johnson, RE, Lee, FK, Nahmias, AJ, and Markowitz, LE (2002) Seroprevalence and coinfection with herpes simplex virus type 1 and type 2 in the United States, 1988-1994. J.Infect.Dis. 185: 1019-1024.

Yaar, M, Zhai, S, Pilch, PF, Doyle, SM, Eisenhauer, PB, Fine, RE, and Gilchrest, BA (1997) Binding of beta-amyloid to the p75 neurotrophin receptor induces apoptosis. A possible mechanism for Alzheimer's disease. J.Clin.Invest 100: 2333-2340.

Yamashita, T, Higuchi, H, and Tohyama, M (2002) The p75 receptor transduces the signal from myelin-associated glycoprotein to Rho. J.Cell Biol. 157: 565-570.

Yamashita, T and Tohyama, M (2003) The p75 receptor acts as a displacement factor that releases Rho from Rho-GDI. Nat.Neurosci. 6: 461-467.

Yamashita, T, Tucker, KL, and Barde, YA (1999) Neurotrophin binding to the p75 receptor modulates Rho activity and axonal outgrowth. Neuron 24: 585-593.

Yang, B, Slonimsky, JD, and Birren, SJ (2002) A rapid switch in sympathetic neurotransmitter release properties mediated by the p75 receptor. Nat.Neurosci. 5: 539-545.

Yang, J, Yu, L, Bi, AD, and Zhao, SY (2000) Assignment of the human reticulon 4 gene (RTN4) to chromosome 2p14-->2p13 by radiation hybrid mapping. Cytogenet.Cell Genet. 88: 101-102.

Yankner, BA, Benowitz, LI, Villa-Komaroff, L, and Neve, RL (1990) Transfection of PC12 cells with the human GAP-43 gene: effects on neurite outgrowth and regeneration. Brain Res.Mol.Brain Res. 7: 39-44.

Yick, LW, Wu, W, So, KF, Yip, HK, and Shum, DK (2000) Chondroitinase ABC promotes axonal regeneration of Clarke's neurons after spinal cord injury. Neuroreport 11: 1063-1067.

Yiu, G and He, Z (2003) Signaling mechanisms of the myelin inhibitors of axon regeneration. Curr.Opin.Neurobiol. 13: 545-551.

York, IA, Roop, C, Andrews, DW, Riddell, SR, Graham, FL, and Johnson, DC (1994) A cytosolic herpes simplex virus protein inhibits antigen presentation to CD8+ T lymphocytes. Cell 77: 525-535.

Yu, JY, DeRuiter, SL, and Turner, DL (2002a) RNA interference by expression of short-interfering RNAs and hairpin RNAs in mammalian cells. Proc.Natl.Acad.Sci.U.S.A 99: 6047-6052.

Yu, JY, DeRuiter, SL, and Turner, DL (2002b) RNA interference by expression of short-interfering RNAs and hairpin RNAs in mammalian cells. Proc.Natl.Acad.Sci.U.S.A 99: 6047-6052.

Zagrebelsky, M, Buffo, A, Skerra, A, Schwab, ME, Strata, P, and Rossi, F (1998) Retrograde regulation of growth-associated gene expression in adult rat Purkinje cells by myelin-associated neurite growth inhibitory proteins. J.Neurosci. 18: 7912-7929.

Zamore, PD, Tuschl, T, Sharp, PA, and Bartel, DP (2000) RNAi: double-stranded RNA directs the ATP-dependent cleavage of mRNA at 21 to 23 nucleotide intervals. Cell 101: 25-33.

Zeman, RJ, Feng, Y, Peng, H, Visintainer, PF, Moorthy, CR, Couldwell, WT, and Etlinger, JD (2001) X-irradiation of the contusion site improves locomotor and histological outcomes in spinal cord-injured rats. Exp.Neurol. 172: 228-234.

Zeng, BY, Anderson, PN, Campbell, G, and Lieberman, AR (1994) Regenerative and other responses to injury in the retinal stump of the optic nerve in adult albino rats: transection of the intraorbital optic nerve. J.Anat. 185 (Pt 3): 643-661.

Zhang, Y, Dijkhuizen, PA, Anderson, PN, Lieberman, AR, and Verhaagen, J (1998) NT-3 delivered by an adenoviral vector induces injured dorsal root axons to regenerate into the spinal cord of adult rats. J.Neurosci.Res. 54: 554-562.

Zhang, Y, Roslan, R, Lang, D, Schachner, M, Lieberman, AR, and Anderson, PN (2000) Expression of CHL1 and L1 by neurons and glia following sciatic nerve and dorsal root injury. Mol.Cell Neurosci. 16: 71-86.

Zhang, Y, Tohyama, K, Winterbottom, JK, Haque, NS, Schachner, M, Lieberman, AR, and Anderson, PN (2001) Correlation between putative inhibitory molecules at the dorsal root entry zone and failure of dorsal root axonal regeneration. Mol.Cell Neurosci. 17: 444-459.

Zhang, Y, Winterbottom, JK, Schachner, M, Lieberman, AR, and Anderson, PN (1997) Tenascin-C expression and axonal sprouting following injury to the spinal dorsal columns in the adult rat. J.Neurosci.Res. 49: 433-450.

Zheng, B, Ho, C, Li, S, Keirstead, H, Steward, O, and Tessier-Lavigne, M (2003) Lack of enhanced spinal regeneration in Nogo-deficient mice. Neuron 38: 213-224.

Zhou, ZM, Sha, JH, Li, JM, Lin, M, Zhu, H, Zhou, YD, Wang, LR, Zhu, H, Wang, YQ, and Zhou, KY (2002) Expression of a novel reticulon-like gene in human testis. Reproduction. 123: 227-234.

Zhu, Q and Julien, JP (1999) A key role for GAP-43 in the retinotectal topographic organization. Exp.Neurol. 155: 228-242.

Zorick, TS, Syroid, DE, Arroyo, E, Scherer, SS, and Lemke, G (1996) The transcription factors SCIP and Krox-20 mark distinct stages and cell fates in Schwann cell differentiation. Mol.Cell Neurosci. 8: 129-145.

Zuccato, C, Ciammola, A, Rigamonti, D, Leavitt, BR, Goffredo, D, Conti, L, MacDonald, ME, Friedlander, RM, Silani, V, Hayden, MR, Timmusk, T, Sipione, S, and Cattaneo, E (2001) Loss of huntingtin-mediated BDNF gene transcription in Huntington's disease. Science 293: 493-498.

Zufferey, R, Donello, JE, Trono, D, and Hope, TJ (1999) Woodchuck hepatitis virus posttranscriptional regulatory element enhances expression of transgenes delivered by retroviral vectors. J.Virol. 73: 2886-2892.

Zuo, J, Hernandez, YJ, and Muir, D (1998a) Chondroitin sulfate proteoglycan with neurite-inhibiting activity is up-regulated following peripheral nerve injury. J.Neurobiol. 34: 41-54.

Zuo, J, Neubauer, D, Dyess, K, Ferguson, TA, and Muir, D (1998b) Degradation of chondroitin sulfate proteoglycan enhances the neurite-promoting potential of spinal cord tissue. Exp.Neurol. 154: 654-662.